

Regulation of planar cell polarity in the mammalian auditory sensory epithelium
by microtubule-mediated processes

Conor Wythe Sipe

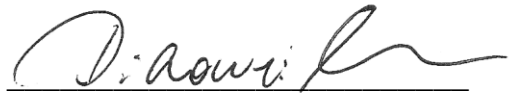
M.A., College of William and Mary, 2003
B.S., College of William and Mary, 2000

A Dissertation Presented to the Graduate Faculty
of the University of Virginia in Candidacy for the Degree of
Doctor of Philosophy

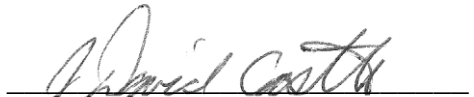
Department of Cell Biology

University of Virginia
May 2013

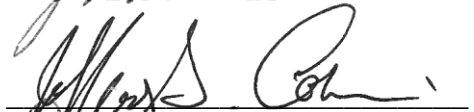
Xiaowei Lu, PhD

A handwritten signature in black ink, appearing to read 'Xiaowei Lu', written over a horizontal line.

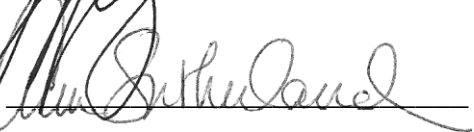
J. David Castle, PhD

A handwritten signature in black ink, appearing to read 'J. David Castle', written over a horizontal line.

Jeffrey T. Corwin, PhD

A handwritten signature in black ink, appearing to read 'Jeffrey T. Corwin', written over a horizontal line.

Ann E. Sutherland, PhD

A handwritten signature in black ink, appearing to read 'Ann E. Sutherland', written over a horizontal line.

Abstract

In the mammalian organ of Corti (OC), planar polarity of individual auditory hair cells is defined by their V-shaped hair bundle. At the tissue level, all hair cells display uniform planar polarity across the epithelium. Although it is known that tissue-level planar polarity of the OC is controlled by non-canonical Wnt/planar cell polarity (PCP) signaling, the mechanisms underlying hair cell-intrinsic polarity are relatively poorly understood. Genetic evidence suggests that hair bundle polarity and orientation are dictated by the position of the microtubule-based kinocilium and its associated basal body, which also organizes the cytoplasmic microtubule array. Based on this idea, I hypothesized that microtubule-mediated processes regulate hair bundle morphology and orientation and set out to investigate this idea by focusing on two microtubule motor-associated proteins. In this work, I have uncovered a role for the plus-end directed motor molecule Kif3a in regulating hair cell planar polarization through both ciliary and non-ciliary mechanisms. Kif3a coordinates hair bundle orientation with basal body positioning through localized activation of Rac-PAK (p21-activated kinase) signaling at the cortex, leading me to speculate that microtubule capture at the hair cell cortex is integral to the polarization process. To examine microtubule-cortical interactions during hair cell polarization, I also investigated the role of the Lissencephaly 1 (*Lis1*) gene, a major regulator of the minus-end directed cytoplasmic dynein microtubule motor. I present evidence that *Lis1* regulates localized Rac-PAK signaling in embryonic hair cells, likely through microtubule-associated Tiam1, a guanine nucleotide exchange factor for

Rac. Lis1 ablation in postnatal hair cells significantly disrupts centrosome anchoring and the normal V-shape of hair bundles, accompanied by defects in the pericentriolar matrix and microtubule organization. Together, my results describe a novel pathway that regulates the hair cell-intrinsic polarity machinery and provide important mechanistic insights into the role of microtubules during hair cell development.

Dedication

This dissertation is dedicated to my family, whose unfailing love and support has brought me to where I am today. Also to Kevin—while you never had a chance to reach these lofty academic heights, your memory continues to inspire me along my own journey.

	v
Abstract	ii
Dedication	iv
Table of Contents	v
List of Abbreviations	x
List of Figures	xii
List of Tables	xiv

Chapter 1: Background

Section 1.1: Development of the inner ear	2
1.1.1 Induction and patterning of the otocyst	2
1.1.2 Specification of the prosensory domain	4
1.1.3 Hair cell differentiation	5
1.1.4 Cochlear morphogenesis	6
Section 1.2: Hair cell structure and function	8
1.2.1 Hair bundle structure and function	8
1.2.2 The hair cell microtubule network	10
1.2.3 Hair cell polarization	11
Section 1.3: Planar cell polarity	14
1.3.1 Manifestation of PCP	15
1.3.2 The noncanonical Wnt/PCP signaling pathway	17
1.3.2.1 Vertebrate noncanonical Wnt/PCP pathway components	18
1.3.3 The Fat/Daschous pathway	22

1.3.4	PCP regulation by mechanical cues	23
1.3.5	Downstream effectors of PCP signaling	24
1.3.6	PCP in the organ of Corti	27
1.3.6.1	Manifestation of PCP in the organ of Corti	27
1.3.6.2	Molecular basis of PCP in the organ of Corti	28
1.3.6.3	The role of the kinocilium in PCP signaling	30
Section 1.4: The role of microtubules in cell polarity		33
1.4.1	Microtubule structure and dynamics	33
1.4.2	Microtubules regulate Rho GTPase activity during cell migration	34
1.4.3	Cortical protein complexes anchor Lis1-dynein during <i>C. elegans</i> spindle positioning	37
1.4.4	Microtubules organize adherens junctions in epithelial cells	40

Chapter 2: Methods

2.1	Mice	44
2.2	Tissue collection and fixation	44
2.3	Genotyping	45
2.4	Immunohistochemistry	45
2.5	Fluorescent image acquisition	46
2.6	Scanning electron microscopy	46
2.7	Organotypic cochlear explant culture	46
2.8	Quantification of hair cell phenotypes	47

2.9	Western blot	50
-----	--------------	----

Chapter 3: Kif3a regulates planar polarization through both ciliary and non-ciliary mechanisms

3.1	Introduction	55
3.2	Results	
3.2.1	Kif3a deletion causes PCP-like phenotypes in the organ of Corti	58
3.2.2	Kif3a is required for the V-shape of the nascent hair bundle	60
3.2.3	Kif3a is required for coupling of hair bundle orientation to basal body position	61
3.2.4	Kif3a is required for apical-basal positioning of the basal body in hair cells	63
3.2.5	Kif3a regulates cortical PAK activity during hair cell polarization	64
3.2.6	Rac-PAK signaling regulates basal body positioning and hair bundle morphogenesis	66
3.2.7	Kif3a associates with the Rac GEF Tiam1	66
3.2.8	Additional Experiments	68
3.3	Discussion	73
3.4	Figures	79

Chapter 4: Lis1 mediates planar polarity through regulation of microtubule organization

4.1	Introduction	104
-----	--------------	-----

4.2	Results	
4.2.1	Lis1 is localized to the pericentriolar region in developing hair cells	106
4.2.2	Lis1 deletion during embryonic development causes defects in hair bundle morphology and orientation	107
4.2.3	Defective cellular organization and nectin localization in <i>Lis1</i> ^{CKO-early} organ of Corti	109
4.2.4	Lis1 regulates Rac-PAK signaling in embryonic hair cells	110
4.2.5	Lis1 is required for maintaining the V-shape of hair bundles during postnatal development	112
4.2.6	Lis1 mediates the positioning of the hair cell centrosome near the lateral cortex	113
4.2.7	Lis1 is required for proper dynein localization and pericentriolar matrix organization	115
4.2.8	Microtubule organization defects in <i>Lis1</i> ^{CKO-late} hair cells	116
4.2.9	Lis1 deficiency leads to organelle distribution defects and subsequent outer hair cell death	117
4.2.10	Additional experiments	118
4.3	Discussion	121
4.4	Figures	126

Chapter 5: JNK signaling is required for hair cell morphogenesis

5.1	Introduction	154
5.2	Results	
5.2.1	Localization of active JNK during cochlear morphogenesis	155
5.2.2	Potential regulators of JNK signaling during cochlear development	156

5.2.3	JNK signaling is required for hair cell morphogenesis	157
5.3	Discussion	157
5.4	Figures	159

Chapter 6: Future Directions

6.1	Summary	165
6.2	Is dynein required to establish and/or maintain hair cell planar polarity?	166
6.3	Are microtubules required for cortical Rac-PAK signaling in embryonic hair cells?	167
6.4	Do Tiam family GEFs regulate microtubule-dependent Rac signaling in embryonic hair cells?	167
6.5	Is Par-3 involved in regulating Rac-PAK activity?	169
6.6	How might Lis1 link microtubule plus-ends to the cell cortex?	170
6.6.1	IQGAP1	170
6.6.2	LGN/GPSM2	171
6.7	How does PAK signaling regulate Lis1-mediated microtubule-cortex interactions?	173
6.8	How do tissue polarity cues impinge on the microtubule-mediated cell polarity machinery?	174
6.9	What is the basis for centrosomal defects in Lis1-deficient hair cells?	176
6.10	Is JNK signaling involved in Lis1-mediated cell death?	177
6.11	Conclusion	178

Chapter 7: Literature Cited

List of Abbreviations

AID	Autoinhibitory domain
AJ	Adherens junction
A-P	Anterior-posterior
APC	Adenomatous polyposis coli
BBS	Bardet-Biedl Syndrome
CE	Convergent extension
CHOP	C/EBP homologous protein
CRS	Craniorachischisis
DMEM	Dulbecco's Modified Eagle Medium
DMSO	Dimethyl Sulfoxide
D-V	Dorsal-ventral
Dvl2	Dishevelled-2
E	Embryonic day
ER	Endoplasmic reticulum
ERM	Ezrin/Radixin/Moesin protein
Fz3	Frizzled 3
GEF	Guanine nucleotide exchange factor
GFP	Green fluorescent protein
GTP	Guanosine triphosphate
HBSS	Hank's Balanced Salt Solution
HC	Hair cell
HEPES	4-(2-hydroxyethyl)-1-piperazineethanesulfonic acid
HIGS	Heat-inactivated goat serum
IHC	Inner hair cell
IFT	Intraflagellar transport
JNK	c-Jun N-terminal kinase
Lis1	Lissencephaly-1
NA	Numerical aperture
OC	Organ of Corti
OHC	Outer hair cell
P	Postnatal day
PAK	p21-activated kinase
PBS	Phosphate Buffered Saline
PBST	Phosphate Buffered Saline and Triton X-100
PCM	Pericentriolar matrix

PCP	Planar cell polarity
PFA	Paraformaldehyde
PLA	Proximity ligation assay
PTK7	Protein tyrosine kinase 7
RA	Retinoic acid
SEM	Scanning electron microscopy
TCA	Trichloroacetic acid
Tiam1	T-cell lymphoma invasion and metastasis 1
Vangl2	Van Gogh-like 2

List of Figures

Figure 1:	Hair cell planar cell polarity	12
Figure 2:	Cochlear extension and hair bundle orientation defects in <i>Kif3a^{ckO}</i> OC	80
Figure 3:	Normal hair cell development in the <i>Kif3a^{ckO}</i> utricle	82
Figure 4:	Localization of Dishevelled-2 in <i>Kif3a^{ckO}</i> OC	83
Figure 5:	Localization of frizzled 3 in <i>Kif3a^{ckO}</i> OC	84
Figure 6:	Kif3a is required for normal hair bundle morphology	85
Figure 7:	Uncoupling of hair bundle orientation from basal body position in <i>Kif3a^{ckO}</i> hair cells	86
Figure 8:	Aberrant apical-basal positioning of basal body in <i>Kif3a^{ckO}</i> hair cells	88
Figure 9:	IFT88 localization is normal in <i>Kif3a^{ckO}</i> hair cells	90
Figure 10:	Abnormal phospho-PAK localization correlates with centriole defects in <i>Kif3a^{ckO}</i> hair cells	91
Figure 11:	Rac-PAK signaling regulates hair cell centriole positioning	92
Figure 12:	Hair cell kinocilia persist after inhibition of Rac-PAK signaling in vitro	94
Figure 13:	The Rac GEF Tiam1 is a likely cargo of kinesin-II	95
Figure 14:	Hair cell phenotype and centriole positioning in <i>Kif3a^{ckO}; Rac1^{ckO}</i> OC	96
Figure 15:	Effects of β -catenin misregulation in hair cells	98
Figure 16:	Levels of canonical Wnt signaling are normal in <i>Kif3a^{ckO}</i> cochleae	100
Figure 17:	Abnormal cochlear morphology and hair bundle phenotypes in <i>axin^{fu/fu}</i> OC	101
Figure 18:	<i>In vivo</i> imaging of centriole search behavior during hair cell polarization	102

Figure 19:	Lis1 expression in developing hair cells	127
Figure 20:	Normal OC patterning and hair cell development in <i>Lis1</i> heterozygote embryos	129
Figure 21:	Planar polarity and microtubule defects in the <i>Lis1</i> ^{CKO-early} organ of Corti	130
Figure 22:	Frizzled-3 localization in the <i>Lis1</i> ^{CKO-early} organ of Corti	132
Figure 23:	Lis1 regulates cellular organization and junctional nectin localization in the organ of Corti	133
Figure 24:	Normal junctional E-cadherin localization in <i>Lis1</i> ^{CKO-early} hair cells	134
Figure 25:	Subcellular localization of dynein, Rac1-GTP and Tiam1 in hair cells at E17.5	135
Figure 26:	Lis1 mediates cortical Rac-PAK signaling likely through microtubule-associated Tiam1	136
Figure 27:	Lis1 is critical for maintaining hair bundle morphology and centrosome position in the postnatal organ of Corti	138
Figure 28:	Normal hair bundle morphology and polarity in the <i>Lis1</i> ^{CKO-late} utricle	140
Figure 29:	Lis1 is required for dynein localization around the hair cell centrosome	141
Figure 30:	Rac1-GTP and Tiam1 localization in wild-type organ of Corti at P3	143
Figure 31:	Pericentriolar matrix and microtubule organization defects in <i>Lis1</i> ^{CKO-late} hair cells	145
Figure 32:	Lis1 is required for organelle positioning and hair cell survival	147
Figure 33:	CHOP induction in <i>Lis1</i> ^{CKO-late} hair cells	148
Figure 34:	Constitutive Rac1 activation disrupts hair bundle morphology	149

Figure 35:	<i>Tiam1</i> is required for cellular patterning in the OC	150
Figure 36:	<i>In vivo</i> imaging of <i>Lis1</i> ^{CKO-late} hair bundle development	151
Figure 37:	A proposed model for Lis1 function in hair cell planar polarity	152
Figure 38:	JNK signaling during embryonic hair cell development	160
Figure 39:	JNK signaling in the early postnatal OC	162
Figure 40:	JNK signaling is required for proper hair bundle morphology and cell shape	163

List of Tables

Table 1:	Genotyping primers	51
Table 2:	Primary antibodies used for immunochemistry	52

Chapter 1

Background

Section 1.1: Development of the vertebrate inner ear

The vertebrate inner ear, housed within the temporal bone, consists of a number of interconnected fluid-filled ducts and chambers containing groups of sensory cells responsible for the sensation of hearing and balance. There are six individual organs positioned precisely in three-dimensional space that mediate different aspects of hearing and balance. Three cristae detect angular acceleration in response to fluid motion in three orthogonal semicircular canals. Two maculae, the utricle and saccule, are oriented at right angles to one another and detect acceleration due to gravity. Finally, the spiral-shaped cochlea houses the organ of Corti (OC), the sensory epithelium specialized for hearing. In addition to these sensory areas, the inner ear generates a population of spiral ganglion neurons that innervate these organs in a topographically precise fashion [1].

1.1.1 Induction and patterning of the otocyst

The entire inner ear develops from the otic placode, a thickened plate of ectodermal tissue that arises adjacent to the dorsal hindbrain around embryonic day (E) 8.5 in the mouse. Evidence suggests that fibroblast growth factor (FGF) signals arising from the underlying mesoderm, endoderm, and adjacent neural ectoderm are necessary and sufficient to induce early otic placode markers in competent ectoderm [2]. The earliest molecular marker of the future inner ear that is induced in response to FGF signaling in mammals is *Pax2* [3]. Graded Wnt signals, originating from the midline and amplified via Notch signaling, act in

combination with FGF to further refine the presumptive placode into otic and non-otic territories [4, 5]. Following specification, the otic placode invaginates, closes, and separates from the surface ectoderm to form the otic vesicle around E9 in the mouse [6].

The complex morphology of the mature inner ear exhibits clear polarity in three axes, the dorsal-ventral (D-V), anterior-posterior (A-P) and medial-lateral (M-L) axes. This polarity, beginning in the form of differential gene expression, is established early in development and is already present by the time of otocyst formation [7]. These early gene expression patterns are established according to axial position as an integrated response to morphogen gradients originating from the tissue surrounding the otocyst. The D-V axis, which functionally divides the inner ear into a dorsal vestibular system and a ventral auditory component, is primarily established by Shh signaling. Analogous to its role in patterning the neural tube, Shh produced by the notochord and ventral neural tube imparts D-V patterning information to the adjacent otocyst [8]. Consistent with this idea, Shh effectors, such as the Gli transcription factors, and direct targets of Shh, including its receptor patched 1, are expressed across the otocyst in a D-V gradient [9]. Likewise, a retinoic acid (RA) signal present in the ectoderm surrounding the inner ear induces distinct responses along the A-P axis, which divides non-sensory structures from neuronal elements and most sensory structures of the inner ear [10]. Importantly, each patterning signal must be integrated with others that emanate from the surrounding tissues, notably Wnts and BMPs, to establish an exact axial identity [7].

1.1.2 Specification of the prosensory domain

Three main lineages of cells, prosensory (cells that become hair cells and closely-associated supporting cells), proneural (cells that develop into the auditory or vestibular neurons) and nonsensory (all other otocyst-derived cells), are derived from the otocyst, and gene expression analyses have led to the identification of genes involved in specifying each cell type.

The prosensory cell lineage gradually becomes restricted to particular regions of the inner ear, including the presumptive organ of Corti. Based on mutant analysis, several studies implicated the Notch ligand *Jag1* as having a critical role in specifying the prosensory domain [11, 12]. Subsequent loss- or gain-of-function experiments have confirmed a crucial role for the Notch signaling pathway in the formation of prosensory domains (see [13]). This function for Notch signaling is in contrast to the well-established role in lateral inhibitory signaling that determines hair cell versus supporting cell fates later in otic development (see **Section 1.1.3**). The transcription factor SOX2 is also a marker of the presumptive prosensory domains, and mice harboring *Sox2* mutations show a loss of both hair cells and supporting cells [14]. Recent work suggests that Notch signaling induces prosensory fate by enforcing *Sox2* expression within competent cells [15]. The transcriptional coactivator gene *Eya1*, associated with syndromic hearing loss in humans, also has an important role in prosensory specification [16]. While genetic analysis has led to the identification of genes necessary for prosensory specification, comparatively little is known about the factors responsible for refining the position and boundaries of

the domain within the cochlear epithelium, though there is strong evidence that the Shh and BMP pathways play a role in this process [13].

1.1.3 Hair cell differentiation

Cells within the prosensory domain are further specified to develop as either hair cells or supporting cells in a precise ratio. A large body of work has shown that lateral inhibition between developing hair cells and surrounding undifferentiated progenitors determines this fate and limits the production of hair cells. This lateral inhibitory process is mediated by the Notch signaling pathway and is independent of Notch's earlier role in prosensory development [17]. While the receptor *Notch1* is expressed throughout the cochlear duct, the Notch ligands *Jag2*, *Dll1*, and *Dll3* are expressed exclusively in developing hair cells [13]. Consistent with this idea, targets of Notch activation that inhibit hair cell specific gene expression, such as the Hes family of proteins, are expressed selectively in supporting cells [18, 19]. As development continues, prosensory cells upregulate the cyclin-dependent kinase inhibitor p27^{Kip1} and withdraw from the cell cycle beginning around E12 in mice [20].

Atoh1 (formerly known as *Math1*), encoding a basic helix-loop-helix transcription factor, has been identified as the earliest hair cell-specific gene required for definitive hair cell development, because the loss of *Atoh1* results in a total failure of hair cell differentiation in the mouse cochlea [21]. Moreover, forced expression of *Atoh1* within the prosensory domain or even outside of it is sufficient to induce hair cell fate [22]. Although the deletion of *Sox2* or *Eya1* also

causes a lack of hair cell differentiation, this is thought to involve a loss of the progenitor cell population in general and not a specific block in hair cell differentiation [13].

1.1.4 Cochlear morphogenesis

The cochlear duct first extends from the postero-lateral region of the otocyst and then descends ventro-laterally to form an L-shaped organ by E12 in the mouse [6]. The murine cochlea continues to elongate over development until reaching a mature length of one and three-quarters turns. After the onset of *Atoh1* expression, sensory cell precursors in the primordial OC exit the cell cycle between E12 and E14 and form a precursor domain that is four to five cells thick [23]. During terminal differentiation, this domain thins to a two cell-layered epithelium that extends in length along the longitudinal axis. Extension and thinning occur independently of cell death and proliferation, indicating that cellular rearrangements within the developing OC are responsible for the final form of the mature cochlea [23]. Such movements are similar to the process of convergent extension (CE) that occurs during *Xenopus* gastrulation and neurulation [24]. Like other morphogenic processes where tissues undergo CE, it is thought that radial and mediolateral cell intercalation behaviors underlie cochlear extension [25–27], and this process is governed, at least in part, by Wnt/planar cell polarity (PCP) signaling (see **Section 1.3.6**) [28, 29]. The small GTPase Rac1 also contributes to cochlear morphogenesis by coordinating cell adhesion, cell proliferation, and cell movements [30, 31].

Terminal differentiation of hair cells in the organ of Corti initiates near the base of the cochlea following the onset of *Atoh1* expression. This wave of differentiation proceeds in a base-to-apex gradient along the length of the cochlea in mouse between E15.5 and E17.5, alongside extension of the cochlear duct. Simultaneous with differentiation along the longitudinal axis, a gradient of differentiation along the mediolateral (i.e. inner hair cell to outer hair cell) axis is also present. By E18.5, nearly all cells in the OC have adopted a mature configuration consisting of three rows of outer hair cells (OHCs) and one row of inner hair cells (IHCs) with several types of supporting cells interdigitated between them (**Fig. 1A**). While Notch signaling is thought to be responsible for segregating hair cell and supporting cell fates, the checkerboard-like pattern of the OC is regulated by the nectin family of immunoglobulin-like cell adhesion proteins [32]. IHCs are located medially (i.e. closer to the center of the cochlear spiral) in the OC, while OHCs are on the lateral side farthest from the cochlear spiral.

The fully mature OC consists of a continuous array of cells that are tonotopically organized along the length of the cochlea. Based on the mechanical properties of the basilar membrane and the electrical properties of the cells themselves, each sensory hair cell is tuned to a particular frequency based on its location along the length of the cochlea [33]. This progressive tonotopical response is organized in ascending order from the apex of the cochlea to its base.

Section 1.2: Hair cell structure and function

1.2.1 Hair bundle structure and function

Vertebrate hair cells are characterized by the presence of a mechanosensory hair bundle (or stereociliary bundle) that projects from their apical surface. The hair bundle consists of two or more rows of modified microvilli, known as stereocilia, and a single microtubule-based kinocilium that develops from the basal body immediately underlying it. The stereocilia are arranged in rows of increasing height with the tallest row of stereocilia adjacent to the kinocilium. In spite of their name, individual stereocilia are composed of F-actin filaments that are highly cross-linked by actin bundling proteins such as espin and fimbrin [34]. Growth of stereocilia occurs via addition of new actin monomers to the barbed ends of filaments which are aligned toward the stereocilia tips. Some actin filaments pass through the tapered base of the stereocilia to form a rootlet which anchors the entire structure in the cuticular plate, a dense meshwork of actin in the apical domain of the hair cell that forms just before birth. Given the fundamental importance of actin in stereocilia, factors that regulate actin filament assembly and dynamics are critical for both the development and maintenance of the hair bundle [35].

Hearing depends on sound-induced deflection of the stereocilia. The actin core of each stereocilia forms a rigid array that allows the stereocilium to pivot at its base in response to stimulation by sound waves traveling through the cochlear duct. The deflection of stereocilia opens mechanically gated ion channels located on the tips of stereocilia. Tip links, extracellular filaments that connect

the tips of adjacent stereocilia, are believed to transmit tension force onto transduction channels [36]. The opening of the mechanotransduction channel allows Ca^{2+} to enter the stereocilia near the lower tip link insertion site depolarizing the hair cell toward 0 mV. This depolarization activates neurotransmitter release at the base of the hair cell, passing the signal on to the central nervous system.

Based on the discovery of genes required for hearing (the so-called “deafness” genes) and the study of mouse and zebrafish mutants, significant progress has been made in identifying the molecular components of the mechanotransduction machinery of auditory hair cells. Notably, these studies have showed that tip links are composed of heterophilic complexes of cadherin 23 and protocadherin 15 homodimers [37]. In addition, a network of other proteins expressed in the stereocilia, many of which encode genes affected by the human sensory disorder Usher syndrome, have been incorporated into an integrated model of the mechanotransduction network. These include adaptor proteins such as harmonin [38], whirlin [39] and sans [40], cell surface receptors such as Usherin [41], actin binding proteins like espin [42], and several myosin motors including myosin VIIa [43], myosin VI [44], and myosin XV [45] (see [46, 47] for a full discussion of the mechanotransduction apparatus). Despite these advances, the identity of the proteins comprising the mechanotransduction channel remains unknown. The channel-like proteins Tmc1 and Tmc2 have been proposed as components of the channel complex, but a definitive

demonstration that they are integral components of the complex awaits further study [48].

1.2.2 The hair cell microtubule network

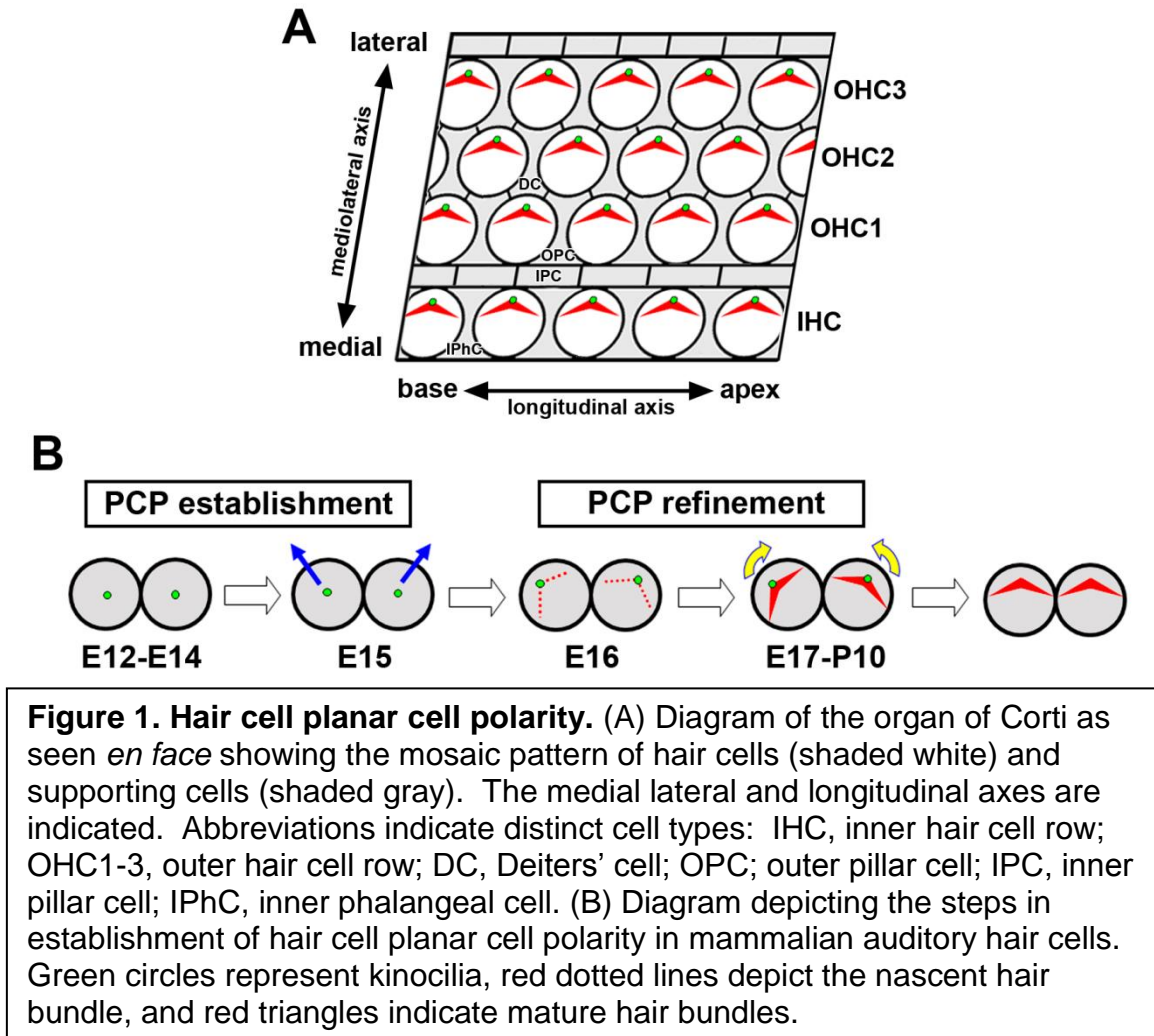
The specialized nature of hair cells in the organ of Corti is reflected in the architecture of their microtubule network, which differs significantly from that found in supporting cells. While tubulin immunofluorescence reveals subtle differences in staining between OHCs and IHCs, several features are common to all hair cells [49]. The kinocilium, a specialized non-motile primary cilium, is found on the apical surface of hair cells [50]. The axoneme of the cilia extends from the basal body, which is derived from the mother centriole of the centrosome and found at the base of the kinocilium within the cuticular plate [51]. In auditory hair cells, the kinocilium is a transient structure that recedes following maturation of the hair bundle, suggesting a crucial role during development (see **Section 1.3.6.3**).

In addition to organizing the kinocilium, the basal body and its associated pericentriolar material (PCM), or centrosome, organize the cytoplasmic microtubule array of the hair cell [50]. This array is highly ordered, with a majority of microtubules radiating outward toward the lateral pole of the cell (see **Fig. 31**). After contacting the cortex with their plus-ends, these microtubules continue to grow, angling back toward the medial pole of the cell between the cell membrane and the cuticular plate. In addition to filaments that span the mediolateral axis of the cell, a portion of microtubules extends from the

centrosome into the cytoplasm toward the base of the hair cell. During the postnatal period, the entire microtubule network grows more diffuse, eventually forming a filamentous mesh that extends to the basal portions of the mature hair cell [52, 53]. Extensive post-translational modification of microtubules is observed in embryonic and postnatal hair cells; a majority of tubulin in hair cells is found in a tyrosinated and/or acetylated state, though the functional implications of these modifications is not known [54].

1.2.3 Hair cell polarization

A prominent feature of the OC is the polarization of hair cells within the plane of the epithelium. Hair cell planar cell polarity (PCP) is manifested by the V-shaped hair bundle formed near the lateral pole of the cell. At the tissue level, each hair cell orients its hair bundle in a uniform direction such that the vertex of the bundle points toward the lateral edge of the OC (**Fig. 1A**). The asymmetric structure of the stereociliary bundle is critical for proper mechanotransduction, as it renders the bundle directionally sensitive to mechanical movement. Hair cells are depolarized (excited) by displacement toward the tallest row of stereocilia and hyperpolarized (inhibited) by movements in the opposite direction [36]. Thus, the directional sensitivity of each bundle makes uniform orientation of stereociliary bundles across the OC critical for proper sensation of sound.



During development, the kinocilium and its associated basal body are thought to play an instructive role in hair bundle polarity (**Fig. 1B**) [55]. Hair cell polarization begins shortly after cell cycle exit when the kinocilium grows from the center of the apical cell surface which is covered by a carpet of short microvilli [56]. Around E16 in the mouse, the kinocilium migrates toward the periphery of the cell in a non-random fashion; the position of the kinocilium after migration is biased toward the side of the cell nearest the lateral edge of the OC [57]. Here, it initiates outgrowth of the surrounding microvilli which subsequently organize into rows, thicken and elongate, and become anchored in the cuticular plate. This

process occurs alongside an extended period of reorientation, when hair bundles rotate to achieve a precise uniform orientation across the plane of hair cells [58, 59]. After bundle formation and orientation are complete, around P10 in the mouse, the kinocilium degenerates, leaving its basal body behind in the fonticulus, an area in the cuticular plate devoid of actin.

On a molecular level, the uniform orientation of hair bundles in the OC is controlled by the Wnt/PCP signaling pathway, an evolutionarily conserved set of proteins that directs morphogenesis in a number of developmental contexts (see **Section 1.3**) [60]. Loss-of-function of mammalian core PCP genes causes a characteristic misorientation of hair bundles (see **Section 1.3.6**). Despite loss of planar polarity on the tissue level in these mutants, the intrinsic asymmetry of the bundle remains intact, indicating that planar polarity on the cell and tissue level are separable. However, the mechanisms that establish hair cell-intrinsic planar polarity are poorly understood. To date, attention has focused on the role of ciliary proteins [61] and the importance of kinociliary links with neighboring stereocilia [62].

Previous work in our laboratory has suggested that the Rac small GTPases and their downstream effector, PAK, serve as polarity cues within hair cells [30]. A major goal of the current study is to elucidate the cellular processes that establish cell-intrinsic polarity through spatial regulation of Rac-PAK signaling on the hair cell cortex.

Section 1.3: Planar cell polarity

Cell polarity is a fundamental characteristic of nearly all cells. Different cell types use polarity to orient themselves in a variety of ways. For example, epithelial cells maintain a strict apical-basal polarity axis, while migrating mesenchymal cells organize their cytoplasm into distinct forward and rear compartments. This variation allows for a wide range of cellular functions, including changes in cell shape, cell adhesion, migration, cell division, cell fate determination, and the uptake and release of molecules [63]. Despite this diversity of function, each of these polarized processes is underpinned by a common molecular mechanism. In each case, molecular polarity determinants localize to specific domains of the plasma membrane where they subsequently act to polarize other cellular systems. A key feature of these polarity determinants is the ability to respond to extracellular cues from neighboring cells or the surrounding environment [64]. However, in some cases, polarity determinants can spontaneously polarize in the absence of external cues [63].

Planar cell polarity (PCP) refers to the coordinated orientation of cells across the plane of a two-dimensional cell sheet. PCP is perhaps most evident in epithelial tissues, such as the organ of Corti of the inner ear, but can occur in a wide range of cell types and contexts. Historically, planar polarity had long been appreciated in the cuticle of *Drosophila*, where hairs and bristles align themselves precisely with respect to the body axes. These observations culminated in the seminal work by Gubb and Garcia-Bellido that identified the genetic basis for this phenomenon [65]. It is now appreciated that a relatively

small set of evolutionarily conserved genes coordinates many of the complex cell movements and polarized structures required to elaborate the final morphology of both invertebrates and vertebrates.

1.3.1 Manifestation of PCP

The biological processes where PCP is important can be broadly categorized based on the tissue or cell context in which they occur. The simplest manifestation of PCP is the uniform alignment of an array of identical cells, as in the wing of *Drosophila*. Here, each epithelial cell extends a single bristle pointing toward the distal axis of the wing [66]. An analogous circumstance occurs in the posterior notochordal plate of vertebrates, where each cell extends its primary cilium toward the posterior of the cell so that left-right fluid flow can be induced by their coordinated beating [67]. A more complex arrangement arises when polarized cells reside in a heterogeneous epithelium where polarity information must be transmitted through non-polarized cell types. Such is the case for multiciliated cells in the epidermis of the frog *Xenopus*, which form in an internal cell layer and subsequently migrate to intercalate with unciliated cells in the outer surface layer [68]. These cells direct fluid flow along the A-P axis by orientating their cilia and underlying basal bodies uniformly. Another example of this type of PCP occurs in hair cells of the mammalian inner ear (**see Section 1.3.6**).

PCP also manifests within multicellular structures. For example, hair follicles in mammalian skin are composed of a number of cell types, each with distinct morphology and gene expression patterns [69]. In rodent skin, body

hairs are directed toward the posterior, and this orientation is based on the angle at which each protrudes from the follicle. Disruption of follicle polarity affects this angle, leading to whorls and ridges in fur [70]. Finally, PCP processes govern morphogenetic processes requiring the transient orientation of cells within a tissue. The prime example is during convergent extension (CE) movements that occur during gastrulation and the elongation of axial tissue. Cells produce polarized protrusions that allow neighboring cells to converge on an axis and intercalate by “pulling” on each other, thereby forming a narrower, longer array [24]. Disruption of these polarized cell movements underpins the open neural tube defects in individuals with compromised PCP signaling.

Throughout each of these circumstances, two unifying functions for PCP signaling are observed. First, it provides individual cells within a group the ability to discriminate their position relative to the overall tissue arrangement. For example, cells undergoing CE must identify a common axis before organized cell movements can occur. Second, it transmits tissue-level information to the cell-intrinsic machinery to direct the placement of polarized structures, the outward manifestations of PCP. For example, polarized regulation of the cytoskeleton brings about asymmetric hair formation in the *Drosophila* wing epithelium and directs stereociliary bundle formation in hair cells of the inner ear.

The establishment of PCP requires polarized cell-cell interactions that align cells with their immediate neighbors and long-range cues to orient this polarization in relation to tissue axes. It is now understood that the establishment of PCP in a diverse assortment of tissues is coordinated by two separate but

highly coordinated molecular systems, the non-canonical Wnt/PCP signaling pathway and the Fat/Dachsous system, both of which generate asymmetric cell-cell contacts through interactions between cell-surface proteins. Recent evidence also suggests that mechanical tension can provide physical cues to direct polarization.

1.3.2 The noncanonical Wnt/PCP signaling pathway

A set of core components, first identified by genetic studies in *Drosophila* but highly conserved in vertebrates, is required for most, if not all, aspects of PCP signaling; a lack of any of these genes (or the vertebrate ortholog) results in polarity defects in a number of tissues [60]. This core cassette of proteins consists of the seven-pass transmembrane receptor Frizzled (Fz), the seven-pass transmembrane cadherin Flamingo (Fmi; also known as Starry Night/Stan), the four-pass transmembrane Strabismus (Stbm; also known as Van Gogh/Vang), and three cytoplasmic proteins, Dishevelled (Dsh), Prickle (Pk), and Diego (Dgo). Fz and Dsh are also components of the canonical Wnt signaling pathway, however both have roles in PCP that are independent of Wnt/ β -catenin signaling [71].

Core PCP proteins are spread uniformly throughout the cell prior to the onset of signaling but become asymmetrically localized and differentially enriched during active signaling [72]. The ability to communicate polarity information between neighboring cells, critical for the maintenance of planar polarity, is thought to be propagated by asymmetric assembly of cell-surface

PCP protein complexes that are set up via both intracellular and cell-autonomous interactions. In support of non-cell-autonomous regulation of PCP protein complex assembly, experiments in *Drosophila* revealed that wild-type cells adjacent to a clone of cells lacking a PCP component adopt a misoriented phenotype, turning either toward or away from the mutant clone (a phenomenon termed ‘domineering non-autonomy’) [73]. It has subsequently been shown that heterophilic interactions between cell-surface PCP protein complexes on adjacent cells propagate the planar polarization signal by enforcing their asymmetric localization in the neighboring cell [74, 75]. Within a given cell, interactions between core PCP proteins also determine their asymmetric localization by interfering with one another’s membrane localization or accumulation [72, 76]. The integration of both intra- and inter-cellular signals results in a self-organizing system; this hypothesis has been further substantiated by conceptual models where the application of relatively simple rules leads to accumulation of PCP protein complexes on opposite sides of the cells [77–79]. Importantly, the interactions with neighboring cells continually reinforce this arrangement of proteins to assure coordinated polarization. In particular, Fmi acts as a central mediator by communicating bi-directionally between neighboring cells [80].

1.3.2.1 Vertebrate noncanonical Wnt/PCP pathway components

A more diverse set of core PCP proteins has radiated in vertebrates, adding complexity to the regulation of PCP signaling compared to lower

organisms. There are at least 10 members of the Frizzled family in vertebrates compared with only four in *Drosophila* [81]. While not all Fz receptors are involved in PCP signaling, those that are have some degree of functional overlap. Fz3 and Fz6 are implicated in PCP signaling and have overlapping asymmetric localization patterns in the cochlea; genetic redundancy accounts for the severe neural tube phenotype of *Fz3^{-/-}/Fz6^{-/-}* mice when individuals lacking either gene alone do not have the defect [82]. Likewise, mammals have three Dishevelled (Dvl) genes [83]. *Dvl1/Dvl2* compound mutants display open neural tube defects and misorientation of stereocilia bundles in the inner ear, despite a lack of such phenotypes in *Dvl1^{-/-}* or *Dvl2^{-/-}* mice [27, 84].

The increased number of cells and greater size of vertebrates have led to the suggestion that a long-range signal might be necessary to coordinate PCP in these organisms [60]. Because Fz proteins function as receptors for diffusible Wnt signals during canonical signaling, Wnts present themselves as likely candidates for a long-range PCP signaling molecule. Indeed, a growing body of evidence from vertebrate species has supported a role for Wnt regulation of PCP processes, ranging from CE movements to polarization of hair cells [85–88]. In contrast, functional evidence for Wnt involvement in *Drosophila* PCP signaling is scarce [80]. Given the expanded role of Wnts in vertebrate PCP, it is not unexpected that vertebrate cells employ several accessory proteins that act as Wnt coreceptors to regulate PCP signaling. Glypican 4 [89] and Ryk [88] both bind Wnts and positively regulate PCP, in the case of Ryk through interactions with Vangl2 (vertebrate homolog of *Drosophila* Stbm) to control downstream

effectors. Similarly, the Ror kinases are a family of transmembrane receptors that form Wnt-induced receptor complexes with Vangl2 to sense Wnt dosage and regulate levels of Vangl2 phosphorylation [90].

Given the importance of asymmetric localization of core PCP proteins in the generation of polarity, their regulated trafficking, transport, and turnover is crucial and highly regulated in vertebrates. In fact, mutations in genes that control these processes can lead to phenotypes indistinguishable from those of the core PCP mutants [91]. *Scribble1* (*Scrb1*), a PDZ-containing protein, was identified on the basis of a neural tube defect in the *circletail* mouse mutant and subsequently shown to be responsible for asymmetric targeting of membrane Vangl2 complexes [58, 92, 93]. Sec24, a component of the coat protein complex II (COP II) that is essential for ER-to-Golgi intracellular transport, selectively sorts PCP proteins, including Vangl2 and *Scrb1*, into vesicles [94, 95]. Convergent extension defects and stereocilia misorientation have also been observed in mice lacking the Smurf1/2 ubiquitin ligases. These phenotypes are attributed to loss of Pk asymmetric localization caused by defective protein degradation, normally mediated by a Smurf/Par6/Dvl complex [96]. In addition, evidence is emerging that vertebrate PCP genes are regulated at the transcriptional level; mutations in *Cdx1/2*, a homeodomain transcription factor that binds in the promoter region of *Ptk7*, cause axial defects that genetically interact with *Scrb1* [97].

Protein tyrosine kinase 7 (Ptk7), an atypical receptor tyrosine kinase, is another regulator of vertebrate PCP for which there is no evidence for a homologous function in *Drosophila* [98]. *Ptk7*-null mice exhibit craniorachischisis

(CRS) and misoriented hair bundles in the inner ear [98], and Ptk7 is required for convergent extension movements in *Xenopus* [98], zebrafish [99], and mammals [100]. However, evidence suggests that Ptk7 is not an obligatory component of the core PCP pathway [101] and likely functions in novel alternative pathways to regulate PCP. In *Xenopus*, Ptk7 appears to mediate PCP signaling by controlling the recruitment of Dvl to the plasma membrane [102]. The interaction of Ptk7 with Dvl is mediated by RACK1 [103], an evolutionarily conserved adapter protein, that is also required for Vangl2 membrane localization [104]. An additional protein, PKC δ , cooperates with Ptk7 and RACK1 to bring about membrane recruitment of Dvl, but its functional role in the process remains unclear [103]. In stark contrast to *Xenopus*, mammalian Ptk7 does not regulate membrane localization of Dvl2 in mesodermal cells [100] or hair cells in the inner ear [101], suggesting heterogeneous molecular functions for Ptk7 during polarization. Recent work in our laboratory indicates that *Ptk7* acts in parallel to the core PCP pathway to orient PCP in the auditory sensory epithelium [101]. In this circumstance, *Ptk7* mediates the assembly of a myosin II network that exerts polarized contractile tension between supporting cells and hair cells. The current model for *Ptk7* function in hair cells speculates that this anisotropic tension acts as a polarity cue by influencing spatial patterns of Rac-PAK activity.

1.3.3 The Fat/Daschous pathway

The second major planar cell polarity signaling pathway has been most extensively characterized in *Drosophila*. Fat (Ft) and Daschous (Ds) encode

atypical cadherins that preferentially bind to one another heterophilically across cell boundaries. Their affinity for one another is modulated by the phosphorylation of their extracellular domains by the Golgi protein Four-jointed (Fj) [105, 106]. Similar to *Fz* mutant clones, groups of cells that lack *Ft* or *Ds* mediate a directional non-autonomous effect on neighboring cells [107, 108]. Despite their role in polarity, these proteins exhibit no obvious asymmetric subcellular localization [109].

Ft/Ds expression domains are organized in developing tissues via coordination with upstream morphogens. In the *Drosophila* eye, *Ft* is expressed uniformly, but opposing gradients of *Ds* and *Fj* expression are set up by *Wg*, leading to a gradient of interactions between the two [106, 110]. The discovery of such gradients in a range of tissues initially led to the supposition that the *Ft/Ds* system might serve as a classical long-range polarity cue [107]. However, evidence argues against this as a universal function of the *Ft/Ds* gradient since its disruption does not interfere with the establishment of PCP in the wing [110, 111]. An alternative model that considers *Ft* and *Ds* expression boundaries rather than gradients as a means of signaling has also been proposed [112].

The interface between *Ft/Ds* and the core PCP signaling pathway remains enigmatic. In the *Drosophila* eye, clones lacking *Ft*, *Ds*, or *Fj* retain core PCP protein asymmetry [113]. However, *Ft* mutant clones lose their ability to affect polarity in clones doubly mutant for core Wnt/PCP signaling genes, suggesting that *Ft/Ds* can act upstream of core PCP signaling [113]. Despite such evidence, there has been no molecular link established between the two pathways to date

[112]. There are also tissue-specific differences in the interpretation of Ds/Ft signaling; in some tissues (such as the eye and anterior segment compartments of the abdomen), core PCP signaling orients toward high levels of Ds expression [113, 114], and in others (the wing and posterior segment compartments of the abdomen) toward low Ds expression [107, 108, 114]. Thus, there is unlikely to be a universal relationship between Ft/Ds activity and the asymmetry of core PCP proteins.

To date, relatively little is known about the extent to which the Fat/Ds polarity system is conserved in vertebrates. Mammals have four Fat-related proteins, two Ds-related proteins, and a single Fj-related protein [115]. Among these, only Fat4 shares similarity with *Drosophila* Ft in its cytoplasmic domain. Mutations in murine *Fat4* or *Dchs1* cause PCP phenotypes in a number of tissues, and disruption of either gene increases the protein levels of the other [116, 117]. The role of the Fat/Ds signaling pathway and the extent to which it interfaces with Wnt/PCP signaling in vertebrates is an area of intense interest.

1.3.4 PCP regulation by mechanical cues

Recent evidence from *Drosophila* has supported the idea that the establishment of PCP can be tightly coupled to active mechanical events. Investigation into this phenomenon revealed that a global planar polarity signal, as measured by Fz/Stbm asymmetry, was present in the imaginal disc cells giving rise to the wing epithelium [118]. At this early stage, PCP is aligned to the wing margin rather than in its final configuration along the proximodistal axis.

During the transition to pupal stages, the wing hinge contracts, generating anisotropic tension across the epithelium. This tension is thought to guide a series of oriented cell divisions, cell elongations, and neighbor exchanges that cause the tissue to elongate and narrow. These morphogenetic movements ultimately result in a realignment of PCP along the proximodistal axis of the wing epithelium. Interestingly, mutation of *Ds* perturbs this pattern by altering epithelial dynamics rather than changing the asymmetric localization of PCP proteins [118], perhaps by influencing microtubule dynamics [119]. A separate study used genetic manipulation to flatten several morphogen gradients emanating from organizer regions in the epithelium [120]. Intracellular polarity was not affected; instead, morphogenetic movements were disrupted, ultimately perturbing the global PCP pattern. Whether a similar mechanism might regulate PCP in vertebrate tissues is only beginning to be explored. Our laboratory has recently suggested that anisotropic tension in the developing OC might control polarity acquisition in hair cells [101].

1.3.5 Downstream effectors of PCP signaling

In addition to the core components of the Wnt/PCP signaling pathway, a wider group of proteins is essential for executing PCP but are not solely dedicated to it. These proteins, which lie downstream of Fz and Dsh, have been implicated in both *Drosophila* and vertebrates, and they are conserved between the two groups. Due to the wide range of processes mediated by PCP signaling, cellular context dictates the contribution of various downstream effectors. This

heterogeneity between organisms and tissues has led some to caution against the use of the term 'PCP signaling' as a general descriptor [121, 122].

Arguably the most important of the PCP effectors are the small Rho-family GTPases, RhoA, Rac and Cdc42, all of which have been implicated as planar polarity effectors during vertebrate gastrulation (see [60] and references therein). These GTPases function as bimolecular switches, existing in a GDP-bound inactive form and an active GTP-bound form, that interact with effector proteins to trigger multiple cellular responses, notably the rearrangement of the actin cytoskeleton to induce changes in cell shape and motility. In general, RhoA regulates assembly of actin/myosin filaments to mediate contractile forces, while Rac and Cdc42 promote actin polymerization at the cell periphery to generate protrusive forces [123].

Dishevelled signals to two parallel pathways that lead to the activation of the Rho GTPases [124, 125]. A direct interaction between Dsh and the formin Daam1, which specifically associates with Dsh at the plasma membrane, activates Rho-associated kinase (ROCK) through its GTP exchange factor, WGEF [126, 127]. A second pathway directly activates Rac and stimulates JNK signaling, which stands atop a MAPK cascade capable of regulating a wide variety of targets, including those involved in actin polymerization [128]. During CE movements in *Xenopus*, Dsh can also form a complex with Ptk7 at the cell membrane to activate JNK signaling [129].

Another group of proteins are thought to function exclusively as planar polarity effectors. In *Drosophila*, these proteins, Fuzzy (Fy), Inturned (In) and

Fritz (Frtz), influence the polarity of wing cells and hair bristles, but not the ommatidia of the eye. In the pupal wing, they colocalize on the proximal edge of cells with Fmi, Stbm, and Pk, though they do not physically associate with core Wnt/PCP proteins [130, 131]. Here, they regulate the subcellular localization of another downstream effector, Multiple Wing Hairs (Mwh), that antagonizes actin polymerization to prevent bristle formation on that side of the cell [132, 133]. The roles of the vertebrate homologs of In, Fy, and Frtz are less clear, as loss of their activity causes only mild gastrulation defects in frog and mouse [134–136]. Further complicating matters, their loss disrupts ciliogenesis, causing widespread defects in Hedgehog (Hh) signaling [136, 137]. This, combined with the importance of cilia in many morphogenetic processes, makes it difficult to separate the contributions of In, Fy, and Frtz to true PCP signaling versus other non-polarity roles.

Defining the effectors of the Ft/Ds signaling pathway has proved challenging because of its dual roles in mediating polarity and tissue growth. In the *Drosophila* wing, the Ft/Ds pathway influences polarity by changing core PCP protein localization, indicating that the core PCP signaling pathway can serve as a downstream effector of Ft/Ds in some contexts [107]. In other tissues, such as the abdomen and larval cuticle, Ft/Ds probably acts directly with unidentified downstream effectors independently of the core PCP proteins [114]. During control of oriented cell division in the wing, Ft/Ds activity does control the polarized distribution of at least one downstream effector, the atypical myosin Dachs [109]. However, Dachs does not appear to be required in all Ft/Ds

signaling contexts (e.g. hair polarity) [109]. To date, the effector proteins lying downstream of the vertebrate Ft/Ds PCP signal are not known.

1.3.6 PCP in the organ of Corti

1.3.6.1 Manifestation of PCP in the organ of Corti

The OC is a complex epithelium composed of hair cells separated from one another by interdigitated supporting cells. Hair cells within the OC have one of the most prominent manifestations of vertebrate PCP: all hair cells exhibit a uniform orientation of their hair bundles in relation to one another, with the vertices of each aligned along the medial-lateral axis of the OC. In addition to planar polarity at the tissue level, hair cells display a cell-intrinsic form of planar polarity. The stereociliary bundle itself is asymmetric, being composed of a V-shaped staircase of stereocilia with the kinocilium eccentrically placed at its vertex. Moreover, the basal body and its associated daughter centriole adopt a precise orientation relative to the mediolateral axis of the OC (see **Fig. 7A,C**).

Cochlear extension defects in PCP mutants also support a role for PCP signaling during the morphogenesis and patterning of the cochlea itself. During terminal differentiation, the postmitotic OC intercalates to thin from an epithelium of 4-5 cells thick to a final two cell-layered structure [23]. This occurs simultaneously with mediolateral cell movements that extend the cochlear duct along the longitudinal axis [29]. Such coordinated cell movements are characteristic of the CE movements observed during vertebrate gastrulation and neurulation, which are governed by PCP signaling [24].

1.3.6.2 Molecular basis of PCP in the OC

Evidence has demonstrated a conserved role for polarized core PCP proteins in establishing PCP in the inner ear. A hallmark of *Drosophila* PCP signaling is the polarized membrane distribution of PCP proteins. In the mammalian inner ear, Dvl2 and Dvl3 [27, 138], Vangl2 [93], Fz3 and Fz6 [82] show asymmetric membrane localization in the OC. In fact, asymmetric localization of Vangl2 is observed prior to the outward manifestation of polarity in hair cells, indicating a key role in establishing the future planar polarity axis [61].

Localization studies indicate that core PCP complexes in the inner ear might diverge from those of *Drosophila*. In the OC, Dvl2 is localized to the lateral pole of hair cells, and Vangl2, Fz3, and Fz6 to the medial pole. The localization of Dvl2 and Vangl2 to opposite poles of the cell mirrors the Dsh-Stbm antagonism observed during PCP signaling in the fly. However, it is unexpected that Dvl2 and Fz3/Fz6 do not colocalize and, instead, Fz3/Fz6 colocalize with Vangl2. It should be noted that inferences drawn from these observations are tempered by the difficulty in distinguishing the cell membranes of tightly juxtaposed hair and supporting cells [26]. Furthermore, observations from the utricle indicate that PCP complex localization is not an absolute determinant of final polarity in all inner ear tissues; Fz6 and Pk2 are localized to the same side of vestibular hair cells regardless of the cell's final polarity in relation to the line of reversal [139].

Loss of mouse core PCP gene function in the inner ear, including *Vangl2* [58], *Dvl1/2* [27, 140], *Fz3/6* [82], and *Celsr1* (vertebrate homolog of *Drosophila* Fmi) [141], causes various degrees of hair bundle misorientation. As in *Drosophila*, loss of any of the core components disrupts asymmetric localization of the others in hair cells. Moreover, many core PCP gene mutations are associated with a shortened, wider cochlear duct and open neural tube phenotypes, ranging in severity from spina bifida to CRS, presumably by virtue of disrupting CE [142].

The long-range signal, if any, that allows cells to discriminate their position relative to the medial-lateral axis of the OC remains unclear. Given the importance of Fz in transmission of the PCP signal, the Wnt proteins, which bind Fz and its coreceptors, present themselves as likely candidates for such a signal. Indeed, many Wnts are expressed in the developing mouse cochlea [59], and they are required for PCP-mediated CE movements in zebrafish and *Xenopus* [85, 86, 143, 144]. However, disruption of Wnt genes in mice has failed to produce dramatic inner ear phenotypes. To date, the best candidate for Wnt involvement in inner ear PCP signaling is *Wnt5a*. It shares a reciprocal expression pattern with the Wnt antagonist, *Frzb*, along the planar polarity axis, and *Wnt5a* knockout mice have shortened, wider cochleae as well as some bundle orientation defects [87]. Experiments involving exogenous application of *Wnt7a* in cochlear explant cultures indicate that Wnt signaling may be involved in reorienting OHC hair bundles during early postnatal development [59]. Despite

these hints of Wnt involvement, no conclusive evidence of an instructive Wnt gradient has been found in the developing OC.

1.3.6.3 The role of the kinocilium in PCP signaling

Both hair cells and supporting cells have a single microtubule-based primary cilium on their apical surface. The kinocilium of hair cells has long been suspected to be involved in establishing polarity. First, the polarized structure of the hair bundle itself is based around the eccentric position of the kinocilium at the vertex of the V-shape. The kinocilium is connected to the adjacent stereocilium via protein links, and this association is required for normal V-shape and orientation of the nascent hair bundle (see **Chapter 3**) [61, 62]. Second, the migration of the kinocilium and its associated basal body is the first outward manifestation of hair cell polarity and precedes hair bundle development. Finally, the kinocilium recedes after hair bundle maturation is complete, suggesting it has a developmental role.

Genetic evidence for a link between primary cilia and PCP signaling first came from genes involved in the human disorder Bardet-Biedl Syndrome (BBS) [145]. BBS proteins, 14 of which have been identified to date, localize preferentially or exclusively to the basal body and/or cilium. A subset of these form a multi-subunit complex called the BBSome that acts as a scaffold to regulate axonemal transport [146, 147]. Similar to PCP mutants, mice lacking BBS genes exhibit CE defects in zebrafish and misoriented hair bundles in the ear [145, 148, 149]. Moreover, *Bbs4*-null mice display CRS and open eyelids,

phenotypes associated with impaired PCP signaling [145]. Localization of BBS proteins in the OC are consistent with a similar role of regulating cilia and/or basal body functioning in the inner ear [149]. A genetic interaction between BBS genes and *Vangl2* in the OC is further evidence for a link between ciliary proteins and PCP signaling in the inner ear [145].

Other studies have taken a more direct approach to addressing the role of the kinocilium in PCP signaling by disrupting the intraflagellar transport (IFT) system in hair cells. IFT transports ciliary components up the axoneme and is absolutely required for ciliogenesis and subsequent maintenance of cilia length (reviewed in [150]). In *Ift88* mutants, which have stunted kinocilia or lack them altogether, the OC is shorter and wider, and hair bundles are misoriented [61]. These defects occur in spite of normal core PCP protein membrane localization, though the hair bundle misorientation and cochlear extension phenotypes were augmented when combined with the *Vangl2* mutation *looptail*. Interestingly, hair cells with disrupted ciliary proteins, including ALMS1 [151], *Ift88* [61] and the BBS [145] proteins, often exhibit abnormally-shaped flat or circular hair bundles, indicating that cell-intrinsic planar polarity is also disrupted. Taken together, there is compelling evidence for a link between ciliogenesis in the OC and PCP signaling, though the exact nature of the relationship remains obscure.

Given that both the canonical (β -catenin dependent) and non-canonical/PCP Wnt signaling pathways rely on shared molecular components that converge on Dvl, they have been hypothesized to have an interconnected, reciprocal relationship [83]. Evidence from cultured cells suggests that the

primary cilium and its associated basal body impact PCP signaling by acting as a switch between the two pathways. Suppression of *Bbs1/4/6* leads to CE extension defects in zebrafish with a concomitant increase in canonical Wnt signaling [148]. Importantly, increased canonical signaling was also observed after disruption of the IFT component *Kif3a* and occurred independently of the microtubule cytoskeleton, indicating the increase was a true ciliary effect. Other studies investigating the effects of ciliary (*Kif3a*, *Ift88*, *Dync2h1*) and basal body (*Odf1*) mutants have reached similar conclusions [152, 153].

Despite the evidence that the primary cilium and its associated proteins generally restrain canonical Wnt signaling, other experiments have failed to detect changes in Wnt activity after disruption of ciliary genes [154–156]. This suggests the existence of cell- or tissue-specific regulatory mechanisms to control canonical versus non-canonical Wnt signaling. To date, the only reported evidence of such a switch in the inner ear comes from mice lacking the ciliopathy protein *Rpgrip1l*, which have both basal body positioning and stereociliary orientation defects in hair cells [157]. *Rpgrip1l*, in complex with other ciliopathy proteins, modulates Dvl levels by regulating its proteasomal degradation. A full understanding of how the balance between canonical and non-canonical/PCP signaling is maintained in the inner ear awaits further study.

Section 1.4: The role of microtubules in cell polarity

While it is long established that actin and actin-associated proteins generate molecular and morphological polarity (see [58, 59]), recent work has shown that cell-intrinsic cues from the microtubule cytoskeleton can likewise induce and/or maintain polarity in a wide range of cell types. A common function for microtubules in the generation of polarity across a range of cell types is the delivery of positional information to the cell cortex. Once microtubules and their associated proteins and cargos have established a specialized cortical domain, it is thought that positive feedback loops between the actin-rich cell cortex and microtubules reinforce and maintain this polarity [64].

This section will introduce three well-studied instances of microtubules and microtubule-associated pathways in regulating cell polarity in different contexts. These pathways represent paradigms for understanding the role of the microtubule cytoskeleton during hair cell polarization. The special case of the primary cilia in the establishment of planar cell polarity is discussed elsewhere (see **Section 1.3.6.3**).

1.4.1 Microtubule structure and dynamics

Microtubules are dynamic polar filaments built from 13 parallel protofilaments, each composed of alternating α -tubulin and β -tubulin molecules [160]. In a typical interphase cell, microtubules form a radial array centered around the centrosome (composed of the basal body, daughter centriole, and their associated pericentriolar material). Microtubule minus-ends are slow

growing and usually anchored at the centrosome, while faster growing plus-ends are closer to the cell cortex. Growing microtubule plus-ends are composed of GTP-bound tubulin which acts to stabilize the ends of the filament. Over time, tubulin hydrolyzes the bound GTP to its GDP form, making the filament more susceptible to depolymerization, or collapse. The constant rate of hydrolysis necessitates continual growth to maintain the microtubule's GTP cap. This cycle of rapid growth and collapse is termed dynamic instability. This behavior confers upon a cell the ability to spatially and temporally regulate its cytoskeletal structure, necessary for any polarization process [64].

A group of proteins, collectively known as the plus-end tracking proteins (+TIPS), localize exclusively to dynamic microtubule plus-ends and are intimately involved in microtubule-mediated polarization processes. +TIPs regulate plus-end dynamics and mediate the microtubule-cortex interactions necessary for cargo delivery, force generation, and cortical signaling [161].

1.4.2 Microtubules regulate Rho GTPase activity during cell migration

Migrating cells display a characteristic polarized morphology that defines their direction of movement. Forward motion occurs through the extension of actin-rich lamellipodia, followed by the establishment and maturation of adhesion plaques and subsequent contraction of the trailing edge of the cell to translocate the cytoplasm and nucleus toward the leading edge [162]. Accordingly, the leading edge of the cell contains a complex arrangement of actin and its

associated polymerization machinery, while the trailing end of the cell contains actin stress fibers and integrin-mediated attachments to the substrate [163].

The microtubule array in a migrating cell is highly polarized, with the minus-ends of microtubules anchored at the centrosome near the middle of the cell and plus-ends contacting the leading edge as well as targeting focal adhesions at the rear of the cell [164]. The importance of microtubules for cell migration was first demonstrated by treating fibroblasts with microtubule-depolymerizing agents, which resulted in unpolarized membrane ruffling and a lack of directional migration [165]. Thus, microtubules are not required for migration *per se*, but they are essential for establishing a polarized leading edge. Subsequent experiments demonstrated that low concentrations of nocodazole or taxol, which arrest microtubule dynamics without affecting filament polarity or abundance, block cell migration [166]. Moreover, a key study by Waterman-Storer et al. [167] showed that the rapid growth of a short microtubule array induced by taxol brought about transient polarized protrusions. Together, these results indicate that long-range microtubule-based intracellular transport is dispensable for polarized protrusive activity and, instead, implicate microtubule-cortex interactions as driving the process.

A clue to the question of how microtubule plus-ends alter cortical polarity was provided by data linking transient microtubule stabilization with increased levels of the activated form of the Rho-family small GTPase Rac1, which regulates actin turnover and stimulates lamellipodial growth [123, 167]. By virtue of its role in regulating levels of Rho GTPase signaling [168], its ability to directly

bind actin [169], and its association with the +TIP CLIP-170 [170], IQGAP1 was identified as a candidate protein linking the microtubule and actin cytoskeletons. In fact, gain- or loss-of-function of IQGAP1 positively or negatively regulates both the levels of Rac1-GTP and cell migration rates [168, 171]. IQGAP1 colocalizes with Rac1 on the cortex on the leading edge of the cell, and this localization requires the presence of another +TIP, adenomatous polyposis coli (APC) [170, 171]. In a process that also involves modulation of signaling by Rho-family GTPases, IQGAP1 forms a complex with CLIP-170 and Lis1 in response to calcium influx, linking the cortical actin network to microtubules at the leading edge of migrating neurons [172]. Whether Lis1 is a constitutive member of the IQGAP/CLIP-170 complexes described in other cell types has not been addressed in the literature to date.

In addition to IQGAP1-dependent mechanisms, crosstalk between the microtubule and the actin cytoskeleton in migrating cells is likely regulated by guanine exchange factors (GEFs), which activate Rho-family GTPases to their GTP-bound form. A leading candidate is GEF-H1, which binds to and is held inactive by its association with microtubules [173]. With increased microtubule instability, GEF-H1 is released and becomes free to activate RhoA, which organizes leading edge extension and ruffling and myosin-mediated contraction at the rear of the cell [174]. More recent work has shown that microtubule-mediated Rac1 activation also occurs through the GEF activity of Tiam1 [175] and Tiam2/STEF [176], possibly through association with MAP1B, a +TIP.

Besides establishing polarity during cell migration, microtubules are also involved in positive feedback loops that stabilize and reinforce the polarity axis. Several intertwined pathways that utilize +TIPs to anchor microtubule ends to the cell cortex via association with cortical protein complexes have been described. For instance, activated Rac1, after its initial activation by IQGAP1, promotes microtubule/IQGAP1/CLIP-170 complex formation and longer microtubule-cortex dwell times [170, 171]. Moreover, the activity of another Rho-family GTPase, Cdc42, regulates the phosphorylation and inactivation of GSK-3 β in concert with the Par-6 and PKC ξ kinases. This phosphorylation event, in turn, recruits APC to microtubule plus-ends where it is necessary for reorientation of the microtubule organizing center (MTOC), an important polarizing event during cell migration [177]. Likewise, microtubule plus-ends are captured and anchored at the leading edge by association of the +TIPs EB1 and APC with the cortical formin mDia [178]. More direct regulation of microtubule turnover can also occur, as when high Rac1 activity represses stathmin function, which normally inhibits tubulin polymerization, promotes catastrophe events, and modulates tubulin GTP hydrolysis [179].

1.4.3 Cortical protein complexes anchor Lis1-dynein during *C. elegans* spindle positioning

The *C. elegans* egg is initially symmetrical, but upon fertilization becomes polarized along its A-P axis. The identity of the first two daughter cells is determined by asymmetric distribution of cortical proteins during the first cell

division. The entry point of the sperm defines the posterior pole in the one-cell zygote [63]. Before the first mitosis can occur, the two pronuclei and their associated centrosomes move to the cell center (known as centration) and rotate 90° to align the centrosome pair along the A-P axis (known as spindle orientation). During early anaphase, the mitotic spindle moves toward the posterior pole (termed spindle positioning), ultimately resulting in a dorsal daughter cell that is smaller than the anterior daughter [180].

A set of polarity determinants crucial in the establishment of asymmetry was discovered in genetic screens for genes regulating the asymmetric partitioning of granules during the first cell division in *C. elegans* [181]. A large body of work has shown that the evolutionarily conserved PAR-3/PAR-6/aPKC complex is localized to the anterior cortex of the zygote, whereas PAR-1 and PAR-2 localize to the posterior cortex [121, 182]. In the absence of any one of the anterior proteins, the localization of the other two is lost and the posterior determinants spread toward the anterior pole [182]. In the absence of PAR-2, PAR-1 is lost from the posterior pole and the anterior determinants spread toward the posterior. Thus, the cortical polarity determinants act to mutually exclude one another from the anterior and posterior domains of the cell, likely by phosphorylating each other to inhibit plasma membrane association [63, 183]. Interestingly, it has recently been proposed that the high density of microtubules around one of the centrosomes induces polarized PAR domains by physically shielding PAR-2 from phosphorylation by aPKC [183]. Loss of cortical Par

polarity disrupts spindle orientation and positioning, resulting in anterior and posterior daughter cells of the same size [181].

Numerous lines of evidence, including spindle disruption experiments [184–186], genetic manipulation [184, 187], and mathematical modeling [186, 187], have demonstrated that spindle orientation and positioning rely on astral microtubule anchoring at the cell cortex. An asymmetric pulling force, larger on the posterior spindle pole, results in generation of a larger anterior and smaller posterior blastomere [180]. Building on evidence of their similar role in other contexts (see [90]), attention focused on the role of cortical dynein complexes in generating this asymmetric force. Dynein heavy chain is enriched on the cell cortex near the plus-ends of microtubule asters, and inactivation of *dhc-1* results in characteristic cell division defects in one-cell-stage embryos [189].

Subsequent work identified Lis1 as essential for all known dynein-mediated process in the one-cell embryo [185, 190]. Dynein and Lis1 are found uniformly throughout the cytoplasm and enriched on the cell cortex during all phases of the cell cycle [189, 190], leading to the question of how dynein-mediated pulling forces are spatially and temporally regulated to direct spindle positioning.

Heterotrimeric G proteins are also required for several aspects of spindle positioning and have a central role in linking asymmetric Par protein distribution to dynein-mediated force generation. Disruption of two partially redundant G α proteins results in spindle positioning defects reminiscent of those caused by dynein loss-of-function [191, 192]. Though canonical heterotrimeric G protein signaling pathways are activated primarily by cell surface receptors, work in

Drosophila neuroblasts revealed receptor-independent mechanisms involving the TPR/GoLoco protein Pins [193]. The *C. elegans* orthologs, GPR-1/2 (known as LGN/GPSM2 in mammals) are enriched on the posterior cortex by Par polarity signaling during anaphase spindle positioning [192, 194]. Here, GPR-1/2 binds Gα and undergoes a conformational change, freeing its TPR domain from autoinhibition. The TPR domain of GPR-1/2 interacts with LIN-5 (known as Mud in flies and NuMA in mammals), and together they associate with Lis1 and dynein to exert a pulling force [195, 196]. The final link between the microtubule machinery and cortical polarity determinants occurs via LET-99, a protein which inhibits cortical accumulation of GPR-1/2 and restricts it to the posterior cortex [194]. On the anterior side of the cell, PAR-3 and PAR-1 inhibit the localization of LET-99, generating differential pulling forces on each centrosome during anaphase [194, 197].

Notably, the major components of the spindle positioning pathway are highly conserved among species and used in similar contexts. Nearly identical functions for the cortical components, including LGN, Gαi and NuMA [198–202], and Lis1-dynein [196, 202–204] have been described in polarized mammalian cell types.

1.4.4 Microtubules organize adherens junctions in epithelial cells

Adherens junctions (AJs) are cell-cell adhesion complexes crucial for embryogenesis and cellular homeostasis [205]. AJs form the zonula adherens of epithelial cells, which link cells into a continuous sheet and separate the apical

and basolateral membrane domains of each polarized cell. The AJs of adjacent cells are directly apposed to one another, and the interacting plasma membranes are held together by homophilic bonds between transmembrane cadherin molecules. Within each cell, a contractile bundle of actin filaments lies adjacent to the AJs, oriented in parallel with the plasma membrane. This actin interacts with a large set of intracellular anchoring proteins that link filaments to cadherin complexes, forming a transcellular network capable of contracting via the action of myosin motor proteins. This actomyosin machinery allows a variety of cell shape changes important in many cell- and tissue-level processes, making the establishment of polarized AJs a fundamental step in morphogenesis.

Several lines of evidence have established that AJs intimately associate with dynamic microtubules, and that these interactions are important for organizing the intracellular microtubule array. The plus-ends of dynamic microtubules have been shown to repeatedly contact cadherin-based cell junctions [206–208]. Moreover, dynamic instability of microtubules is reduced with cell-cell contact, suggesting that AJs stabilize microtubule plus-ends [207]. By contrast, microtubule integrity is required for AJ stability since treatment with depolymerizing agents disrupts morphology and organization of E-cadherin contacts [206, 207, 209]. Interactions between microtubules and AJs are mediated, at least in part, by +TIPs. CLIP-170 and EB1 localize adjacent to cadherin clusters, and disruption of CLIP-170 results in a loss of cadherin clustering without lowering the overall levels of cell surface cadherin [206, 208]. Furthermore, cytoplasmic dynein localizes at nascent and mature AJs via an

association with β -catenin [210] and/or PLAC24 [211], and injection of dynein antibodies causes microtubules to dissociate from AJs [209]. Thus, AJs can function as dynein-mediated microtubule anchoring sites that tether filaments to the cell cortex. During polarization processes, these anchored microtubules could serve as tracks for targeted delivery of AJ components or allow dynein-mediated force generation in a configuration analogous to that described in the *C. elegans* zygote.

In *Drosophila* development, microtubules have a key role in AJ assembly during cellularization, the process whereby the syncytial embryo compartmentalizes into an epithelium of columnar cells [212]. Polarized apical junctions first form as cadherin-catenin clusters located between microvilli on the apical plasma membrane. These clusters subsequently shift position to the apicolateral membrane domain to form spot AJs in a cytoplasmic dynein-dependent process that is guided by the minus-ends of centrosomal microtubules [213]. Microtubules also influence AJ position through the cortical polarity determinant Bazooka (the *Drosophila* Par3 ortholog) [214]. Bazooka colocalizes at spot AJs with cadherin clusters, and both become mislocalized together when dynein function is compromised [214]. Without Bazooka, cadherin-catenin clusters still form at microvilli but are unable to reposition and instead become spread throughout the plasma membrane [214]. Current evidence suggests a model whereby the minus-ends of centrosomal microtubules provide a polarity cue for the deposition of Bazooka clusters, which, in turn, engage cadherin-catenin clusters to promote polarized AJ assembly [215].

Chapter 2

Materials and Methods

2.1 Mice

Animal care and use were performed in compliance with NIH guidelines and the Animal Care and Use Committee at the University of Virginia. Mice were obtained from either the Jackson Laboratory or the referenced sources and maintained on a mixed genetic background. For timed pregnancies, the morning of the plug was designated as E0.5 and the day of birth as P0. The primers used to genotype each strain are listed in **Table 1**. Specific mating schemes for each strain can be found within the appropriate section of Results.

2.2 Tissue collection and fixation

For tissue collection, pups were decapitated and their heads placed in PBS for dissection. The roof of the skull and brain were immediately removed and discarded. Excess tissue was removed, and the temporal bone was pierced in two locations to enhance fixative permeation. The skull was then transferred into a 12-well dish containing fixative. Tissue was fixed in 4% PFA for 1 hour at room temperature or overnight at 4°C. For some antibodies (see **Table 2**), skulls were fixed in 10% TCA for 1 hour on ice. Following fixation, tissue was rinsed three times in PBS for 5 minutes, and the temporal bones subsequently removed from the skull in PBS. For whole-mount preparations, cochleae were dissected out of the temporal bones and Reissner's membrane was removed to expose the sensory epithelium. For utricle preparations, dissected utricles were transferred to PBS containing protease XXVII (50 µg/ml) for 5 min at room temperature to remove the otolithic membrane. For sectioning, fixed temporal bones were

equilibrated in 30% sucrose, snap frozen in OCT (Tissue Tek), and cryosectioned at 12 μ m thickness.

2.3 Genotyping

The distal portion of each pup tail was clipped, placed into 100 μ l 50 mM NaOH, and incubated at 95°C for 30 minutes. The mixture was subsequently neutralized with 30 μ l of 1M Tris-HCl (pH 7.5) and centrifuged for 1 minute to pellet insoluble material. This DNA was used as a template to amplify products via PCR for genotyping using the primers indicated in **Table 1**. PCR products were analyzed on 0.8% or 2% agarose gels.

2.4 Immunohistochemistry

Sections or dissected cochleae were incubated in PBS containing 5% HGS, 0.1% Triton-X 100, 0.02% NaN₃ (blocking solution) for 1 hour at room temperature, followed by overnight incubation with primary antibodies (**Table 2**) diluted in blocking solution at 4°C. After three 5 minute washes in PBST, samples were incubated with secondary antibodies diluted in blocking buffer for 1 hour at room temperature. Samples were then washed in PBST three times for 5 minutes each. Cochleae or utricles were flat-mounted on glass slides in Mowiol containing 5% N-propyl gallate. Alexa- conjugated secondary antibodies (1:1000), Alexa-488 and rhodamine-conjugated phalloidin (1:200) and Hoechst 33342 (1:10,000) were obtained from Invitrogen.

2.5 Fluorescent image acquisition

Z-stacks of images were collected using a Deltavision deconvolution microscope equipped with a Plan-Apochromat N 60×/1.42 oil objective (Olympus) and a CoolSNAP HQ2 CCD camera (Photometrics) at 0.2 μm intervals using the Softworx software package (Applied Precision). Alternatively, image stacks were collected using a Zeiss LSM 510 confocal microscope equipped with a Plan-Apochromat 100×/1.40 oil objective at 0.2-0.5 μm intervals using the Zeiss image acquisition software. Optical slices along the Z-axis and maximum intensity Z-projections were generated using the Zeiss LSM Image Browser program or ImageJ 1.45s (NIH). Individual images were cropped and levels adjusted using Adobe Photoshop (Adobe Systems).

2.6 Scanning electron microscopy

For SEM, temporal bones were dissected from embryos of the indicated age and fixed at 4°C in 0.1 M sodium cacodylate buffer containing 4% PFA, 2.5% glutaraldehyde and 2 mM CaCl_2 . Cochleae were then dissected from temporal bones in cacodylate buffer and postfixed for 2 hours in 1% osmium tetroxide. After three 30 minute washes, cochleae were dehydrated in a series of graded ethanol washes (25%, 50%, 80%, 90%, 100%), critical point dried, mounted on metal stubs, and sputter coated with gold. Samples were imaged on a JEOL 6400 scanning electron microscope (SEM) at 20 kV.

2.7 Organotypic cochlear explant cultures

Explant cultures of cochleae were established at the indicated ages. Cochleae were dissected from temporal bones in sterile HBSS containing 10 mM HEPES (pH 7.5). After dissection, cochleae were transferred to glass slides coated with Cell-Tak (BD Biosciences) and flat mounted. Culture media consisted of DMEM/F12 (1:1) supplemented with N2 (1:100; Invitrogen) and penicillin, and cultures were maintained in 5% CO₂ at 37°C. Cultures were maintained for the indicated number of days, fixed for 30 minutes in 4% PFA, and then processed for immunohistochemistry. For FM1-43 uptake assays, explants were treated with 5 µM FM1-43 (Invitrogen) for 10 seconds and then washed three times with fresh culture media and imaged immediately. For PAK inhibition experiments, explant cultures from *GFP-centrin2* mice were established on E16.5, treated with 10 µM IPA-3 (Calbiochem) or vehicle (DMSO) the following day, and processed for immunohistochemistry after 3 days in vitro. For Rac1 inhibition experiments, explant cultures from *GFP-centrin2* mice were established on E16.5, treated with 100 µM NSC 23766 (Calbiochem) after 3 hours in vitro, and processed for immunohistochemistry after 2 days in vitro.

2.8 Quantification of hair cell phenotype

Care was taken to ensure that an equivalent mid-basal region of the cochlea was compared between experimental groups. The data presented for hair bundle and centriole measurements include only those of outer hair cells (OHCs), because the tilt of the tissue surrounding and including the inner hair cells (IHCs) precluded an accurate measurement of their centriole position.

Cochlear length was determined from whole-mount images using ImageJ software (NIH). For all experiments, measurements were obtained from hair cells in the basal region of the cochlea (25% cochlear length; at least 3 cochleae per genotype).

2.8.1 Hair bundle orientation: For quantification of hair bundle orientation, the angle formed by the intersection of a line drawn through the axis of symmetry of the hair bundle and one parallel to the mediolateral axis of the OC (assigned as 0°) was measured using ImageJ. Clockwise deviations from 0° were assigned positive values and counterclockwise negative values. The orientation of flat hair bundles in *Kif3a*^{CKO} hair cells was apparent owing to the asymmetric distribution of short microvilli on their apical surface. Mutant cells with dysmorphic bundles lacking a discernible orientation were not included in the analysis.

2.8.2 Centriole/centrosome position: To generate rose diagrams of the planar position of hair cell centrioles, projected z-stacks were used to assign centriole positions to one of six 60° sectors within the hair cell. Rose diagrams were plotted using the CircStats library in the R software package (<http://www.r-project.org/>).

To quantify the deviation of basal body position from the mediolateral axis, the intersection of a line drawn from the hair cell center through the basal body and one parallel to the mediolateral axis of the OC (assigned as 0°) was measured in ImageJ. Clockwise deviations from 0° were assigned positive values and counterclockwise negative values. Microsoft Excel was used to calculate Pearson's correlation coefficient and generate scatter plots.

To quantify hair cell centriole pair distance, the three-dimensional coordinates of each centriole were recorded using the point plotting function in Softworx and the Euclidean distance calculated. Typically, GFP fluorescence from a single centriole was visible in multiple z-planes. The coordinate of the plane with the brightest GFP fluorescence was used for distance measurement. Box plots of hair cell measurements were generated using Sigmaplot 11 (Systat Software). The boundary of the box closest to zero indicates the 25th percentile, a line within the box marks the median, and the boundary of the box farthest from zero indicates the 75th percentile. Whiskers (error bars) above and below the box indicate the 90th and 10th percentiles, respectively. Experimental data sets were tested for significance using a Student's t-test in the R software package or Microsoft Excel, and data are presented in the form of mean \pm standard error of the mean (s.e.m.).

To quantify basal body migration, a line was drawn from the center of the hair cell through the basal body to the cell membrane. The distance between the basal body and cell membrane along this line was measured with ImageJ. Hair cells and support cells were readily distinguished by their morphology and position in the epithelium.

To quantify the distance of the centrosome from the cell membrane, a line was drawn from the center of the centrosome (visualized by α -tubulin immunostaining) to the closest edge of the cell. The distance along this line between the centrosome and the edge of the cell was measured using ImageJ.

2.9 Western blot

For each sample, two cochleae were dissected from the temporal bone, immediately lysed in 1% TritonX-100 lysis buffer (0.14M NaCl, 20 mM HEPES (pH 7.4), 25 mM NaF, 1 mM Na₃VO₄, 5 mM Na₄P₂O₇, 4 mM EDTA) with 1X Protease inhibitor cocktail (Roche) and diluted with 4X SDS sample buffer. Samples were boiled at 95°C for 5 minutes and run on 12.5% acrylamide gels. Transfer was carried out on nitrocellulose membranes at 300mA. Membranes were blocked in 5% milk/PBST for 1 hour at room temperature and then incubated with primary antibodies diluted in PBST containing 3% BSA and 0.02% NaN₃ overnight at 4°C. Primary antibodies were: rabbit anti-PAK1 (1:1000; Cell Signaling #2602), rabbit anti-phospho-PAK1/2/3 (1:2500, Invitrogen #44940G, lot #980627A), mouse anti-GAPDH (1:10,000; Invitrogen #AM4300). Membranes were then incubated with IRDye-labeled secondary antibodies (1:15,000; LI-COR, Inc.) in PBST with 2% fish gelatin for 1 hour at room temperature, washed 3 times in PBST, and scanned using the Odyssey Infrared Imaging System (LI-COR, Inc.). Absolute band intensities were quantified using Image Studio (LI-COR, Inc.). The relative levels of PAK1 and phospho-PAK were normalized to their respective GAPDH loading controls, and the ratio of pPAK to PAK in each sample was calculated. Data from control (n=9) and Lis1cKO-early (n=5) samples were tested for significance using a two-tailed Student's t-test, and data are presented as mean \pm standard error of the mean (s.e.m.).

Table 1. Genotyping Primers

<u>Strain</u>	<u>Sequence (5' to 3')</u>
<i>Cre</i>	AGAACCTGAAGATGTTTCGCG
	GGCTATACGTAACAGGGTGT
<i>Kif3a^{flox}/Kif3a⁺</i>	AGGGCAGACGGAAGGGTGG
	TCTGTGAGTTTGTGACCAGCC
<i>Lis1^{flox}/Lis1⁻/Lis1⁺</i>	TGAATGCATCAGAACCATGC
	CCTCTACCACTAAAGCTTGTTT
	ATCTCCGATGTTTGAGTATG
<i>GFP-centrin2</i>	ACGACTTCTTCAAGTCCGCCATGCC
	GATCTTGAAGTTCACCTTGATGCC

Table 2. Primary antibodies used for immunohistochemistry

<u>Antigen</u>	<u>Host</u>	<u>Dilution</u>	<u>Source / Catalog #</u>
acetylated-tubulin	mouse mAb	1:500	Sigma T6793
α -tubulin	mouse mAb	1:1000	Sigma T6074
β 1/ β 2 tubulin	mouse mAb	1:200	Sigma T8535
cleaved caspase-3	rabbit	1:200	Cell Signaling 9661
Dvl2 ¹	rabbit mAb	1:100	Cell Signaling 3224
dynein intermediate chain (74.1) ¹	mouse mAb	1:100	Kevin Pfister UVA
E-cadherin	rat	1:200	Sigma U3254
Fz3	rabbit	1:200	Jeremy Nathans JHU
GM130	mouse	1:250	BD Biosciences 610822
Lis1	goat	1:50	Santa Cruz sc-7577
Lis1	rabbit	1:250	Abcam ab2607
mitochondria ¹	mouse mAb	1:50	Abcam ab3298
myosin VI	rabbit	1:1000	Proteus Biosciences 25-6791
myosin VIIa	rabbit	1:1000	Proteus Biosciences 25-6790
nectin 1	mouse mAb	1:100	MBL D146-3
nectin 2	rabbit mAb	1:200	Epitomics 6580-1
nectin 3	mouse mAb	1:100	MBL D084-3
p27 ^{kip1}	mouse mAb	1:200	Thermo Scientific MS-256
PCM-1 ¹	rabbit	1:400	Andreas Merdes Université de Toulouse
phospho- β -catenin (ser33/37/Thr41)	rabbit	1:100	Cell Signaling 9561
phospho-ERM ¹	rabbit	1:1000	Cell Signaling

			3141
phospho-PAK1/2/3	rabbit	1:200	Invitrogen 44-940G
Rac1 ¹	mouse	1:100	Millipore 05-389
Rac1-GTP ¹	mouse IgM	1:500	NewEast Biosciences 26903
α -spectrin	mouse mAb	1:100	Millipore MAB1622
Tiam1	rabbit	1:100	Santa Cruz Biotechnology sc-872
ZO-1	mouse mAb	1:300	Invitrogen 33-9100

¹ Antibodies used with 10% trichloroacetic acid (TCA) fixation protocol

Chapter 3

**Kif3a regulates planar polarization through both ciliary
and non-ciliary mechanisms**

3.1 Introduction

Sensory hair cells in the hearing organ, the cochlea, convert sound energy into electrical signals, which are in turn transmitted to the central nervous system. The mechanotransduction organelle of the hair cell is the hair bundle, consisting of rows of actin-based stereocilia with graded heights that form a V-shaped staircase pattern. The asymmetric structure of the hair bundle renders it directionally sensitive to deflection. Hair cells are depolarized by deflections toward the tallest stereocilia, hyperpolarized by deflections toward the shortest stereocilia, and insensitive to perpendicular stimuli [36].

Because of their directional sensitivity, hair bundles in the cochlea must be uniformly oriented for correct perception of sound. In the auditory sensory epithelium, the organ of Corti, the vertex of the V-shaped hair bundle on every hair cell points toward the lateral edge of the cochlear duct. The uniform hair bundle orientation is controlled by the PCP/tissue polarity pathway, which regulates cytoskeletal remodeling during tissue morphogenesis in many systems [131]. In addition, the PCP pathway is also required for extension of the cochlear duct [28]. In PCP mutants, hair bundles are frequently misoriented relative to the medial-lateral axis of the cochlea. However, the structural polarity of individual V-shaped hair bundles is not affected. Thus, planar polarization of auditory hair cells is manifested at both cell and tissue levels, which are genetically separable. Planar polarization at the single cell level is independent of the PCP/tissue polarity pathway. The molecular machinery that controls polarization of individual hair cells is poorly understood.

The kinocilium, a specialized primary cilium, is thought to serve as the 'guidepost' for hair bundle morphogenesis [55]. The axoneme of the kinocilium extends from the basal body, which is derived from the mother centriole of the centrosome [51, 216]. In addition to organizing the cilia, the basal body, along with the associated pericentriolar material (PCM), also organizes cytoplasmic microtubules and anchor their minus-end [217]. During development of mammalian auditory hair cells, before the onset of bundle morphogenesis, the kinocilium migrates from the center of the hair cell apex to the lateral edge of the hair cell apex. The surrounding microvilli then undergo selective elongation to form a V-shaped hair bundle, with the kinocilium at the vertex of the V next to the tallest stereocilia. Thus, migration of the kinocilium/basal body appears to be the critical polarizing event that orchestrates hair bundle morphogenesis and orientation.

Indeed, there is a growing body of evidence for a role of the kinocilium/basal body in hair bundle morphogenesis and orientation. It has been proposed that the PCP/tissue polarity pathway coordinates hair bundle orientation by controlling the direction of the kinocilium/basal body migration [58]. Mutations in BBS genes that underlie the Bardet-Biedl syndrome, a human ciliopathy, cause defects in hair bundle morphology and inner ear PCP in mice [145, 149]. Mouse models for human Usher syndrome type I have defects in kinocilium positioning and hair bundle fragmentation and misorientation [218]. In particular, an isoform-specific knockout of *protocadherin 15* (*PCDH15-ΔCD2*) caused disruption of the kinociliary links that connect the kinocilium to the

adjacent stereocilia, leading to hair bundle orientation and polarity defects [62]. Moreover, the Alström Syndrome protein ALMS1 has been shown to localize to basal bodies of cochlear hair cells and regulate hair bundle shape and orientation [151]. Finally, a role for the kinocilium in hair cell PCP regulation has been demonstrated by genetic ablation of the kinocilium [61]. Cilia assembly and maintenance require the intraflagellar transport (IFT) process, in which particles are transported bidirectionally along axonemal microtubules [51, 216]. Deletion of *Ift88*, which encodes one component of IFT particles, in the inner ear resulted in the absence of kinocilia and basal body migration defects, causing PCP phenotypes including a shortened cochlear duct and hair bundle misorientation [61].

In spite of the evidence pointing to a pivotal role for the kinocilium/basal body in planar polarization of hair cells, the cellular and molecular mechanisms by which basal body migration instructs hair cell polarity remain unresolved. Because the basal body is the microtubule organizing center of the hair cell, we speculated that microtubule-dependent processes control hair cell polarization. To gain mechanistic insights into microtubule-mediated processes, we investigated the role of Kif3a, a component of the microtubule plus-end directed, heterotrimeric kinesin-II motor complex. Kinesin-II is the motor for anterograde IFT required for ciliogenesis [216]. Kif3a-deficient mice lack nodal cilia, have left-right asymmetry defects and die around embryonic day 10.5 [219, 220]. In addition to ciliogenesis, the kinesin-II motor is also required for intracellular transport of various cargos in different cell types [219, 221, 222]. In this study we

uncover a non-ciliary function of Kif3a critical for basal body positioning during hair cell polarization. We show that Kif3a mediates localized p21-activated kinase (PAK) activation on the hair cell cortex, which in turn regulates basal body positioning. Together with published results, we describe a model in which Kif3a is a component of the cell-intrinsic polarity machinery.

3.2 Results

3.2.1 Kif3a deletion causes PCP-like phenotypes in the organ of Corti

To investigate the function of *Kif3a* in inner ear development, we generated *Kif3a* conditional mutants using a floxed allele of *Kif3a* [219] and a *Foxg1^{Cre}* allele that drives Cre expression in the otic epithelium, including precursor cells of the OC [223]. As the conditional *Kif3a* mutants (referred to as *Kif3a^{ckO}*) die shortly after birth, we first examined cochlear development *in vivo* at late embryonic stages.

Consistent with an essential role for Kif3a in ciliogenesis, primary cilia were absent from all cochlear epithelial cells as early as E14.5 in *Kif3a^{ckO}* mutants (**Fig. 2B**). The length of the *Kif3a^{ckO}* cochlea was much shorter than wild-type (**Fig. 2C,D**). At E18.5, wild-type cochleae had a length of 5225 $\mu\text{m} \pm 149$ (n=3). By contrast, *Kif3a^{ckO}* cochleae were 2503 $\mu\text{m} \pm 104$ (n=6) in length. Toward the apex of the *Kif3a^{ckO}* cochlea, many supernumerary rows of hair cells were observed (bracket, **Fig. 2F**). These defects are reminiscent of PCP/tissue polarity mutant phenotypes and suggest that Kif3a regulates the convergent extension-like movements thought to underlie cochlear extension [28, 224].

We next examined hair bundle orientation, another event regulated by the PCP/tissue polarity pathway. In the basal and middle turns of the *Kif3a^{CKO}* OC, where patterning of hair cells and support cells appeared normal, hair bundle orientation defects were mild (**Fig. 2H,K**). Of note, compared to the normal V-shaped hair bundles (**Fig. 2G**), *Kif3a^{CKO}* hair bundles appeared to have a flattened morphology (**Fig. 2H**). Toward the apex of the *Kif3a^{CKO}* OC, where the hair cell rows were very disorganized, hair cells with misoriented hair bundles were more prevalent (**Fig. 2J,K**). We also examined the *Kif3a^{CKO}* utricular macula and observed no overt defect in PCP of utricular hair cells (**Fig. 3**). Taken together, these results suggest that Kif3a regulates aspects of planar polarity in the OC.

To further assess if PCP/tissue polarity signaling was affected in *Kif3a^{CKO}* OC, we asked if Kif3a regulates the asymmetric localization of the core PCP proteins Dishevelled-2 (Dvl2) and Frizzled3 (Fz3). In E17.5 wild-type OC, Dvl2-EGFP is localized to the lateral side of hair cell membranes [27], whereas Frizzled3 is enriched on the medial side of plasma membrane in hair cells and support cells [82]. Using immunostaining, we found that in the wild-type, Dvl2 is asymmetrically localized in hair cells and support cells and appeared enriched on the lateral side of hair cell membranes (**Fig. 4A,C,E,G**). In the basal region of the *Kif3a^{CKO}* OC, Dvl2 localization was largely normal (**Fig. 4B,D**), as was the asymmetric localization of Frizzled3 (**Fig. 5B,D**). Towards the apex of the *Kif3a^{CKO}* OC, where hair cells and support cells form disorganized rows, asymmetric membrane localization of Dvl2 (**Fig. 4F,H**) and Frizzled3 (**Fig. 5F,H**)

was also apparent, albeit somewhat disorganized. Of note, the pattern of Deiters cells was disturbed in *Kif3a*^{CKO} mutants, particularly towards the apex. In the wild type, the apical extension of a single Deiters cell can be found in between neighboring hair cells. In *Kif3a*^{CKO} mutants, however, the number and position of Deiters cell extensions in contact with hair cells were abnormal (**Fig. 4B,F**). Together, these results suggest that PCP/tissue polarity signaling is still active in the *Kif3a*^{CKO} OC, and that Kif3a may regulate support cell movements during cochlear extension.

3.2.2 Kif3a is required for the V-shape of the nascent hair bundle

Confirming the light microscopy results (**Fig. 2H**), SEM analysis showed that *Kif3a*^{CKO} hair cells displayed abnormal hair bundle morphology. At E18.5, in contrast to the normal V shape (**Fig. 6A**), stereocilia in *Kif3a*^{CKO} hair cells were arranged in straight rows (**Fig. 6B-D**), indicating that Kif3a is required for the normal V-shape of the nascent hair bundle. Notably, in control hair bundles, the heights of individual stereocilia decrease in relation to their distance from the vertex of the bundle. In contrast, stereocilia in *Kif3a*^{CKO} hair bundles lack this taper and appear to maintain a uniform height across the entirety of the bundle.

To evaluate functional maturation of auditory hair bundles that normally takes place in the early postnatal period [225], we examined hair bundle morphology and FM1-43 dye uptake in explant cultures derived from *Kif3a*^{CKO} cochleae. FM1-43 is a fluorescent styryl dye that can be taken up by hair cells through their mechanotransduction channels upon brief exposure [226–228]. We

found that many *Kif3a*^{CKO} hair bundles became fragmented (**Fig. 6G-H,J**), suggesting that Kif3a is required for hair bundle cohesion. Despite hair bundle deformation, the stereocilia still formed a staircase with graded heights (**Fig. 6F-H**), and FM1-43 uptake was normal in *Kif3a*^{CKO} explants (**Fig. 6L**), suggesting that *Kif3a* is dispensable for staircase formation and acquisition of the mechanotransduction apparatus. Of note, many flattened *Kif3a*^{CKO} hair bundles adopted a C-shape over time in explant cultures (**Fig. 6F,J**), probably as a result of remodeling of the cortical actomyosin network in OHCs during the early postnatal period [229].

3.2.3 Kif3a is required for coupling of hair bundle orientation to basal body position

To investigate how Kif3a functions to shape the nascent hair bundle, we examined basal body migration, a key event during hair cell polarization, in *Kif3a*^{CKO} hair cells. To identify the centrioles, we used a *GFP-centrin2* transgenic mouse line, which ubiquitously expresses GFP-tagged centrin2, a centrosomal protein [230]. In the OC, the expression pattern of GFP-centrin2 was identical to that of the centrosomal proteins γ -tubulin and pericentrin (**Fig. 7A** and data not shown), indicating that it faithfully marks the centrioles. To distinguish between the basal body and the daughter centriole, we used an antibody against phospho- β -catenin, which labels the basal body as well as the tips of the stereocilia (**Fig. 7A** and data not shown). In E18.5 wild-type OC, hair cell centrioles were invariably found near the lateral edge of the hair cell, and they

displayed remarkable planar polarity: they were aligned along the medial-lateral axis, with the basal body always positioned medial to the daughter centriole (arrows, **Fig. 7A,C,E**). Notably, centrioles in the surrounding support cells lacked apparent planar polarity (arrowheads, **Fig. 7A,C,E**). In E18.5 *Kif3a*^{CKO} hair cells, centrioles have migrated to the edge of hair cells, however their position along the medial-lateral planar polarity axis was severely disrupted (**Fig. 7B,D,F**). While most of the centrioles were located in the lateral-most sector in wild-type hair cells, centrioles in *Kif3a*^{CKO} mutants were found at positions all around the edge of the hair cell (**Fig. 7G**), even near the medial edge (arrowheads, **Fig. 7B,D,F**).

The severe defect in planar position of basal bodies stood in contrast with the mild hair bundle orientation defects in *Kif3a*^{CKO} hair cells. This prompted us to examine if the coupling between hair bundle orientation and basal body position was affected. In the wild-type, there was a tight correlation between bundle orientation and basal body position (**Fig. 7H,I**; Pearson's coefficient, $r = 0.9$), indicating that hair bundle orientation is coupled to basal body position. This coupling was intact in the PCP mutants examined, including PTK7 [98] (**Fig. 7H**) and *Vangl2*^{Lp/Lp}, which is mutant for the core PCP gene Van gogh-like 2 (**Fig. 7I**; $r = 0.96$). In *Kif3a*^{CKO} hair cells, on the other hand, this correlation was lost (**Fig. 7H,I**; $r = 0.6$). Hair cells with a mispositioned basal body can have normal hair bundle orientation (arrowheads, **Fig. 7B,D,F**). Conversely, the occasional hair cells with misoriented bundles can have a normally positioned basal body (arrows, **Fig. 7B,D,F**). These observations demonstrate that in the *Kif3a*^{CKO} mutant, hair bundle orientation is uncoupled from basal body position, and that

hair bundle orientation can proceed normally when uncoupled from basal body position.

3.2.4 Kif3a is required for apical-basal positioning of the basal body in hair cells

To further investigate the cause for the uncoupling of hair bundle orientation from basal body position in *Kif3a*^{ckO} mutants, we closely followed the positions of hair cell centrioles over the course of hair bundle development. At E16.5, basal body migration toward the hair cell periphery had occurred in both control and *Kif3a*^{ckO} mutants (**Fig. 8A,B**). The distance from the basal body to the cell membrane was $1.35 \mu\text{m} \pm 0.11$ in control versus $1.21 \mu\text{m} \pm 0.09$ in *Kif3a*^{ckO} hair cells ($p=0.34$), confirming that Kif3a is not required for basal body migration. We also examined the localization of IFT88, a protein that is normally localized to the basal body and kinocilium and partially required for basal body migration [61]. We found that IFT88 was still recruited to the basal bodies in the *Kif3a*^{ckO} mutants (arrows, **Fig. 9B,D**). However, there was a striking difference in basal body position along the apical-basal axis between control and *Kif3a*^{ckO} hair cells. The basal body in wild-type hair cells was positioned just underneath the apical surface, and the daughter centriole was positioned more basally (**Fig. 8C**). By contrast, in *Kif3a*^{ckO} hair cells, the basal body appeared to have descended to the same level as the daughter centriole (**Fig. 8D**). The aberrant positioning of the basal body persisted through later developmental stages (E17.5 and E18.5) in *Kif3a*^{ckO} hair cells (**Fig. 8F,K**). By contrast, basal body positioning in *Kif3a*^{ckO}

support cells (pillar and Deiters cells) was not affected compared to controls (data not shown). These results indicate that Kif3a regulates basal body positioning along the apical-basal axis of hair cells.

The apical-basal positioning defect of the basal body in *Kif3a^{CKO}* hair cells may reflect a requirement of Kif3a in apical docking of the basal body at the onset of ciliogenesis. We therefore examined basal body positioning at E15.5, before basal body migration. We found that the apical-basal position of the basal body was normal in *Kif3a^{CKO}* hair cells compared to controls (**Fig. 8G-K**).

Therefore we conclude that Kif3a is not required for the initial apical docking of the basal body. Taken together, our results reveal that Kif3a controls an active developmental process that positions the basal body along both the apical-basal and planar polarity axes during hair cell polarization and raise the possibility that uncoupling of hair bundle orientation from basal body position may be related to the aberrant basal body position in *Kif3a^{CKO}* mutants.

3.2.5 Kif3a regulates cortical PAK activity during hair cell polarization

To investigate the mechanisms by which Kif3a regulates basal body positioning in hair cells, we hypothesized that Kif3a is involved in generating or transducing a hair cell-intrinsic polarity cue to position the basal body near the lateral membrane. Previously, we discovered that activated p21-activated kinases (PAK), cytoskeletal regulators downstream of the small GTPases Rac and Cdc42 [231], are asymmetrically distributed in developing auditory hair cells as detected by an antibody specific for phosphorylated PAK (pPAK) [30]. Both

the developmental onset of PAK activation and its subcellular localization coincide with migration of the basal body to the lateral edge of hair cells, making PAK an attractive candidate component of the hair cell polarity machinery. During normal development, cortical localization of pPAK was first detected in hair cells between E16.5 and E17.5 at the base of the cochlea, where the basal body has migrated to the periphery [30]. By E17.5, pronounced pPAK staining correlated with the locations of hair cell centrioles (**Fig. 10A,B,E**). Just beneath the apical cell surface, pPAK was localized in a triangle-shaped ring around the basal body and the stereocilia insertion sites. We found that the basal body was stereotypically positioned at the lateral tip of the ring (**Fig. 10A,G**). Around 1 μm basal to the ring, pPAK was asymmetrically localized to the lateral side of the hair cell membrane, immediately adjacent to the location of the daughter centriole (**Fig. 10B,G'**).

In the *Kif3a*^{CKO} mutant, pPAK staining was present but disorganized at both subcellular locations (**Fig. 10C,D,F**). At the base of the hair bundle, pPAK staining lost its triangular pattern and instead conformed to the shape of the flat bundle (**Fig. 10C,H-J**). Strikingly, basal bodies were no longer positioned within the ring of pPAK staining around the base of the hair bundle. Instead, both centrioles were located approximately 1 μm below the base of the hair bundle, closely juxtaposed to the plasma membrane (arrows, **Fig. 10D, H'-J'**). At this level, instead of the normal horseshoe-shaped pattern on the lateral membrane, pPAK was localized around the entire perimeter of the plasma membrane, albeit still relatively enriched on the lateral side (**Fig. 10D,H'-J'**). These results suggest

that Kif3a regulates localized PAK activation at the hair cell cortex adjacent to the centrioles, and show an intriguing correlation between mislocalized PAK activity and basal body positioning defects in *Kif3a*^{CKO} hair cells.

3.2.6 Rac-PAK signaling regulates basal body positioning and hair bundle morphogenesis

If PAK activity was indeed a polarity cue that mediates basal body positioning downstream of Kif3a, then PAK signaling should be required for correct basal body positioning in hair cells. To test this hypothesis, we applied IPA-3, a small-molecule inhibitor of PAK [232], to cochlear explants and assessed the effect on basal body positioning and hair bundle morphogenesis. We found that IPA-3 treatment resulted in basal body positioning defects, as well as bundle morphology and orientation defects (**Fig. 11B,C**). Because PAK kinases are downstream effectors of the small GTPases Rac and Cdc42, we also tested if Rac activity is required for basal body positioning by treating cochlear explants with NSC 23766, a small molecule inhibitor of Rac [233]. We found that Rac inhibition also resulted in basal body positioning and bundle morphogenesis defects (**Fig. 11E,F**). Inhibitor treatment had no effect on ciliogenesis, suggesting that the basal body positioning defect is due directly to impaired Rac-PAK signaling rather than the absence of the kinocilium (**Fig. 12**). Taken together, these results support the hypothesis that Rac-PAK signaling acts downstream of Kif3a to regulate basal body positioning during hair cell polarization.

3.2.7 Kif3a associates with the Rac GEF Tiam1

Rac GTPases are activated to the GTP-bound state by GEFs, and inactivated by GTPase-activating proteins (GAPs). We therefore considered Rac GEFs as potential kinesin-II cargos in hair cells and focused on those with reported expression in the nervous system. T-cell lymphoma invasion and metastasis 1 (Tiam1) emerged as the leading candidate. Tiam1 associates with microtubules in neurons, and, like Kif3a [221, 234], Tiam1 is implicated in regulation of neuronal polarity [235]. We first examined Tiam1 localization during hair cell polarization, and found that Tiam1 is highly expressed in hair cells and is localized to the kinocilium and cytoplasmic microtubules (**Fig. 13A-C**). Interestingly, microtubule localization of Tiam1 was unaffected in *Kif3a^{CKO}* hair cells (data not shown), suggesting microtubule association of Tiam1 is independent of the kinesin-II motor.

We next asked if Tiam1 forms a complex with Kif3a *in vivo*. Because the small number of hair cells present in the mouse cochlea precludes biochemical analysis, we turned to embryonic brains as a source of tissue, where both Kif3a and Tiam1 are expressed. Endogenous Tiam1 was immunoprecipitated from brain lysates. Kif3a was present in the Tiam1 immunoprecipitates, but was undetectable in immunoprecipitates using normal IgG or antibodies against β -PIX, a Rac/Cdc42 GEF highly expressed in the brain [236] (**Fig. 13D**). To further determine the specificity of the Kif3a-Tiam1 interaction, we took advantage of the fact that Kif3a was also deleted in the neocortex of *Kif3a^{CKO}* mutants (**Fig. 13E**) and performed immunoprecipitation using *Kif3a^{CKO}* cortices. Kif3a was detected

in the Tiam1 immunoprecipitates from control cortices but not *Kif3a^{ckO}* cortices (**Fig. 13E**). Together, these data demonstrate that Kif3a specifically interacts with Tiam1 *in vivo* and support a model in which Kif3a mediates localized Rac activation at the cell cortex by delivering the Rac GEF Tiam1.

3.2.8 Additional experiments

3.2.8.1 Effects of reduced Rac1 dosage

Our results suggest that a tightly regulated domain of PAK signaling acts as a polarity cue for basal body positioning downstream of Kif3a. In *Kif3a^{ckO}* hair cells, Rac-PAK signaling is misregulated, allowing PAK to become activated around the entire cell cortex (**Fig. 10D**). We reasoned that a global reduction in the levels of Rac1 signaling might limit unconstrained PAK activity at the cell cortex and rescue the phenotypes we observed in *Kif3a^{ckO}* hair cells. To investigate this idea, we reduced the dosage of Rac1 in *Kif3a^{ckO}* OC by introducing a conditional knockout allele of Rac1 (*Rac1^{ckO}*) [30] and examined cochlear extension, hair bundle orientation, and centriole positioning in these cochleae.

Cochlear extension:

At E18.5, temporal bones from *Kif3a^{ckO}; Rac1^{ckO}* embryos were reduced in size, resembling those of *Rac1^{ckO}* single mutants (**Fig. 14A**) [30]. The length of the *Kif3a^{ckO}; Rac1^{ckO}* cochlea was considerably shorter than that of control cochleae (**Fig. 14B**). While a small sample size prevented a quantitative analysis of cochlear length, *Kif3a^{ckO}; Rac1^{ckO}* cochleae appeared to be shorter than either

Kif3a^{ckO} (**Fig. 2D**) or *Rac1*^{ckO} [30] single mutant cochleae, indicating a possible genetic interaction between *Kif3a* and *Rac1* during cochlear extension.

Hair bundle orientation:

Hair bundle morphology in *Kif3a*^{ckO}; *Rac1*^{ckO} was highly disrupted and resembled that of *Rac1*^{ckO} mutants, with most hair bundles exhibiting flattened, split, or generally dysmorphic morphologies (**Fig. 14D,F**). Moreover, roughly the same degree of hair bundle misorientation was observed as in *Rac1*^{ckO} mutants.

Interestingly, the disruptions to the mosaic pattern of hair and supporting cells observed in single *Rac1*^{ckO} mutants were largely absent in *Kif3a*^{ckO}; *Rac1*^{ckO} OC. Consistent with what is observed in *Kif3a*^{ckO} single mutants, apical regions of the cochlea had supernumerary rows of hair cells (**Fig. 14F**).

Planar position of centrioles:

We also examined the planar and apical-basal position of centrioles in E18.5 *Kif3a*^{ckO}; *Rac1*^{ckO} mutants. In comparison to control hair cells where centrioles were found exclusively on the medial side of the cell, *Kif3a*^{ckO}; *Rac1*^{ckO} centrioles were observed in all sectors of the cell (**Fig. 14G**). Centriole distribution was roughly similar to that observed in *Kif3a*^{ckO} single mutants, though a higher percentage of centrioles were found on the side of the cell nearest the apex of the cochlea (**Fig. 14G**, sectors 4 and 5).

Apical-basal centriole positioning:

Apical-basal distance between the basal body and daughter centriole in *Kif3a*^{ckO}; *Rac1*^{ckO} hair cells was significantly shorter than that of control cells (**Fig. 14H**). However, reduced *Rac1* dosage significantly increased this distance compared

to *Kif3a*^{CKO} hair cells, indicating a partial rescue of apical-basal centriole positioning defects. These results lend support to the hypothesis that Kif3a is involved in regulating Rac signaling at the cell cortex to position hair cell centrioles appropriately along the apical-basal axis.

3.2.8.2 The role of β -catenin

Recent evidence indicates that disruption of the primary cilium stabilizes β -catenin and leads to an overactivation of the Wnt transcriptional program *in vitro* [152]. Moreover, Rac signaling is involved in regulating nuclear localization of β -catenin during canonical Wnt signaling [237]. Given the localization of phospho- β -catenin to the hair cell basal body (**Fig. 7**) and the importance of β -catenin regulation in other planar polarization processes [148], we investigated whether misregulation of β -catenin could be contributing to the observed defects in *Kif3a*^{CKO} hair cells.

We specifically expressed the *Catnb*^{ex3} allele, which encodes a dominant stable mutant of β -catenin that lacks the phosphorylation residues in exon 3 necessary for normal degradation [238], in developing hair cells using *Atoh1-Cre*. At E18.5, *Atoh1-Cre; Catnb*^{ex3/+} hair cells did not exhibit any obvious OC patterning or hair bundle morphology defects when compared to controls (**Fig. 15B**). To enforce β -catenin stability in a larger set of cells with greater temporal control, we also used a ubiquitously-expressed tamoxifen-inducible Cre allele, *CAGGSCre-ER* [239]. The cochleae of embryos collected from a pregnant female injected with tamoxifen at E14.5 were examined. At E18.5, *CAGGSCre-*

ER; *Catnb*^{ex3/+} OC displayed gross defects in cell patterning that appeared to arise from pockets of overproliferating supporting cells (**Fig. 15C,D**). While hair bundle morphology was largely normal, some cells with abnormal hair bundles were observed around the pockets of supporting cells. These results are consistent with a subsequently published study reporting that misregulation of β -catenin in the cochlea using *Catnb*^{ex3} initiates proliferation in sensory precursor cells in the postnatal OC [240].

We reasoned that if *Kif3a*^{cKO} cells suffered from an overabundance of stabilized β -catenin, reducing β -catenin dosage might ameliorate *Kif3a*^{cKO} hair cell defects. To investigate this, we introduced one copy of a β -catenin knockout allele (*Catnb*^{KO}) into the *Kif3a*^{cKO} line. At E18.5, *Catnb*^{KO/+} OC were completely normal, and we could detect no patterning or hair bundle defects (**Fig. 15E**). However, *Kif3a*^{cKO}; *Catnb*^{KO/+} OC continued to exhibit flattened hair bundle defects (**Fig. 15G**) and supernumerary apical hair cell rows and were indistinguishable from *Kif3a*^{cKO} OC. We also examined canonical Wnt signaling using a transgenic reporter line, BATgal, which expresses LacZ under the control of Tcf/Lef binding sites [225] and did not observe any overt changes in the level of Wnt/ β -catenin signaling in *Kif3a*^{cKO} cochleae by X-gal staining (**Fig. 16**). Taken together, these results suggest that disruption of Kif3a function likely does not lead to misregulation of β -catenin in developing hair cells.

3.2.8.3 Axin

Axin is a multifunctional protein involved in several important regulatory pathways, most notably β -catenin-mediated canonical Wnt signaling. In Wnt signaling, axin provides a platform for the assembly of the β -catenin degradation complex, consisting of APC, casein kinase 1 (CK1) and glycogen synthase kinase 3 (GSK3), to negatively regulate the activity of β -catenin [241].

To investigate further if misregulation of β -catenin contributes to the *Kif3a*^{CKO} phenotype, we examined OC from mice harboring a naturally-occurring transposon insertion into the axin locus (*axin*^{fu}). *Axin*^{fu/fu} mice display widely varied phenotypes ranging from embryonic lethality to relatively normal adults with kinked tails [242]. Interestingly, it has been reported that some *axin*^{fu/fu} mice are deaf [243]. At E18.5, the gross cochlear morphology of *axin*^{fu/fu} ranged from near normal to some having an extremely dilated cochlear duct (**Fig. 17B**). *Axin*^{fu/fu} OC exhibited minor patterning defects, with occasional extra cells in IHC and OHC rows (**Fig. 17D**), and a subset of *axin*^{fu/fu} hair cells displayed flat or splitting hair bundle morphology defects which persisted into early postnatal stages (**Fig. 17D,E**). Both patterning and hair bundle defects were more severe in cochleae that also had gross morphological defects. Despite occasional abnormalities, the defects we observed in *axin*^{fu/fu} OC were less prevalent and dissimilar to the predominant *Kif3a*^{CKO} flattened bundle phenotype, again suggesting that β -catenin misregulation likely does not contribute to defects in *Kif3a*^{CKO} hair cells.

3.2.8.4 *In vivo* imaging of centriole search behavior

Imaging of fixed samples is limited to the visualization of a single “snapshot” of centriole positioning during planar polarization. In order to more fully characterize centriole behavior during hair cell planar polarization, we imaged live cochlear explants. Explants from E16.5 *GFP-centrin2* embryos were established, allowed to adhere to coverslips overnight, and imaged the following morning. Z-stacks encompassing the apical region of hair cells were collected every hour. We observed fluid centriole movements at E17, with centriole pairs moving toward and away from the cell center over the course of 7 hours (**Fig. 18**). During this time, the alignment of the centrioles in relation to the medial-lateral axis of the OC also changed over time. Moreover, the distance between the basal body and daughter centriole appeared to oscillate, with the maximum distance between them roughly doubling (**Fig. 18A**, arrowheads). The lack of fluorescent landmarks on the cell apex precluded an accurate assessment of changes in the apical-basal position of the centrioles. The centrioles of supporting cells were also observed to change position over the course of an hour (**Fig. 18B**, arrows). We speculate that the observed centriole behaviors constitute a search for the cortical domain established by Rac signaling which ultimately defines the polarized position of the basal body at the lateral pole of the hair cell.

3.3 Discussion

In this study, we identify the kinesin-II subunit Kif3a as a key component of the hair cell-intrinsic polarity machinery that couples hair bundle morphogenesis

and orientation to basal body positioning. In *Kif3a*^{CKO} hair cells, in addition to the absence of the kinocilium, basal body positioning along both epithelial polarity axes was disrupted, hair bundles failed to develop the stereotypical V-shape, and their orientation became uncoupled from basal body position. These phenotypes indicate that, by serving the dual functions of IFT and intracellular transport, *Kif3a* coordinates planar polarization of the hair bundle and the centrioles.

Both *Kif3a*^{CKO} and *Ift88* mutants [61] lack primary cilia and display PCP/tissue polarity defects, including shortened cochlear ducts and hair bundle misorientation, demonstrating a general requirement of the primary cilium/basal body for tissue polarity. Interestingly, while the PCP/tissue polarity pathway acts in both hearing and vestibular organs, neither *Kif3a* nor *Ift88* [61] mutations appear to affect PCP of utricular hair cells. It is conceivable that cell-cell interactions necessary for the propagation of polarity signals are different in hearing and balance organs due to their distinct mosaic patterns of hair cells and support cells. Moreover, distinct expression patterns of cell-adhesion molecules may contribute to differences in cell-adhesion and cytoskeletal organization between hearing and balance organs [244, 245]. Interestingly, there is evidence that an additional, as yet unidentified, patterning event operates together with the tissue polarity pathway to regulate PCP in the utricular macula [139].

The signaling events mediated by the IFT molecules during cochlear extension remain to be elucidated. An intriguing possible role of cilia/IFT is to maintain the balance between Wnt/ β -catenin and Wnt/PCP signaling, however experimental evidence for this idea is controversial [148, 152, 154, 246]. We did

not detect changes in the localization of β -catenin or phospho- β -catenin in *Kif3a*^{CKO} OC, although it is possible that there are quantitative differences not revealed by immunofluorescence. β -catenin was localized to cellular junctions (data not shown), while phospho- β -catenin, destined for proteasome-mediated degradation, was localized to cellular junctions, the basal body and the tips of the stereocilia. Others have reported localization of phospho- β -catenin to the centrosome of cultured cells [152, 247]. The significance of the different localization of β -catenin versus phospho- β -catenin we observed in hair cells is currently unknown.

Furthermore, using a transgenic Wnt-signaling reporter line, BATgal, which expresses *LacZ* under the control of *Tcf/Lef* binding sites [248], we did not observe any overt changes in the level of Wnt/ β -catenin signaling in *Kif3a*^{CKO} cochleae by X-gal staining (**Fig. 16**). *Kif3a* deletion in mouse embryonic fibroblasts causes hyperphosphorylation of Dishevelled proteins [152]. We showed that *Kif3a* is not required for asymmetric localization of Dvl2 in the OC, but it remains possible that *Kif3a* may regulate the activity of Dishevelled proteins in the OC. At present the relative contributions by hair cells and support cells to cochlear extension is not known. In the *Kif3a*^{CKO} OC, we often observed multiple Deiters cells in contact with one hair cell, particularly in the apical region where the hair cell rows were more disorganized. This suggests that Deiters cell movements could be regulated by *Kif3a* and may play a role in cochlear extension.

Our cochlear explant experiments further delineate the role of Kif3a in hair bundle morphogenesis. Kif3a function is important for the V-shape of the nascent hair bundle and for the structural cohesion of the hair bundle during functional maturation. However, Kif3a and the kinocilium are dispensable for selective elongation of the stereocilia (staircase formation) or acquisition of the mechanotransduction apparatus. Consistent with our results, in *PCDH15-ΔCD2* mutant hair cells, where the kinocilium became detached from the hair bundle, staircase formation and mechanotransduction were also unaffected [62].

Although both *Kif3a^{ckO}* and *Ift88* [61] mutants have defects in bundle orientation and planar positioning of the basal body, there are important differences in their phenotypes. By comparing the differences, we can begin to tease apart the ciliary and non-ciliary functions of Kif3a in hair cell development. In contrast to *Ift88* mutants, where a fraction of hair cells form circular hair bundles with a centrally positioned basal body [61], we did not observe any circular hair bundles or centrally positioned basal bodies in *Kif3a^{ckO}* mutants, indicating that Kif3a is not required for basal body migration. Another key difference in the phenotypes lies in the coupling between basal body position and hair bundle orientation. In *Ift88* mutants, hair bundle orientation defects strongly correlated with basal body positioning defects [61]. By contrast, we show that in *Kif3a^{ckO}* hair cells, hair bundle orientation is no longer coupled to basal body position, and basal bodies are mispositioned along both apical-basal and planar polarity axes. These phenotypes are novel and striking in that they are not observed in previously reported PCP or ciliogenesis (*Ift88*) mutants. These

results suggest that coupling of hair bundle orientation and basal body position is, at least in part, mediated by a non-ciliary function of Kif3a. Interestingly, it has been suggested recently that the links between the kinocilium and stereocilia also play a role in coordinating hair bundle orientation and basal body position [62].

We present evidence for a non-ciliary function of Kif3a in regulating cortical PAK activity. PAK activity exhibits several key properties of a polarity cue. First, it is asymmetrically localized in hair cells. Second, PAK activity is required for normal basal body positioning. Third, in *Kif3a*^{cko} hair cells, mislocalized PAK activity correlated with basal body positioning defects, suggesting that the precise spatial pattern of PAK activation may also be important. Together with our previous findings, these results reveal multiple critical functions for PAK signaling in hair bundle morphogenesis. During the early phase of hair bundle formation, cortical PAK activity serves to position the basal body and direct hair bundle orientation. Subsequently, PAK signaling is required for the cohesion of the nascent hair bundles [30].

As a motor molecule, Kif3a may regulate PAK activity through direct or indirect mechanisms. Since our *in vitro* results indicate that both Rac and PAK signaling are required for basal body positioning, we speculate that Kif3a may transport a cargo that regulates activation of Rac GTPases at cortical locations. We have identified the Rac GEF Tiam1 as a candidate cargo of kinesin-II in hair cells. We showed in cochlear explants that pharmacological inhibition of Rac activation by GEFs, including Tiam1 [233], disrupted basal body positioning,

indicating a requirement for Rac activity in this process. Rac inhibition also severely disrupted hair bundle morphogenesis, probably a combined effect of inhibiting Tiam1 and other Rac GEFs in hair cells. The *in vivo* function of Tiam1 in hair cell polarization remains to be determined. Tiam1 knock-out mice are viable and fertile with no reported inner ear phenotypes, suggesting that the closely related paralog TIAM2/STEF may functionally compensate for Tiam1-deficiency [249].

We propose that kinesin-II-mediated delivery of Tiam1 to the cell cortex and subsequent local activation of Rac is a key step in establishing the positive feedback loop between localized PAK activation and basal body positioning in hair cells. In the absence of kinesin-II-mediated transport, Tiam1 may still be able to translocate from microtubules to the cortex and activate Rac, for example, by virtue of microtubule growth (Waterman-Storer et al., 1999). However, the spatial and temporal dynamics of Rac activation are disrupted due to the lack of a positive feedback mechanism, leading to diffused PAK activation on the cortex and “trapping” of the basal body at an aberrantly basal position.

Taken together, our results argue that the hair-cell intrinsic polarity machinery regulated by Kif3a acts in parallel to the PCP/tissue polarity pathway. First, we showed previously that the formation of the asymmetric pPAK domain *per se* was not affected in *Vangl2*^{Lp/Lp} mutants; rather, it is misoriented in a manner that precisely correlates with hair bundle misorientation [30]. Thus, in PCP mutants, individual hair cells were able to polarize in response to hair cell-intrinsic cues, using both morphological (V-shaped hair bundle) and molecular

criteria (asymmetric pPAK localization). By contrast, both forms of readout for hair cell polarization were disrupted in *Kif3a^{CKO}* mutants: hair bundles adopted a flattened morphology and pPAK staining became mislocalized around hair cell membranes. Second, Kif3a, but neither PTK7 nor Vangl2 (data not shown), is required for correct apical-basal positioning of the basal body. Third, there is evidence that PCP signaling is still active in *Kif3a^{CKO}* mutants. The core PCP proteins Dvl2 and Frizzled3 were still asymmetrically localized in the *Kif3a^{CKO}* OC. Moreover, cortical PAK activity, though diffused around the hair cell membrane, was still somewhat enriched on the lateral side, suggesting that PAK activity is still regulated by tissue polarity cues in *Kif3a^{CKO}* mutants. Finally, hair bundle misorientation in *Kif3a^{CKO}* mutants was mild compared to the PCP mutants. Together, our data provide strong support for the model that the Kif3a-mediated cell-intrinsic and the PCP/tissue polarity pathways act in concert and converge on PAK kinases to regulate hair cell polarity.

3.4 Figures

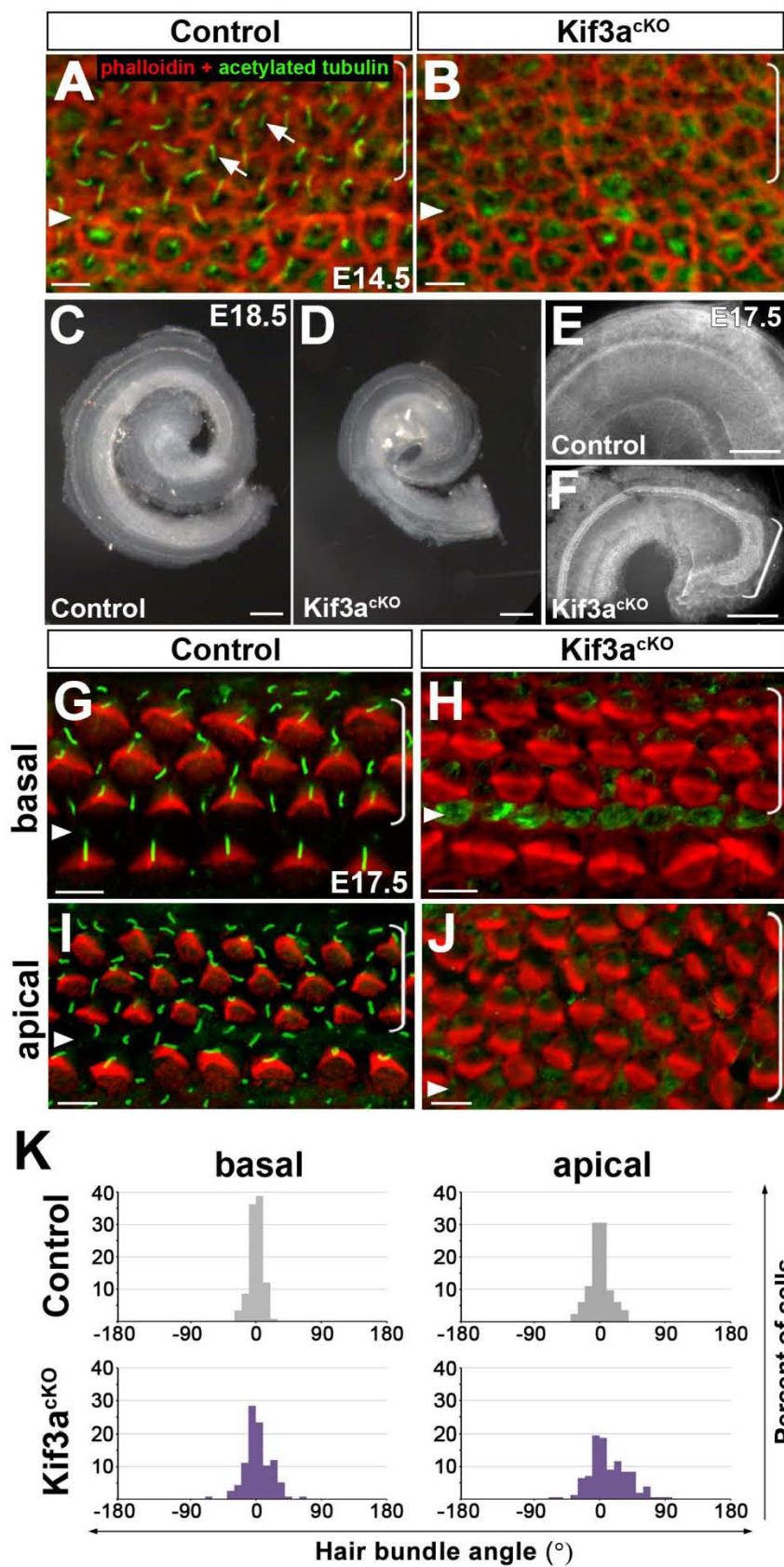


Figure 2. Cochlear extension and hair bundle orientation defects in *Kif3a*^{cko} OC. (A,B) Acetylated tubulin (green) and phalloidin (red) stained images of E14.5 control (A) and *Kif3a*^{cko} (B) OC. Kinocilia are present in control (arrows, A) but undetectable in *Kif3a*^{cko} hair cells (B). (C,D) E18.5 *Kif3a*^{cko} cochleae (D) are shorter than controls (C). (E,F) *Kif3a*^{cko} cochleae (stained with phalloidin) exhibit an expansion of hair cell rows near the apex of the cochlea (bracket in F). (G-J) Acetylated tubulin (green) and phalloidin (red) staining of control (G, I) and *Kif3a*^{cko} (H, J) cochleae at E17.5. Triangles mark the row of pillar cells, and brackets indicate outer hair cell rows. (K) Quantification of hair bundle orientation in E18.5 control (basal, n=116; apical, n=82) and *Kif3a*^{cko} (basal, n=116; apical n=154) cochleae. Scale bars: A-B, 5 μ m; C-D, 200 μ m; E-F, 100 μ m; G-J, 5 μ m.

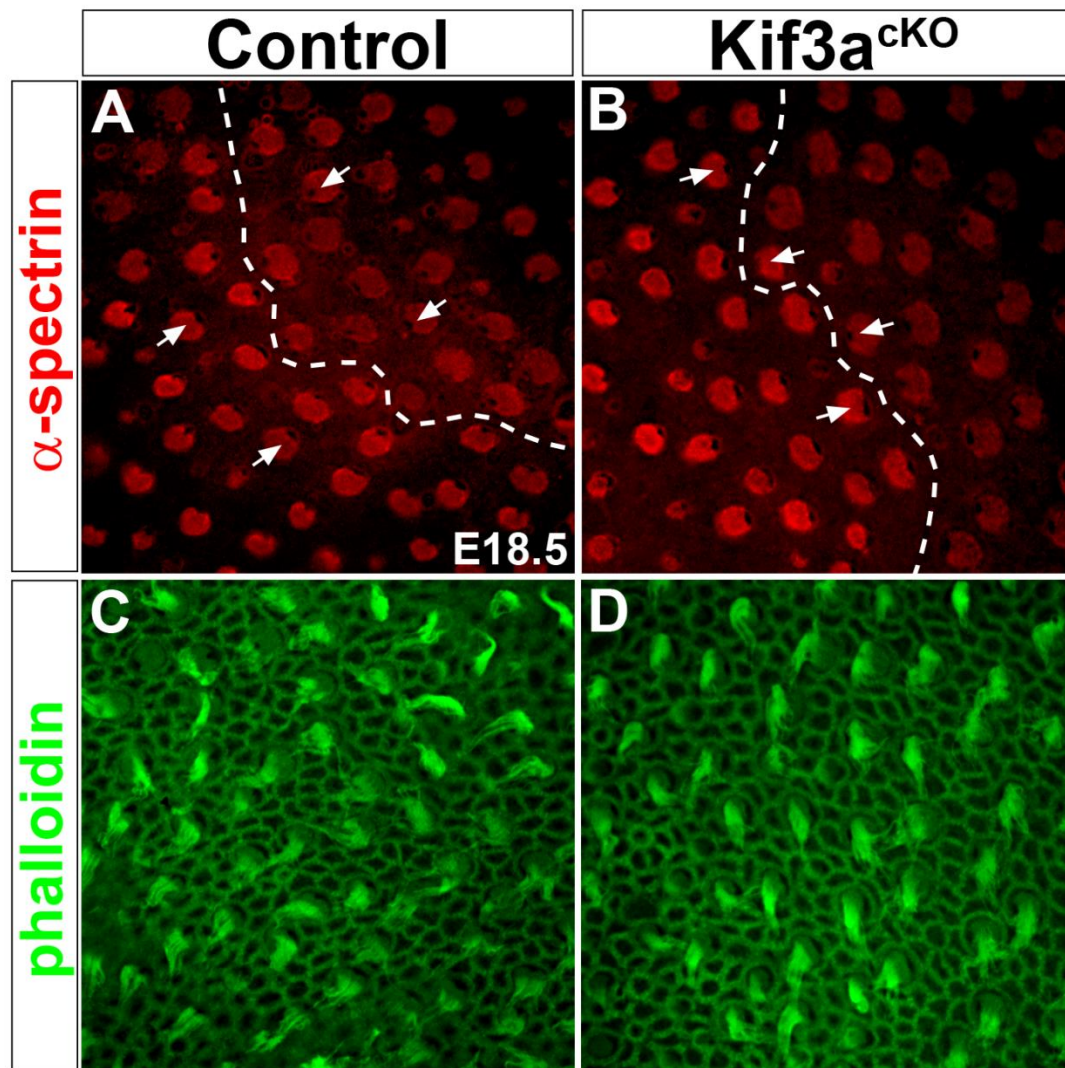


Figure 3. Normal hair cell development in the *Kif3a*^{cKO} utricle. (A-D) α -Spectrin (red) and phalloidin (green) stained images of E18.5 control (A,C) and *Kif3a*^{cKO} (B,D) utricles. (A,B) Planar polarity of hair cells appears normal in *Kif3a*^{cKO} utricles (B) compared with controls (A). Arrows indicate planar polarity as revealed by staining of the cuticular plate component, α -spectrin. Broken lines indicate the line of reversal. (C,D) Stereocilia organization appears normal in *Kif3a*^{cKO} utricular hair cells (D) compared with controls (C).

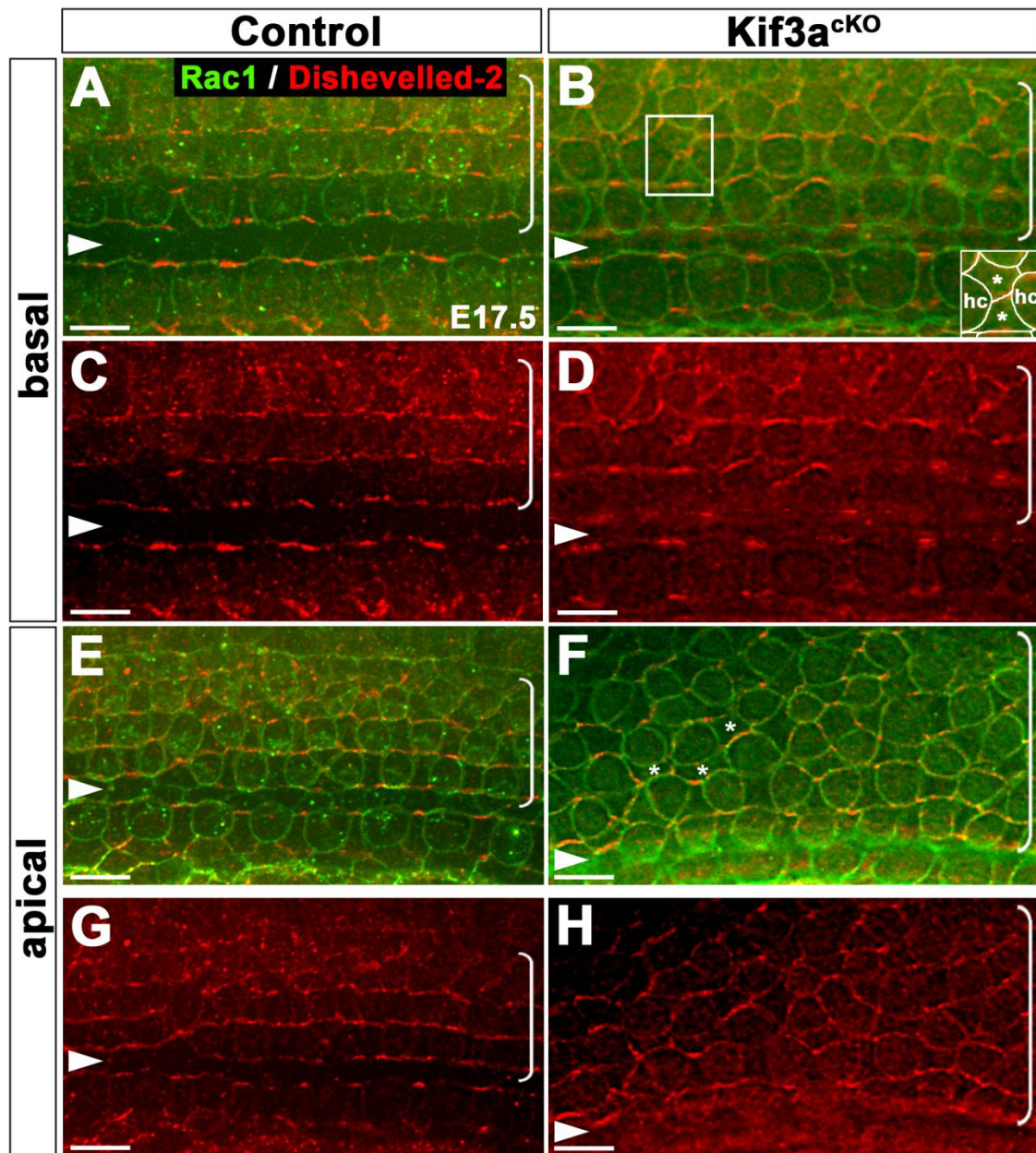


Figure 4. Localization of Dishevelled-2 in *Kif3a*^{CKO} OC. (A-H) Dishevelled-2 immunostaining (red) in basal (A-D) or apical (E-H) regions of E17.5 control and *Kif3a*^{CKO} OC. Cell boundaries are labeled by Rac1 immunostaining (green). The box in B indicates the apical membranes of two Deiters cells found in between hair cells and is shown in a schematic diagram in the inset (hc, hair cell; *, support cell). The asterisks in F indicate examples of abnormal Deiters cell extensions in contact with hair cells. Triangles indicate the row of pillar cells, and brackets indicate outer hair cell rows. Scale bars: A-H, 6 μ m.

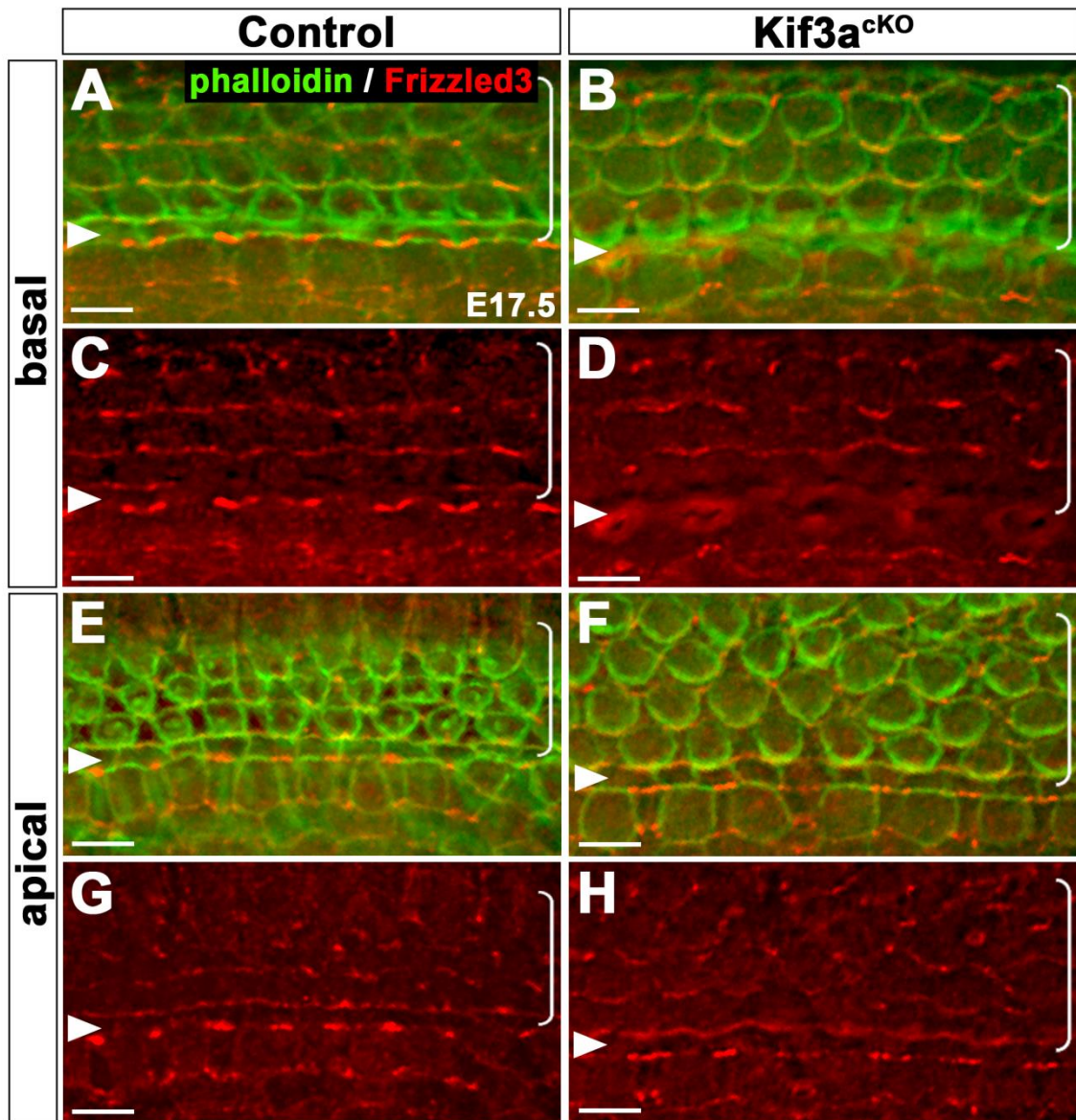


Figure 5. Localization of frizzled 3 in *Kif3a*^{ckO} OC. (A-H) Frizzled 3 immunostaining (red) in basal (A-D) or apical (E-H) regions of E17.5 control (left panels) and *Kif3a*^{ckO} (right panels) OC. Cell boundaries are labeled by phalloidin staining (green). Triangles indicate the row of pillar cells, and brackets indicate outer hair cell rows. Scale bars: 6 μ m.

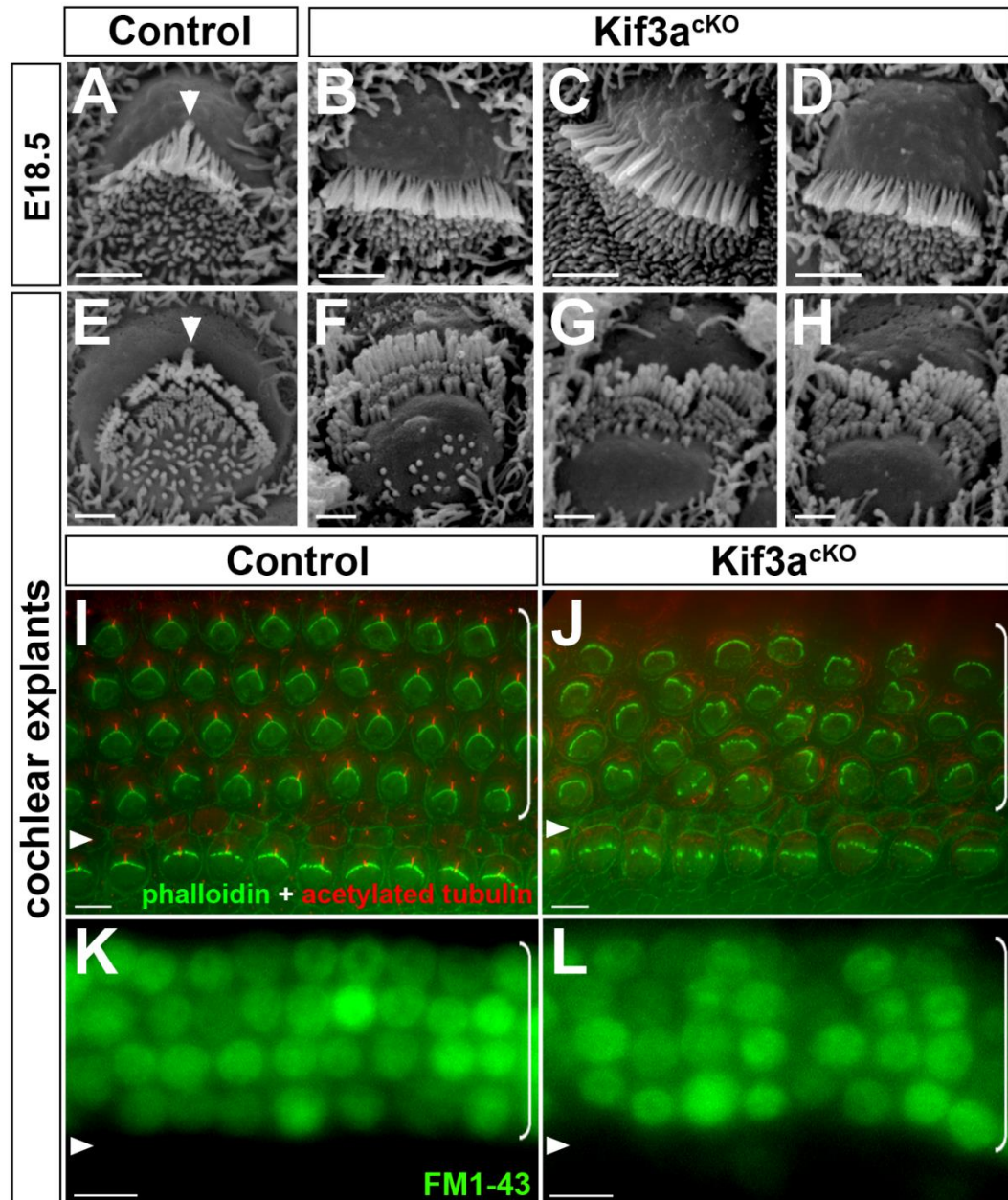


Figure 6. *Kif3a* is required for normal hair bundle morphology. (A-D) Scanning electron micrographs of control (A) and *Kif3a*^{cKO} outer hair cells (B-D) from the mid-basal region of E18.5 cochleae. (E-L) Hair cell maturation in explant cultures derived from E18.5 cochleae and maintained for 3.5-4 days *in vitro*. (E-H) Scanning electron micrographs of outer hair cells from control (E) and *Kif3a*^{cKO} explants (F-H). White triangles in A and E indicate the kinocilium in control cells. (I, J) Control (I) and *Kif3a*^{cKO} (J) explants stained for acetylated-tubulin (red) and phalloidin (green). (K, L) FM1-43 dye (green) uptake is normal in *Kif3a*^{cKO} explants (L) compared to the control (K). Triangles mark the row of pillar cells, and brackets indicate outer hair cell rows. Scale bars: A-H, 1 μ m; I-J, 5 μ m; K-L, 10 μ m.

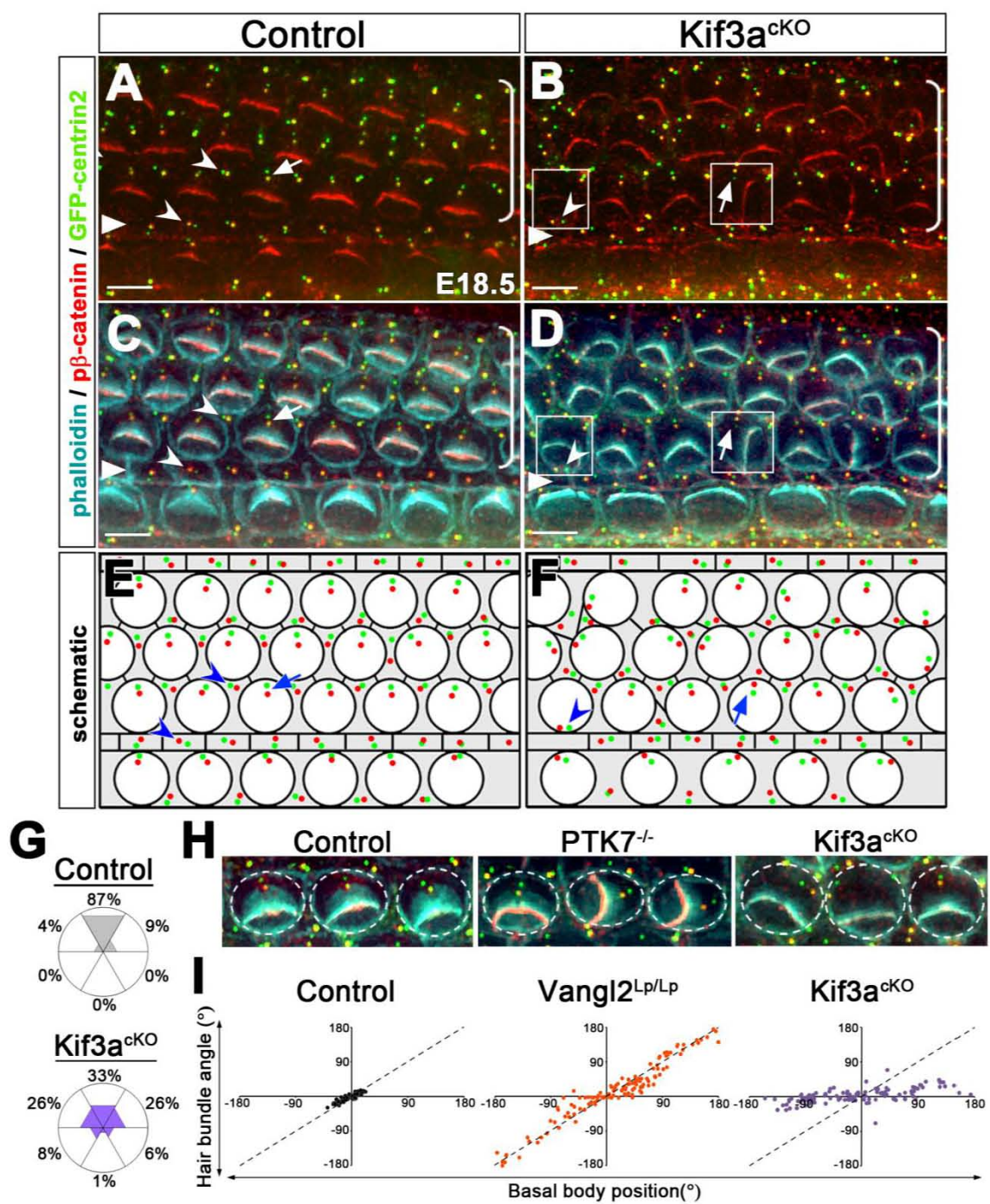


Figure 7. Uncoupling of hair bundle orientation from basal body position in *Kif3a*^{CKO} hair cells. (A-D) Planar position of centrioles in E18.5 control (A, C) and *Kif3a*^{CKO} (B,D) hair cells. Green, GFP-centrin2; red, phospho- β -catenin; cyan, phalloidin. Examples of *Kif3a*^{CKO} hair cells showing uncoupling of hair bundle orientation from basal body position are boxed. Triangles mark the row of pillar cells, and brackets indicate outer hair cell rows. Scale bars: 6 μ m. (E,F) Schematic diagrams of C and D, respectively. Green dots, daughter centrioles; red dots, basal bodies. Support cells are shaded. (G) Rose diagrams showing the percentage of centrioles located within the indicated 60° sectors in E18.5 control (shaded grey; n=153) and *Kif3a*^{CKO} (shaded blue; n=142) hair cells. (H) Hair bundle orientation is coupled to basal body position in wild-type (left) and PTK7^{-/-} (middle) but not *Kif3a*^{CKO} (right) hair cells. Green, GFP-centrin2; red, phospho- β -catenin; cyan, phalloidin. Hair cell boundaries are outlined by dashed circles. The lateral side of the cochlea is up in all diagrams. (I) Scatter plots showing hair bundle orientation in relation to the planar position of the basal body. Control (n=73), Vangl2^{Lp/Lp} (n=128) and *Kif3a*^{CKO} (n=115) hair cells were all from the mid-basal region of the cochlea. The dashed reference line in each graph indicates a perfect correlation.

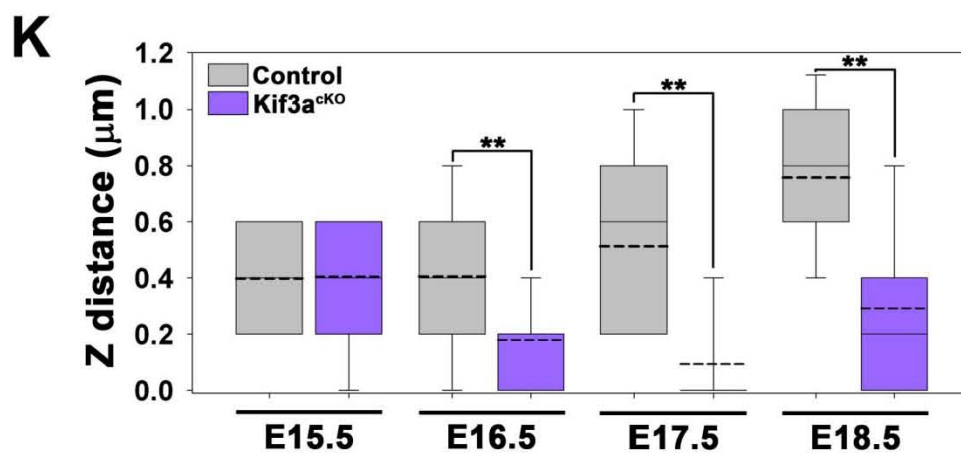
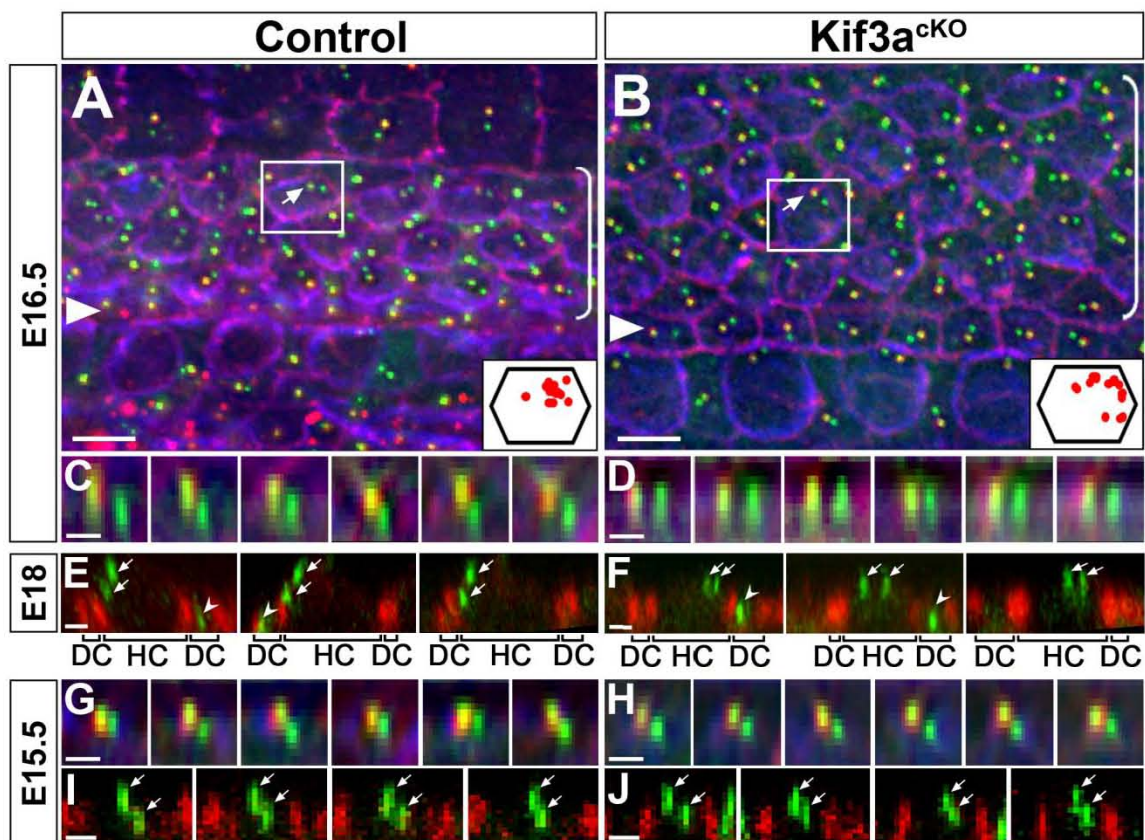


Figure 8. Aberrant apical-basal positioning of basal body in *Kif3a*^{CKO} hair cells. (A, B) Basal body migration in E16.5 control (A) and *Kif3a*^{CKO} (B) hair cells. Green, GFP-centrin2; red, phospho- β -catenin; blue, phalloidin. Schematic diagrams summarizing the planar positions of the hair cell basal bodies are shown in the insets. Triangles mark the row of pillar cells, and brackets indicate outer hair cell rows. (C, D) Optical slices along the Z-axis of E16.5 control (C) or *Kif3a*^{CKO} (D) hair cells showing the apical-basal position of the centriole pairs. (E, F) Optical slices along the Z-axis showing the apical-basal position of hair cell centrioles relative to the tight junctions (as marked by ZO-1 immunostaining) in E18.5 control (E) and *Kif3a*^{CKO} (F) OC. Green, GFP-centrin2; red, ZO-1. Brackets indicate the domains of hair cells (HC) and Deiters cells (DC) demarcated by ZO-1 staining. Arrows indicate hair cell centrioles. Arrowheads indicate the centrioles of DC. (G-J) Optical slices along the Z-axis showing normal apical-basal position of centrioles in *Kif3a*^{CKO} hair cells (H,J) compared to controls (G,I) at E15.5. (G,H) Green, GFP-centrin2; red, phospho- β -catenin; blue, phalloidin. (I,J) Green, GFP-centrin2; red, ZO-1. (K) Distance along the Z-axis between the basal body and the daughter centriole in control (shaded gray) and *Kif3a*^{CKO} (shaded blue) hair cells at different developmental stages. Compared to controls, the Z distance between centriole pairs in *Kif3a*^{CKO} mutant hair cells is similar at E15.5, but significantly shorter at E16.5, E17.5 and E18.5. **, $p < 0.001$. Scale bars: A-B, 5 μ m; C-J, 1 μ m.

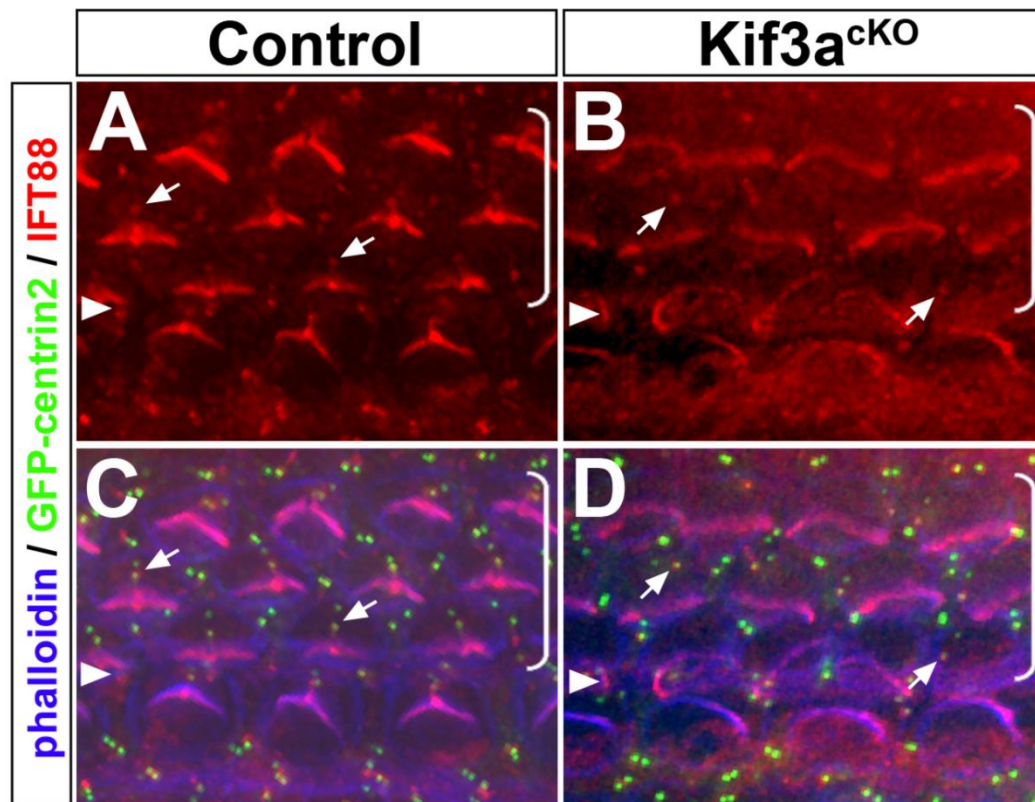


Figure 9. IFT88 localization is normal in *Kif3a*^{cKO} hair cells. (A-D) IFT88 (red) localization at E18.5 in control (A,C) and *Kif3a*^{cKO} (B,D) hair cells. GFP-centrin2 marks the hair cell centrioles (green). Arrows indicate IFT88 localization on the basal body. Triangles mark the row of pillar cells, and brackets indicate outer hair cell rows.

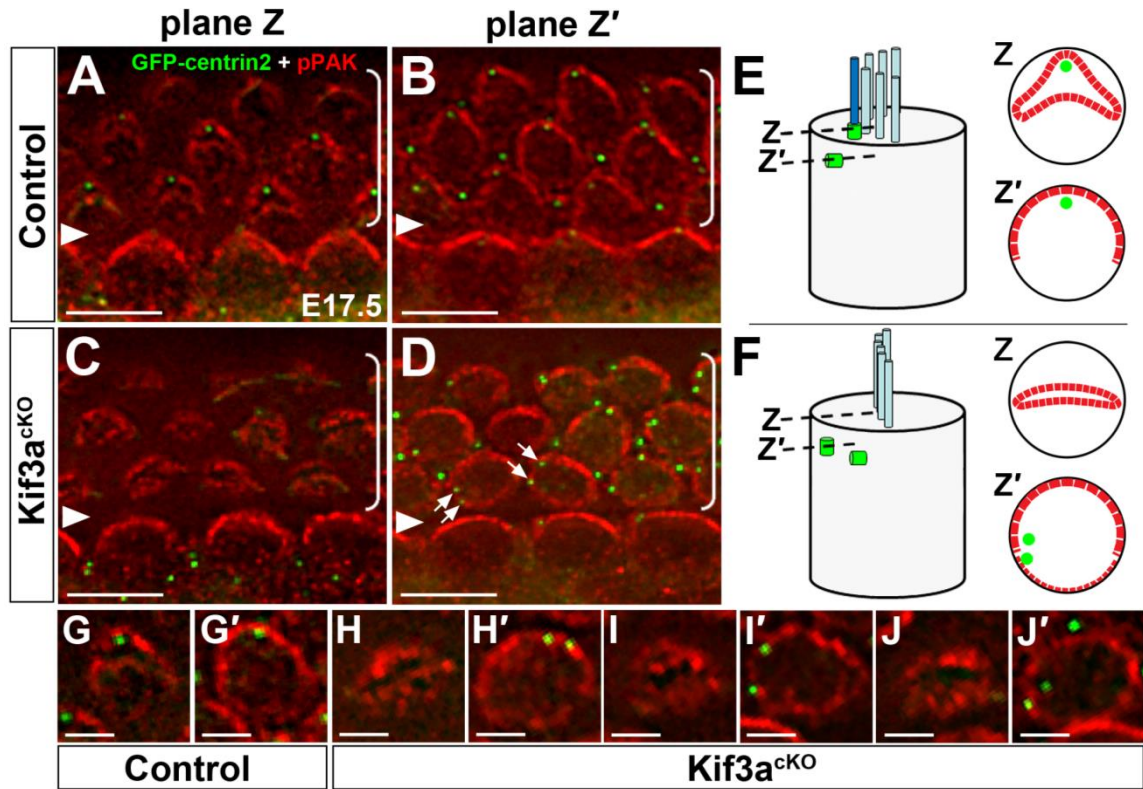


Figure 10. Abnormal phospho-PAK localization correlates with centriole defects in *Kif3a*^{cKO} hair cells. (A-D) Single Z-sections showing centriole (green, GFP-centrin2) location in relation to phospho-PAK staining (red) in E17.5 control (A,B) and *Kif3a*^{cKO} (C,D) hair cells. Plane Z' is approximately 1 μm basal to plane Z. Arrows in D indicate aberrantly positioned centriole pairs. Triangles mark the row of pillar cells, and brackets indicate outer hair cell rows. (E,F) Schematic diagrams of centriole positions relative to pPAK localization in a control (E) and a *Kif3a*^{cKO} (F) hair cell. On the left are side-views of a hair cell showing centriole (green barrels) positions relative to the hair bundle. Circles to the right represent cross sections through the hair cell at plane Z and plane Z' and show the localization of pPAK (red) and the position of the centrioles (green dots). (G-J') Higher magnification images of single Z sections showing pPAK localization (red) and centriole (green, GFP-centrin2) location at plane Z (G,H,I,J) and Z' (G',H',I',J') in control (G,G') and *Kif3a*^{cKO} hair cells (H-J'). Scale bars: A-D, 6 μm; G-J', 3 μm.

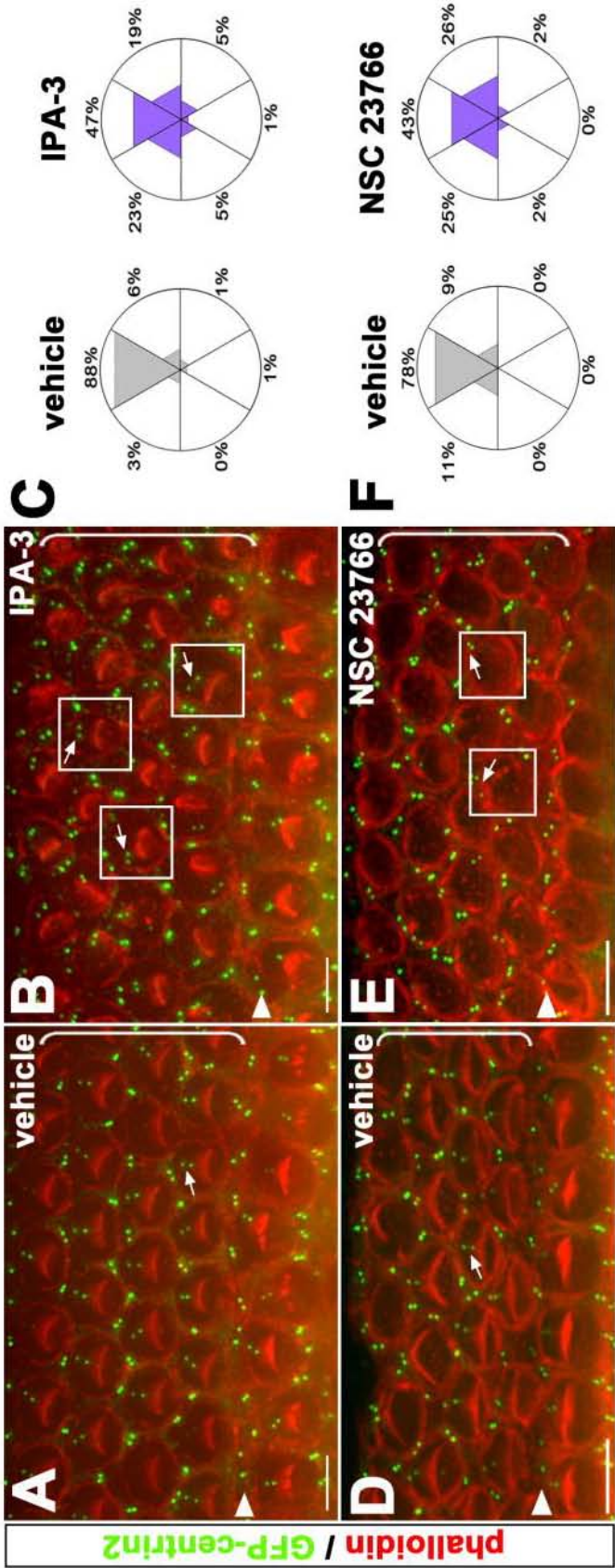


Figure 11. Rac-PAK signaling regulates hair cell centriole positioning. (A, B) Cochlear explants treated with vehicle (A) or 10 μ M IPA-3 (B). Green, GFP-centrin2; red, phalloidin staining. Arrows indicate centriole pairs. Examples of hair cells with centriole positioning defects are boxed in B. Triangles mark the row of pillar cells, and brackets indicate outer hair cell rows. (C) Rose diagrams showing the percentage of centrioles located within the indicated 60° sectors in hair cells of explants treated with vehicle (shaded gray, n=270) or 10 μ M IPA-3 (shaded blue, n=432). (D, E) Cochlear explants treated with vehicle (D) or 100 μ M NSC 23766 (E). Arrows indicate centriole pairs. Examples of hair cells with mispositioned centrioles are boxed in E. (F) Rose diagrams showing the percentage of centrioles located within the indicated 60° sectors in hair cells of explants treated with vehicle (shaded gray, n=218) or 100 μ M NSC 23766 (shaded blue, n=218). The lateral side of the cochlea is up in all diagrams. Scale bars: A-B, 5 μ m; D-E, 5 μ m.

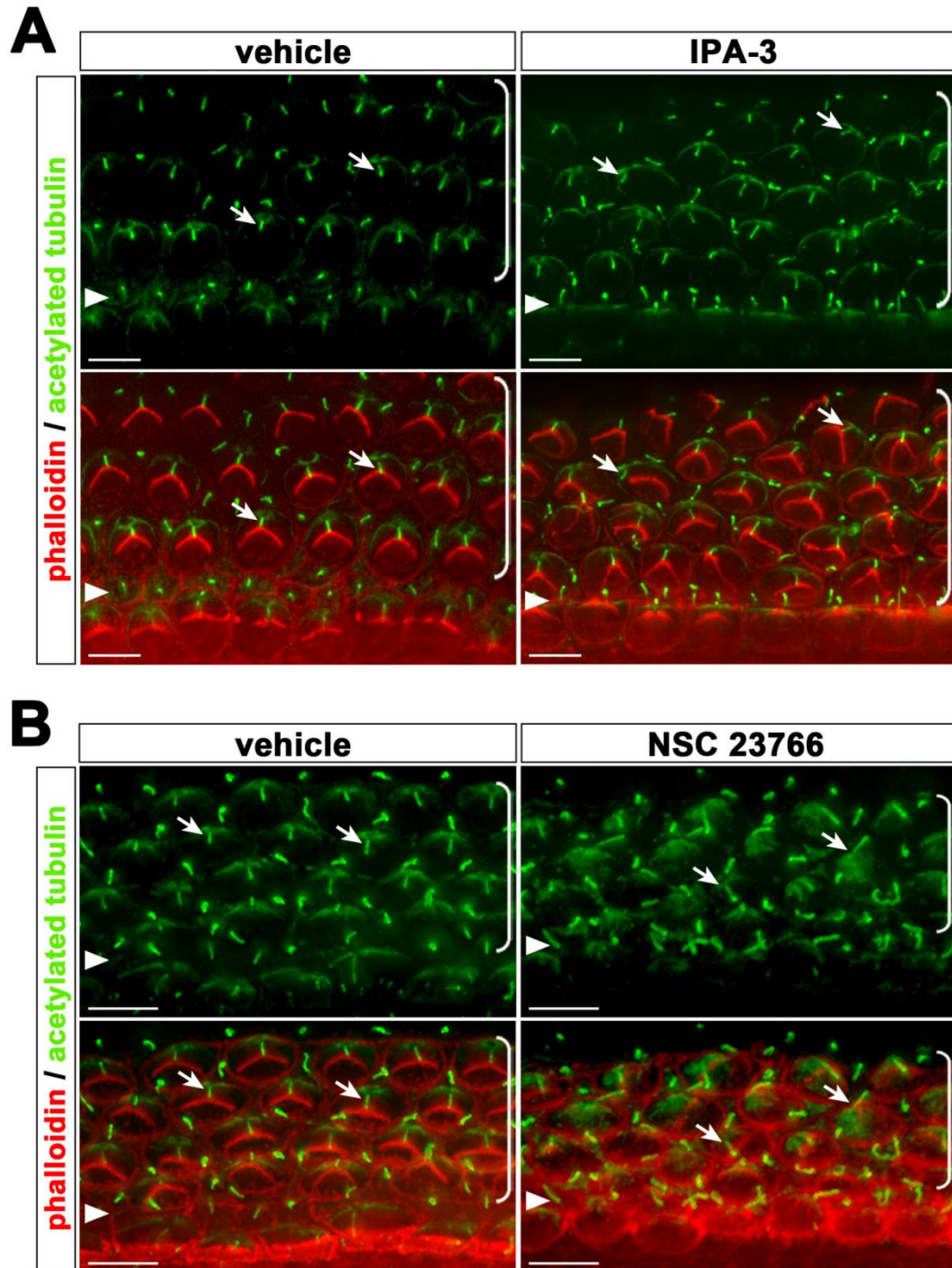


Figure 12. Hair cell kinocilia persist after inhibition of Rac-PAK signaling in vitro. (A) Cochlear explants treated with vehicle or 10 μ M IPA-3. (B) Cochlear explants treated with vehicle or 100 μ M NSC 23766. Green, acetylated tubulin antibody staining; red, phalloidin staining. Arrows indicate examples of hair cell kinocilia. Triangles indicate the row of pillar cells, and brackets indicate outer hair cell rows. Scale bars: 6 μ m.

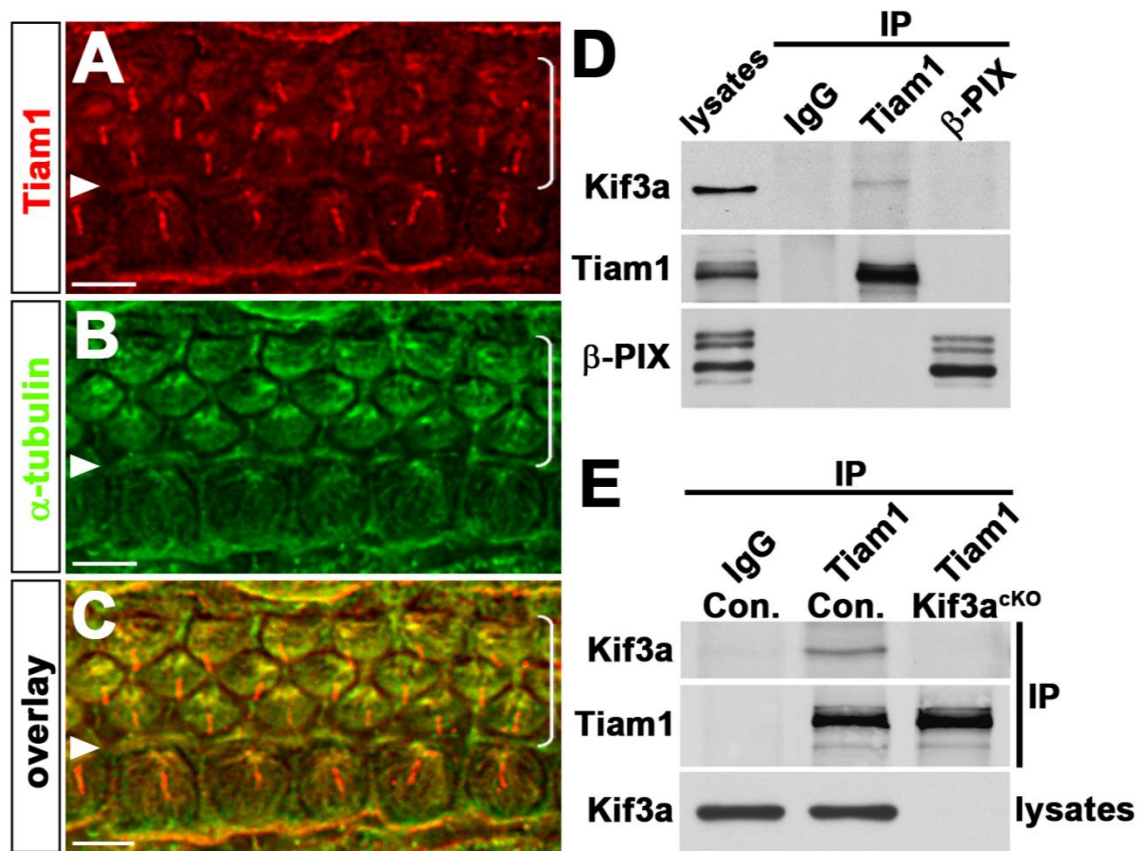


Figure 13. The Rac GEF Tiam1 is a likely cargo of kinesin-II. (A-C) Tiam1 (red) and α -tubulin (green) immunostaining in E17.5 control OC. Triangles mark the row of pillar cells, and brackets indicate outer hair cell rows. Scale bars: A-C, 6 μ m. (D) Co-immunoprecipitation assays from E16.5 wild-type brain lysates. Lysates were incubated with normal rabbit IgG, anti-Tiam1, or anti- β -PIX antibodies, and the immunoprecipitates were analyzed by immunoblotting with the indicated antibodies. (E) Co-immunoprecipitation assays from E16.5 control (Con.) or *Kif3a*^{CKO} mutant cortices. Lysates were incubated with normal rabbit IgG or anti-Tiam1 antibodies as indicated, and the immunoprecipitates (IP) analyzed by Western blot for Kif3a.

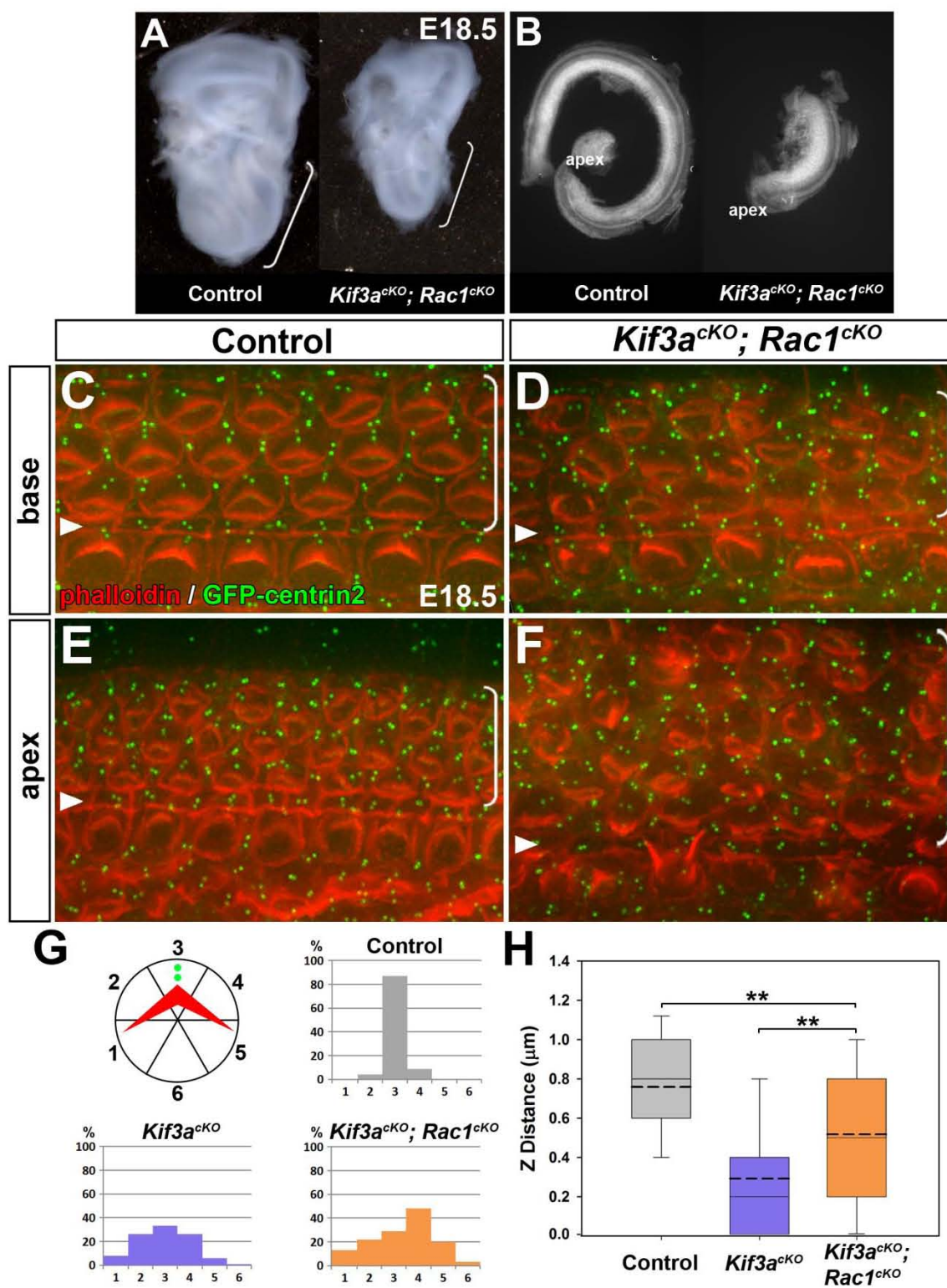


Figure 14. Hair cell phenotype and centriole positioning in *Kif3a*^{cko}; *Rac1*^{cko} OC. (A,B) E18.5 control and *Kif3a*^{cko}; *Rac1*^{cko} temporal bones (A) and flat-mounted cochleae (B). *Kif3a*^{cko}; *Rac1*^{cko} cochleae are shorter in length than control and *Kif3a*^{cko} cochleae (compare to **Fig. 2D**). Brackets in A indicate the cochlear region. (C-F) Centrin2-GFP (green) and phalloidin (red) staining of control (C,E) and *Kif3a*^{cko}; *Rac1*^{cko} (D,F) at E18.5. Triangles mark the row of pillar cells, and brackets indicate outer hair cell rows. (G) Graphs show the percentage of centrioles located within the indicated 60° sectors in E18.5 control (n=153), *Kif3a*^{cko} (n=142), and *Kif3a*^{cko}; *Rac1*^{cko} (n=172) hair cells. Distance along the z-axis between the basal body and the daughter centriole in E18.5 control (shaded gray), *Kif3a*^{cko} (shaded blue), and *Kif3a*^{cko}; *Rac1*^{cko} (shaded orange) hair cells. *Kif3a*^{cko}; *Rac1*^{cko} centrioles are closer together in the Z-axis than control centrioles but farther apart than those of single *Kif3a*^{cko} mutants (**,p<0.001).

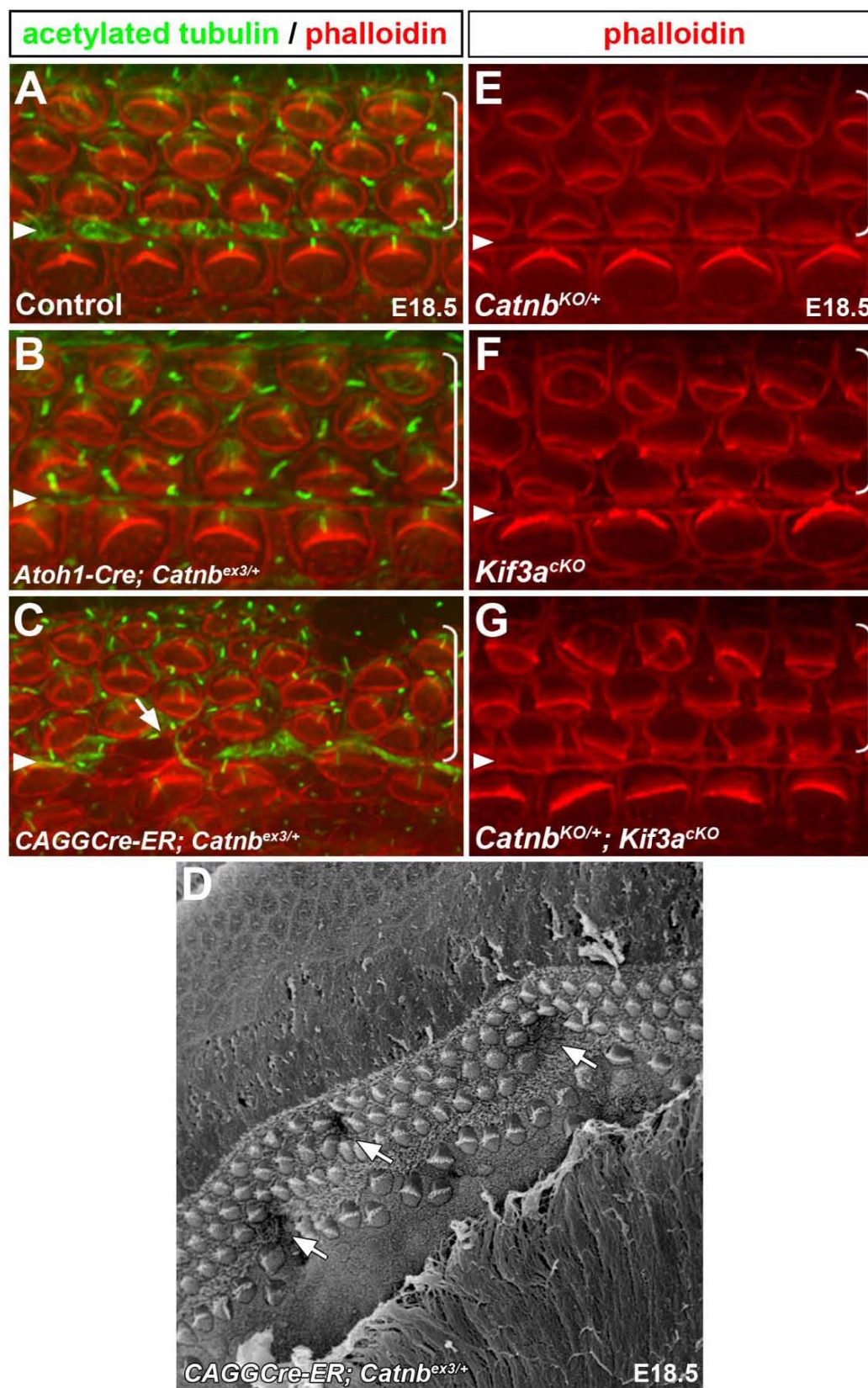


Figure 15. Effects of β -catenin misregulation in hair cells. (A-C) Acetylated tubulin (green) and phalloidin (red) staining in E18.5 control (A), hair cell-specific β -catenin gain-of-function (B), and tamoxifen-inducible β -catenin gain-of-function (C) OC. Arrow in C indicates a region of overproliferating supporting cells. (D) SEM image of an E18.5 OC expressing the tamoxifen-inducible β -catenin gain-of-function mutation. Arrows indicate pockets of overproliferating supporting cells. (E-G) Phalloidin (red) staining of *Catnb*^{KO/+}, single *Kif3a*^{cKO} (F), and double *Catnb*^{KO/+}; *Kif3a*^{cKO} (G) OC. Loss of β -catenin function in hair cells does not ameliorate the *Kif3a*^{cKO} flattened bundle phenotype. Triangles mark the row of pillar cells, and brackets indicate outer hair cell rows.

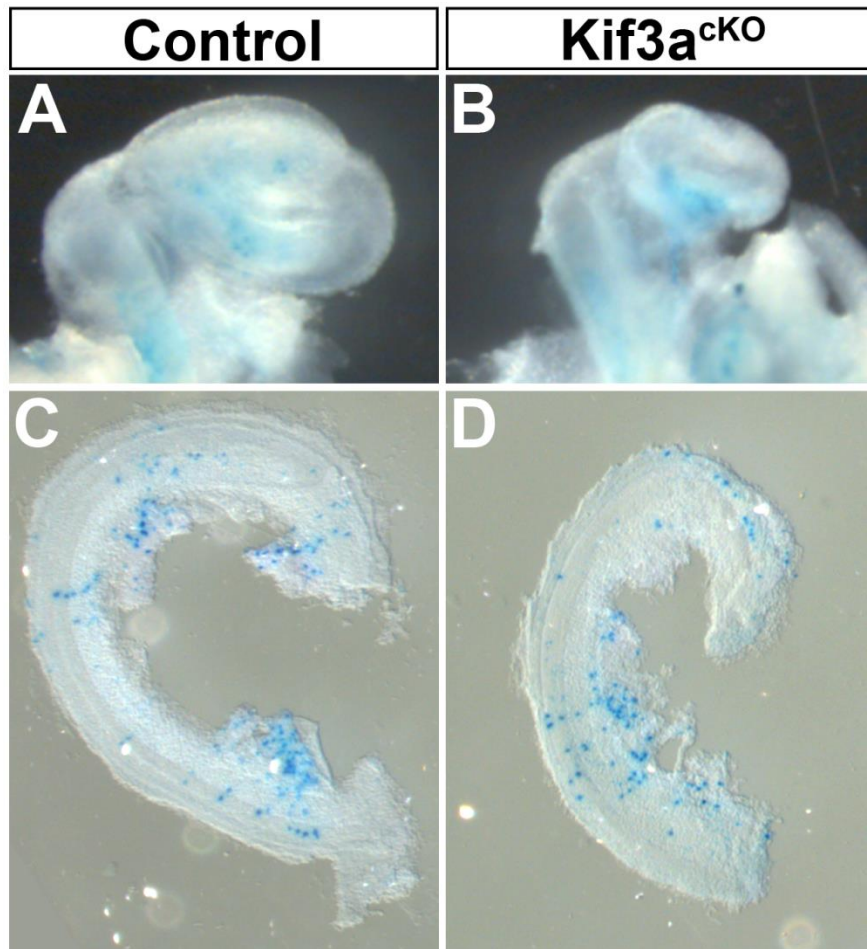


Figure 16. Levels of canonical Wnt signaling are normal in *Kif3a*^{cKO} cochleae. (A,B) Whole mount images of cochleae from control (A) or *Kif3a*^{cKO} (B) mice that have been crossed with the BATGAL reporter line. X-gal staining (blue) indicates active canonical Wnt signaling. (C,D) Flat-mounted cochleae from control (C) or *Kif3a*^{cKO} (D) stained with X-gal. The roof of the cochlear duct has been removed to show BATgal expressing-cells in and around the organ of Corti.

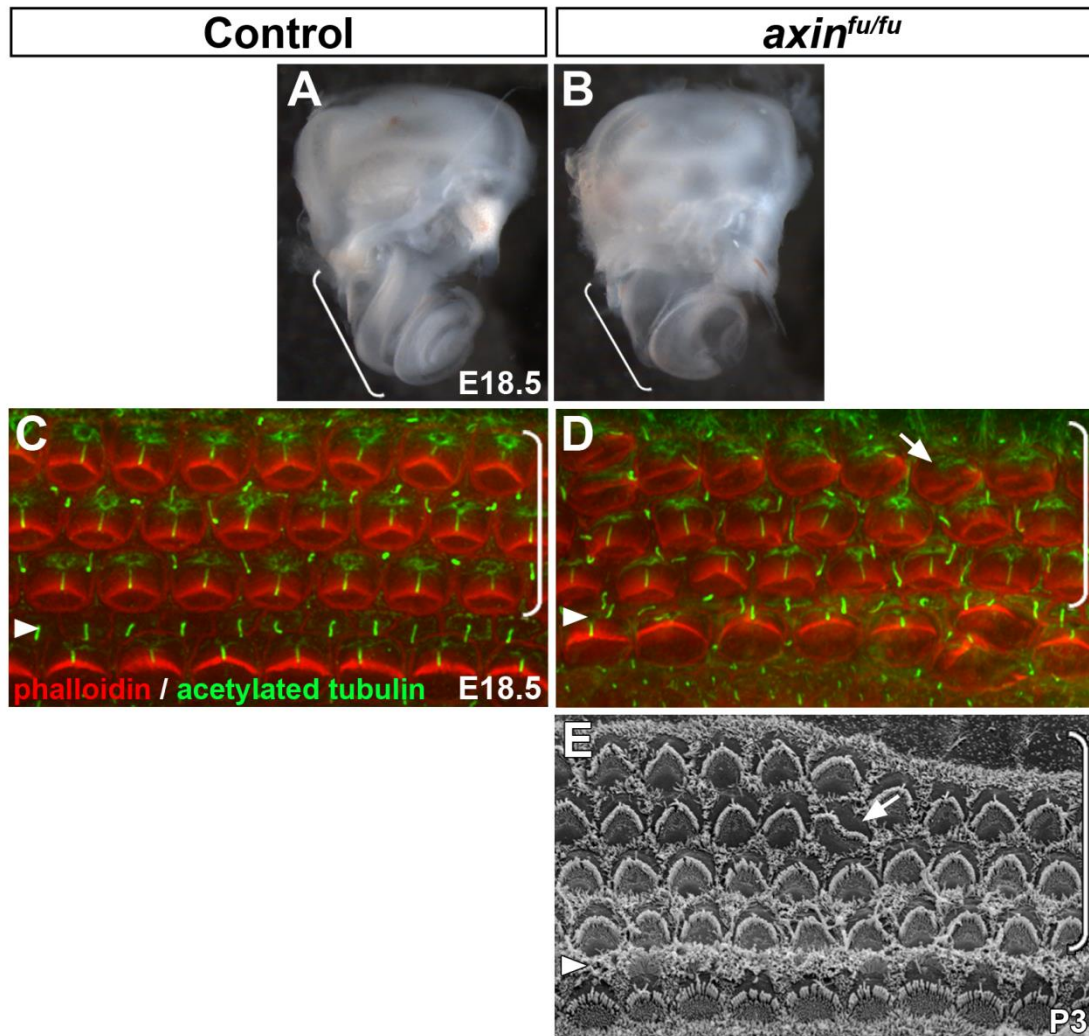


Figure 17. Abnormal cochlear morphology and hair bundle phenotypes in *axin^{fu/fu}* OC. (A,B) Dissected temporal bones from control (A) and *axin^{fu/fu}* (B) mice. *Axin^{fu/fu}* cochleae often have a shorter, dilated cochlear duct. Brackets indicate the cochlea. (C,D) Acetylated tubulin (green) and phalloidin (red) staining of E18.5 control (C) and *axin^{fu/fu}* (D) OC. *Axin^{fu/fu}* OC have minor patterning disruptions of HC rows, and a subset of hair bundles display an abnormal flattened phenotype (arrow). (E) SEM image of P3 *axin^{fu/fu}* OC showing disruption of OHC patterning and an abnormal flattened hair bundle (arrow). Triangles mark the row of pillar cells, and brackets indicate outer hair cell rows.

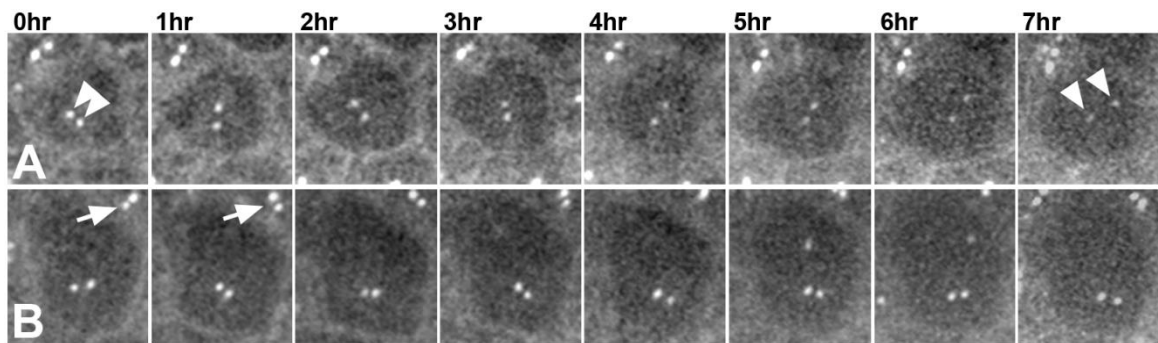


Figure 18. *In vivo* imaging of centriole search behavior during hair cell polarization. (A,B) Collapsed Z-stacks show the centrioles (marked with *GFP-centrin2*) of single hair cells at E17. Images were collected every hour. Arrowheads in A indicate the increased distance between the basal body and daughter centriole at 7hr compared to 0hr. Arrows in B indicate supporting cell centrioles that have changed alignment over the course of an hour.

Chapter 4

**Lis1 mediates planar polarity through regulation of
microtubule organization**

4.1 Introduction

In addition to apical-basal polarity, PCP, or polarity within an epithelial cell sheet, is critical for epithelial morphogenesis and function. Sensory hair cells are specialized neuroepithelial cells that convert mechanical stimuli into electrical nerve impulses. Mechanotransduction is accomplished by the V-shaped stereociliary bundle (or hair bundle) located on the apex of each hair cell. Each hair bundle consists of rows of actin-based stereocilia arranged in a staircase pattern with a single microtubule-based kinocilium next to the tallest row of stereocilia. This polarized structure renders the hair bundle directionally sensitive to deflections [47]. As a result, hair cells must be uniformly oriented across the plane of the auditory sensory epithelium, the organ of Corti, such that the vertex of each bundle points toward the lateral edge of the cochlear duct. Proper hair bundle polarity and orientation is essential for normal hearing.

Hair cell planar polarity is established during embryogenesis in vertebrates. One of the earliest manifestations of planar polarization is the migration of the axonemal kinocilium from the center of the hair cell apex toward the cell periphery [55, 57]. The kinocilium is a specialized primary cilium that extends from the basal body located just below the apical surface. Following its migration toward the lateral edge of the cochlear duct, microvilli adjacent to the kinocilium thicken and elongate, eventually forming a V-shaped bundle of stereocilia, with the kinocilium at its vertex. Nascent hair bundles then refine and align their orientation during late embryonic and early postnatal development [59]. Thus, positioning of the kinocilium/basal body near the lateral pole is tightly

coupled with hair bundle polarity and orientation, and together they constitute morphological features of hair cell planar polarity.

Hair cell planar polarity is coordinated at the tissue level by the evolutionarily conserved, core Wnt/PCP pathway [60]. Downstream of the core PCP genes, the small GTPase Rac and its effector p21-activated kinases (PAK) have been shown to mediate basal body positioning and hair bundle orientation [30, 250]. Wnt/PCP signaling spatially orients localized Rac-PAK signaling on the hair cell cortex [30]; however, the underlying mechanisms remain incompletely understood.

Accumulating evidence suggests that tissue-level PCP signaling impinges on a hair cell-intrinsic pathway that controls planar polarization of individual hair cells. The kinocilium and its connection to the adjacent stereocilium, via the kinociliary links, are required for the normal V-shape and orientation of the nascent hair bundle [61, 62, 250]. Moreover, a non-ciliary function of Kif3a, a component of the kinesin-II plus-end-directed microtubule motor complex, coordinates basal body positioning and hair bundle orientation through spatial regulation of Rac-PAK signaling, thus implicating microtubule-based intracellular transport in hair cell planar polarization [250]. In addition to templating the kinocilium, the basal body (or the mother centriole), along with the daughter centriole and the associated pericentriolar matrix, organize cytoplasmic microtubules in hair cells [49].

To further elucidate the microtubule-mediated hair cell polarity pathway, we investigated the function of a well-established microtubule regulator, Lis1.

Lis1 mutations cause type I lissencephaly, a human brain malformation [251]. Functionally, Lis1 controls microtubule organization as a microtubule-associated protein and regulator of cytoplasmic dynein, a minus-end directed microtubule motor complex that participates in a range of cellular processes, including cell migration, organelle positioning and mitotic spindle assembly [188, 252, 253]. Lis1 regulates localization of dynein to microtubule plus-ends and the cell cortex, as well as the motor function of dynein [253, 254]. In addition to mediating dynein function, Lis1 also regulates actin dynamics and Rho GTPase signaling [172, 255, 256]. Thus, Lis1 is a strong candidate regulator of hair cell planar polarity.

Here, we analyzed the inner ears of conditional *Lis1* mouse mutants during both embryonic and postnatal development. *Lis1* mutant embryos show defects in hair cell planar polarity and cellular organization of the organ of Corti due to impaired Rac-PAK signaling. In addition, we also uncover a critical role for Lis1 in maintaining planar polarity in postnatal hair cells by regulating cytoplasmic dynein and microtubule organization. Lastly, our results reveal a function of Lis1-dynein in organelle positioning and hair cell survival.

4.2 Results

4.2.1 Lis1 is localized to the pericentriolar region in developing hair cells

To investigate a potential role for Lis1 in auditory hair cell development, we first determined the subcellular localization of Lis1 in the developing organ of Corti. At E17.5, Lis1 was detected on the stereocilia and the hair cell centrioles

(**Fig. 19A-C**, arrows). At P1, Lis1 was prominently localized to the pericentriolar region in hair cells, forming a cloud surrounding the centrioles (**Fig. 19G-I**, circles), and was also detected at low levels on the centrioles of supporting cells (**Fig. 18G-I**, arrows). These localization patterns are consistent with those reported in other cell types and suggest a function for Lis1 in the regulation of the hair cell microtubule network [257, 258].

4.2.2 Lis1 deletion during embryonic development causes defects in hair bundle morphology and orientation

To investigate the function of Lis1 in developing hair cells, we generated *Lis1* conditional mutants using a floxed allele of *Lis1* [259] and an *Atoh1^{Cre}* driver line that expresses Cre in developing hair cells and a subset of supporting cells starting around E14.5 [260]. We also used a *Lis1* null allele (*Lis1^{-/-}*) that was derived from the *Lis1^{flox}* allele by germline Cre expression. To perturb *Lis1* function in embryonic hair cells, we generated *Atoh1^{Cre}; Lis1^{flox/-}* embryos (hereafter referred to as *Lis1^{CKO-early}*). As expected, Lis1 levels in *Lis1^{CKO-early}* hair cells were greatly reduced, and Lis1 no longer localized on the centrioles (**Fig. 19D-F**). *Lis1^{+/-}*, *Lis1^{flox/-}* and *Lis1^{flox/+}* mice did not exhibit any inner ear phenotypes at P0 (**Fig. 20**) and served as controls for subsequent experiments.

At E17.5, a subset of *Lis1^{CKO-early}* hair cells had bundles with an abnormal, flattened morphology (**Fig. 21B**, arrow). Moreover, *Lis1^{CKO-early}* hair cells displayed hair bundle misorientation (**Fig. 21B,F**; average bundle deviation = $20.1^{\circ} \pm 1.5$) compared to littermate controls (**Fig. 21A,E**; average bundle

deviation = $8.6^{\circ} \pm 0.7$). We also examined the position of the kinocilium and found that it had migrated to the hair cell periphery (**Fig. 21B**). However, kinocilia were often mispositioned with respect to both the hair bundle and the medial-lateral axis of the cochlea (**Fig. 21B,D**, arrows and arrowheads). These defects in kinocilium/basal body positioning correlated with hair bundle misorientation. Furthermore, in contrast to the regular aster-shaped array in control hair cells (**Fig. 21C**), cytoplasmic microtubules appeared disorganized in *Lis1*^{CKO-early} hair cells (**Fig. 21D**, arrow and arrowhead). These results demonstrate that Lis1 regulates microtubule organization and planar polarization of embryonic hair cells.

Hair bundle orientation is coordinated by the core Wnt/PCP pathway [60]. Therefore, we sought to determine if Wnt/PCP signaling was compromised in *Lis1*^{CKO-early} cochleae by examining the asymmetric membrane localization of the core PCP protein Dishevelled 2 (Dvl2). In E17.5 wild-type cochleae, Dvl2 was localized to the lateral side of hair cell membranes (**Fig. 21G,J**). This localization was essentially unchanged in *Lis1*^{CKO-early} hair cells (**Fig. 21H,I,K,L**). Of note, the hair cell rows in *Lis1*^{CKO-early} cochleae were slightly jumbled, and abnormal apical contacts between two supporting cells with Dvl2 staining were observed (**Fig. 21L**, arrow). Likewise, normal Fz3 localization at the lateral pole of hair cells was maintained in *Lis1*^{CKO-early} hair cells, though at somewhat reduced levels (**Fig. 22B,D**). These results demonstrate that Lis1 is not required for asymmetric membrane localization of Dvl2 or Fz3, suggesting that Wnt/PCP signaling is at least partially active in *Lis1*^{CKO-early} hair cells.

4.2.3 Defective cellular organization and nectin localization in *Lis1*^{CKO-early} organ of Corti

To further assess cellular organization in *Lis1*^{CKO-early} cochleae, we stained E18.5 tissue with myosin VI and $\beta 1/\beta 2$ tubulin to label hair cells and supporting cells, respectively. Instead of the normal “checkerboard” pattern of hair cells interdigitated with supporting cells (**Fig. 23A**), pairs of *Lis1*^{CKO-early} hair cells often appeared to be in direct contact, without an intervening supporting cell (**Fig. 23B**, arrow). Moreover, the apical surfaces of both hair cells and supporting cells in *Lis1*^{CKO-early} cochleae were misshapen. Many hair cells adopted an oblong or irregular shape (**Fig. 23B**, asterisk), and the evenly spaced “hourglass” shape of supporting cell apical domains was frequently jumbled and distorted (**Fig. 23B**). We next examined transverse cochlear sections. In control sections, hair cell nuclei were invariably located a uniform distance from the luminal surface of the epithelium (**Fig. 23C**). In contrast, the *Lis1*^{CKO-early} sensory epithelium was disorganized with hair cell nuclei frequently found at varying distances from the luminal surface (**Fig. 23D**).

The checkerboard pattern of the organ of Corti is regulated by the nectin family of cell adhesion molecules [32]. We therefore examined the localizations of nectin-1, -2 and -3 in E18.5 cochleae. In the control, all three nectins were localized to hair cell-supporting cell contacts, consistent with their role in mediating heterotypic adhesion between these two cell types [32] (**Fig. 23G,I,K**). By contrast, localization of all three nectins at cell-cell contacts was reduced in

Lis1^{CKO-early} cochleae, with nectin-1 and -3 more affected than nectin-2 (**Fig. 23H,J,L**). Junctional localization of E-cadherin, on the other hand, was not significantly changed (**Fig. 24B**). These results suggest that impaired nectin-mediated cell adhesion contributes to the cellular organization defects in the *Lis1*^{CKO-early} organ of Corti.

4.2.4 Lis1 regulates Rac-PAK signaling in embryonic hair cells

Given the role of Lis1 as a regulator of cytoplasmic dynein in other systems, we investigated dynein localization using an antibody against the dynein intermediate chain [261]. Immunostaining of E17.5 control hair cells revealed a cloud of dynein in the apical cytoplasm, with a higher concentration in the pericentriolar region (**Fig. 25A**). In *Lis1*^{CKO-early} hair cells, dynein is still found in the pericentriolar region, but it was more diffuse (**Fig. 25A**), indicating a role for Lis1 in regulating dynein localization in hair cells.

To elucidate the mechanisms underlying the planar polarity and cellular organization defects, we next examined Rac-PAK signaling in *Lis1*^{CKO-early} cochleae. Our previous work suggests a model in which microtubule-mediated transport regulates localized activation of Rac-PAK signaling on the hair cell cortex [250]. This model predicts that regulators of microtubule organization may be important for cortical Rac-PAK signaling. In support of this idea, *Lis1*^{CKO-early} and *Rac1*^{CKO} mutants have similar planar polarity and cellular organization defects [30]. To further test this hypothesis, we measured the levels of activated PAK using a phospho-specific antibody (pPAK). Immunoblotting of *Lis1*^{CKO-early}

cochleae showed a significant decrease in the ratio of pPAK to total PAK1 in mutants (0.77 ± 0.05) when compared to controls (1.14 ± 0.09 ; $p=0.006$) (**Fig. 26A**).

To more directly assess Rac signaling *in situ*, we examined the localization of active, GTP-bound Rac1 in E17.5 cochleae using an antibody specific for Rac1-GTP alongside a pan-Rac1 antibody to localize the total pool of Rac1 simultaneously. In agreement with previously reported pPAK localization [30, 250], Rac1-GTP was enriched on the lateral hair cell cortex in the control, whereas total Rac1 was uniformly distributed along the circumference of the hair cell (**Fig. 26B,D,F,H**). In addition, Rac1-GTP was also detected in the pericentriolar region and on the stereocilia (**Fig. 25B**). In *Lis1*^{CKO-early} cochleae, the cortical domain of Rac1-GTP was significantly reduced and/or misoriented relative to the medial-lateral axis of the cochlea (**Fig. 26C,E,G,I**). In addition, localization of Rac1-GTP in the pericentriolar region was also disorganized and diffuse, while it was still detected on the hair bundle (**Fig. 25B**). These results indicate that Lis1 regulates localized Rac1 activity at the hair cell cortex and other subcellular locations.

Our previous work identified the Rac GEF Tiam1 as a possible cargo of kinesin-II implicated in activating Rac signaling during planar polarization of hair cells [250]. In other systems, Tiam1 associates with microtubules and regulates polarity [235]. Furthermore, the Tiam1 homolog Tiam 2/STEF has been shown to mediate microtubule-dependent Rac activation during cell migration [176]. We sought to determine if the microtubule disorganization observed in *Lis1*^{CKO-early}

hair cells could impact Tiam1 distribution. At E17.5, Tiam1 is highly enriched on microtubules and the kinocilium in control hair cells (**Fig. 26J,L,N**, arrows; **Fig. 25C-E**). In *Lis1*^{CKO-early} hair cells, while still detected on microtubules, Tiam1 staining was greatly disorganized or diminished in cells with disorganized microtubules (**Fig. 26K,M,O**, arrows). These data suggest a potential role for microtubule-associated Tiam1 in stimulating cortical Rac-PAK activity.

4.2.5 Lis1 is required for maintaining the V-shape of hair bundles during postnatal development

Having demonstrated a role for Lis1 in planar polarization of embryonic hair cells, we next sought to determine the function of Lis1 in postnatal hair cells. To this end, we generated *Atoh1*^{Cre}; *Lis1*^{flox/flox} mice (hereafter referred to *Lis1*^{CKO-late}). In contrast to *Lis1*^{CKO-early} mutants, two Cre-mediated recombination events are required to generate a *Lis1* deficient hair cell. Since Lis1 protein levels correlate tightly with gene dosage [262], we reasoned that the combined effects of slower DNA excision and longer protein perdurance in *Lis1*^{CKO-late} would enable slower depletion of Lis1 compared to *Lis1*^{CKO-early} mutants. Immunostaining confirmed a near complete absence of Lis1 protein in hair cells in the basal region of P1 *Lis1*^{CKO-late} OC (**Fig. 19J,K**).

At P0, the *Lis1*^{CKO-late} OC had normal cellular organization (**Fig. 27B**). Hair bundle morphology and orientation were also normal, suggesting that Lis1 function in the *Lis1*^{CKO-late} cochlea was sufficient to sustain the embryonic phase of hair cell morphogenesis. However, starting around P2 and following a base-

to-apex gradient along the cochlea, some *Lis1*^{CKO-late} outer hair cells displayed hair bundle morphology defects ranging from a flattened bundle (**Fig. 27D**, arrow; **27F,G**) to splitting of the bundle into two separate groups of stereocilia (**Fig. 27D**, arrowheads; **27H-J**). Rarely, hair bundles were severely dysmorphic or completely fragmented (**Fig. 27K**). Overall, 13% of *Lis1*^{CKO-late} hair bundles in outer hair cell rows exhibited a flattened morphology, 8% were split, and 1% were dysmorphic (**Fig. 27E**). By contrast, *Lis1*^{CKO-late} vestibular hair cells in the utricular macula at P4 had no overt defects in hair bundle morphology or orientation (**Fig. 28**). These results indicate that, in addition to its earlier function, *Lis1* is required for maintaining the normal V-shape of the auditory hair bundle during postnatal development.

4.2.6 *Lis1* mediates the positioning of the hair cell centrosome near the lateral cortex

To understand the basis for the hair bundle defects in *Lis1*^{CKO-late} hair cells, we examined basal body positioning at P2. In control hair cells, the centrosome (the basal body and daughter centriole) was invariably found near the lateral pole and aligned along the medial-lateral axis of the cochlear duct (**Fig. 27L**). In contrast, the centrosome in many *Lis1*^{CKO-late} hair cells was located away from the lateral pole and toward the center of the cell, particularly in those cells with a flattened or split hair bundle (**Fig. 27M**, arrows). Indeed, the distance between the centrosome and the lateral hair cell membrane (D_{C-M}) closely correlated with hair bundle morphology defects (**Fig. 27N**). On average, D_{C-M} in *Lis1*^{CKO-late} hair

cells with a normal bundle morphology ($0.90 \mu\text{m} \pm 0.05$; $n=42$) was similar to that of controls ($0.87 \mu\text{m} \pm 0.02$; $n=60$). However, D_{C-M} was dramatically increased in *Lis1*^{CKO-late} hair cells with a flattened hair bundle ($1.55 \mu\text{m} \pm 0.06$; $n=45$) and increased still further in cells with a split hair bundle ($2.04 \mu\text{m} \pm 0.07$; $n=34$) (**Fig. 27N**). Thus, using basal body position and V-shaped hair bundle as morphological readouts for planar polarity, we conclude that Lis1 is required for the maintenance of planar polarity in postnatal hair cells.

To investigate if Wnt/PCP signaling plays a role in postnatal hair cells, we examined Dvl2 localization at P2. Similar to embryonic hair cells, Dvl2 was asymmetrically localized on the lateral hair cell membranes, suggesting a potential role for Wnt/PCP signaling in maintaining planar polarity (**Fig. 29A,E**). In *Lis1*^{CKO-late} cochleae, asymmetric Dvl2 localization was unchanged (**Fig. 29B,F**), suggesting that Wnt/PCP signaling remains intact in *Lis1*^{CKO-late} hair cells. We also wondered whether localized cortical Rac signaling persists in postnatal hair cells to maintain planar polarity. In control hair cells at P3, the cortical domain of Rac1-GTP on the lateral side of hair cells was no longer detectable (**Fig. 30A-C**), whereas Rac1-GTP was still localized to the hair bundle and pericentriolar region (**Fig. 30D-I**). Furthermore, Tiam1 localization to microtubules but not the kinocilium was greatly reduced compared to embryonic hair cells (**Fig. 30J-O**). Together, these results suggest a developmental downregulation of Tiam1-mediated cortical Rac activation.

4.2.7 Lis1 is required for proper dynein localization and pericentriolar matrix organization

To understand the basis for the centrosome positioning defects in *Lis1*^{CKO-late} hair cells, we next examined the localization of cytoplasmic dynein.

Immunostaining of dynein intermediate chain in control hair cells at P2 revealed a three-dimensional lattice of dynein in the pericentriolar region, extending from the centrosome basally for approximately 2 μ m to the level of Dvl2 membrane localization (**Fig. 29C**, arrowhead). At the plane of the centrosome, dynein formed an organized ring surrounding the centrosome and also localized to one of the centrioles (**Fig. 29G,I**, arrow). Dynein staining was also detected on the cell cortex, partially overlapping with Dvl2 (**Fig. 29E**, inset). In *Lis1*^{CKO-late} hair cells, instead of an organized three-dimensional lattice, dynein formed an irregular, diffuse cloud. At the plane of the centrosome, dynein collapsed inward toward the centrosome and was no longer detectable on centrioles (**Fig. 29H,J**). At the level of Dvl2 crescents, dynein was still detected extending basally from the pericentriolar cloud (**Fig. 29D**, arrowheads) and on the cell cortex, partially overlapping with Dvl2 (**Fig. 29F**, inset). These results indicate that Lis1 is required for normal dynein localization around the centrosome in hair cells. Next we asked if Lis1-dynein function is important for hair cell pericentriolar matrix organization, similar to other cell types [263–265]. We examined the localization of the PCM-1 protein (pericentriolar material 1), a pericentriolar matrix component important for recruitment of other centrosomal proteins [266, 267]. In control hair cells at P3, PCM-1 was localized in a tight ring in the

pericentriolar region, which formed interior to the dynein lattice approximately 0.2 μm below the daughter centriole (**Fig. 31A; 31C**, inset). In contrast, PCM-1 in *Lis1*^{CKO-late} hair cells failed to organize into a ring-like structure and instead collapsed inward toward the centrioles, forming a diffuse cloud interior to the dynein clusters (**Fig. 31B; 31D**, inset). Thus, centrosome mispositioning in *Lis1*^{CKO-late} hair cells is associated with dynein and pericentriolar matrix organization defects.

4.2.8 Microtubule organization defects in *Lis1*^{CKO-late} hair cells

Lis1-dynein function in pericentriolar matrix organization regulates the interphase microtubule array in other systems [268, 269]. We therefore examined microtubule organization in *Lis1*^{CKO-late} hair cells at P2, when hair bundle and dynein defects are beginning to manifest. In control hair cells, an aster-shaped microtubule array emanated from the pericentriolar matrix toward the cortex in all directions but was more prominent on the lateral side of the cell (**Fig. 31E,G,I**). Individual microtubules appear to extend laterally and basally to contact the cortex and then curl around the circumference of the cell (**Fig. 31I**). In *Lis1*^{CKO-late} hair cells, the organization of the cytoplasmic microtubule array was severely disrupted; the ring-like organization of the minus-ends of microtubules collapsed inward and became more focused around the centrosome (**Fig. 31F,H**). This was particularly evident in *Lis1*^{CKO-late} cells with flattened or split bundles (**Fig. 31F,H**, arrowhead; **31J**, plane z). Instead of fanning out basally to form an aster shaped array, microtubules in many *Lis1*^{CKO-late} cells lacked apparent organization

and directionality (**Fig. 31F,H**, arrows; **31J,K**). In some cells, microtubules organized into thick bundles that wrapped around the circumference of the cell (**Fig. 31J**, plane z'). Overall, *Lis1*^{CKO-late} hair cells appeared to have a reduced concentration of microtubules on the lateral side of the hair cell and more microtubules on the medial side of the cell (**Fig. 31K**, plane z'). Together, these results suggest that dynein and pericentriolar matrix defects in *Lis1*^{CKO-late} hair cells result in disorganization of the microtubule network.

4.2.9 Lis1 deficiency leads to organelle distribution defects and subsequent outer hair cell death

In cultured cells, Lis1 and dynein regulate organelle position [270, 271]. We therefore determined if the distributions of the Golgi and mitochondria were perturbed in *Lis1*^{CKO-late} hair cells. At P2, the Golgi complex in control hair cells consisted of complex tubule structures (**Fig. 32A**) that were confined to a region just basal to the cuticular plate of the hair cell (**Fig. 32B**, bracket). Similarly, mitochondria were distributed throughout the cell body but were enriched in the apical cytoplasm (**Fig. 32E,F**). By contrast, in *Lis1*^{CKO-late} hair cells, the Golgi complex appeared fragmented with vesicles spread throughout the cytoplasm (**Fig. 32C,D**). Mitochondria were also highly dispersed, and the apical population of mitochondria was greatly diminished (**Fig. 32G,H**). Taken together, these Golgi and mitochondria defects support a universal function of Lis1-dynein in organelle positioning.

To determine if the organelle positioning defects triggered stress responses in *Lis1*^{CKO-late} hair cells, we immunostained for CHOP, a transcription factor induced by both endoplasmic reticulum (ER) and mitochondrial stress [272, 273]. CHOP was not detectable in control hair cells. In *Lis1*^{CKO-late} hair cells, though we did see occasional CHOP-positive cells, they were in the process of being extruded from the sensory epithelium (**Fig. 33**, arrows), suggesting that *Lis1*-deficiency does not induce a global unfolded protein response.

To determine the fate of *Lis1*^{CKO-late} hair cells, we examined *Lis1*^{CKO-late} cochleae a few days after the onset of hair bundle and organelle defects. Beginning around P5 and proceeding in a wave from the basal region of the cochlea toward the apex, outer hair cells began to undergo apoptotic cell death, as indicated by cleaved caspase-3 immunostaining, and were extruded from the sensory epithelium (**Fig. 32J**). By P7 the basal region of the *Lis1*^{CKO-late} cochlea was devoid of outer hair cells (**Fig. 32M,N**). These results reveal a requirement for *Lis1* for auditory hair cell survival.

4.2.10 Additional experiments

4.2.10.1 Constitutive Rac1 activity disrupts hair bundle morphology

Our results indicate that *Lis1* regulates localized Rac-PAK signaling at the hair cell cortex and other subcellular locations. Without *Lis1*-dynein function in hair cells, we predict that the Rac GEF Tiam1 would not be delivered efficiently to the cell cortex, leading to decreased Rac-PAK signaling and defects in polarization. Therefore, increasing the levels of active Rac might compensate for

Lis1 deficiency. To test this idea, we used a constitutively active allele of Rac1 (*R26Rac1**) that is expressed upon Cre-mediated excision of a STOP cassette [274]. Expression of *R26Rac1** should result in a cell-wide increase in Rac signaling levels. *Atoh1-Cre* was used to induce Rac1 activation in developing hair cells. At P0, *R26Rac1** OC contain some hair cells with flattened (**Fig. 34B**, arrowhead) or split (**Fig. 34B**, arrow) hair bundles.

We next generated *Lis1*^{ckO-early}; *R26Rac1** mice and examined their hair bundle morphology for rescue of the *Lis1*^{ckO-early} phenotypes. We were able to recover a single P1 *Lis1*^{ckO-early} survivor for comparison, likely due to its relatively mild phenotype (**Fig. 34D**). *Lis1*^{ckO-early}; *R26Rac1** OC contained hair cells with both flattened and split hair bundles (**Fig. 34E**, arrows). Notably, the patterning of the OC was relatively normal, though we did occasionally observe dying hair cells. These results are difficult to interpret given that *R26Rac1** activates Rac1 throughout the cell and, thus, does not reflect the normal level and/or spatial distribution of Rac signaling. In particular, the precise cortical localization of Rac signaling, which we believe crucial for proper hair cell polarization, is unlikely to be reproduced in the *R26Rac1** hair cells. Moreover, the hair bundle defects we observed could be due to Rac1's role in regulating the actin of the stereocilia.

4.2.10.2 *Tiam1* regulates OC cellular patterning

Our results suggest that the GEF *Tiam1* regulates the activation of Rac-PAK signaling at the hair cell cortex during planar polarization. If this is the case, depletion of *Tiam1* should disrupt normal hair bundle development by inducing

changes in the levels or localization of Rac-PAK signaling, perhaps mimicking the *Lis1*^{CKO-early} phenotype. To substantiate an *in vivo* requirement of Tiam1 for Rac activation in hair cells, we analyzed the phenotype of *Tiam1*-deficient hair cells (kindly provided by John Collard, The Netherlands Cancer Institute). At P0, *Tiam1*^{+/-} OCs exhibited normal cellular organization, and hair bundle morphology and orientation were normal (**Fig. 35A,C**). In contrast, the patterning of *Tiam1*^{-/-} OCs was disrupted, with jumbled OHC rows that frequently contained stretches either lacking an OHC row or with an extra OHC row (**Fig. 35B,D**). Notably, the hair bundle morphology and orientation of *Tiam1*-null hair cells were completely normal. Limited amounts of tissue precluded us from analyzing the levels of Rac-PAK signaling in *Tiam1*^{-/-} hair cells.

These preliminary results indicate that *Tiam1* is required for establishing normal cellular patterning in the OC, while it is dispensable for planar polarization of the hair bundle. The lack of hair bundle defects in *Tiam1*^{-/-} could be explained by functional overlap between related Tiam GEFs, which show redundancy in structure and binding partners [275, 276]. Experiments designed to further investigate the role of Tiam family GEFs during hair cell polarization are presented in **Section 6.4**.

4.2.10.3 *In vivo* imaging of *Lis1*^{CKO-late} hair bundle development

In order to characterize the progression of the cytoskeletal changes leading to the *Lis1*^{CKO-late} hair bundle defects, we imaged live cochlear explants using an upright multiphoton confocal microscope. These experiments used

GFP-centrin2 to mark the position of the centrosome [230]. In addition, the *Rosa26-mT/mG* line, which expresses membrane-bound Tomato or GFP depending on the presence of Cre, was used to label the hair bundle and cell membranes [277]. Cochlear explant cultures from early postnatal *Lis1*^{CKO-late}, *GFP-centrin2*; *mT/mG* mice were established on coverslips and maintained until the equivalent of P5 when they were imaged. Z-stacks encompassing the apical region of hair cells were collected every 30 minutes for 6 hours. Hair bundles were clearly labeled with GFP, and individual hair cell centrioles could be discerned (**Fig. 36**, arrow). Hair bundles exhibiting the characteristic *Lis1*^{CKO-late} flattened (**Fig. 36**, yellow box) or split (**Fig. 36**, orange box) morphologies were prevalent in the culture. Despite apparently capturing hair bundles in the process of splitting (**Fig. 36**, red box), we were unable to detect significant changes in hair bundle morphology over the course of six hours. Nevertheless, these pilot experiments demonstrate the feasibility of using live imaging in cochlear explants to investigate the behaviors of the hair bundle and hair cell centrosome during development *in vivo*.

4.3 Discussion

In this study, we have undertaken a comprehensive analysis of *Lis1* and dynein function in developing auditory hair cells. Our results reveal a critical function of *Lis1* in dynein localization and microtubule organization and provide novel insights into the *Lis1*- and microtubule-mediated processes critical for hair cell planar polarity during both embryonic and postnatal development. In addition,

we demonstrate that *Lis1* is required for proper organelle positioning and hair cell survival.

Together with recent advances, our results provide strong support for a two-tier hierarchy of hair cell planar polarity regulation. The core PCP pathway generates extrinsic or tissue polarity cues that are interpreted within hair cells by a cell-intrinsic effector machinery. These cell-intrinsic processes are capable of operating independently of inputs from the tissue polarity pathway to drive planar polarization of individual cells, as core PCP genes are not required for establishing planar polarity features including polarized basal body position, V-shaped hair bundle, and the asymmetric cortical domain of Rac-PAK activity.

We show that asymmetric localization of Dvl2 is maintained when *Lis1* is deleted in hair cells, suggesting that tissue polarity cues set up by the core PCP pathway remain intact. Of note, while *Atoh1^{Cre}* is expressed predominantly in hair cells, we cannot rule out the possibility that supporting cells contribute to the phenotypes we observed in *Lis1*-null OC. We propose that *Lis1* is a component of the cell-intrinsic effector machinery in embryonic hair cells that controls localized cortical Rac-PAK activity through microtubule-mediated transport. At the onset of planar polarization, the arrival of the basal body at the lateral pole of the hair cell tightly correlates with asymmetric cortical PAK activity [30]. Importantly, hair cell planar polarization is disrupted in *Kif3a*-deficient hair cells, where active PAK on the cell cortex is mislocalized and diffuse, indicating that plus-end directed transport is important for constraining the cortical domain of Rac-PAK signaling [250]. Here we show a correlation between reduced cortical

Rac-PAK signaling and microtubule organization defects in *Lis1*^{ckO-early} hair cells, suggesting that Lis1-dependent microtubule organization is crucial for Rac-PAK activation on the cell cortex. Lis1 also appears to regulate Rac activity in the pericentriolar region, which likely controls hair bundle cohesion and the position of the kinocilium within the hair bundle. Furthermore, we show that the Rac GEF Tiam1 is associated with microtubules in a manner that is sensitive to microtubule organization and developmentally regulated, making it a strong candidate activator of cortical Rac-PAK signaling during planar polarization of hair cells.

Taken together, these results suggest a model whereby microtubule-associated Tiam1 translocates to the cell cortex through Lis1-mediated microtubule-cell cortex interactions to stimulate cortical Rac-PAK activation (**Fig. 37A**). Migration of the basal body to the hair cell periphery is the symmetry-breaking event that sets the cell-intrinsic effector machinery in motion. Following migration of the basal body to the hair cell periphery, centriolar microtubules interact with the nearby cell cortex, allowing translocation of the Rac GEF Tiam1 from microtubules to the cell cortex, which enables it to activate Rac-PAK signaling [278]. This cortical Rac-PAK activity strengthens local interactions between microtubules and the cell cortex through as yet unidentified cortical and cytoskeletal proteins, thus setting up a positive feedback loop that establishes the constrained domain of Rac-PAK signaling essential for proper positioning of the basal body (**Fig. 37A**). Lis1 could regulate microtubule-cell cortex interactions directly by binding to cortical proteins, such as IQGAP1 [172], and/or indirectly

through dynein-mediated cortical capture of microtubules [279–282]. Of note, similar mechanisms involving feedback loops between Rho family GTPases and polarized trafficking via the cytoskeleton have been proposed for self-polarization of unicellular organisms and other polarized cell types in the absence of extrinsic cues [283–285].

Acting upstream of the cell-intrinsic effector pathway, tissue-level PCP signaling may spatially coordinate cortical Rac-PAK activity through two potential mechanisms, which are not mutually exclusive. First, mechanical tension between hair cells and supporting cells may be involved in tissue-level PCP signaling. Genetic evidence suggests that the core PCP pathway acts in conjunction with a *Ptk7*-mediated pathway to modulate apical junctional actomyosin contractility [98, 101]. Anisotropic mechanical forces exerted on hair cells may bias the positioning of the basal body toward the lateral pole to orient centriolar microtubules and align planar polarity in embryonic hair cells. In addition to actomyosin-mediated forces, the core PCP pathway may also regulate dynein-mediated microtubule capture at the hair cell cortex. Interestingly, Dishevelled has been shown to regulate dynein-mediated mitotic spindle orientation through interaction with NuMA (nuclear mitotic apparatus protein) in other systems [286]. NuMA, together with LGN (Leucine-Glycine-Asparagine repeat-enriched protein) and Gα, forms an evolutionarily conserved cortical protein complex which recruits cytoplasmic dynein to the cell cortex to generate pulling forces that position spindle microtubules [185, 287]. Recently, G protein-signaling modulator 2 (GPSM2), the human homolog of LGN, has been

identified as the causative gene for the nonsyndromic deafness DFNB82 [288, 289]. Thus, we speculate that a Dishevelled-dynein pathway analogous to that which mediates mitotic spindle orientation may regulate cortical microtubule capture thereby orienting centriolar microtubules in both embryonic and postnatal hair cells (**Fig. 37**).

In postnatal *Lis1*^{CKO-late} hair cells, planar polarity is established normally but is subsequently lost, as indicated by the observed basal body anchoring and bundle morphology defects. This is, to our knowledge, the first direct evidence that hair cell planar polarity must be actively maintained during early postnatal development. In contrast to embryonic hair cells, cortical Rac activity is significantly downregulated in P3 hair cells, suggesting that asymmetric cortical Rac-PAK activity is critical for the initial planar polarization process, but alternative mechanisms are employed to maintain planar polarity. Our data suggest that Dishevelled may act upstream of Lis1-dynein to maintain the centrosome position in postnatal hair cells.

Intriguingly, microtubule arrays were often more tightly focused around the centrosome in *Lis1*^{CKO-late} hair cells, consistent with loss of cortical anchoring of microtubule plus-ends. In other systems, cortical dynein plays a critical role in the regulation of microtubule growth and exerts pulling forces to position microtubule associated-structures [282, 290–293]. The buckling and bending of long microtubules around the cell cortex observed in a subset of *Lis1*^{CKO-late} hair cells is similar to the *in vitro* behavior of microtubules in the absence of end-on capture by cortical dynein (Laan et al., 2012). Based on these observations, we propose

that Lis1-dynein mediated cortical capture of microtubules, together with a microtubule organizing function at the centrosome, controls anchoring of the basal body at the lateral pole of hair cells. Proper basal body position, in turn, maintains the V-shape of the hair bundle during early postnatal development (**Fig. 37B**).

Although defects in dynein and microtubule organization were widespread in *Lis1*^{CKO-late} hair cells, only a subset develops flat or split hair bundles, suggesting that hair cells employ redundant mechanisms for maintaining proper hair bundle morphology. During early postnatal development, the apical region of the hair cell undergoes a shape change driven by actomyosin forces [229]. Also during this time period, densely bundled rootlet structures form at the base of the stereocilia to anchor them into the cuticular plate, an actin meshwork that provides rigid support [294, 295]. We suggest that the rootlets of the stereocilia and the cuticular plate serve as additional physical constraints to maintain the position of the basal body and the V-shape of the hair bundle in conjunction with Lis1-dynein. Lis1 is also required for positioning of the Golgi and mitochondria as well as hair cell survival. Importantly, cell death is not limited to cells with abnormal hair bundles, suggesting it is not merely a consequence of hair bundle defects. Further study is needed to understand these additional functions of Lis1-dynein.

4.4 Figures

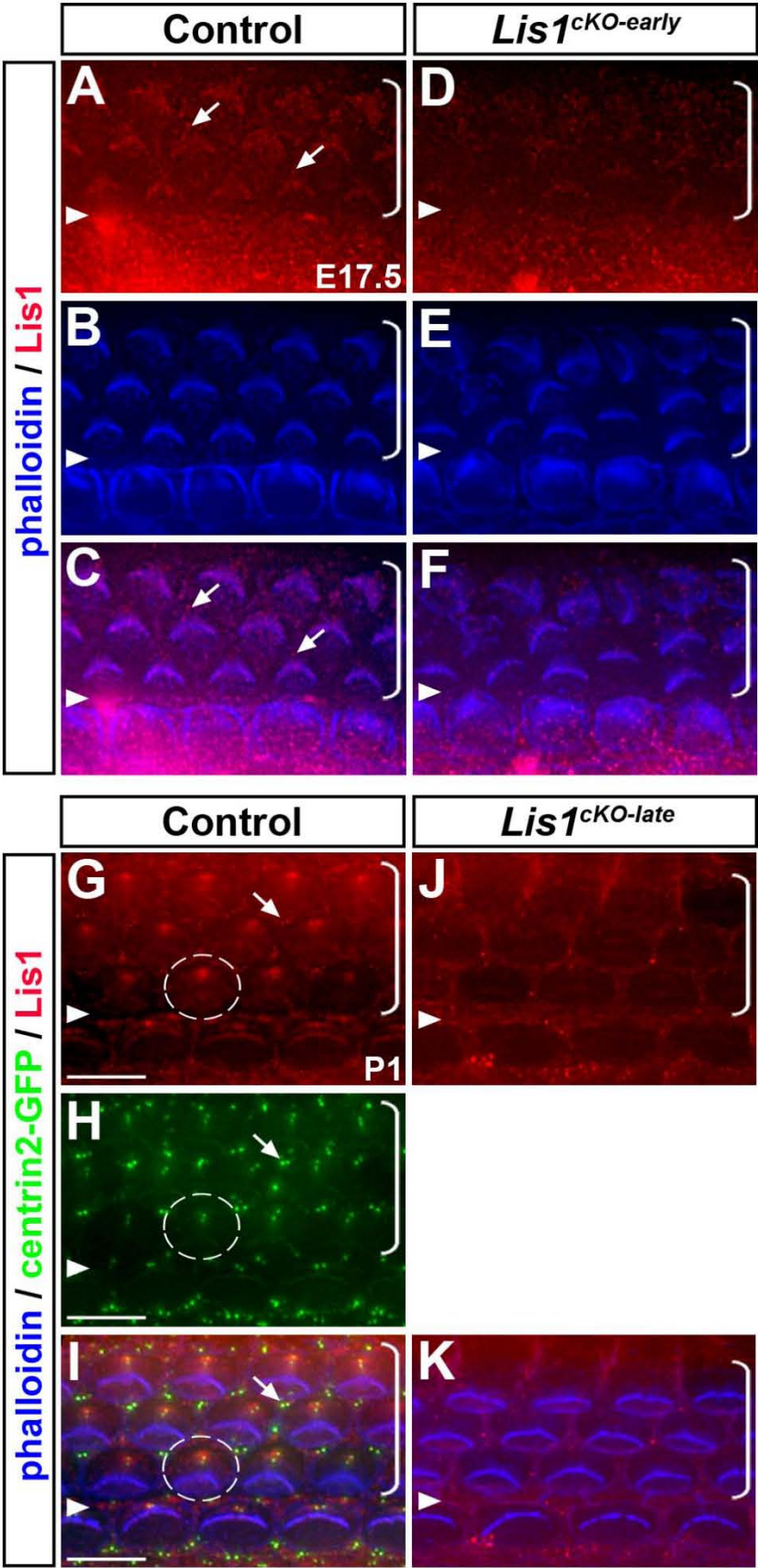


Figure 19. Lis1 expression in developing hair cells. (A-K) Immunostaining for Lis1 (red) and phalloidin (blue) in flat-mounted cochleae. (A-C) At E17.5, Lis1 is localized along the stereocilia and on the centrioles (arrows). (D-F) Lis1 expression is greatly reduced in E17.5 *Lis1^{ckO-early}* OC and no longer detectable on hair cell centrioles. (G-I) At P1, Lis1 is found in a diffuse cloud around hair cell centrioles and on the centrioles of supporting cells (arrows). Centrioles are marked with GFP-centrin2 (green). White circles outline hair cell boundaries, and arrows indicate Lis1 localization on supporting cell centrioles. (J,K) Lis1 is no longer detected in the pericentriolar region in the basal region of P1 *Lis1^{ckO-late}* OC. Triangles mark the pillar cell row, and brackets indicate outer hair cell rows. Scale bars: 6 μ m.

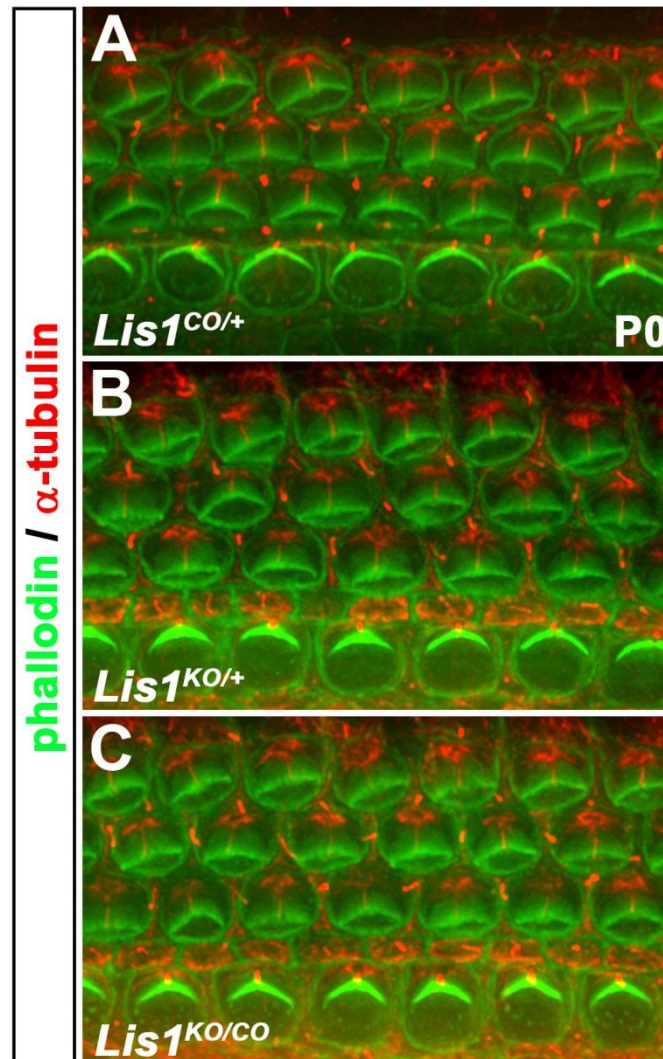


Figure 20. Normal OC patterning and hair cell development in *Lis1* heterozygote embryos. (A-C) Phalloidin (green) and α-tubulin (red) stained OC from P0 *Lis1*^{CO/+} (A), *Lis1*^{KO/+} (B) and *Lis1*^{KO/CO} (C) embryos. OC patterning, hair bundle morphology, and microtubule organization are normal.

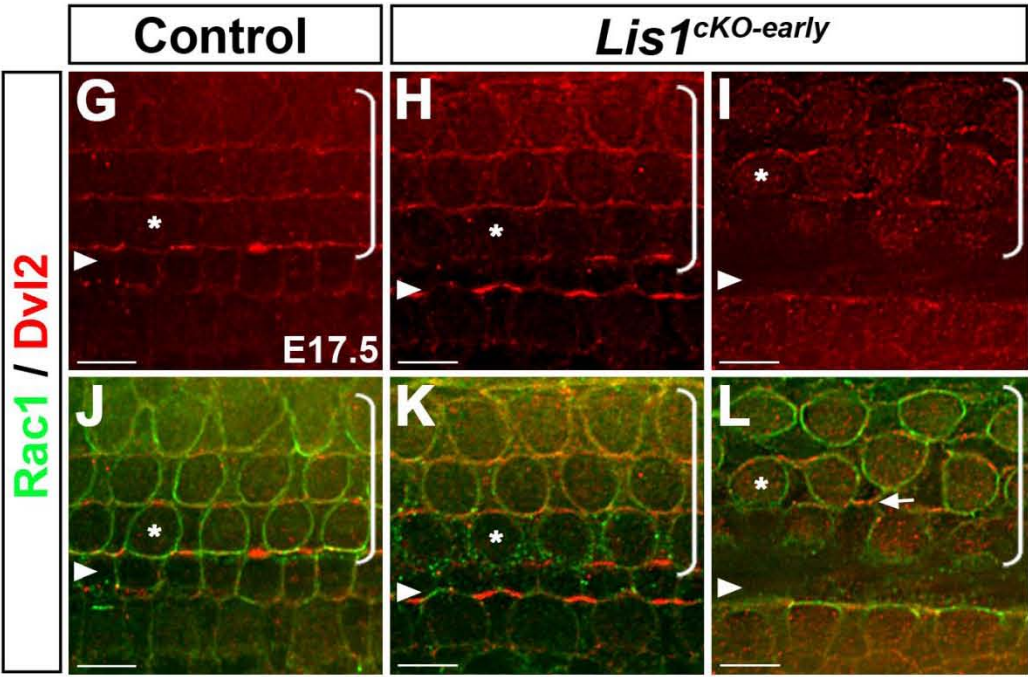
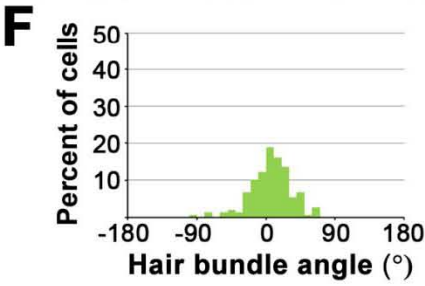
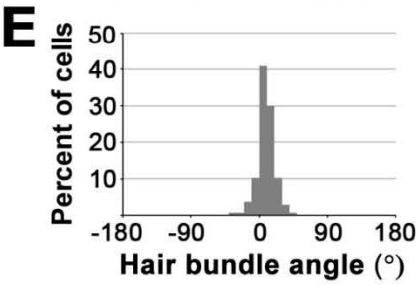
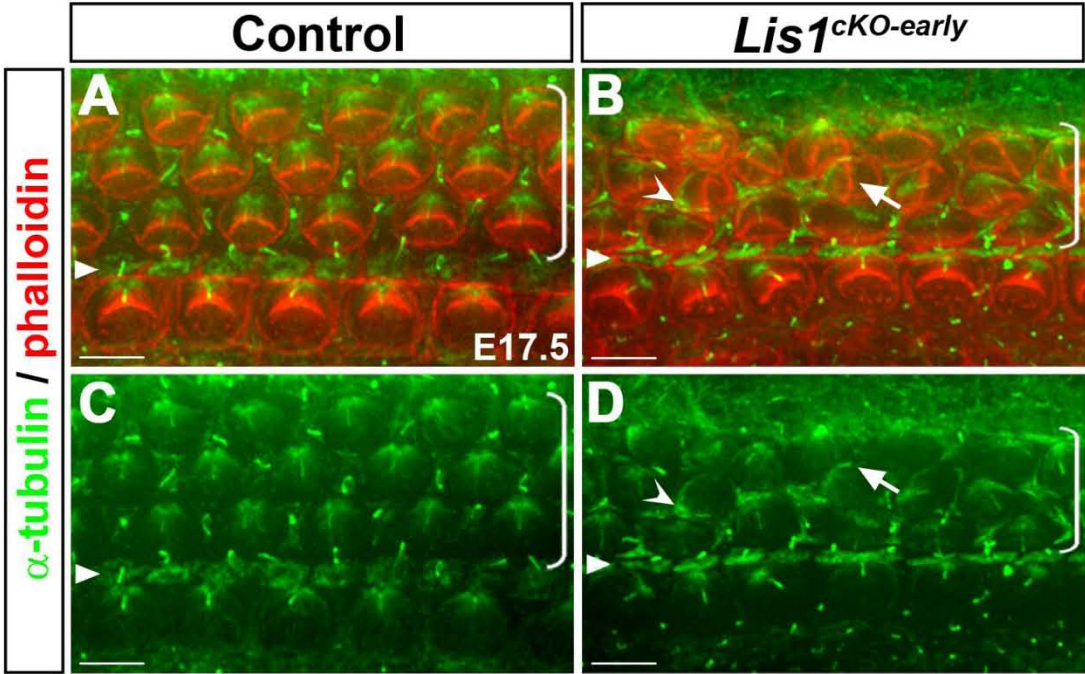


Figure 21. Planar polarity and microtubule defects in the *Lis1*^{CKO-early} organ of Corti. (A-D) E17.5 control (A,C) and *Lis1*^{CKO-early} (B,D) cochleae stained for phalloidin (red) and α -tubulin (green) to label the hair bundle and microtubules, respectively. Arrows indicate a flattened hair bundle with an off-center kinocilium. Arrowheads indicate a mispositioned centrosome. (E,F) Quantification of hair bundle orientation in E18.5 control (E; n=137) and *Lis1*^{CKO-early} (F; n=148) cochleae. (G-L) Dvl2 immunostaining (red) in control (G,J) and *Lis1*^{CKO-early} organ of Corti (H,K and I,L show two representative images). Asterisks indicate examples of hair cells with Dvl2 staining on the lateral pole. Arrow in L indicates Dvl2 staining on the cell contact between two supporting cells. Cell boundaries are labeled by Rac1 immunostaining (green). Scale bars: 6 μ m.

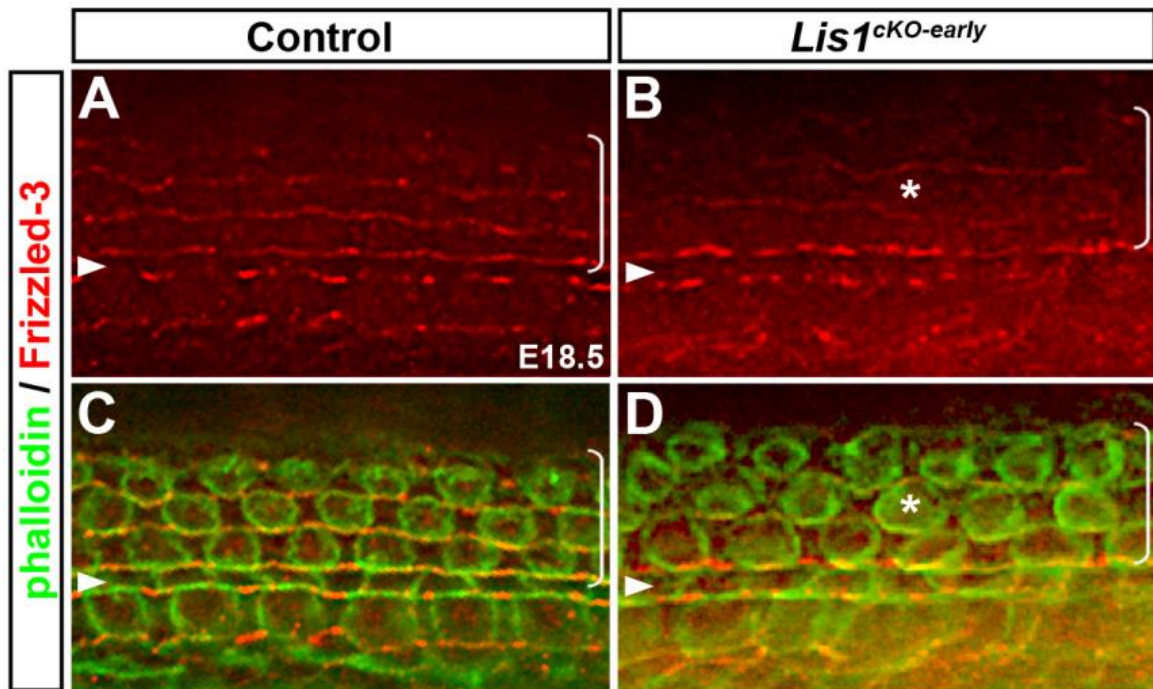


Figure 22. Frizzled-3 localization in the *Lis1*^{CKO-early} organ of Corti. (A-D) Frizzled-3 (red) and phalloidin (green) staining in E18.5 control (A,C) and *Lis1*^{CKO-early} (B,D) OC. Asterisk indicates a *Lis1*^{CKO-early} hair cell with asymmetric Frizzled-3 localization.

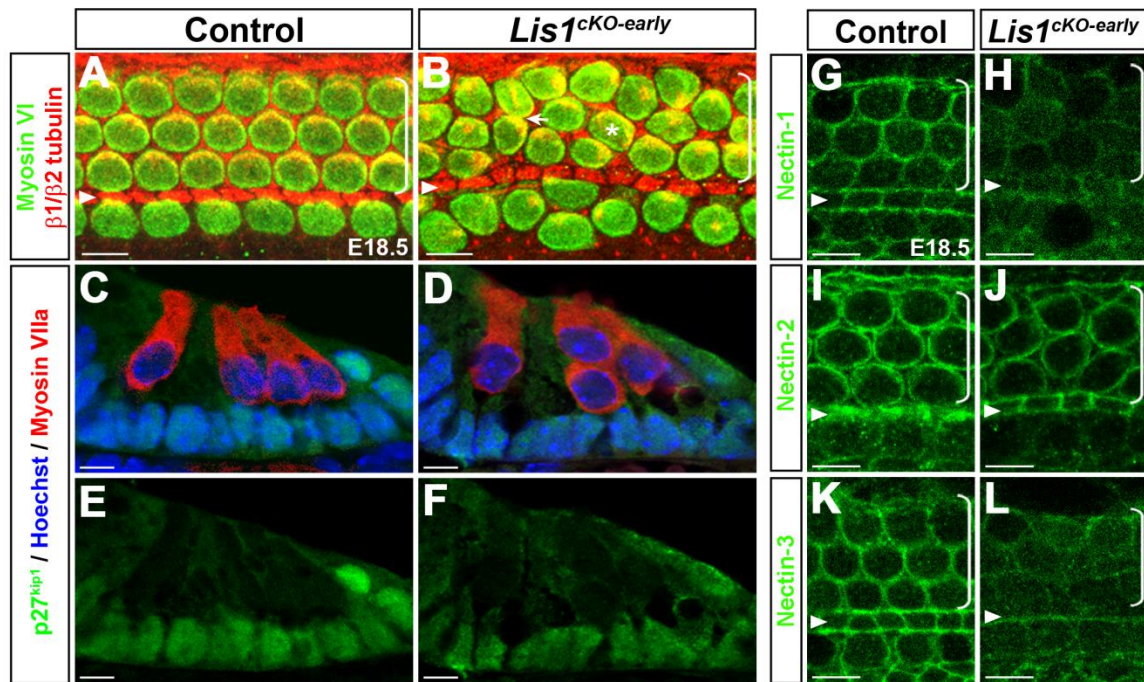


Figure 23. Lis1 regulates cellular organization and junctional nectin localization in the organ of Corti. (A,B) Myosin VI (green) and $\beta 1/\beta 2$ tubulin (red) immunostaining in E18.5 control (A) and *Lis1*^{CKO-early} (B) cochleae. The arrow in B indicates two hair cells in contact with one another, and the asterisk marks a hair cell with an abnormal shape. (C-F) Cross sections of E18.5 control (C,E) and *Lis1*^{CKO-early} (D,F) cochleae stained for the supporting cell marker p27^{kip1} (green), the hair cell marker Myosin VIIa (red) and Hoechst (blue) to label cell nuclei. (G-L) Localization of nectin-1 (G,H), nectin-2 (I,J) and nectin-3 (K,L) in E18.5 control (G,I,K) and *Lis1*^{CKO-early} (H,J,L) organ of Corti. Scale bars: 6 μ m.

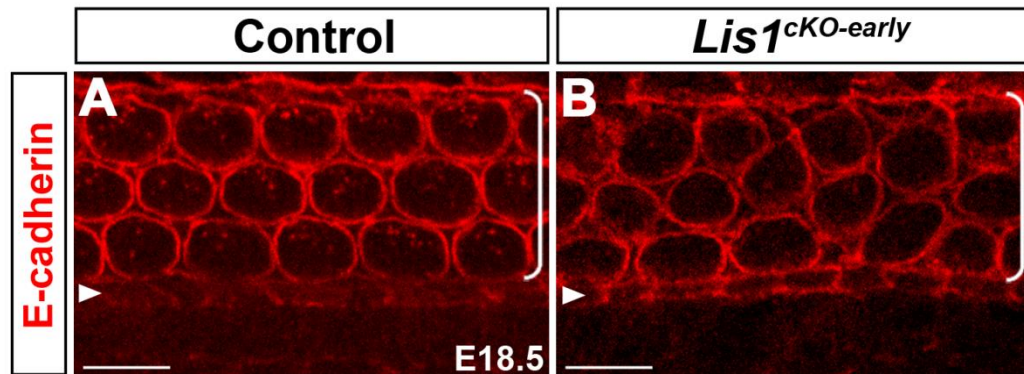


Figure 24. Normal junctional E-cadherin localization in *Lis1*^{cKO-early} hair cells. E-cadherin immunostaining (red) in E18.5 control (A) and *Lis1*^{cKO-early} (B) organ of Corti at the level of the adherens junctions. Triangles mark the pillar cell row, and brackets indicate outer hair cell rows. Scale bars: 6 μ m.

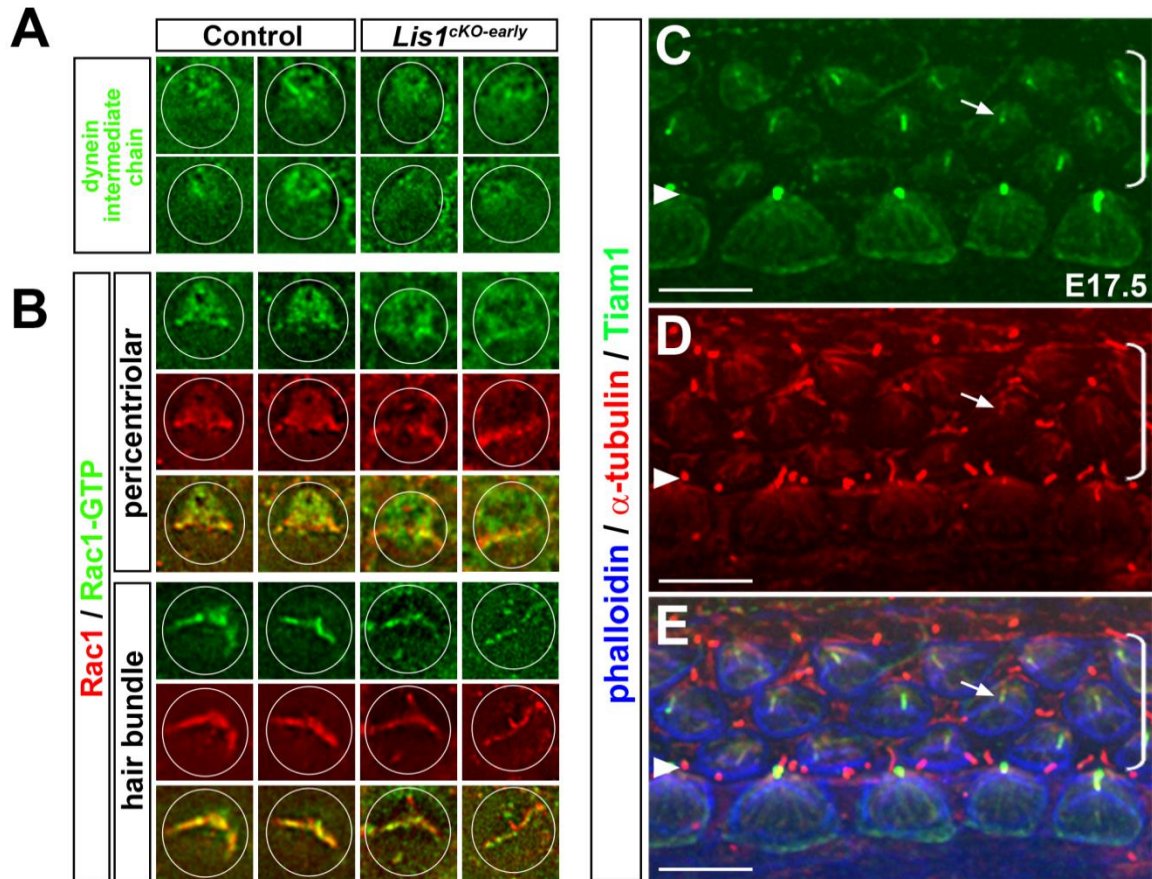


Figure 25. Subcellular localization of dynein, Rac1-GTP and Tiam1 in hair cells at E17.5. (A) Dynein intermediate chain immunostaining (green) in individual control (left panels) and *Lis1*^{cKO-early} (right panels) hair cells. Dynein in control hair cells is enriched in the pericentriolar region. In *Lis1*^{cKO-early} hair cells, dynein staining in the pericentriolar region is more diffuse. (B) Rac1-GTP (green) and Rac1 (red) immunostaining in individual control (left panels) and *Lis1*^{cKO-early} (right panels) hair cells. Each panel is an optical section taken at the level of the hair cell centrosome or the hair bundle as indicated. White circles mark individual hair cell boundaries. (C-E) Tiam1 (green) and α -tubulin (red) immunostaining in a wild-type organ of Corti. Tiam1 is enriched on the hair cell kinocilium (arrows). Triangles mark the pillar cell row, and brackets indicate outer hair cell rows. Scale bars: 6 μ m.

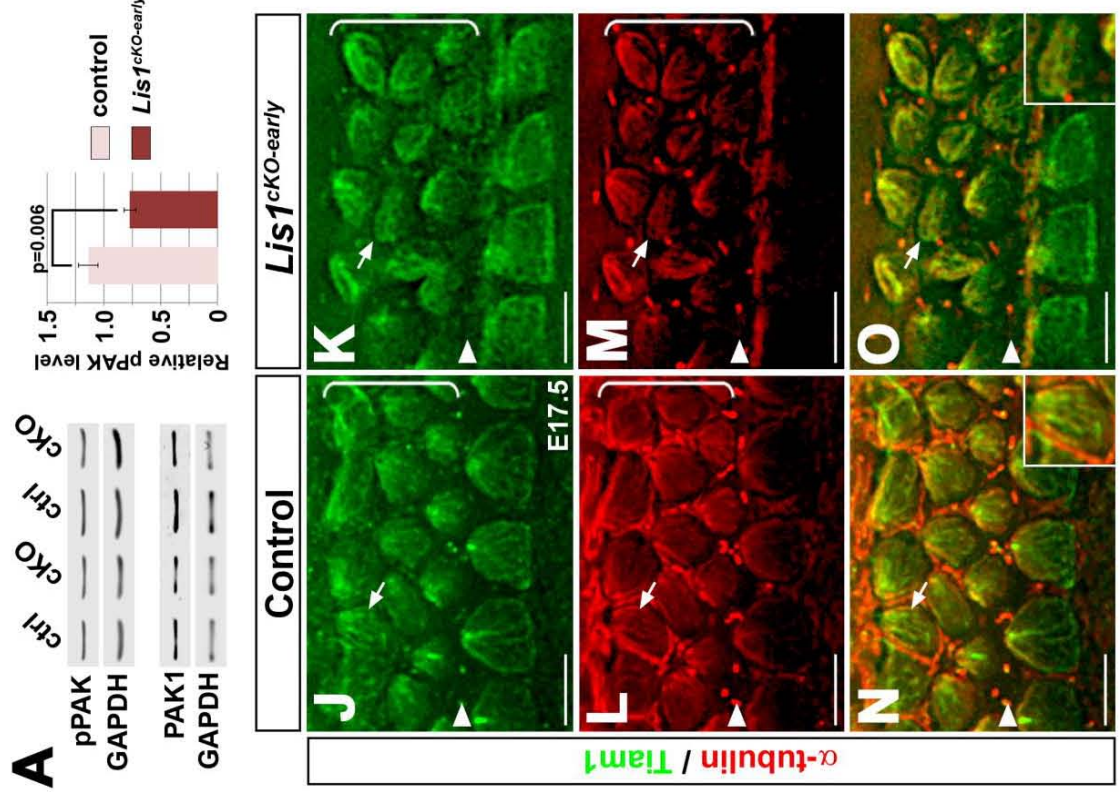
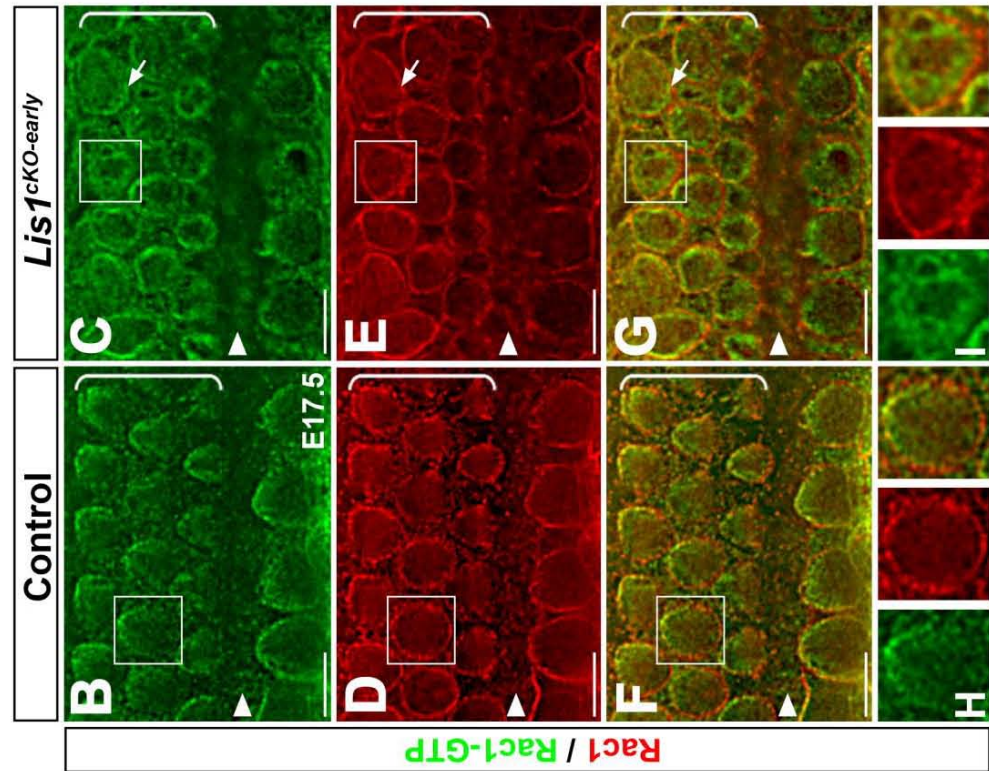


Figure 26. Lis1 mediates cortical Rac-PAK signaling likely through microtubule-associated Tiam1. (A) Western blot analysis of the levels of pPAK and PAK1 in control (ctrl) and *Lis1*^{CKO-early} (cKO) cochleae. Lysates of two cochleae from the same embryo were loaded in each lane. GAPDH served as loading control. (B-I) Localization of Rac1-GTP (green) and total Rac1 (red) in E17.5 control (B,D,F,H) and *Lis1*^{CKO-early} (C,E,G,I) cochleae. Boxed control and *Lis1*^{CKO-early} cells are shown in higher magnification in H and I, respectively. (J-O) Colocalization of Tiam1 (green) and α -tubulin (red) in E17.5 control (J,L,N) and *Lis1*^{CKO-early} (K,M,O) organ of Corti. The cells indicated by arrows are shown in higher magnification insets. Scale bars: 6 μ m.

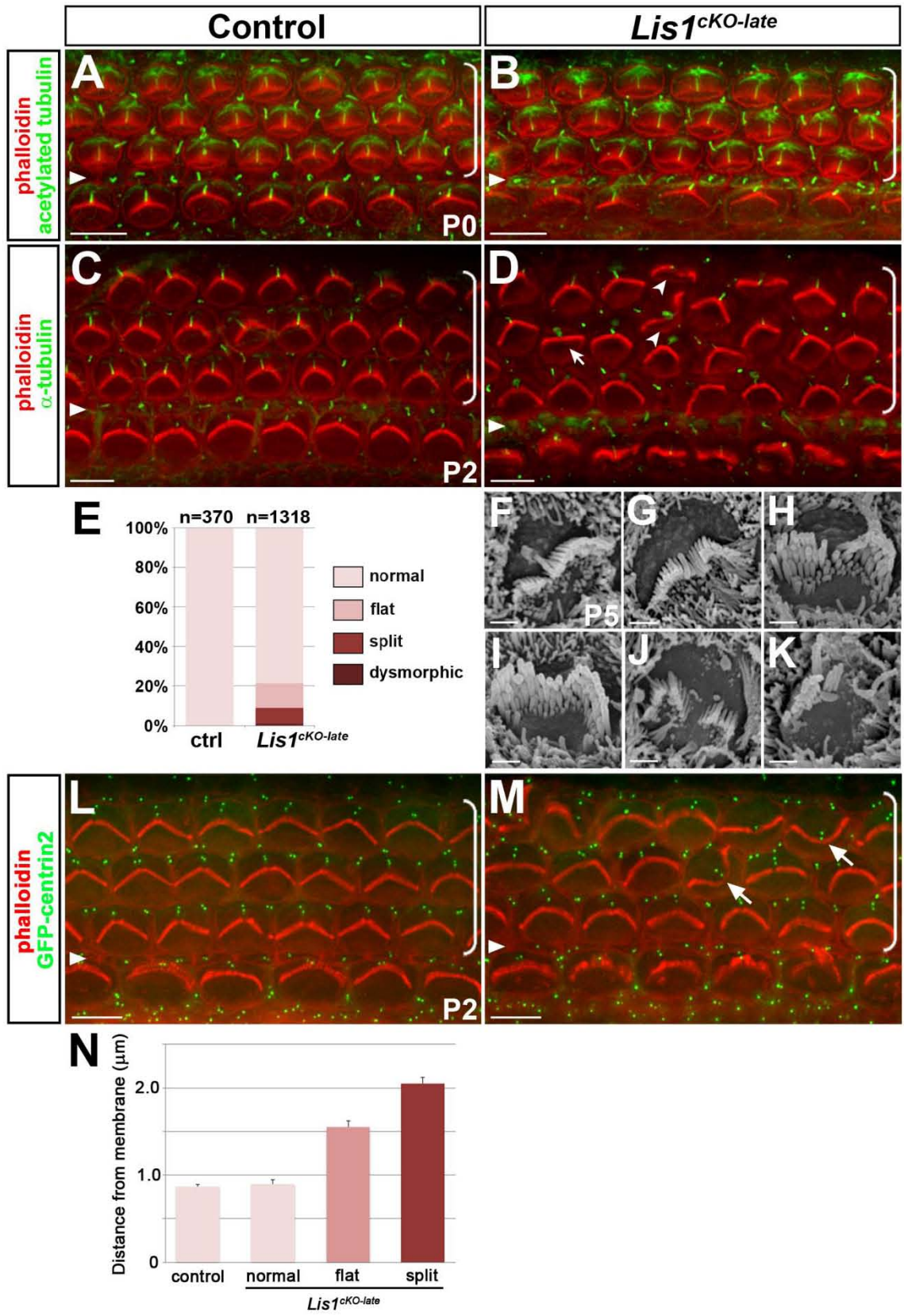


Figure 27. Lis1 is critical for maintaining hair bundle morphology and centrosome position in the postnatal organ of Corti. (A,B) Acetylated-tubulin (green) and phalloidin (red) staining of P0 control (A) and *Lis1*^{CKO-late} (B) cochleae. (C,D) α -tubulin (green) and phalloidin (red) staining of P2 control (C) and *Lis1*^{CKO-late} (D) cochleae. (E) Graph shows the penetrance of the hair bundle morphology phenotypes observed in the *Lis1*^{CKO-late} cochleae. (F-K) Scanning electron micrographs of P5 *Lis1*^{CKO-late} outer hair cells showing hair cells with flattened (F,G), split (H-J), and dysmorphic hair bundles (K). (L,M) Centrosome position (marked by GFP-centrin2, green) correlates with hair bundle morphology in P2 control (L) and *Lis1*^{CKO-late} (M) hair cells. Arrows in M indicate *Lis1*^{CKO-late} hair cells with split hair bundles and centrally placed centrosomes. (N) Quantification of the distance between the centrosome and the lateral hair cell membrane (D_{C-M}) in control and *Lis1*^{CKO-late} hair cells. Scale bars: A-D, L-M, 6 μ m; F-K, 2 μ m.

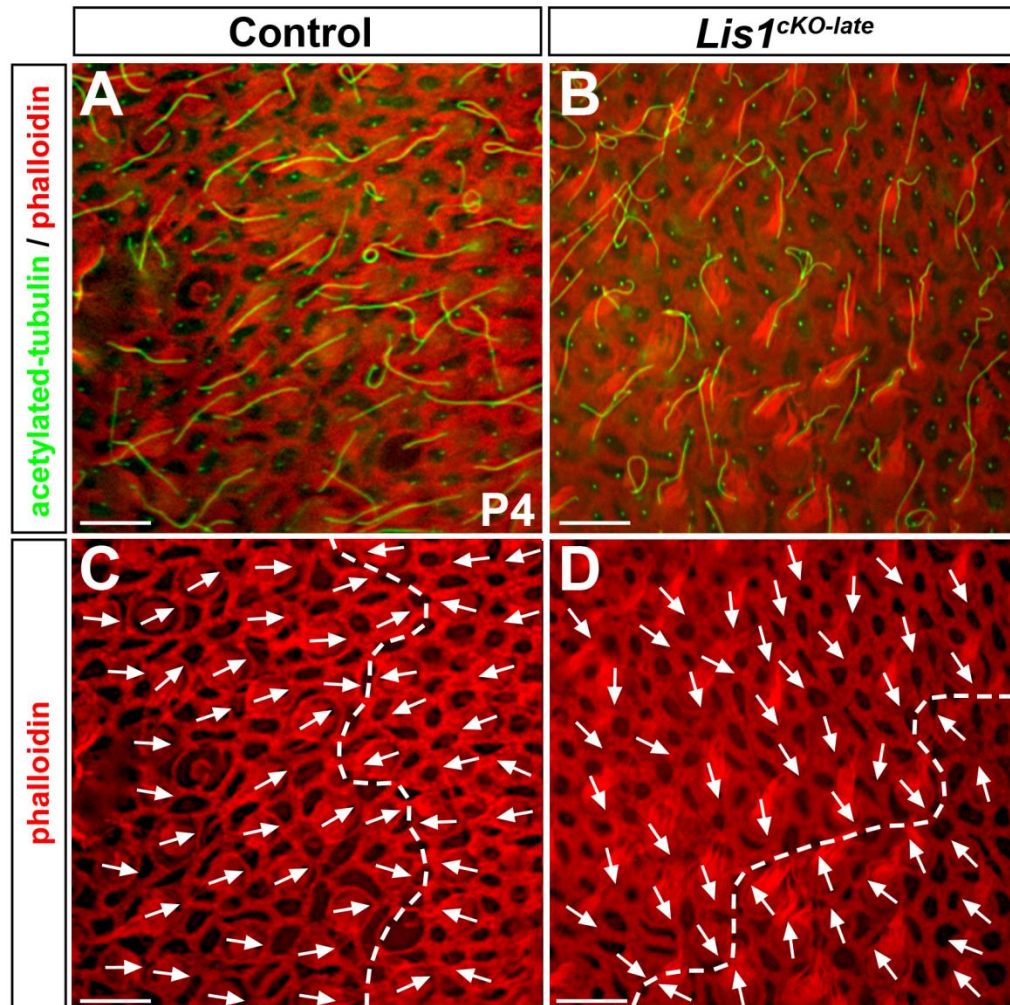


Figure 28. Normal hair bundle morphology and polarity in the *Lis1*^{CKO-late} utricle. (A-D) Acetylated-tubulin (green) and phalloidin (red) staining in P4 control (A,C) and *Lis1*^{CKO-late} (B,D) utricles. (A,B) Hair bundle morphology and kinocilium position are normal in *Lis1*^{CKO-late} utricular hair cells (B) compared to controls (A). (C,D) Planar polarity of hair cells appears normal in *Lis1*^{CKO-late} utricles (D) compared to controls (C). Panels show Z-sections taken at the level of the cuticular plate. Arrows indicate planar polarity as revealed by actin staining of the cuticular plate. Dotted lines indicate the line of reversal. Scale bars: 6 μm.

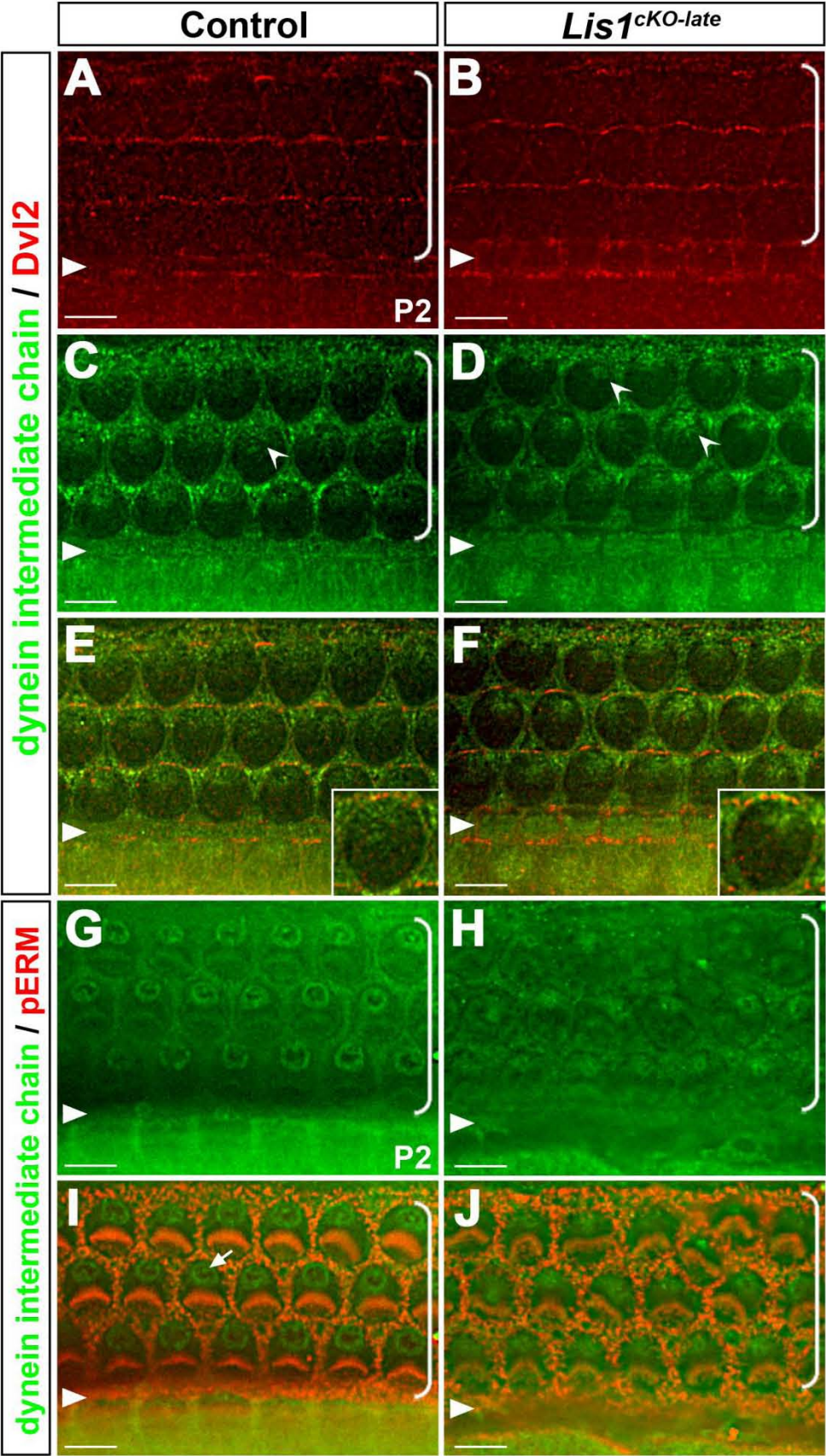


Figure 29. Lis1 is required for dynein localization around the hair cell centrosome. (A-F) Immunostaining of Dvl2 (red) and dynein intermediate chain (green) in P2 control (A,C,E) and *Lis1*^{CKO-late} (B,D,F) hair cells. Higher magnification insets in E and F show overlapping cortical staining of Dvl2 and dynein. Arrowheads indicate the basal terminus of the dynein lattice that surrounds the centrosome, which had a more variable and irregular shape in *Lis1*^{CKO-late} hair cells (D). (G-J) Immunostaining of dynein intermediate chain (green) at the level of the hair cell centrosome in P2 control (G,I) and *Lis1*^{CKO-late} (H,J) organ of Corti. phospho-ERM (pERM, red) labels stereocilia and supporting cell microvilli. Scale bars: 6 μ m.

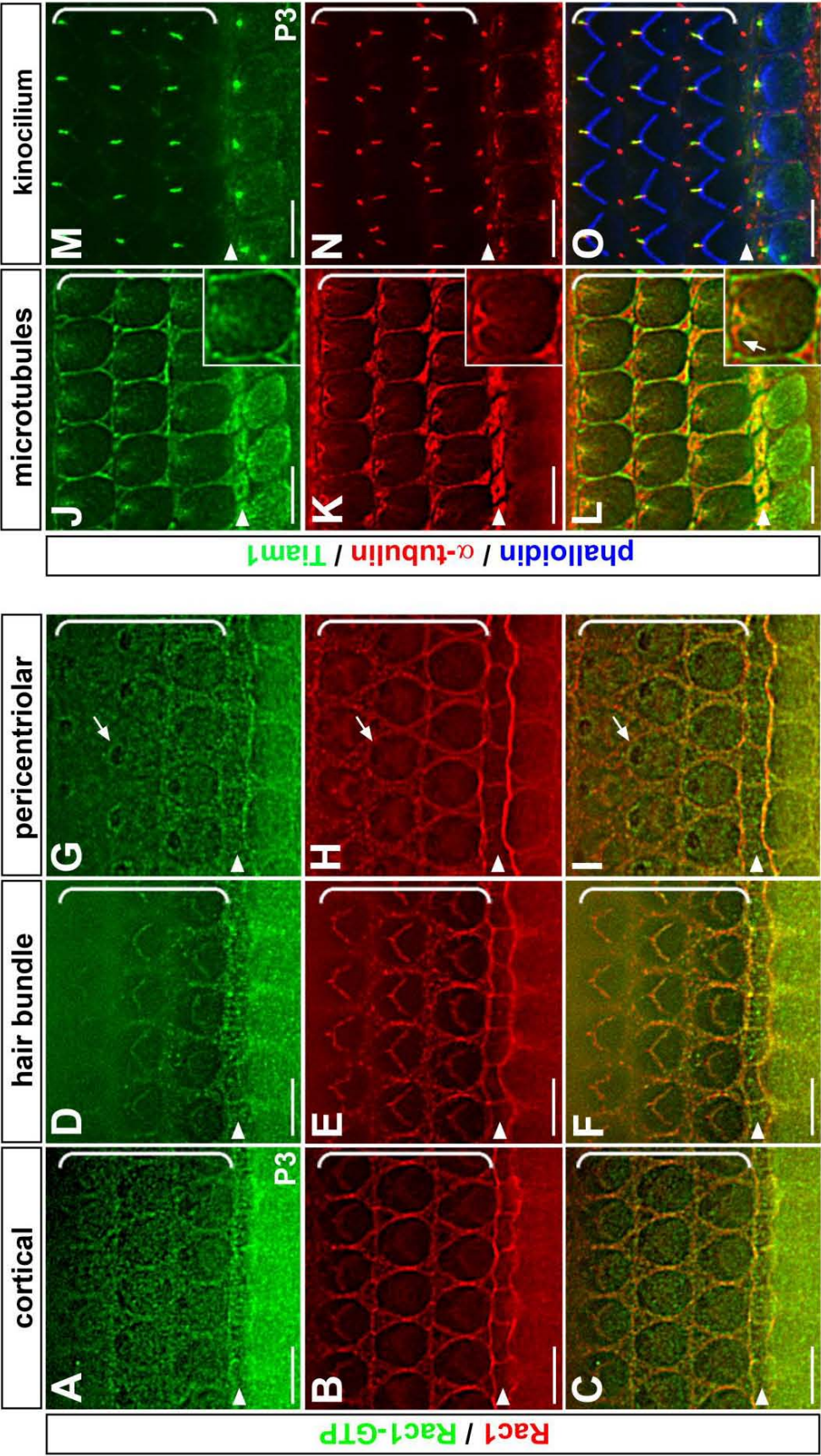


Figure 30. Rac1-GTP and Tiam1 localization in wild-type organ of Corti at P3. (A-I) Rac1-GTP (green) and total Rac1 (red) immunostaining at the level of Dvl2 cortical crescents (A-C), the hair bundle (D-F) and the pericentriolar region (G-I). (J-O) Tiam1 (green) and α -tubulin (red) immunostaining at the level of centriolar microtubules (J-L) and the kinocilium (M-O). Tiam1 localization on microtubules is restricted to the pericentriolar region (J-L); bundled microtubules along the cell cortex lack significant Tiam1 staining (insets, arrow). Triangles mark the pillar cell row, and brackets indicate outer hair cell rows. Scale bars: 6 μ m.

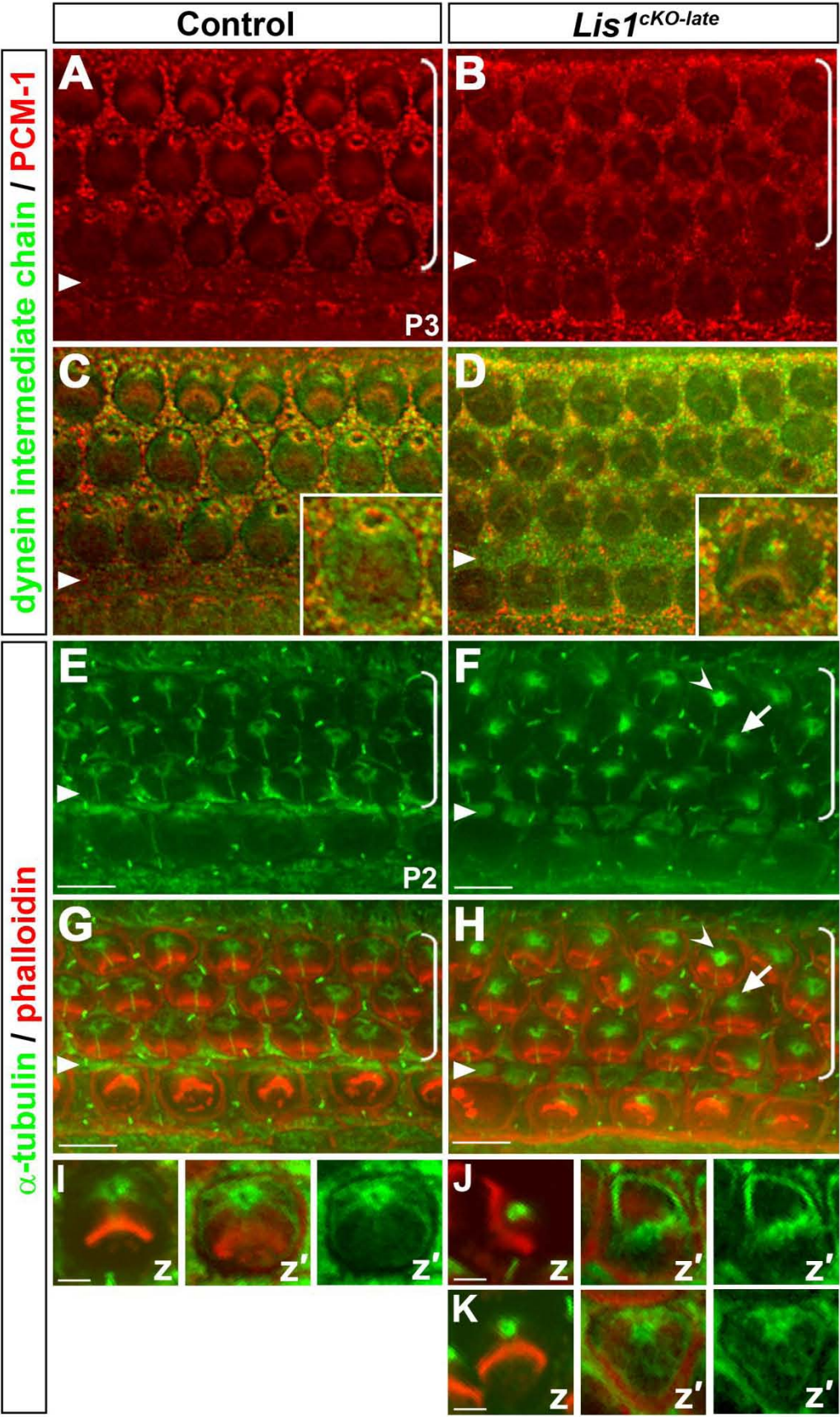


Figure 31. Pericentriolar matrix and microtubule organization defects in *Lis1*^{CKO-late} hair cells. (A-D) Immunostaining of PCM-1 (red) and dynein intermediate chain (green) in P3 control (A,C) and *Lis1*^{CKO-late} (B,D) cochleae. Higher magnification insets in C and D show distribution of PCM-1 in relation to dynein. (E-K) α -tubulin (green) and phalloidin staining (red) in P2 control (E,G,I) and *Lis1*^{CKO-late} (F,H,J,K) cochleae. (I-K) Higher magnification optical sections of individual hair cells taken at the level of the hair cell basal body (z) and 1 μ m basal to z (z'). Scale bars: A-H, 6 μ m; I-K, 2 μ m.

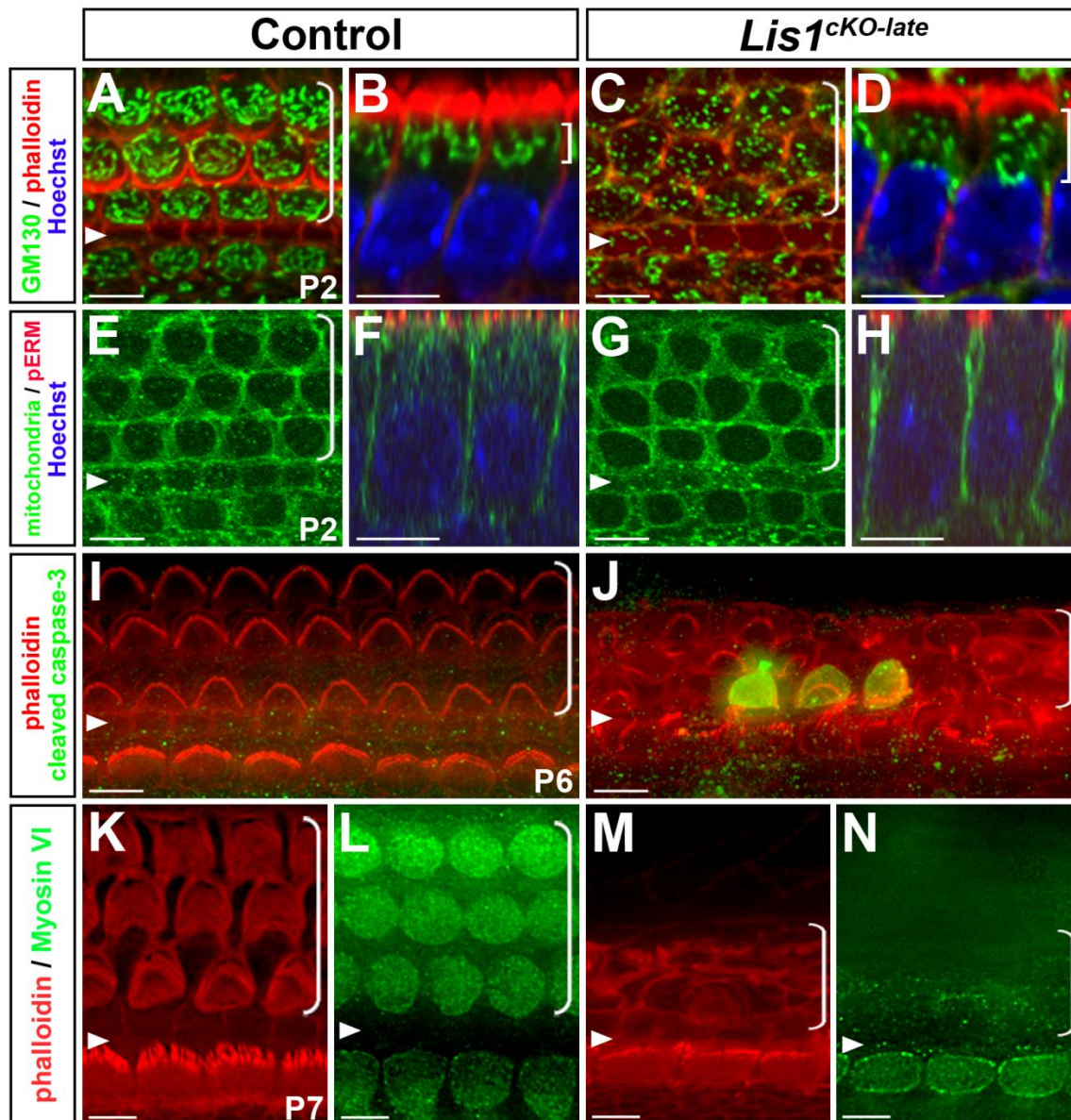


Figure 32. *Lis1* is required for organelle positioning and hair cell survival. (A-D) P2 control (A,B) and *Lis1*^{CKO-late} (C,D) cochleae stained for the Golgi marker GM130 (green), phalloidin (red) and Hoechst (blue) to label cell nuclei. B and D are optical slices along the Z-axis to show hair cells in profile. Brackets in B and D indicate the distribution of Golgi complexes in the apical cytoplasm. (E-H) P2 control (E,F) and *Lis1*^{CKO-late} (G,H) organ of Corti stained for mitochondria (green), phospho-ERM (red) and Hoechst (blue) to label cell nuclei. F and H are optical slices along the Z-axis. (I,J) Cleaved caspase-3 (green) and phalloidin staining (red) in P6 control (I) and *Lis1*^{CKO-late} (J) hair cells. *Lis1*^{CKO-late} hair cells undergo apoptosis and are subsequently extruded from the epithelium. (K-N) Myosin VI (green) and phalloidin (red) staining in the basal region of P7 control (K,L) and *Lis1*^{CKO-late} (M,N) cochleae. The *Lis1*^{CKO-late} cochlea is devoid of outer hair cells. Scale bars: 6 μ m.

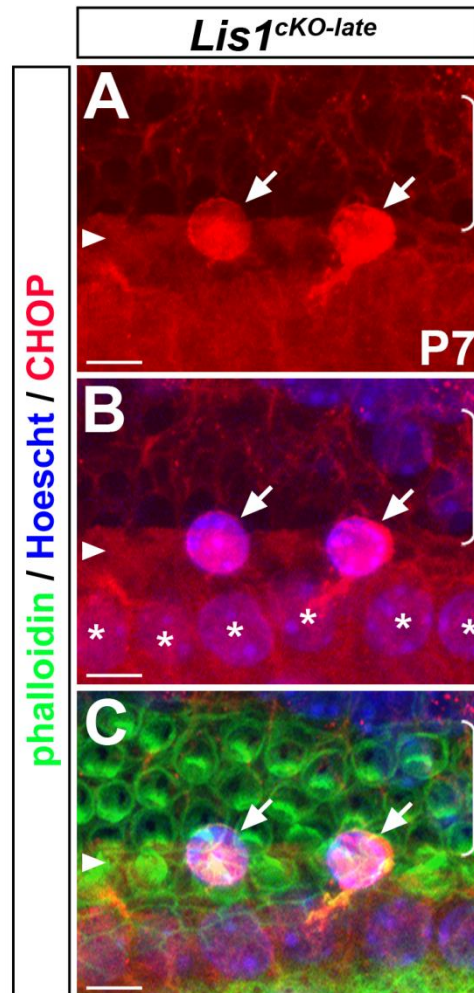


Figure 33. CHOP induction in *Lis1*^{CKO-late} hair cells. (A-C) Collapsed Z-stacks showing representative staining of CHOP (red), nuclei (blue) and phalloidin (green) in P7 *Lis1*^{CKO-late} hair cells from the mid-apical region of the cochlea (70% cochlear length). CHOP is upregulated in a small number of hair cells as they are extruded from the sensory epithelium (arrows). Asterisks in B indicate the row of IHC nuclei. Triangles mark the row of pillar cells, and brackets indicate OHC rows. Scale bars: 6 μm.

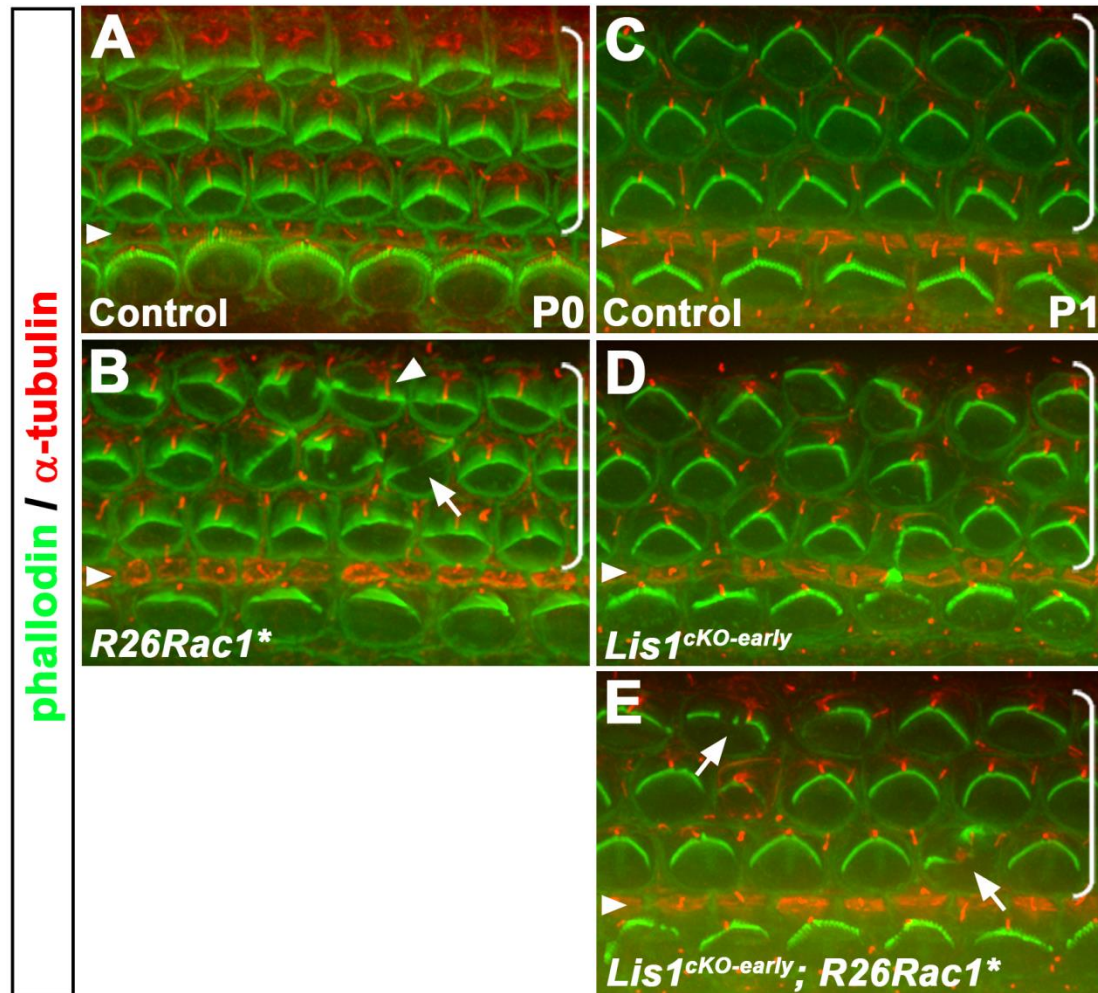


Figure 34. Constitutive Rac1 activation disrupts hair bundle morphology. (A,B) Phalloidin (green) and α -tubulin (red) staining in P0 control (A) and *R26Rac1** (B) OC. Arrowhead in B indicates a hair cell with a flattened bundle, and the arrow points to a hair cell with a split bundle. (C-E) Hair bundle morphology in P1 control (C), *Lis1^{CKO-early}* (D) and *Lis1^{CKO-early}; R26Rac1** (E) OC. Constitutive Rac1 activation does not rescue the *Lis1^{CKO-early}* hair bundle defects. Arrows in E indicate cells with split hair bundles. Triangles mark the row of pillar cells, and brackets indicate OHC rows.

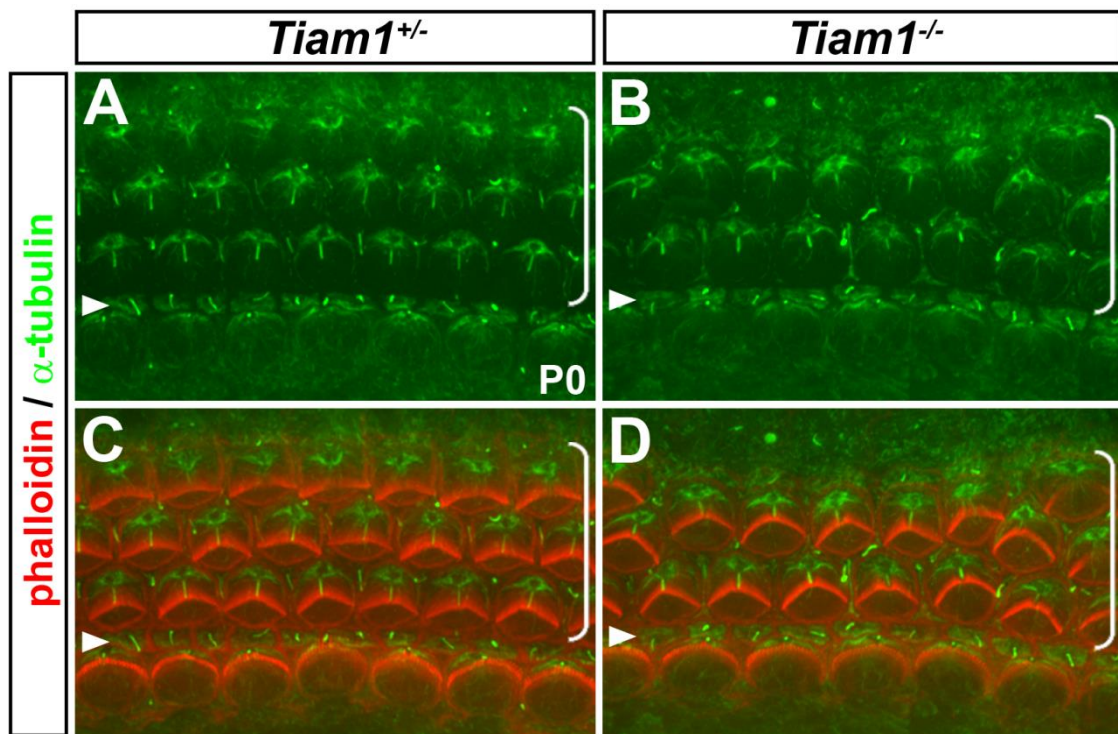


Figure 35. *Tiam1* is required for cellular patterning in the OC. (A-D) Phalloidin (red) and α -tubulin (green) staining in P0 *Tiam1*^{+/-} (A,C) and *Tiam1*^{-/-} (B,D) OC. Disruption of *Tiam1* causes OC patterning defects, including loss or gain of OHC rows, but does not affect hair bundle morphology. Triangles mark the row of pillar cells, and brackets indicate OHC rows.

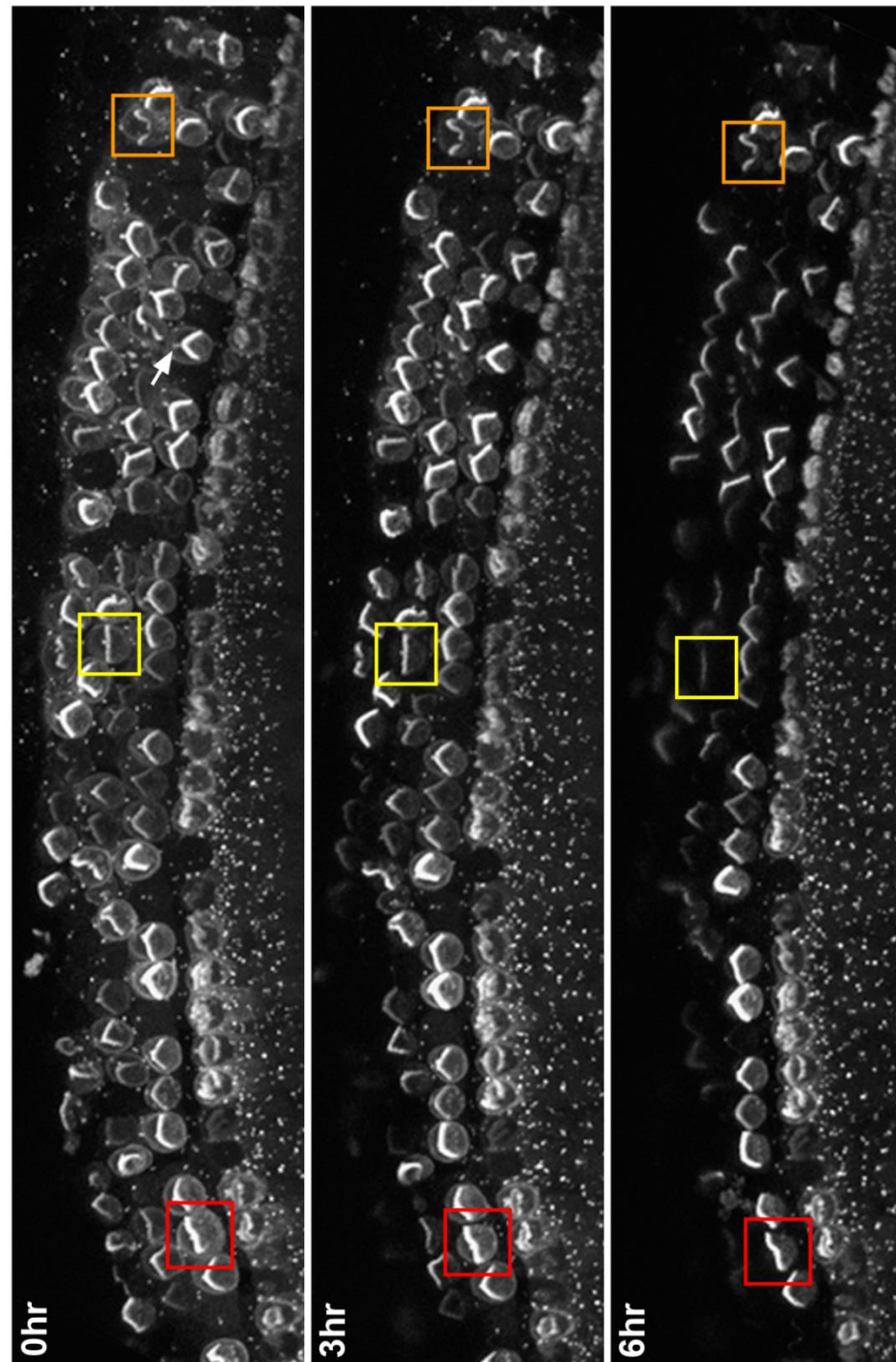


Figure 36. *In vivo* imaging of *Lis1^{CKO-late}* hair bundle development. Panels show collapsed Z-stacks of P5 *Lis1^{CKO-late}* OC expressing *GFP-centrin2* and *mT/mG* to mark the centrioles and membrane/hair bundle, respectively. Colored boxes indicate hair cells with a flattened (yellow), splitting (red) or completely split (orange) phenotype at the initial time point. The arrow in the top panel indicates a pair of hair cell centrioles.

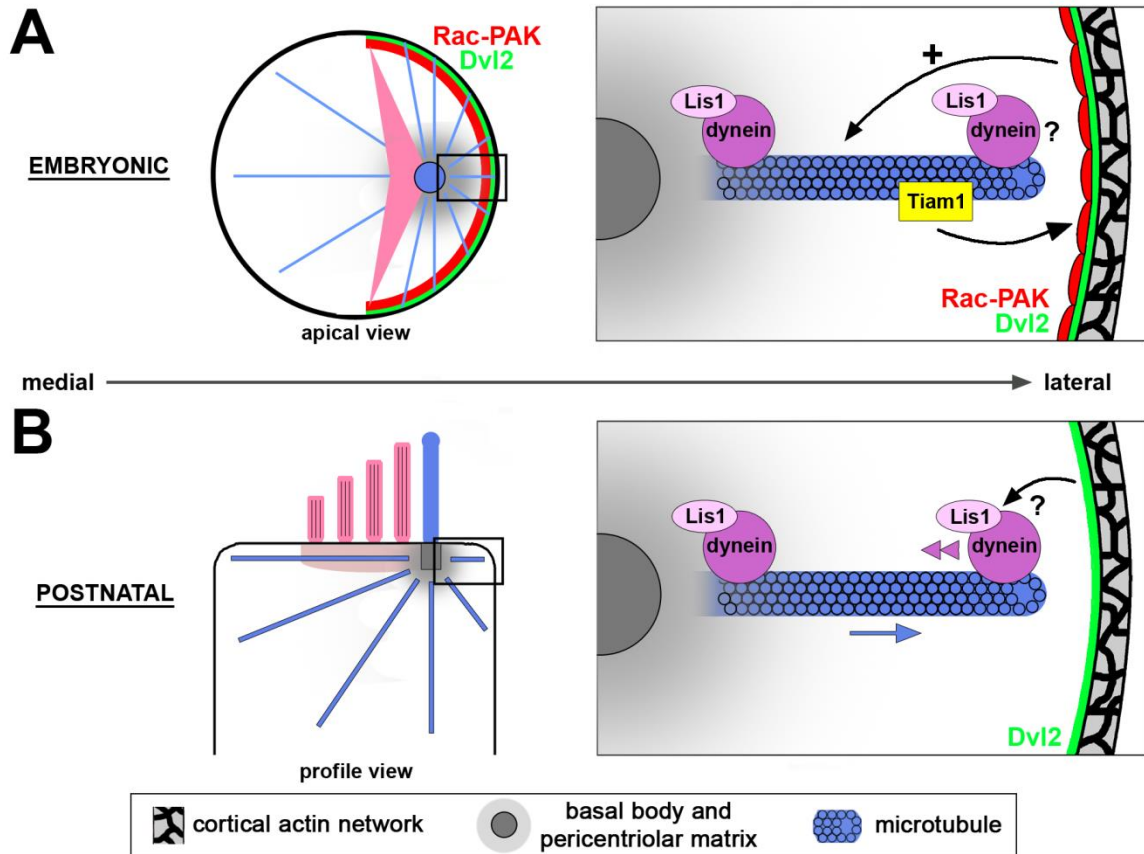


Figure 37. A proposed model for Lis1 function in hair cell planar polarity. (A) During embryonic development, Lis1 regulates the organization of centriolar microtubules and their interactions with the nearby cell cortex. These interactions allow cortical translocation of microtubule-associated Tiam1, leading to local activation of Rac-PAK signaling. In turn, localized Rac-PAK activity serves as a polarity cue to position the basal body. The core PCP pathway spatially orients the cortical domain of Rac-PAK signaling. (B) In postnatal hair cells, Lis1 regulates both pericentriolar matrix organization and cortical dynein, which together allow generation of the pulling force on centriolar microtubules necessary to maintain centrosome positioning. The core PCP pathway may coordinate with cortical proteins to spatially regulate dynein activity.

Chapter 5

JNK signaling is required for hair cell morphogenesis

5.1 Introduction

c-Jun N-terminal kinases (JNKs) belong to the superfamily of MAP kinases (MAPK), which are involved in regulating a wide range of cellular processes, including proliferation, differentiation and apoptosis [296]. The JNK family consists of three isoforms (JNK1, JNK2 and JNK3) that differ in their expression patterns and affinities toward a given substrate [297]. JNK signal transduction requires that upstream and downstream kinases are brought into close proximity to one another via the c-Jun interacting proteins (JIPs) which act as molecular scaffolds [298]. The composition of these individual complexes, or signalosomes, imparts specificity to JNK signaling, ultimately leading to activation of specific target proteins. Once activated, JNKs are able to bind and phosphorylate substrates in a variety of cellular compartments, including the cytoskeleton, mitochondria and nucleus.

The JNK pathway is increasingly recognized as a regulator of cell morphogenesis through its control of the cytoskeleton [299]. During *Drosophila* development, JNK is required for the maturation of actin-nucleating centers, the formation of filopodia and lamellipodia, and cell spreading [300]. JNK signaling is likewise required for mammalian neural tube [301] and eyelid [302] closure, possibly by regulating actin stress fiber formation. Studies in neurons have demonstrated that JNK localizes to microtubules and maintains their stability by phosphorylating microtubule-associated proteins (MAPs) [303, 304]. Reported JNK substrates include a number of cytoskeleton-associated proteins, signaling molecules and adaptor proteins, including the MAPs MAP1B, MAP2, DCX and

SCG10, actin-binding proteins such as spir, and paxillin, a major component of focal adhesions (see [305] and references therein).

As downstream effectors of noncanonical Wnt signaling pathways, the Rho family of small GTPases, including Rho, Rac and Cdc42, control PCP-mediated processes in both *Drosophila* [125] and vertebrates [126]. In this context, Rac1 functions at least in part by activating JNK, presumably to effect the cytoskeletal changes necessary for altering cell shape and behavior [123, 124, 128, 306]. Given our previous findings that genetic ablation [30, 31] or pharmacological inhibition of Rac function [250] perturbs hair cell development, we set out to investigate the effects of inhibiting JNK signaling in developing hair cells. We also characterized JNK activation both spatially and temporally during development in the OC.

5.2 Results

5.2.1 Localization of active JNK during cochlear morphogenesis

To investigate the importance of JNK signaling during hair cell development, we first examined the temporal and spatial pattern of JNK activation using an antibody that specifically recognizes phosphorylated and activated JNK (pJNK). At E15.5, shortly after hair cells begin to differentiate, pJNK localized to the cellular junctions of hair and supporting cells and seemed to be concentrated where multiple cells contacted each other (**Fig. 38A,B**). At E17.5, pJNK continued to localize to hair and supporting cell cellular junctions but was also found at the tips of stereocilia (**Fig. 38C-E**), consistent with a role

for JNK in regulating hair bundle development. In the basal region of the cochlea at P2, pJNK was largely confined to the hair bundle, where it is concentrated in individual stereocilia (**Fig. 39A,B**). In more apical regions, where hair cells are less mature, in addition to the hair bundle, activated pJNK was observed in the pericentriolar region, likely decorating the hair cell microtubule array (**Fig. 39C**). Taken together, these results demonstrate that JNK signaling is active during the early stages of hair cell development, and this activity is maintained in the postnatal hair bundle.

5.2.2 Potential regulators of JNK signaling during cochlear development

JNK has been shown to be activated by Wnt/PCP signaling [128, 307] and acts as a downstream effector of Rac GTPases [124, 125]. We therefore tested whether proteins with a demonstrated function in hair cell PCP might regulate JNK signaling *in vivo*. In E17.5 *PTK7*^{-/-} cochleae, pJNK staining was unchanged compared to controls and continued to be found at cellular junctions and on the tips of the stereocilia (**Fig. 38F-H**). Similarly, E17.5 *Kif3a*^{CKO} hair cells did not show a change in pJNK activation on stereocilia (**Fig. 38I**). Fixation conditions precluded us from determining the status of pJNK at cellular junctions in *Kif3a*^{CKO-early} OC. Finally, P2 *Lis1*^{CKO-late} hair cells showed a similar pattern of JNK activation compared to controls in both the basal and apical regions of the cochlea (**Fig. 39D-F**). Whether JNK signaling is perturbed in Lis1-deficient embryonic hair cells remains to be determined. Taken together, these data argue against a role for PTK7, Kif3a or Lis1 in regulating JNK signaling.

5.2.3 JNK signaling is required for hair cell morphogenesis

To assess the role of JNK signaling in cochlear morphogenesis, we applied SP600125, a small-molecule inhibitor of JNK [308], to E18.5 rat cochlear explant cultures and assessed the effects on hair cell development. We found that SP600125 treatment resulted in dose-dependent hair bundle morphology defects (**Fig. 40B,C**). Affected hair cells displayed a range of hair bundle phenotypes, from split bundles to those that were completely fragmented or absent. The kinocilium in affected hair bundles was often found in an ectopic location close to one side of the hair cell. In addition to hair bundle defects, JNK inhibition resulted in changes to hair cell shape. Explant cultures treated with vehicle contained hair cells that maintained a circular shape and had a regular array of supporting cells interspersed between hair cells (**Fig. 40D**). In contrast, hair cells treated with a high dose of JNK inhibitor varied considerably in diameter and were often directly contacting one another (**Fig. 40E**). These results indicate a requirement of JNK signaling for proper hair bundle morphology and patterning of the OC.

5.3 Discussion

Previous investigations of JNK activity in the cochlea have been largely confined to investigating its role in apoptotic cell death following insult or injury [309, 310]. While JNK activity has been shown to be required for reorienting stereociliary bundles during regeneration in the chick utricle [311], our results

provide the first evidence for active JNK signaling during mammalian cochlear morphogenesis.

In mammals, hair bundle development is divided into distinct stages: initial stereocilia sprouting, staircase initiation, ordered bundle formation, and elongation and pruning [312]. Interestingly, the active form of JNK was enriched in the stereocilia of the nascent hair bundle during the early phases of development and was maintained through the later stereocilia elongation phase. The height of a stereocilium is determined by the length of the actin filaments that form its core, and actin polymerization and depolymerization within stereocilia are tightly regulated [55]. Indeed, a large number of proteins are implicated in regulating the height of stereocilia by modulating actin filament elongation or bundling [313]. Moreover, a high percentage of genes shown to cause nonsyndromic deafness interact directly or indirectly with actin [314]. Our results are consistent with a role for JNK signaling in regulating actin dynamics; however, it remains to be seen whether any actin-regulating stereociliary proteins are JNK substrates.

During morphogenesis, it is critical that cells are able to arrange into a proper configuration during tissue or organ development, and this remodeling often involves changes in cell shape and/or size. JNK signaling has an evolutionarily conserved role as a regulator of cell shape through direct targeting of cytoskeletal proteins and/or by regulating the expression of genes that modulate the physical properties of cells [305, 315]. Our results indicate that JNK signaling is required to maintain hair cell size and shape during embryonic

cochlear morphogenesis. First, JNK is activated specifically at the cortex of hair and supporting cells. Second, chronic JNK inhibition resulted in hair cells with highly variable shapes and sizes. We speculate that JNK signaling regulates the local cortical environment to maintain the physical properties of hair cells via actin function and/or allow formation of the junctional complexes responsible for intercellular adhesion and signaling. Nectin proteins, which control the regular patterning of hair and supporting cells [32], are possible candidates whose localization and function might rely on JNK signaling.

5.4 Figures

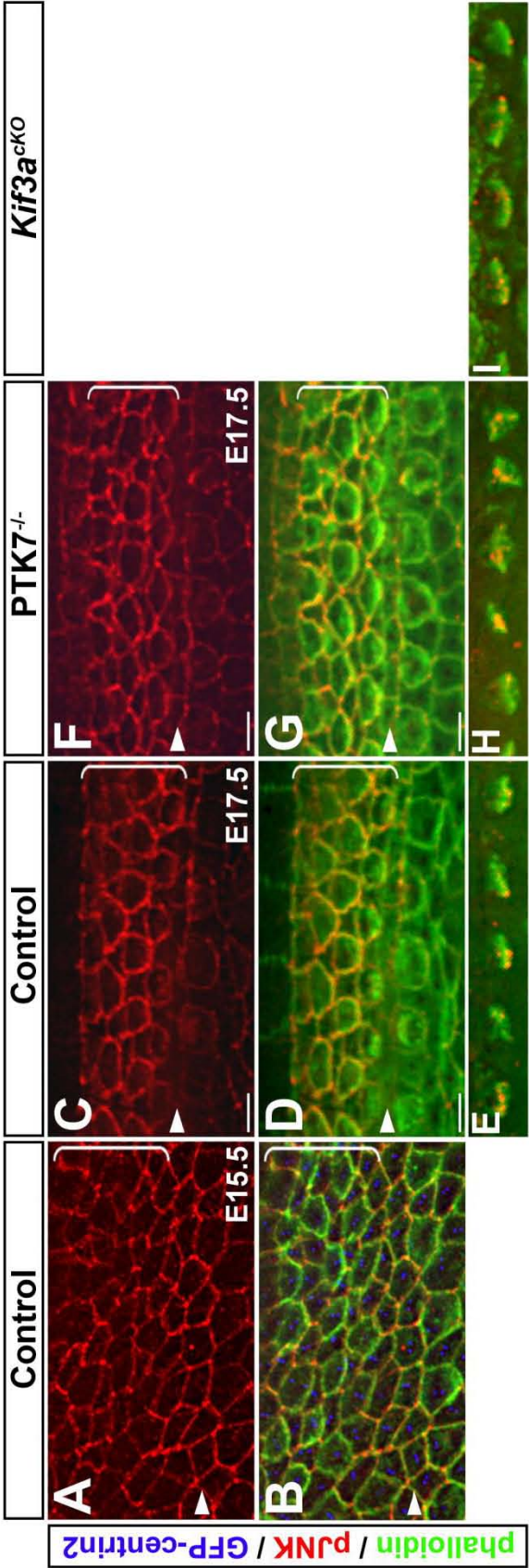


Figure 38. JNK signaling during embryonic hair cell development. (A-I) phospho-JNK (red) and phalloidin (green) staining in E15.5 control (A,B), E17.5 control (C-E), E17.5 *PTK7*^{-/-} (F-H) and E17.5 *Kif3a*^{ckO} (I) OC. pJNK is localized primarily to cellular junctions and the tips of stereocilia. The centrioles in A are marked by GFP-centrin2 (blue). (E,H,I) Single Z-sections at the level of the hair bundle show pJNK localization at the tips of stereocilia. Triangles mark the pillar cell row, and brackets indicate outer hair cell rows.

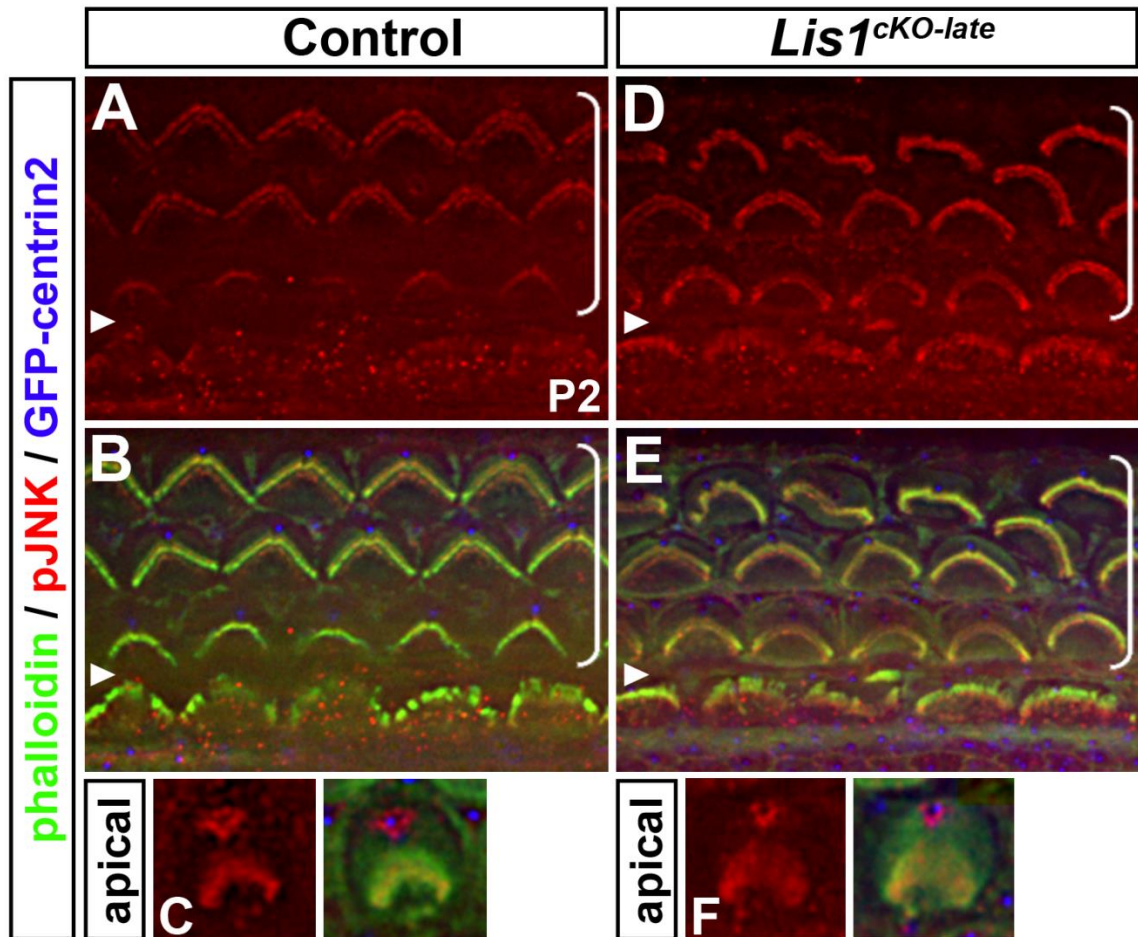


Figure 39. JNK signaling in the early postnatal OC. (A-F) phospho-JNK (red), GFP-centrin2 (blue) and phalloidin (green) staining in P2 control (A-C) and *Lis1*^{cKO-late} (D-F) OC. (A,B,D,E) In the basal region of the cochlea, pJNK localizes to the stereocilia of the hair bundle. (C,F) Single Z-sections at the level of the basal body show pJNK decorating the pericentriolar microtubule array as well as the hair bundle. Triangles mark the pillar cell row, and brackets indicate outer hair cell rows.

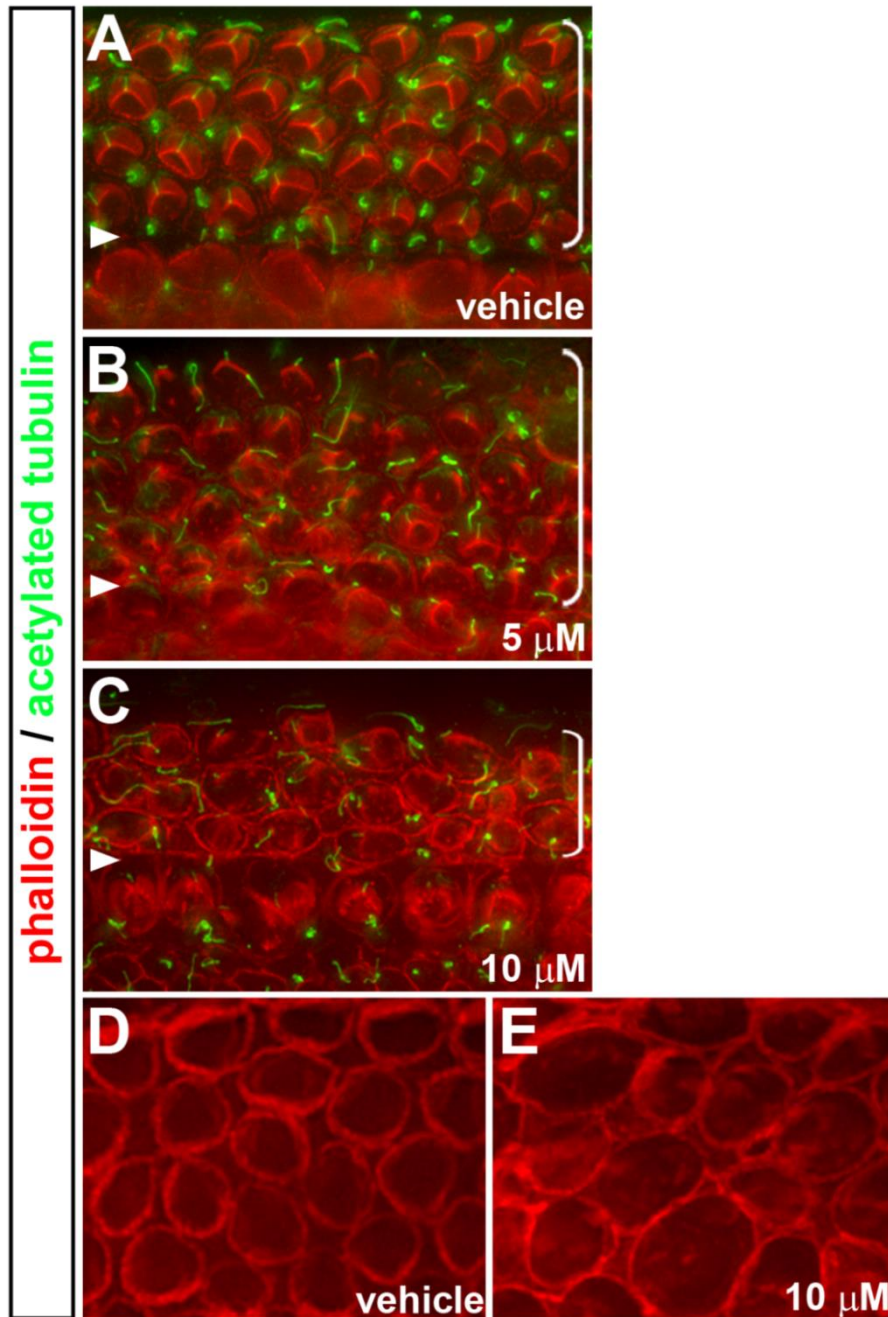


Figure 40. JNK signaling is required for proper hair bundle morphology and cell shape. (A-E) E18.5 rat cochlear explant cultures treated for 48 hours with vehicle (A, D), 5 μ M (B) or 10 μ M (C,E) of the JNK inhibitor SP600125. Phalloidin (red) and acetylated-tubulin (green) mark the hair bundle and microtubules, respectively. Inhibition of JNK signaling resulted in dose-dependent hair bundle defects. (D,E) Single Z-sections at the level of the hair cell body showing the effects of JNK inhibition on OC patterning and cell shape. Triangles mark the row of pillar cells, and brackets indicate OHC rows.

Chapter 6

Future Directions

6.1 Summary

To understand the role of the microtubule cytoskeleton in hair cell planar polarization, I set out to analyze the function of two microtubule motor-associated proteins, Kif3a and Lis1. Based on this work, I have described a novel hair cell-intrinsic pathway for establishing planar polarity. I suggest a model whereby interactions between centriolar microtubules and the cell cortex establish a constrained domain of Rac-PAK signaling which functions as a cell-intrinsic polarity cue. In this model, factors that activate Rac-PAK signaling are translocated to the hair cell cortex, perhaps as cargos carried by plus-end directed motors. Rac-PAK activation on the cortex, in turn, promotes microtubule capture in this region, forming a positive feedback loop to position the basal body at the lateral edge of the hair cell. I speculate that Lis1-dynein facilitates microtubule-cortical interactions, with dynein potentially generating force to position the basal body at the lateral pole of the cell. Lis1-dynein function continues to be important in the maintenance of planar polarity at early postnatal ages by organizing the pericentriolar region and its associated microtubule array and/or maintaining microtubule anchoring to the cortex.

A number of unanswered questions surround my model of microtubule-mediated hair cell polarization. Arguably, foremost among these is an elucidation of the mechanism by which Lis1 facilitates microtubule-cortical interactions. Also pressing is an identification of the molecular components of the Rac-PAK signaling cascade. This chapter explores several of these issues and how they might be addressed experimentally.

6.2 Is dynein required to establish and/or maintain hair cell planar polarity?

While we present evidence that Lis1 regulates cytoplasmic dynein localization in both embryonic and postnatal hair cells, the functional requirement of dynein for hair bundle development has not been established. To test this requirement in embryonic and postnatal hair cells, hair bundle morphology and basal body positioning could be examined in the *Legs-at-odd-angles (Loa)* heterozygous mouse, which contains a point mutation in the dynein heavy chain. *Loa* heterozygous mice are viable but develop early onset neurodegenerative disease with neuronal migration defects similar to those of *Lis1* mutants (homozygous mice die early during embryogenesis) [316, 317]. Furthermore, to test if Lis1 and dynein act in a common genetic pathway, *Lis1; Loa* double heterozygote hair cells could be compared to those from single heterozygote mice. *Lis1* heterozygous mice have no detectable hair cell phenotypes (**Fig. 20**). If, as our model predicts, Lis1 and dynein function in a common genetic pathway, an enhancement of hair bundle and/or basal body positioning defects should be seen in *Lis1; Loa* double heterozygote hair cells. Alternately, ciliobrevin, a recently described small-molecule inhibitor of dynein [318], could be applied to developing cochlear explant cultures and the resultant hair cell and basal body positioning phenotypes analyzed. These experiments would lend further support to our hypothesis that Lis1 mediates hair bundle morphogenesis specifically through regulation of dynein.

6.3 Are microtubules required for cortical Rac-PAK signaling in embryonic hair cells?

A key component in our model of embryonic hair cell polarization is the population of centriolar microtubules whose plus-ends lie proximal to the cell cortex. We speculate that these microtubules are involved in regulating cortical Rac-PAK signaling via two potential functions. First, these microtubules might serve as tracks for targeted delivery of cargos required for localized activation of Rac signaling. Alternately, they could sequester a Rac-activating factor away from the cell cortex, a mode of regulation previously described for the Rac GEF, GEF-H1 [174]. Despite strong evidence that two molecular motors are involved in the regulation of Rac signaling at the hair cell cortex, a formal test of the requirement for microtubules in this process has not been carried out. This requirement could be tested by treating cochlear explant cultures derived from early embryonic stages with a microtubule depolymerizing agent. Our pilot experiments indicate that a modest dose of nocodazole can disrupt the hair cell cytoplasmic microtubule array without significantly affecting the kinocilium. Changes in the localization or levels of activated Rac and/or pPAK in nocodazole-treated hair cells would substantiate the requirement for microtubules in our model of hair cell polarization.

6.4 Do Tiam family GEFs regulate microtubule-dependent Rac signaling in embryonic hair cells?

In our model, centriolar microtubules regulate the delivery of a factor that activates Rac signaling to the hair cell cortex during planar polarization. Based on our data, we speculate that the identity of this factor is the Rac GEF Tiam1. First, we observed the Tiam1 in complex with the plus-end directed motor component Kif3a *in vivo* (**Fig. 13**). Second, Tiam1 associated with the centriolar population of microtubules in embryonic hair cells (**Fig. 26**). These microtubules were highly disorganized in Lis1-deficient hair cells, and this correlated with a loss of asymmetric localization of activated Rac localization. While we observed no overt defects in hair bundle morphogenesis in *Tiam1*^{-/-} hair cells (**Fig. 35**), this analysis may have been complicated by the presence of the related GEF Tiam2 (also known as STEF). Both GEFs share similar structure and binding partners [275, 276] and can regulate microtubule-dependent Rac activation [176]. To address this issue, the function of both Tiam proteins could be blocked via transgenic expression of the dominant negative PH-CC-Ex domain to exclude binding partners from interacting with Tiam1/2 [275].

If Tiam family GEFs are responsible for activating Rac-PAK signaling on the hair cell cortex, the question of how they localize there remains. The most parsimonious explanation is that Tiam is a cargo of the anterograde motor kinesin-II, of which Kif3a is a component. While we have shown a specific association between Kif3a and Tiam1 in embryonic brain lysates (**Fig. 13**), their interaction in hair cells has not been demonstrated. The *in situ* proximity ligation assay (PLA) provides an excellent tool to test for specific Kif3a-Tiam interactions in developing hair cells. PLA allows the *in vivo* detection of two proteins in close

proximity with high specificity; it relies on modified primary antibodies that, when adjacent, allow an enzymatic reaction on a substrate to yield a product that can be detected by fluorescent microscopy [319]. This assay can not only determine if Kif3a and Tiam interact but also provide spatial information about where in the hair cell this association occurs. In addition, this technique can be combined with microtubule immunostaining; PLA signal on the hair cell microtubule array would support the idea that kinesin-II transports Tiam GEFs toward the hair cell cortex.

6.5 Is Par-3 involved in regulating Rac-PAK activity?

Par-3 is a key member of the evolutionarily conserved Par-3/Par-6/aPKC complex that is essential for cell polarity in a variety of organisms [320]. Par-3 functions as a scaffold protein, bringing together members of the complex and localizing them to specific areas of the cell. In polarizing neurons, Par-3 directly interacts with Kif3a, allowing the transport of aPKC to the tips of growing axons by kinesin-II [221]. Work in our laboratory has shown that Par-3 is asymmetrically localized on the hair cell cortex during development in a pattern similar to that of activated PAK (data not shown). In fact, in other cell types, Par-3 can spatially restrict Rac activation by directly binding Tiam1 [321, 322]. Taken together, these data suggest that Par-3 might regulate asymmetric Rac-PAK activity in hair cells through Tiam1 and/or the kinesin-II motor.

As a first step toward validating this hypothesis, the dependence of Par-3 localization on Kif3a could be tested. Disruptions in asymmetric localization of Par-3 in *Kif3a*^{CKO} hair cells would lend support to the idea that kinesin-II

transports Par-3 to the cortex. Additionally, PLA could be used to tease apart interactions between Par-3, Kif3a, and Tiam and whether they associate on the hair cell microtubule array. If Par-3 regulates Tiam during hair cell planar polarization, we would expect Par-3-Tiam PLA signal to overlap with cortical Par-3 localization. Furthermore, if Par-3 acts as a scaffold to facilitate Tiam transport to the cell cortex, analogous to its role described in neurons, Par-3-Tiam interactions should be detected on the hair cell microtubule array. It is also possible that Par-3 interacts with Kif3a on microtubules independently of Tiam, instead recruiting Tiam to the hair cell cortex after it arrives there.

6.6 How might Lis1 link microtubule plus-ends to the cell cortex?

During embryonic stages, Lis1-dependent microtubule organization is critical for Rac-PAK activation on the cell cortex. Similarly, postnatal hair cells require Lis1 to maintain hair bundle polarity, likely by tethering the basal body/kinocilium on the lateral side of the cell. In both cases, we believe that the plus-ends of centriolar microtubules are anchored at the cell cortex, but how Lis1 establishes a link between microtubules and cortical proteins and the identity of its binding partners remain unresolved. Lis1 could potentially interface with the hair cell cortex via direct interaction with cortical proteins and/or indirectly through dynein-mediated cortical microtubule capture.

6.6.1 IQGAP1

IQGAP1 is a leading candidate for a cortical factor that directly interacts with Lis1. Work in cerebellar neurons has identified a tripartite complex of Lis1, the +TIP CLIP-170, and IQGAP1 that is important for migration [172]. Interestingly, disruption of this complex leads to changes in the levels of activated Rac1, Cdc42, and RhoA, supporting a role for Lis1 in the regulation of cortical actin and its coordination with the microtubule cytoskeleton. Given our results in hair cells, we hypothesize that a similar complex might mediate microtubule capture and Rac activation at the cell cortex. Indeed, IQGAP1 is highly expressed in developing hair cells (SHIELD: Shared Harvard Inner-Ear Laboratory Database, <https://shield.hms.harvard.edu/>).

A PLA assay could be used to determine whether Lis1 associates with IQGAP1 in hair cells. PLA signals in proximity to the hair cell cortex would support the idea that Lis1 and IQGAP1 act together in a cortical complex. Co-staining for microtubules in these cells would also be informative, since Lis1-IQGAP1 complexes would be expected to form adjacent to microtubule plus-ends if they are involved in cortical anchoring.

6.6.2 LGN/GPSM2

The evolutionarily conserved polarity protein LGN (also known as GPSM2), the mammalian ortholog of *C. elegans* LGN and *Drosophila* Pins, is another candidate that might link Lis1 to cortical protein complexes. LGN homologs are involved in regulating spindle orientation in a number of cell types, including the *C. elegans* zygote (see **Section 1.4.2**). In these systems, LGN is a

component of cortical protein complexes that binds cytoplasmic dynein, anchoring it to the cortex where it exerts tension on astral microtubules necessary for asymmetric cell division [64, 180, 323]. In both invertebrate and mammalian cells, Lis1, by virtue of regulating dynein, is an integral part of the LGN complex and required to translate microtubule-cortex contact into spindle movement [201, 203, 324].

Recent work has identified *LGN* as the causative gene for DFNB82, a recessive nonsyndromic hereditary disorder in humans that results in severe-to-profound sensorineural hearing loss [288, 289]. In hair cells, LGN is localized near the lateral cortex, possibly decorating the microtubule array. Though its function in human deafness remains completely unknown, it is tempting to speculate that LGN is involved in mediating microtubule-cortex interactions via interactions with Lis1-dynein in hair cells.

To investigate the requirement of LGN for hair cell development, hair bundle morphology and basal body position should be analyzed in *LGN* knockout mice. The timing of the onset of defects would indicate whether LGN is involved in the establishment and/or the maintenance of planar polarization. If LGN is required for Lis1-mediated microtubule anchoring during the maintenance phase of polarization, postnatal LGN-deficient hair cells should develop flat or split hair bundle morphologies concomitant with basal bodies positioned away from the lateral membrane. Given its role in other cell types, we predict that LGN functions in hair cells to regulate cortical dynein. Thus, dynein localization should be examined via immunostaining or with a PLA assay designed to detect

interactions between Lis1 and/or dynein and LGN. Changes in microtubule organization, cortical dynein localization, or PLA signal at the cell cortex would lend strong support to the idea that cortical LGN mediates microtubule-cortical interactions via Lis1-dynein.

6.7 How does PAK signaling regulate Lis1-mediated microtubule-cortex interactions?

A key feature of our model is that localized Rac-PAK activity facilitates microtubule capture at the hair cell cortex, forming a positive feedback loop to reinforce additional PAK activation (**Fig. 37**). We speculate that PAK signaling at the cell cortex facilitates interactions between the Lis1-dynein complex and other cortical proteins. While both Rac and PAK have demonstrated roles regulating the microtubule cytoskeleton in other cell types [325, 326], the downstream effectors of PAK signaling in hair cells have not been identified.

To identify targets of PAK signaling important for Lis1-mediated microtubule capture in hair cells, a dominant-negative approach might be used to block PAK signaling in hair cells. Activation of PAK by phosphorylation results in relief of the inhibitory interaction between its autoinhibitory domain (AID) and kinase domain [231]. Thus, transgenic overexpression of the AID domain in hair cells should specifically block PAK signaling [327]. Hair bundle morphology and basal body position can be used to assay the functional effects of inhibiting PAK signaling. Moreover, PLA assays could test for changes in interactions between Lis1 and candidate cortical binding partners (e.g. IQGAP1, LGN). Changes in

the levels or localization of PLA signals would indicate that PAK signaling regulates Lis1 interaction with binding partners and lend support to our model that sustained cortical PAK signaling reinforces Lis1-mediated microtubule capture in hair cells.

PAK signaling might affect interactions between Lis1 and its partners directly or indirectly. PAK-AID mice would also provide a means of identifying PAK substrates that are relevant to microtubule capture. Candidates substrates include IQGAP1 [328] and the microtubule destabilizing protein Op18/stathmin [326].

6.8 How do tissue polarity cues impinge on the microtubule-mediated cell polarity machinery?

Taken together, our data indicate that tissue-level PCP signals lie upstream of microtubule-mediated polarity processes. In the absence of PCP signaling, cell-intrinsic cues still direct hair cells to polarize morphologically and at the molecular level. Thus, we speculate that tissue-level PCP signaling provides an extrinsic signal that is interpreted within individual hair cells to direct microtubule-mediated polarity. How polarity information from tissue-level signals is transduced to the cell-intrinsic microtubule polarity machinery remains an open question.

PCP signaling potentially regulates Lis1-dynein-mediated microtubule attachment at the hair cell cortex by influencing the localization of cortical proteins. To test this idea, the localization of IQGAP1, LGN, Par-3, and other

candidates that might be involved in establishing microtubule-cortex interactions should be examined in core PCP mutants. Changes in the localization of these cortical proteins in the absence of PCP signaling would provide strong evidence that they link tissue-level polarity cues to the microtubule machinery that establishes cell-intrinsic polarity.

Recent work in our laboratory also suggests that mechanical tension may provide a tissue-level polarity cue to orient hair cells. In this model, the core PCP pathway acts in conjunction with a *Ptk7*-mediated pathway to regulate actomyosin contractility at the medial borders of hair and supporting cells [101]. During polarization, such tension could lead to changes in cortical actin on the medial side of the hair cell, producing conditions antagonistic to microtubule-cortical interactions. As a result, force-generating microtubule-cortex attachments would only be established on the lateral side of the cell, biasing the position of the basal body toward that side of the cell and ultimately orienting centriolar microtubules in a process analogous to the events of mitotic spindle positioning in other cell types [180]. To determine if mechanical tension can prevent microtubule-cortex interactions, live imaging of the microtubule array in hair cells during the period of increased cortical tension would be informative. Unfortunately, the small size of hair cells makes this approach technically challenging. Alternatively, live imaging of hair cell centrioles would provide key information about movement behaviors and the timing of events surrounding basal body polarization. Comparing wild-type centriole behavior to that observed

in *Ptk7*-null hair cells, where mechanical tension is reduced, would also be germane.

Importantly, these two potential mechanisms for linking tissue-level PCP signals to the hair cell-intrinsic polarity machinery are not mutually exclusive.

6.9 What is the basis for centrosomal defects in *Lis1*-deficient hair cells?

Our results indicate that *Lis1* is required to maintain the integrity of the centrosome in postnatal hair cells (**Fig. 31**). We suspect that the observed defects are partly due to impaired dynein accumulation at the centrosome, which is critical for the retrograde transport of some centrosomal components [264, 329] as well as the retention of microtubules in the interphase centrosomal array [330]. While the centrosomal localization of PCM-1 is disrupted in *Lis1*^{CKO-late} hair cells, our preliminary data indicate that γ -tubulin, another integral centrosomal protein [329], remains appropriately localized at the centrioles (data not shown), indicating there are likely multiple mechanisms for the recruitment of proteins to the hair cell centrosome. As an initial step toward understanding centrosome organization in hair cells and the role of *Lis1* in this process, the localization of other key centrosomal proteins should be assessed in *Lis1*^{CKO-late} hair cells. Of particular interest are factors that influence the accumulation of other PCM components, including pericentrin [264], dynactin [331], Aurora-A [332] and NEDD1 [333]. To assess the role of dynein in the centrosomal recruitment of these factors, changes in the localization of these proteins could be assessed in the hair cells of *Loa* mice.

6.10 Is JNK signaling involved in Lis1-mediated cell death?

We have established that Lis1-deficient OHCs undergo apoptosis in early postnatal stages (**Fig. 32**), though the connection between the Lis1 phenotype and cell death remains enigmatic. JNK signaling is central to the intrinsic apoptotic pathway where it activates apoptotic signaling by upregulating pro-apoptotic genes or directly modulating the activities of mitochondrial proteins via phosphorylation [334]. In hair cells, JNK signaling is significantly upregulated during noise- or drug-induced hair cell death, and blockade of the JNK pathway attenuates hair cell death [310, 335].

JNK-interacting proteins (JIPs) potentiate JNK activation by organizing components of the pathway into specific signaling complexes that are transported on microtubules by the kinesin-1 motor [336]. Therefore, disruption of the microtubule array in *Lis1* mutant hair cells might lead to aberrant JNK signaling, thereby activating the apoptotic pathway. Though we did not observe gross changes in activated pJNK localization in *Lis1*^{CKO-late} hair cells (**Fig. 39**), our analysis did not focus on mitochondria or the nucleus, the main sites of JNK action during apoptosis.

If JNK signaling is indeed responsible for inducing apoptosis in Lis1-deficient hair cells, then inhibition of JNK activation should have a protective effect against hair cell death. To test this hypothesis, a small molecule inhibitor of JNK activation (e.g. SP600125 [308]), could be applied to *Lis1*^{CKO-late} cochlear explant cultures prior to the onset of hair cell death. Hair cell survival could then

be assessed by quantifying the number of hair cells or the expression of pro-apoptotic markers (e.g. activated caspase-3) and comparing this data to of control cultures.

6.11 Conclusion

Discerning the basis of hearing impairment is of paramount importance to public health. Sensorineural defects, which account for a majority of cases of hearing loss, are often caused by defects in hair bundle structure or function. Therefore, an understanding of the cellular events involved in hair bundle development is of critical importance for establishing future therapeutic strategies to restore hearing. The promise of stem cell therapy to replace lost or damaged hair cells cannot be realized without a basic understanding of hair cell biology. Studies like the current investigation, which seek to understand specific aspects of hair cell biology, are critical to achieving this goal.

In this work, I have described a novel pathway regulating hair cell-intrinsic polarity and developed a working model of hair cell planar polarization that awaits further refinement. My analysis of *Kif3a* and *Lis1* has revealed important basic mechanistic insights into the role of microtubules in hair cell development and revealed previously unappreciated functions for microtubule-associated proteins during planar polarization of hair cells. This work provides a new entry point into understanding the cellular basis of hair bundle morphogenesis and affords new insights into the etiology of deafness.

Chapter 7

Literature Cited

1. Appler JM, Goodrich L V: **Connecting the ear to the brain: Molecular mechanisms of auditory circuit assembly.** *Progress in neurobiology* 2011, **93**:488–508.
2. Schimmang T: **Expression and functions of FGF ligands during early otic development.** *The International journal of developmental biology* 2007, **51**:473–81.
3. Ohyama T, Groves AK: **Generation of Pax2-Cre mice by modification of a Pax2 bacterial artificial chromosome.** *Genesis (New York, N.Y. : 2000)* 2004, **38**:195–9.
4. Ohyama T, Mohamed O a, Taketo MM, Dufort D, Groves AK: **Wnt signals mediate a fate decision between otic placode and epidermis.** *Development (Cambridge, England)* 2006, **133**:865–75.
5. Jayasena CS, Ohyama T, Segil N, Groves AK: **Notch signaling augments the canonical Wnt pathway to specify the size of the otic placode.** *Development (Cambridge, England)* 2008, **135**:2251–61.
6. Bok J, Chang W, Wu DK: **Patterning and morphogenesis of the vertebrate inner ear.** *The International journal of developmental biology* 2007, **51**:521–33.
7. Groves AK, Fekete DM: **Shaping sound in space: the regulation of inner ear patterning.** *Development (Cambridge, England)* 2012, **139**:245–57.
8. Riccomagno MM, Martinu L, Mulheisen M, Wu DK, Epstein DJ: **Specification of the mammalian cochlea is dependent on Sonic hedgehog.** *Genes & development* 2002, **16**:2365–78.
9. Bok J, Dolson DK, Hill P, Rüther U, Epstein DJ, Wu DK: **Opposing gradients of Gli repressor and activators mediate Shh signaling along the dorsoventral axis of the inner ear.** *Development (Cambridge, England)* 2007, **134**:1713–22.
10. Bok J, Raft S, Kong K-A, Koo SK, Dräger UC, Wu DK: **Transient retinoic acid signaling confers anterior-posterior polarity to the inner ear.** *Proceedings of the National Academy of Sciences of the United States of America* 2011, **108**:161–6.
11. Kiernan AE, Xu J, Gridley T: **The Notch ligand JAG1 is required for sensory progenitor development in the mammalian inner ear.** *PLoS genetics* 2006, **2**:e4.
12. Kiernan a E, Ahituv N, Fuchs H, Balling R, Avraham KB, Steel KP, Hrabé de Angelis M: **The Notch ligand Jagged1 is required for inner ear sensory**

development. *Proceedings of the National Academy of Sciences of the United States of America* 2001, **98**:3873–8.

13. Driver EC, Kelley MW: **Specification of cell fate in the mammalian cochlea.** *Birth defects research. Part C, Embryo today : reviews* 2009, **87**:212–21.

14. Kiernan AE, Pelling AL, Leung KKH, Tang ASP, Bell DM, Tease C, Lovell-Badge R, Steel KP, Cheah KSE: **Sox2 is required for sensory organ development in the mammalian inner ear.** *Nature* 2005, **434**:1031–5.

15. Neves J, Parada C, Chamizo M, Giráldez F: **Jagged 1 regulates the restriction of Sox2 expression in the developing chicken inner ear: a mechanism for sensory organ specification.** *Development (Cambridge, England)* 2011, **138**:735–44.

16. Zou D, Erickson C, Kim E-H, Jin D, Fritzsche B, Xu P-X: **Eya1 gene dosage critically affects the development of sensory epithelia in the mammalian inner ear.** *Human molecular genetics* 2008, **17**:3340–56.

17. Kiernan AE, Cordes R, Kopan R, Gossler A, Gridley T: **The Notch ligands DLL1 and JAG2 act synergistically to regulate hair cell development in the mammalian inner ear.** *Development (Cambridge, England)* 2005, **132**:4353–62.

18. Zheng JL, Shou J, Guillemot F, Kageyama R, Gao WQ: **Hes1 is a negative regulator of inner ear hair cell differentiation.** *Development (Cambridge, England)* 2000, **127**:4551–60.

19. Lanford PJ, Shailam R, Norton CR, Ridley T, Kelley MW: **Expression of Math1 and HES5 in the Cochleae of Wildtype and Jag2 Mutant Mice.** *Journal of the Association for Research in Otolaryngology* 2000, **1**:161–171.

20. Chen P, Segil N: **p27(Kip1) links cell proliferation to morphogenesis in the developing organ of Corti.** *Development (Cambridge, England)* 1999, **126**:1581–90.

21. Bermingham N a., Hassan BA, Price SD, Vollrath MA, Ben-Arie N, Eatock RA, Bellen HJ, Lysakowski A, Zoghbi HY: **Math1: an essential gene for the generation of inner ear hair cells.** *Science (New York, N.Y.)* 1999, **284**:1837–41.

22. Zheng JL, Gao WQ: **Overexpression of Math1 induces robust production of extra hair cells in postnatal rat inner ears.** *Nature neuroscience* 2000, **3**:580–6.

23. Chen P, Johnson JE, Zoghbi HY, Segil N: **The role of Math1 in inner ear development: Uncoupling the establishment of the sensory primordium from hair cell fate determination.** *Development (Cambridge, England)* 2002, **129**:2495–505.
24. Keller R: **Shaping the vertebrate body plan by polarized embryonic cell movements.** *Science (New York, N.Y.)* 2002, **298**:1950–4.
25. McKenzie E, Krupin A, Kelley MW: **Cellular growth and rearrangement during the development of the mammalian organ of Corti.** *Developmental dynamics : an official publication of the American Association of Anatomists* 2004, **229**:802–12.
26. Jones C, Chen P: **Planar cell polarity signaling in vertebrates.** *BioEssays : news and reviews in molecular, cellular and developmental biology* 2007, **29**:120–32.
27. Wang J, Mark S, Zhang X, Qian D, Yoo S-J, Radde-Gallwitz K, Zhang Y, Lin X, Collazo A, Wynshaw-Boris A, Chen P: **Regulation of polarized extension and planar cell polarity in the cochlea by the vertebrate PCP pathway.** *Nature genetics* 2005, **37**:980–5.
28. Rida PCG, Chen P: **Line up and listen: Planar cell polarity regulation in the mammalian inner ear.** *Seminars in cell & developmental biology* 2009, **20**:978–85.
29. Chacon-Heszele MF, Ren D, Reynolds AB, Chi F, Chen P: **Regulation of cochlear convergent extension by the vertebrate planar cell polarity pathway is dependent on p120-catenin.** *Development (Cambridge, England)* 2012, **139**:968–78.
30. Grimsley-Myers CM, Sipe CW, Géléoc GSG, Lu X: **The small GTPase Rac1 regulates auditory hair cell morphogenesis.** *The Journal of neuroscience : the official journal of the Society for Neuroscience* 2009, **29**:15859–69.
31. Grimsley-Myers CM, Sipe CW, Wu DK, Lu X: **Redundant functions of Rac GTPases in inner ear morphogenesis.** *Developmental Biology* 2012, **362**:172–186.
32. Togashi H, Kominami K, Waseda M, Komura H, Miyoshi J, Takeichi M, Takai Y: **Nectins establish a checkerboard-like cellular pattern in the auditory epithelium.** *Science (New York, N.Y.)* 2011, **333**:1144–7.
33. Kelly M, Chen P: **Shaping the mammalian auditory sensory organ by the planar cell polarity pathway.** *The International journal of developmental biology* 2007, **51**:535–47.

34. Sekerková G, Zheng L, Loomis PA, Mugnaini E, Bartles JR: **Espins and the actin cytoskeleton of hair cell stereocilia and sensory cell microvilli.** *Cellular and molecular life sciences : CMLS* 2006, **63**:2329–41.
35. Nayak GD, Ratnayaka HSK, Goodyear RJ, Richardson GP: **Development of the hair bundle and mechanotransduction.** *The International journal of developmental biology* 2007, **51**:597–608.
36. Gillespie PG, Müller U: **Mechanotransduction by hair cells: models, molecules, and mechanisms.** *Cell* 2009, **139**:33–44.
37. Kazmierczak P, Sakaguchi H, Tokita J, Wilson-Kubalek EM, Milligan R a, Müller U, Kachar B: **Cadherin 23 and protocadherin 15 interact to form tip-link filaments in sensory hair cells.** *Nature* 2007, **449**:87–91.
38. Verpy E, Leibovici M, Zwaenepoel I, Liu XZ, Gal a, Salem N, Mansour a, Blanchard S, Kobayashi I, Keats BJ, Slim R, Petit C: **A defect in harmonin, a PDZ domain-containing protein expressed in the inner ear sensory hair cells, underlies Usher syndrome type 1C.** *Nature genetics* 2000, **26**:51–5.
39. Ebermann I, Scholl HPN, Charbel Issa P, Becirovic E, Lamprecht J, Jurklics B, Millán JM, Aller E, Mitter D, Bolz H: **A novel gene for Usher syndrome type 2: mutations in the long isoform of whirlin are associated with retinitis pigmentosa and sensorineural hearing loss.** *Human genetics* 2007, **121**:203–11.
40. Weil D: **Usher syndrome type I G (USH1G) is caused by mutations in the gene encoding SANS, a protein that associates with the USH1C protein, harmonin.** *Human Molecular Genetics* 2003, **12**:463–471.
41. Eudy JD: **Mutation of a Gene Encoding a Protein with Extracellular Matrix Motifs in Usher Syndrome Type IIa.** *Science* 1998, **280**:1753–1757.
42. Naz S, Griffith a J, Riazuddin S, Hampton LL, Battey JF, Khan SN, Wilcox ER, Friedman TB: **Mutations of ESPN cause autosomal recessive deafness and vestibular dysfunction.** *Journal of medical genetics* 2004, **41**:591–5.
43. Weil D, Blanchard S, Kaplan J, Guilford P, Gibson F, Walsh J, Mburu P, Varela A, Levilliers J, Weston MD: **Defective myosin VIIA gene responsible for Usher syndrome type 1B.** *Nature* 1995, **374**:60–1.
44. Avraham KB, Hasson T, Steel KP, Kingsley DM, Russell LB, Mooseker MS, Copeland NG, Jenkins NA: **The mouse Snell's waltzer deafness gene encodes an unconventional myosin required for structural integrity of inner ear hair cells.** *Nature genetics* 1995, **11**:369–75.

45. Liang Y, Wang a, Belyantseva I a, Anderson DW, Probst FJ, Barber TD, Miller W, Touchman JW, Jin L, Sullivan SL, Sellers JR, Camper S a, Lloyd R V, Kachar B, Friedman TB, Fridell R a: **Characterization of the human and mouse unconventional myosin XV genes responsible for hereditary deafness DFNB3 and shaker 2.** *Genomics* 1999, **61**:243–58.
46. Schwander M, Kachar B, Müller U: **Review series: The cell biology of hearing.** *The Journal of cell biology* 2010, **190**:9–20.
47. Kazmierczak P, Müller U: **Sensing sound: molecules that orchestrate mechanotransduction by hair cells.** *Trends in neurosciences* 2012, **35**:220–9.
48. Kawashima Y, Géléoc GSG, Kurima K, Labay V, Lelli A, Asai Y, Makishima T, Wu DK, Santina CC Della, Holt JR, Griffith AJ: **Mechanotransduction in mouse inner ear hair cells requires transmembrane channel – like genes.** 2011, **121**.
49. Steyger PS, Furness DN, Hackney CM, Richardson GP: **Tubulin and microtubules in cochlear hair cells: comparative immunocytochemistry and ultrastructure.** *Hearing research* 1989, **42**:1–16.
50. Sobkowicz HM, Slapnick SM, August BK: **The kinocilium of auditory hair cells and evidence for its morphogenetic role during the regeneration of stereocilia and cuticular plates.** *Journal of neurocytology* 1995, **24**:633–53.
51. Nigg E a, Raff JW: **Centrioles, centrosomes, and cilia in health and disease.** *Cell* 2009, **139**:663–78.
52. Hallworth R, McCoy M, Polan-Curtain J: **Tubulin expression in the developing and adult gerbil organ of Corti.** *Hearing research* 2000, **139**:31–41.
53. Troutt LL, Van Heumen WR, Pickles JO: **The changing microtubule arrangements in developing hair cells of the chick cochlea.** *Hearing research* 1994, **81**:100–8.
54. Tannenbaum J, Slepecky NB: **Localization of microtubules containing posttranslationally modified tubulin in cochlear epithelial cells during development.** *Cell motility and the cytoskeleton* 1997, **38**:146–62.
55. Tilney LG, Tilney MS, DeRosier DJ: **Actin filaments, stereocilia, and hair cells: how cells count and measure.** *Annual review of cell biology* 1992, **8**:257–74.
56. Zine a, Romand R: **Development of the auditory receptors of the rat: a SEM study.** *Brain research* 1996, **721**:49–58.

57. Denman-Johnson K, Forge A: **Establishment of hair bundle polarity and orientation in the developing vestibular system of the mouse.** *Journal of neurocytology* 1999, **28**:821–35.
58. Montcouquiol M, Rachel R a, Lanford PJ, Copeland NG, Jenkins N a, Kelley MW: **Identification of Vangl2 and Scrb1 as planar polarity genes in mammals.** *Nature* 2003, **423**:173–7.
59. Dabdoub A, Donohue MJ, Brennan A, Wolf V, Montcouquiol M, Sassoon DA, Hseih J-C, Rubin JS, Salinas PC, Kelley MW: **Wnt signaling mediates reorientation of outer hair cell stereociliary bundles in the mammalian cochlea.** *Development (Cambridge, England)* 2003, **130**:2375–84.
60. Goodrich L V, Strutt D: **Principles of planar polarity in animal development.** *Development (Cambridge, England)* 2011, **138**:1877–92.
61. Jones C, Roper VC, Foucher I, Qian D, Banizs B, Petit C, Yoder BK, Chen P: **Ciliary proteins link basal body polarization to planar cell polarity regulation.** *Nature genetics* 2008, **40**:69–77.
62. Webb SW, Grillet N, Andrade LR, Xiong W, Swarthout L, Della Santina CC, Kachar B, Müller U: **Regulation of PCDH15 function in mechanosensory hair cells by alternative splicing of the cytoplasmic domain.** *Development (Cambridge, England)* 2011, **138**:1607–17.
63. Thompson BJ: **Cell polarity: models and mechanisms from yeast, worms and flies.** *Development (Cambridge, England)* 2013, **140**:13–21.
64. Siegrist SE, Doe CQ: **Microtubule-induced cortical cell polarity.** *Genes & development* 2007, **21**:483–96.
65. Gubb D, García-Bellido a: **A genetic analysis of the determination of cuticular polarity during development in Drosophila melanogaster.** *Journal of embryology and experimental morphology* 1982, **68**:37–57.
66. Adler PN: **Planar signaling and morphogenesis in Drosophila.** *Developmental cell* 2002, **2**:525–35.
67. Hashimoto M, Shinohara K, Wang J, Ikeuchi S, Yoshida S, Meno C, Nonaka S, Takada S, Hatta K, Wynshaw-Boris A, Hamada H: **Planar polarization of node cells determines the rotational axis of node cilia.** *Nature cell biology* 2010, **12**:170–6.
68. Mitchell B, Stubbs JL, Huisman F, Taborek P, Yu C, Kintner C: **The PCP pathway instructs the planar orientation of ciliated cells in the Xenopus larval skin.** *Current biology : CB* 2009, **19**:924–9.

69. Devenport D, Fuchs E: **Planar polarization in embryonic epidermis orchestrates global asymmetric morphogenesis of hair follicles.** *Nature cell biology* 2008, **10**:1257–68.
70. Guo N, Hawkins C, Nathans J: **Frizzled6 controls hair patterning in mice.** *Proceedings of the National Academy of Sciences of the United States of America* 2004, **101**:9277–81.
71. Axelrod JD, Miller JR, Shulman JM, Moon RT, Perrimon N: **Differential recruitment of Dishevelled provides signaling specificity in the planar cell polarity and Wingless signaling pathways.** *Genes & Development* 1998, **12**:2610–2622.
72. Tree DRP, Shulman JM, Rousset R, Scott MP, Gubb D, Axelrod JD: **Prickle mediates feedback amplification to generate asymmetric planar cell polarity signaling.** *Cell* 2002, **109**:371–81.
73. Vinson CR, Adler PN: **Directional non-cell autonomy and the transmission of polarity information by the frizzled gene of Drosophila.** *Nature* 1987, **329**:549–51.
74. Wu J, Mlodzik M: **The frizzled extracellular domain is a ligand for Van Gogh/Stbm during nonautonomous planar cell polarity signaling.** *Developmental cell* 2008, **15**:462–9.
75. Struhl G, Casal J, Lawrence P a: **Dissecting the molecular bridges that mediate the function of Frizzled in planar cell polarity.** *Development (Cambridge, England)* 2012, **139**:3665–74.
76. Jenny A, Darken RS, Wilson P a, Mlodzik M: **Prickle and Strabismus form a functional complex to generate a correct axis during planar cell polarity signaling.** *The EMBO journal* 2003, **22**:4409–20.
77. Klein TJ, Mlodzik M: **Planar cell polarization: an emerging model points in the right direction.** *Annual review of cell and developmental biology* 2005, **21**:155–76.
78. Amonlirdviman K, Khare N a, Tree DRP, Chen W-S, Axelrod JD, Tomlin CJ: **Mathematical modeling of planar cell polarity to understand domineering nonautonomy.** *Science (New York, N.Y.)* 2005, **307**:423–6.
79. Le Garrec J-F, Lopez P, Kerszberg M: **Establishment and maintenance of planar epithelial cell polarity by asymmetric cadherin bridges: a computer model.** *Developmental dynamics : an official publication of the American Association of Anatomists* 2006, **235**:235–46.

80. Chen W-S, Antic D, Matis M, Logan CY, Povelones M, Anderson G a, Nusse R, Axelrod JD: **Asymmetric homotypic interactions of the atypical cadherin flamingo mediate intercellular polarity signaling.** *Cell* 2008, **133**:1093–105.
81. Huang H, Klein PS: **Protein family review The Frizzled family : receptors for multiple signal transduction pathways.** 2004, **2**:1–7.
82. Wang Y, Guo N, Nathans J: **The role of Frizzled3 and Frizzled6 in neural tube closure and in the planar polarity of inner-ear sensory hair cells.** *The Journal of neuroscience : the official journal of the Society for Neuroscience* 2006, **26**:2147–56.
83. Wallingford JB, Habas R: **The developmental biology of Dishevelled: an enigmatic protein governing cell fate and cell polarity.** *Development (Cambridge, England)* 2005, **132**:4421–36.
84. Hamblet NS, Lijam N, Ruiz-Lozano P, Wang J, Yang Y, Luo Z, Mei L, Chien KR, Sussman DJ, Wynshaw-Boris A: **Dishevelled 2 is essential for cardiac outflow tract development, somite segmentation and neural tube closure.** *Development (Cambridge, England)* 2002, **129**:5827–38.
85. Tada M, Smith JC: **Xwnt11 is a target of Xenopus Brachyury: regulation of gastrulation movements via Dishevelled, but not through the canonical Wnt pathway.** *Development (Cambridge, England)* 2000, **127**:2227–38.
86. Heisenberg CP, Tada M, Rauch GJ, Saúde L, Concha ML, Geisler R, Stemple DL, Smith JC, Wilson SW: **Silberblick/Wnt11 mediates convergent extension movements during zebrafish gastrulation.** *Nature* 2000, **405**:76–81.
87. Qian D, Jones C, Rzadzinska A, Mark S, Zhang X, Steel KP, Dai X, Chen P: **Wnt5a functions in planar cell polarity regulation in mice.** *Developmental biology* 2007, **306**:121–33.
88. Macheda ML, Sun WW, Kugathasan K, Hogan BM, Bower NI, Halford MM, Zhang YF, Jacques BE, Lieschke GJ, Dabdoub A, Stacker S a: **The Wnt Receptor Ryk Plays a Role in Mammalian Planar Cell Polarity Signaling.** *The Journal of biological chemistry* 2012, **287**:29312–29323.
89. Ohkawara B, Yamamoto TS, Tada M, Ueno N: **Role of glypican 4 in the regulation of convergent extension movements during gastrulation in Xenopus laevis.** *Development (Cambridge, England)* 2003, **130**:2129–38.
90. Gao B, Song H, Bishop K, Elliot G, Garrett L, English M a, Andre P, Robinson J, Sood R, Minami Y, Economides AN, Yang Y: **Wnt signaling gradients**

establish planar cell polarity by inducing Vangl2 phosphorylation through Ror2. *Developmental cell* 2011, **20**:163–76.

91. May-Simera H, Kelley MW: *Planar cell polarity in the inner ear*. 1st edition. Elsevier Inc.; 2012, **101**:111–40.

92. Murdoch JN, Henderson DJ, Doudney K, Gaston-Massuet C, Phillips HM, Paternotte C, Arkell R, Stanier P, Copp AJ: **Disruption of scribble (Scrb1) causes severe neural tube defects in the circletail mouse.** *Human molecular genetics* 2003, **12**:87–98.

93. Montcouquiol M, Sans N, Huss D, Kach J, Dickman JD, Forge A, Rachel R a, Copeland NG, Jenkins N a, Bogani D, Murdoch J, Warchol ME, Wenthold RJ, Kelley MW: **Asymmetric localization of Vangl2 and Fz3 indicate novel mechanisms for planar cell polarity in mammals.** *The Journal of neuroscience : the official journal of the Society for Neuroscience* 2006, **26**:5265–75.

94. Wansleebe C, Feitsma H, Montcouquiol M, Kroon C, Cuppen E, Meijlink F: **Planar cell polarity defects and defective Vangl2 trafficking in mutants for the COPII gene Sec24b.** *Development (Cambridge, England)* 2010, **137**:1067–73.

95. Merte J, Jensen D, Wright K, Sarsfield S, Wang Y, Schekman R, Ginty DD: **Sec24b selectively sorts Vangl2 to regulate planar cell polarity during neural tube closure.** *Nature cell biology* 2010, **12**:41–6; sup pp 1–8.

96. Narimatsu M, Bose R, Pye M, Zhang L, Miller B, Ching P, Sakuma R, Luga V, Roncari L, Attisano L, Wrana JL: **Regulation of planar cell polarity by Smurf ubiquitin ligases.** *Cell* 2009, **137**:295–307.

97. Savory JG a, Mansfield M, Rijli FM, Lohnes D: **Cdx mediates neural tube closure through transcriptional regulation of the planar cell polarity gene Ptk7.** *Development (Cambridge, England)* 2011, **138**:1361–70.

98. Lu X, Borchers AGM, Jolicoeur C, Rayburn H, Baker JC, Tessier-Lavigne M: **PTK7/CCK-4 is a novel regulator of planar cell polarity in vertebrates.** *Nature* 2004, **430**:93–8.

99. Golubkov VS, Chekanov A V, Cieplak P, Aleshin AE, Chernov A V, Zhu W, Radichev I a, Zhang D, Dong PD, Strongin AY: **The Wnt/planar cell polarity protein-tyrosine kinase-7 (PTK7) is a highly efficient proteolytic target of membrane type-1 matrix metalloproteinase: implications in cancer and embryogenesis.** *The Journal of biological chemistry* 2010, **285**:35740–9.

100. Yen WW, Williams M, Periasamy A, Conaway M, Burdsal C, Keller R, Lu X, Sutherland A: **PTK7 is essential for polarized cell motility and convergent extension during mouse gastrulation.** *Development (Cambridge, England)* 2009, **136**:2039–48.
101. Lee J, Andreeva A, Sipe CW, Liu L, Cheng A, Lu X: **PTK7 Regulates Myosin II Activity to Orient Planar Polarity in the Mammalian Auditory Epithelium.** *Current biology : CB* 2012, **22**:956–966.
102. Shnitsar I, Borchers A: **PTK7 recruits dsh to regulate neural crest migration.** *Development (Cambridge, England)* 2008, **135**:4015–24.
103. Wehner P, Shnitsar I, Urlaub H, Borchers A: **RACK1 is a novel interaction partner of PTK7 that is required for neural tube closure.** *Development (Cambridge, England)* 2011, **138**:1321–7.
104. Li S, Esterberg R, Lachance V, Ren D, Radde-gallwitz K, Chi F: **Rack1 is required for Vangl2 membrane localization and planar cell polarity signaling while attenuating canonical Wnt activity.** 2010.
105. Ishikawa HO, Takeuchi H, Haltiwanger RS, Irvine KD: **Four-jointed is a Golgi kinase that phosphorylates a subset of cadherin domains.** *Science (New York, N.Y.)* 2008, **321**:401–4.
106. Simon M a, Xu A, Ishikawa HO, Irvine KD: **Modulation of fat:dachsous binding by the cadherin domain kinase four-jointed.** *Current biology : CB* 2010, **20**:811–7.
107. Ma D, Yang C, McNeill H, Simon M, Axelrod J: **Fidelity in planar cell polarity signalling.** *Nature* 2003, **6**:543–547.
108. Adler PN, Charlton J, Liu J: **Mutations in the cadherin superfamily member gene dachsous cause a tissue polarity phenotype by altering frizzled signaling.** *Development (Cambridge, England)* 1998, **125**:959–68.
109. Mao Y, Rauskolb C, Cho E, Hu W-L, Hayter H, Minihan G, Katz FN, Irvine KD: **Dachs: an unconventional myosin that functions downstream of Fat to regulate growth, affinity and gene expression in Drosophila.** *Development (Cambridge, England)* 2006, **133**:2539–51.
110. Simon M a: **Planar cell polarity in the Drosophila eye is directed by graded Four-jointed and Dachsous expression.** *Development (Cambridge, England)* 2004, **131**:6175–84.

111. Matakatsu H, Blair SS: **Interactions between Fat and Dachshous and the regulation of planar cell polarity in the Drosophila wing.** *Development (Cambridge, England)* 2004, **131**:3785–94.
112. Thomas C, Strutt D: **The roles of the cadherins Fat and Dachshous in planar polarity specification in Drosophila.** *Developmental dynamics : an official publication of the American Association of Anatomists* 2012, **241**:27–39.
113. Yang C, Axelrod JD, Simon M a: **Regulation of Frizzled by fat-like cadherins during planar polarity signaling in the Drosophila compound eye.** *Cell* 2002, **108**:675–88.
114. Casal J, Lawrence P a, Struhl G: **Two separate molecular systems, Dachshous/Fat and Starry night/Frizzled, act independently to confer planar cell polarity.** *Development (Cambridge, England)* 2006, **133**:4561–72.
115. Rock R, Schrauth S, Gessler M: **Expression of mouse dchs1, fjc1, and fat-j suggests conservation of the planar cell polarity pathway identified in Drosophila.** *Developmental dynamics : an official publication of the American Association of Anatomists* 2005, **234**:747–55.
116. Mao Y, Mulvaney J, Zakaria S, Yu T, Morgan KM, Allen S, Basson MA, Francis-West P, Irvine KD: **Characterization of a Dchs1 mutant mouse reveals requirements for Dchs1-Fat4 signaling during mammalian development.** *Development (Cambridge, England)* 2011, **138**:947–57.
117. Saburi S, Hester I, Fischer E, Pontoglio M, Eremina V, Gessler M, Quaggin SE, Harrison R, Mount R, McNeill H: **Loss of Fat4 disrupts PCP signaling and oriented cell division and leads to cystic kidney disease.** *Nature genetics* 2008, **40**:1010–5.
118. Aigouy B, Farhadifar R, Staple DB, Sagner A, Röper J-C, Jülicher F, Eaton S: **Cell flow reorients the axis of planar polarity in the wing epithelium of Drosophila.** *Cell* 2010, **142**:773–86.
119. Harumoto T, Ito M, Shimada Y, Kobayashi TJ, Ueda HR, Lu B, Uemura T: **Atypical cadherins Dachshous and Fat control dynamics of noncentrosomal microtubules in planar cell polarity.** *Developmental cell* 2010, **19**:389–401.
120. Sagner A, Merkel M, Aigouy B, Gaebel J, Brankatschk M, Jülicher F, Eaton S: **Establishment of global patterns of planar polarity during growth of the Drosophila wing epithelium.** *Current biology : CB* 2012, **22**:1296–301.
121. Lapébie P, Borchiellini C, Houliston E: **Dissecting the PCP pathway: one or more pathways?: Does a separate Wnt-Fz-Rho pathway drive**

morphogenesis? *BioEssays : news and reviews in molecular, cellular and developmental biology* 2011, **33**:759–68.

122. Wallingford JB: **Planar Cell Polarity and the Developmental Control of Cell Behavior in Vertebrate Embryos.** *Annual review of cell and developmental biology* 2012.

123. Jaffe AB, Hall A: **Rho GTPases: biochemistry and biology.** *Annual review of cell and developmental biology* 2005, **21**:247–69.

124. Habas R, Dawid IB, He X: **Coactivation of Rac and Rho by Wnt/Frizzled signaling is required for vertebrate gastrulation.** *Genes & development* 2003, **17**:295–309.

125. Fanto M, Weber U, Strutt DJ, Mlodzik M: **Nuclear signaling by Rac and Rho GTPases is required in the establishment of epithelial planar polarity in the Drosophila eye.** *Current biology : CB* 2000, **10**:979–88.

126. Habas R, Kato Y, He X: **Wnt/Frizzled activation of Rho regulates vertebrate gastrulation and requires a novel Formin homology protein Daam1.** *Cell* 2001, **107**:843–54.

127. Tanegashima K, Zhao H, Dawid IB: **WGEF activates Rho in the Wnt-PCP pathway and controls convergent extension in Xenopus gastrulation.** *The EMBO journal* 2008, **27**:606–17.

128. Yamanaka H, Moriguchi T, Masuyama N, Kusakabe M, Hanafusa H, Takada R, Takada S, Nishida E: **JNK functions in the non-canonical Wnt pathway to regulate convergent extension movements in vertebrates.** *EMBO reports* 2002, **3**:69–75.

129. Kinoshita N, Iioka H, Miyakoshi A, Ueno N: **PKC delta is essential for Dishevelled function in a noncanonical Wnt pathway that regulates Xenopus convergent extension movements.** *Genes & development* 2003, **17**:1663–76.

130. Adler PN, Zhu C, Stone D: **Inturned Localizes to the Proximal Side of Wing Cells under the Instruction of Upstream Planar Polarity Proteins.** 2004, **14**:2046–2051.

131. Simons M, Mlodzik M: **Planar cell polarity signaling: from fly development to human disease.** *Annual review of genetics* 2008, **42**:517–40.

132. Strutt D, Warrington SJ: **Planar polarity genes in the Drosophila wing regulate the localisation of the FH3-domain protein Multiple Wing Hairs to**

control the site of hair production. *Development (Cambridge, England)* 2008, **135**:3103–11.

133. Yan J, Huen D, Morely T, Johnson G, Gubb D, Roote J, Adler PN: **The multiple-wing-hairs gene encodes a novel GBD-FH3 domain-containing protein that functions both prior to and after wing hair initiation.** *Genetics* 2008, **180**:219–28.

134. Heydeck W, Zeng H, Liu A: **Planar cell polarity effector gene Fuzzy regulates cilia formation and Hedgehog signal transduction in mouse.** *Developmental dynamics : an official publication of the American Association of Anatomists* 2009, **238**:3035–42.

135. Kim SK, Shindo A, Park TJ, Oh EC, Ghosh S, Gray RS, Lewis R a, Johnson C a, Attie-Bittach T, Katsanis N, Wallingford JB: **Planar cell polarity acts through septins to control collective cell movement and ciliogenesis.** *Science (New York, N.Y.)* 2010, **329**:1337–40.

136. Park TJ, Haigo SL, Wallingford JB: **Ciliogenesis defects in embryos lacking inturned or fuzzy function are associated with failure of planar cell polarity and Hedgehog signaling.** *Nature genetics* 2006, **38**:303–11.

137. Gray RS, Abitua PB, Wlodarczyk BJ, Szabo-Rogers HL, Blanchard O, Lee I, Weiss GS, Liu KJ, Marcotte EM, Wallingford JB, Finnell RH: **The planar cell polarity effector Fuz is essential for targeted membrane trafficking, ciliogenesis and mouse embryonic development.** *Nature cell biology* 2009, **11**:1225–32.

138. Etheridge SL, Ray S, Li S, Hamblet NS, Lijam N, Tsang M, Greer J, Kardos N, Wang J, Sussman DJ, Chen P, Wynshaw-Boris A: **Murine dishevelled 3 functions in redundant pathways with dishevelled 1 and 2 in normal cardiac outflow tract, cochlea, and neural tube development.** *PLoS genetics* 2008, **4**:e1000259.

139. Deans MR, Antic D, Suyama K, Scott MP, Axelrod JD, Goodrich L V: **Asymmetric distribution of prickle-like 2 reveals an early underlying polarization of vestibular sensory epithelia in the inner ear.** *The Journal of neuroscience : the official journal of the Society for Neuroscience* 2007, **27**:3139–47.

140. Wang J, Hamblet NS, Mark S, Dickinson ME, Brinkman BC, Segil N, Fraser SE, Chen P, Wallingford JB, Wynshaw-Boris A: **Dishevelled genes mediate a conserved mammalian PCP pathway to regulate convergent extension during neurulation.** *Development (Cambridge, England)* 2006, **133**:1767–78.

141. Curtin JA, Quint E, Tsipouri V, Arkell RM, Cattanach B, Copp AJ, Henderson DJ, Spurr N, Stanier P, Fisher EM, Nolan PM, Steel KP, Brown SDM, Gray IC, Murdoch JN: **Mutation of Celsr1 Disrupts Planar Polarity of Inner Ear Hair Cells and Causes Severe Neural Tube Defects in the Mouse.** 2003, **13**:1129–1133.
142. Ybot-Gonzalez P, Savery D, Gerrelli D, Signore M, Mitchell CE, Faux CH, Greene NDE, Copp AJ: **Convergent extension, planar-cell-polarity signalling and initiation of mouse neural tube closure.** *Development (Cambridge, England)* 2007, **134**:789–99.
143. Kilian B, Mansukoski H, Barbosa FC, Ulrich F, Tada M, Heisenberg C-P: **The role of Ppt/Wnt5 in regulating cell shape and movement during zebrafish gastrulation.** *Mechanisms of Development* 2003, **120**:467–476.
144. Smith JC, Conlon FL, Saka Y, Tada M: **Xwnt11 and the regulation of gastrulation in Xenopus.** *Philosophical transactions of the Royal Society of London. Series B, Biological sciences* 2000, **355**:923–30.
145. Ross AJ, May-Simera H, Eichers ER, Kai M, Hill J, Jagger DJ, Leitch CC, Chapple JP, Munro PM, Fisher S, Tan PL, Phillips HM, Leroux MR, Henderson DJ, Murdoch JN, Copp AJ, Eliot M-M, Lupski JR, Kemp DT, Dollfus H, Tada M, Katsanis N, Forge A, Beales PL: **Disruption of Bardet-Biedl syndrome ciliary proteins perturbs planar cell polarity in vertebrates.** *Nature genetics* 2005, **37**:1135–40.
146. Nachury M V, Loktev A V, Zhang Q, Westlake CJ, Peränen J, Merdes A, Slusarski DC, Scheller RH, Bazan JF, Sheffield VC, Jackson PK: **A core complex of BBS proteins cooperates with the GTPase Rab8 to promote ciliary membrane biogenesis.** *Cell* 2007, **129**:1201–13.
147. Wei Q, Zhang Y, Li Y, Zhang Q, Ling K, Hu J: **The BBSome controls IFT assembly and turnaround in cilia.** *Nature cell biology* 2012, **14**:950–7.
148. Gerdes JM, Liu Y, Zaghloul N a, Leitch CC, Lawson SS, Kato M, Beachy P a, Beales PL, DeMartino GN, Fisher S, Badano JL, Katsanis N: **Disruption of the basal body compromises proteasomal function and perturbs intracellular Wnt response.** *Nature genetics* 2007, **39**:1350–60.
149. May-Simera HL, Ross A, Rix S, Forge A, Beales PL, Jagger DJ: **Patterns of expression of Bardet-Biedl syndrome proteins in the mammalian cochlea suggest noncentrosomal functions.** *The Journal of comparative neurology* 2009, **514**:174–88.
150. Avasthi P, Marshall WF: **Stages of ciliogenesis and regulation of ciliary length.** *Differentiation; research in biological diversity* 2012, **83**:S30–42.

151. Jagger D, Collin G, Kelly J, Towers E, Nevill G, Longo-Guess C, Benson J, Halsey K, Dolan D, Marshall J, Naggert J, Forge A: **Alström Syndrome protein ALMS1 localizes to basal bodies of cochlear hair cells and regulates cilium-dependent planar cell polarity.** *Human molecular genetics* 2011, **20**:466–81.
152. Corbit KC, Shyer AE, Dowdle WE, Gaulden J, Singla V, Chen M-H, Chuang P-T, Reiter JF: **Kif3a constrains beta-catenin-dependent Wnt signalling through dual ciliary and non-ciliary mechanisms.** *Nature cell biology* 2008, **10**:70–6.
153. Lancaster M a, Schroth J, Gleeson JG: **Subcellular spatial regulation of canonical Wnt signalling at the primary cilium.** *Nature cell biology* 2011, **13**:700–7.
154. Ocbina PJR, Tuson M, Anderson K V: **Primary cilia are not required for normal canonical Wnt signaling in the mouse embryo.** *PloS one* 2009, **4**:e6839.
155. Grimsley-myers CM, Chen P: *Cilia and Nervous System Development and Function.* Dordrecht: Springer Netherlands; 2013:131–163.
156. Leightner AC, Hommerding CJ, Peng Y, Salisbury JL, Gainullin VG, Czarnecki PG, Sussman CR, Harris PC: **The Meckel syndrome protein meckelin (TMEM67) is a key regulator of cilia function but is not required for tissue planar polarity.** *Human molecular genetics* 2013:1–17.
157. Mahuzier A, Gaudé H-M, Grampa V, Anselme I, Silbermann F, Leroux-Berger M, Delacour D, Ezan J, Montcouquiol M, Saunier S, Schneider-Maunoury S, Vesque C: **Dishevelled stabilization by the ciliopathy protein Rpgrip11 is essential for planar cell polarity.** *The Journal of cell biology* 2012, **198**:927–40.
158. Pilot F, Lecuit T: **Compartmentalized morphogenesis in epithelia: from cell to tissue shape.** *Developmental dynamics : an official publication of the American Association of Anatomists* 2005, **232**:685–94.
159. Salbreux G, Charras G, Paluch E: **Actin cortex mechanics and cellular morphogenesis.** *Trends in cell biology* 2012, **22**:536–45.
160. Etienne-Manneville S: **From signaling pathways to microtubule dynamics: the key players.** *Current opinion in cell biology* 2010, **22**:104–11.
161. Galjart N: **Plus-end-tracking proteins and their interactions at microtubule ends.** *Current biology : CB* 2010, **20**:R528–37.

162. Ridley AJ, Schwartz M a, Burridge K, Firtel R a, Ginsberg MH, Borisy G, Parsons JT, Horwitz AR: **Cell migration: integrating signals from front to back.** *Science (New York, N.Y.)* 2003, **302**:1704–9.
163. Vicente-Manzanares M, Horwitz AR: **Cell migration: an overview.** *Methods in molecular biology (Clifton, N.J.)* 2011, **769**:1–24.
164. Kaverina I, Straube A: **Regulation of cell migration by dynamic microtubules.** *Seminars in cell & developmental biology* 2011, **22**:968–74.
165. Vasiliev JM, Gelfand IM, Domnina L V, Ivanova OY, Komm SG, Olshevskaja L V: **Effect of colcemid on the locomotory behaviour of fibroblasts.** *Journal of embryology and experimental morphology* 1970, **24**:625–40.
166. Mikhailov a, Gundersen GG: **Relationship between microtubule dynamics and lamellipodium formation revealed by direct imaging of microtubules in cells treated with nocodazole or taxol.** *Cell motility and the cytoskeleton* 1998, **41**:325–40.
167. Waterman-Storer CM, Worthylake R a, Liu BP, Burridge K, Salmon ED: **Microtubule growth activates Rac1 to promote lamellipodial protrusion in fibroblasts.** *Nature cell biology* 1999, **1**:45–50.
168. Mataraza JM, Briggs MW, Li Z, Entwistle A, Ridley AJ, Sacks DB: **IQGAP1 promotes cell motility and invasion.** *The Journal of biological chemistry* 2003, **278**:41237–45.
169. Fukata M, Kuroda S, Fujii K, Nakamura T, Shoji I, Matsuura Y, Okawa K, Iwamatsu a, Kikuchi a, Kaibuchi K: **Regulation of cross-linking of actin filament by IQGAP1, a target for Cdc42.** *The Journal of biological chemistry* 1997, **272**:29579–83.
170. Fukata M, Watanabe T, Noritake J, Nakagawa M, Yamaga M, Kuroda S, Matsuura Y, Iwamatsu A, Perez F, Kaibuchi K: **Rac1 and Cdc42 capture microtubules through IQGAP1 and CLIP-170.** *Cell* 2002, **109**:873–85.
171. Watanabe T, Wang S, Noritake J, Sato K, Fukata M, Takefuji M, Nakagawa M, Izumi N, Akiyama T, Kaibuchi K: **Interaction with IQGAP1 links APC to Rac1, Cdc42, and actin filaments during cell polarization and migration.** *Developmental cell* 2004, **7**:871–83.
172. Kholmanskih SS, Koeller HB, Wynshaw-Boris A, Gomez T, Letourneau PC, Ross ME: **Calcium-dependent interaction of Lis1 with IQGAP1 and Cdc42 promotes neuronal motility.** *Nature neuroscience* 2006, **9**:50–7.

173. Krendel M, Zenke FT, Bokoch GM: **Nucleotide exchange factor GEF-H1 mediates cross-talk between microtubules and the actin cytoskeleton.** *Nature cell biology* 2002, **4**:294–301.
174. Nalbant P, Chang Y, Chang Z, Bokoch GM: **Guanine Nucleotide Exchange Factor-H1 Regulates Cell Migration via Localized Activation of RhoA at the Leading Edge.** 2009, **20**:4070–4082.
175. Montenegro-venegas C, Tortosa E, Rosso S, Peretti D, Bollati F, Bisbal M, Jausoro I, Avila J, Ca A, Gonzalez-billault C: **MAP1B Regulates Axonal Development by Modulating Rho-GTPase Rac1 Activity.** 2010, **21**:3518–3528.
176. Rooney C, White G, Nazgiewicz A, Woodcock S a, Anderson KI, Ballestrem C, Malliri A: **The Rac activator STEF (Tiam2) regulates cell migration by microtubule-mediated focal adhesion disassembly.** *EMBO reports* 2010, **11**:292–8.
177. Etienne-manneville S, Hall A: **Cdc42 regulates GSK-3 b and adenomatous polyposis coli to control cell polarity.** 2003, **421**:753–756.
178. Wen Y, Eng CH, Schmoranz J, Cabrera-Poch N, Morris EJS, Chen M, Wallar BJ, Alberts AS, Gundersen GG: **EB1 and APC bind to mDia to stabilize microtubules downstream of Rho and promote cell migration.** *Nature cell biology* 2004, **6**:820–30.
179. Wittmann T, Bokoch GM, Waterman-Storer CM: **Regulation of microtubule destabilizing activity of Op18/stathmin downstream of Rac1.** *The Journal of biological chemistry* 2004, **279**:6196–203.
180. Siller KH, Doe CQ: **Spindle orientation during asymmetric cell division.** *Nature cell biology* 2009, **11**:365–74.
181. Kemphues KJ, Priess JR, Morton DG, Cheng NS: **Identification of genes required for cytoplasmic localization in early C. elegans embryos.** *Cell* 1988, **52**:311–20.
182. Schneider SQ, Bowerman B: **Cell polarity and the cytoskeleton in the Caenorhabditis elegans zygote.** *Annual review of genetics* 2003, **37**:221–49.
183. Motegi F, Zonies S, Hao Y, Cuenca A a, Griffin E, Seydoux G: **Microtubules induce self-organization of polarized PAR domains in Caenorhabditis elegans zygotes.** *Nature cell biology* 2011, **13**:1361–7.

184. Grill SW, Gönczy P, Stelzer EH, Hyman a a: **Polarity controls forces governing asymmetric spindle positioning in the *Caenorhabditis elegans* embryo.** *Nature* 2001, **409**:630–3.
185. Nguyen-Ngoc T, Afshar K, Gönczy P: **Coupling of cortical dynein and G alpha proteins mediates spindle positioning in *Caenorhabditis elegans*.** *Nature cell biology* 2007, **9**:1294–302.
186. Grill SW, Howard J, Schäffer E, Stelzer EHK, Hyman A a: **The distribution of active force generators controls mitotic spindle position.** *Science (New York, N.Y.)* 2003, **301**:518–21.
187. Pecreaux J, Röper J-C, Kruse K, Jülicher F, Hyman A a, Grill SW, Howard J: **Spindle oscillations during asymmetric cell division require a threshold number of active cortical force generators.** *Current biology : CB* 2006, **16**:2111–22.
188. Vallee RB, McKenney RJ, Ori-McKenney KM: **Multiple modes of cytoplasmic dynein regulation.** *Nature cell biology* 2012, **14**:224–30.
189. Gönczy P, Pichler S, Kirkham M, Hyman a a: **Cytoplasmic dynein is required for distinct aspects of MTOC positioning, including centrosome separation, in the one cell stage *Caenorhabditis elegans* embryo.** *The Journal of cell biology* 1999, **147**:135–50.
190. Cockell MM, Baumer K, Gönczy P: **lis-1 is required for dynein-dependent cell division processes in *C. elegans* embryos.** *Journal of cell science* 2004, **117**:4571–82.
191. Gotta M, Ahringer J: **Distinct roles for Galpha and Gbetagamma in regulating spindle position and orientation in *Caenorhabditis elegans* embryos.** *Nature cell biology* 2001, **3**:297–300.
192. Colombo K, Grill SW, Kimple RJ, Willard FS, Siderovski DP, Gönczy P: **Translation of polarity cues into asymmetric spindle positioning in *Caenorhabditis elegans* embryos.** *Science (New York, N.Y.)* 2003, **300**:1957–61.
193. Schaefer M, Petronczki M, Dorner D, Forte M, Knoblich J a: **Heterotrimeric G proteins direct two modes of asymmetric cell division in the *Drosophila* nervous system.** *Cell* 2001, **107**:183–94.
194. Tsou M-FB, Hayashi A, Rose LS: **LET-99 opposes Galpha/GPR signaling to generate asymmetry for spindle positioning in response to PAR and MES-1/SRC-1 signaling.** *Development (Cambridge, England)* 2003, **130**:5717–30.

195. Srinivasan DG, Fisk RM, Xu H, Van den Heuvel S: **A complex of LIN-5 and GPR proteins regulates G protein signaling and spindle function in *C. elegans*.** *Genes & development* 2003, **17**:1225–39.
196. Kotak S, Busso C, Gönczy P: **Cortical dynein is critical for proper spindle positioning in human cells.** *The Journal of cell biology* 2012, **199**:97–110.
197. Wu J, Rose LS: **PAR-3 and PAR-1 Inhibit LET-99 Localization to Generate a Cortical Band Important for Spindle Positioning in *Caenorhabditis elegans* Embryos** □. 2007, **18**:4470–4482.
198. Zheng Z, Zhu H, Wan Q, Liu J, Xiao Z, Siderovski DP, Du Q: **LGN regulates mitotic spindle orientation during epithelial morphogenesis.** *The Journal of cell biology* 2010, **189**:275–88.
199. Du Q, Macara IG: **Mammalian Pins is a conformational switch that links NuMA to heterotrimeric G proteins.** *Cell* 2004, **119**:503–16.
200. Du Q, Taylor L, Compton D a, Macara IG: **LGN blocks the ability of NuMA to bind and stabilize microtubules. A mechanism for mitotic spindle assembly regulation.** *Current biology : CB* 2002, **12**:1928–33.
201. Peyre E, Jaouen F, Saadaoui M, Haren L, Merdes A, Durbec P, Morin X: **A lateral belt of cortical LGN and NuMA guides mitotic spindle movements and planar division in neuroepithelial cells.** *The Journal of cell biology* 2011, **193**:141–54.
202. Merdes a, Ramyar K, Vechio JD, Cleveland DW: **A complex of NuMA and cytoplasmic dynein is essential for mitotic spindle assembly.** *Cell* 1996, **87**:447–58.
203. Yingling J, Youn YH, Darling D, Toyo-Oka K, Pramparo T, Hirotsune S, Wynshaw-Boris A: **Neuroepithelial stem cell proliferation requires LIS1 for precise spindle orientation and symmetric division.** *Cell* 2008, **132**:474–86.
204. Faulkner NE, Dujardin DL, Tai CY, Vaughan KT, O'Connell CB, Wang Y, Vallee RB: **A role for the lissencephaly gene LIS1 in mitosis and cytoplasmic dynein function.** *Nature cell biology* 2000, **2**:784–91.
205. Gumbiner BM: **Regulation of cadherin-mediated adhesion in morphogenesis.** *Nature reviews. Molecular cell biology* 2005, **6**:622–34.
206. Stehbens SJ, Paterson AD, Crampton MS, Shewan AM, Ferguson C, Akhmanova A, Parton RG, Yap AS: **Dynamic microtubules regulate the local**

concentration of E-cadherin at cell-cell contacts. *Journal of cell science* 2006, **119**:1801–11.

207. Waterman-Storer CM, Salmon WC, Salmon ED: **Feedback interactions between cell-cell adherens junctions and cytoskeletal dynamics in newt lung epithelial cells.** *Molecular biology of the cell* 2000, **11**:2471–83.

208. Bellett G, Carter JM, Keynton J, Goldspink D, James C, Moss DK, Mogensen MM: **Microtubule plus-end and minus-end capture at adherens junctions is involved in the assembly of apico-basal arrays in polarised epithelial cells.** *Cell motility and the cytoskeleton* 2009, **66**:893–908.

209. Ligon L a, Holzbaur ELF: **Microtubules tethered at epithelial cell junctions by dynein facilitate efficient junction assembly.** *Traffic (Copenhagen, Denmark)* 2007, **8**:808–19.

210. Ligon L a, Karki S, Tokito M, Holzbaur EL: **Dynein binds to beta-catenin and may tether microtubules at adherens junctions.** *Nature cell biology* 2001, **3**:913–7.

211. Karki S, Ligon LA, Desantis J, Tokito M, Holzbaur ELF: **PLAC-24 Is a Cytoplasmic Dynein-Binding Protein That Is Recruited to Sites of Cell-Cell Contact.** 2002, **13**:1722–1734.

212. Harris TJC, Sawyer JK, Peifer M: *How the cytoskeleton helps build the embryonic body plan: models of morphogenesis from Drosophila.* 1st edition. Elsevier Inc.; 2009, **89**:55–85.

213. McGill M a, McKinley RFA, Harris TJC: **Independent cadherin-catenin and Bazooka clusters interact to assemble adherens junctions.** *The Journal of cell biology* 2009, **185**:787–96.

214. Harris TJC, Peifer M: **The positioning and segregation of apical cues during epithelial polarity establishment in Drosophila.** *The Journal of cell biology* 2005, **170**:813–23.

215. Harris TJC, Tepass U: **Adherens junctions: from molecules to morphogenesis.** *Nature reviews. Molecular cell biology* 2010, **11**:502–14.

216. Goetz SC, Anderson K V: **The primary cilium: a signalling centre during vertebrate development.** *Nature reviews. Genetics* 2010, **11**:331–44.

217. Moser JJ, Fritzler MJ, Ou Y, Rattner JB: **The PCM-basal body/primary cilium coalition.** *Seminars in cell & developmental biology* 2010, **21**:148–55.

218. Lefèvre G, Michel V, Weil D, Lepelletier L, Bizard E, Wolfrum U, Hardelin J-P, Petit C: **A core cochlear phenotype in USH1 mouse mutants implicates fibrous links of the hair bundle in its cohesion, orientation and differential growth.** *Development (Cambridge, England)* 2008, **135**:1427–37.
219. Marszalek JR, Ruiz-Lozano P, Roberts E, Chien KR, Goldstein LS: **Situs inversus and embryonic ciliary morphogenesis defects in mouse mutants lacking the KIF3A subunit of kinesin-II.** *Proceedings of the National Academy of Sciences of the United States of America* 1999, **96**:5043–8.
220. Takeda S, Yonekawa Y, Tanaka Y, Okada Y, Nonaka S, Hirokawa N: **Left-right asymmetry and kinesin superfamily protein KIF3A: new insights in determination of laterality and mesoderm induction by kif3A-/- mice analysis.** *The Journal of cell biology* 1999, **145**:825–36.
221. Nishimura T, Kato K, Yamaguchi T, Fukata Y, Ohno S, Kaibuchi K: **Role of the PAR-3-KIF3 complex in the establishment of neuronal polarity.** *Nature cell biology* 2004, **6**:328–34.
222. Teng J, Rai T, Tanaka Y, Takei Y, Nakata T, Hirasawa M, Kulkarni AB, Hirokawa N: **The KIF3 motor transports N-cadherin and organizes the developing neuroepithelium.** *Nature cell biology* 2005, **7**:474–82.
223. Hébert JM, McConnell SK: **Targeting of cre to the Foxg1 (BF-1) locus mediates loxP recombination in the telencephalon and other developing head structures.** *Developmental biology* 2000, **222**:296–306.
224. Yamamoto N, Okano T, Ma X, Adelstein RS, Kelley MW: **Myosin II regulates extension, growth and patterning in the mammalian cochlear duct.** *Development (Cambridge, England)* 2009, **136**:1977–86.
225. Lelli A, Asai Y, Forge A, Holt JR, Géléoc GSG: **Tonotopic gradient in the developmental acquisition of sensory transduction in outer hair cells of the mouse cochlea.** *Journal of neurophysiology* 2009, **101**:2961–73.
226. Gale JE, Marcotti W, Kennedy HJ, Kros CJ, Richardson GP: **FM1-43 dye behaves as a permeant blocker of the hair-cell mechanotransducer channel.** *The Journal of neuroscience : the official journal of the Society for Neuroscience* 2001, **21**:7013–25.
227. Géléoc GSG, Holt JR: **Developmental acquisition of sensory transduction in hair cells of the mouse inner ear.** *Nature neuroscience* 2003, **6**:1019–20.
228. Meyers JR, MacDonald RB, Duggan A, Lenzi D, Standaert DG, Corwin JT, Corey DP: **Lighting up the senses: FM1-43 loading of sensory cells through**

nonselective ion channels. *The Journal of neuroscience : the official journal of the Society for Neuroscience* 2003, **23**:4054–65.

229. Etournay R, Lepelletier L, De Monvel JB, Michel V, Cayet N, Leibovici M, Weil D, Foucher I, Hardelin J-P, Petit C: **Cochlear outer hair cells undergo an apical circumference remodeling constrained by the hair bundle shape.** *Development* 2010, **137**:1373–1383.

230. Higginbotham H, Bielas S, Tanaka T, Gleeson JG: **Transgenic mouse line with green-fluorescent protein-labeled Centrin 2 allows visualization of the centrosome in living cells.** *Transgenic research* 2004, **13**:155–64.

231. Bokoch GM: **Biology of the p21-activated kinases.** *Annual review of biochemistry* 2003, **72**:743–81.

232. Deacon SW, Beeser A, Fukui J a, Rennefahrt UEE, Myers C, Chernoff J, Peterson JR: **An isoform-selective, small-molecule inhibitor targets the autoregulatory mechanism of p21-activated kinase.** *Chemistry & biology* 2008, **15**:322–31.

233. Gao Y, Dickerson JB, Guo F, Zheng J, Zheng Y: **Rational design and characterization of a Rac GTPase-specific small molecule inhibitor.** *Proceedings of the National Academy of Sciences of the United States of America* 2004, **101**:7618–23.

234. Shi S, Cheng T, Jan LY, Jan Y: **APC and GSK-3 β Are Involved in mPar3 Targeting to the Nascent Axon and Establishment of Neuronal Polarity.** 2004, **14**:2025–2032.

235. Kunda P, Paglini G, Quiroga S, Kosik K, Caceres a: **Evidence for the involvement of Tiam1 in axon formation.** *The Journal of neuroscience : the official journal of the Society for Neuroscience* 2001, **21**:2361–72.

236. Frank SR, Hansen SH: **The PIX-GIT complex: a G protein signaling cassette in control of cell shape.** *Seminars in cell & developmental biology* 2008, **19**:234–44.

237. Wu X, Tu X, Joeng KS, Hilton MJ, Williams D a, Long F: **Rac1 activation controls nuclear localization of beta-catenin during canonical Wnt signaling.** *Cell* 2008, **133**:340–53.

238. Boerboom D, White LD, Dalle S, Courty J, Richards JS: **Dominant-stable beta-catenin expression causes cell fate alterations and Wnt signaling antagonist expression in a murine granulosa cell tumor model.** *Cancer research* 2006, **66**:1964–73.

239. Hayashi S, McMahon AP: **Efficient recombination in diverse tissues by a tamoxifen-inducible form of Cre: a tool for temporally regulated gene activation/inactivation in the mouse.** *Developmental biology* 2002, **244**:305–18.
240. Chai R, Kuo B, Wang T, Liaw EJ, Xia A, Jan T a, Liu Z, Taketo MM, Oghalai JS, Nusse R, Zuo J, Cheng AG: **Wnt signaling induces proliferation of sensory precursors in the postnatal mouse cochlea.** *Proceedings of the National Academy of Sciences of the United States of America* 2012, **109**:8167–72.
241. MacDonald BT, Tamai K, He X: **Wnt/beta-catenin signaling: components, mechanisms, and diseases.** *Developmental cell* 2009, **17**:9–26.
242. Rakyan VK, Chong S, Champ ME, Cuthbert PC, Morgan HD, Luu KVK, Whitelaw E: **Transgenerational inheritance of epigenetic states at the murine Axin(Fu) allele occurs after maternal and paternal transmission.** *Proceedings of the National Academy of Sciences of the United States of America* 2003, **100**:2538–43.
243. Lu Z, Liu W, Huang H, He Y, Han Y, Rui Y, Wang Y, Li Q, Ruan K, Ye Z, Low BC, Meng A, Lin S-C: **Protein encoded by the Axin(Fu) allele effectively down-regulates Wnt signaling but exerts a dominant negative effect on c-Jun N-terminal kinase signaling.** *The Journal of biological chemistry* 2008, **283**:13132–9.
244. Hackett L: **E-cadherin and the Differentiation of Mammalian Vestibular Hair Cells.** *Experimental Cell Research* 2002, **278**:19–30.
245. Simonneau L, Gallego M, Pujol R: **Comparative expression patterns of T-, N-, E-cadherins, beta-catenin, and polysialic acid neural cell adhesion molecule in rat cochlea during development: implications for the nature of Kölliker's organ.** *The Journal of comparative neurology* 2003, **459**:113–26.
246. Huang P, Schier AF: **Dampened Hedgehog signaling but normal Wnt signaling in zebrafish without cilia.** *Development (Cambridge, England)* 2009, **136**:3089–98.
247. Huang P, Senga T, Hamaguchi M: **A novel role of phospho-beta-catenin in microtubule regrowth at centrosome.** *Oncogene* 2007, **26**:4357–71.
248. Maretto S, Cordenonsi M, Dupont S, Braghetta P, Broccoli V, Hassan a B, Volpin D, Bressan GM, Piccolo S: **Mapping Wnt/beta-catenin signaling during mouse development and in colorectal tumors.** *Proceedings of the National Academy of Sciences of the United States of America* 2003, **100**:3299–304.

249. Malliri A, Van der Kammen R a, Clark K, Van der Valk M, Michiels F, Collard JG: **Mice deficient in the Rac activator Tiam1 are resistant to Ras-induced skin tumours.** *Nature* 2002, **417**:867–71.
250. Sipe CW, Lu X: **Kif3a regulates planar polarization of auditory hair cells through both ciliary and non-ciliary mechanisms.** *Development* 2011, **138**:3441–9.
251. Wynshaw-Boris A, Pramparo T, Youn YH, Hirotsune S: **Lissencephaly: mechanistic insights from animal models and potential therapeutic strategies.** *Seminars in cell & developmental biology* 2010, **21**:823–30.
252. Vallee RB, Tsai J-W: **The cellular roles of the lissencephaly gene LIS1, and what they tell us about brain development.** *Genes & development* 2006, **20**:1384–93.
253. Huang J, Roberts AJ, Leschziner AE, Reck-Peterson SL: **Lis1 Acts as a “Clutch” between the ATPase and Microtubule-Binding Domains of the Dynein Motor.** *Cell* 2012, **150**:975–986.
254. McKenney RJ, Vershinin M, Kunwar A, Vallee RB, Gross SP: **LIS1 and NudE induce a persistent dynein force-producing state.** *Cell* 2010, **141**:304–14.
255. Kholmanskikh SS, Dobrin JS, Wynshaw-Boris A, Letourneau PC, Ross ME: **Disregulated RhoGTPases and actin cytoskeleton contribute to the migration defect in Lis1-deficient neurons.** *The Journal of neuroscience : the official journal of the Society for Neuroscience* 2003, **23**:8673–81.
256. Rehberg M, Kleylein-Sohn J, Faix J, Ho T, Schulz I, Gräf R: **Dictyostelium LIS1 is a centrosomal protein required for microtubule/cell cortex interactions, nucleus/centrosome linkage, and actin dynamics.** *Molecular biology of the cell* 2005, **16**:2759–71.
257. Sasaki S, Shionoya a, Ishida M, Gambello MJ, Yingling J, Wynshaw-Boris a, Hirotsune S: **A LIS1/NUDEL/cytoplasmic dynein heavy chain complex in the developing and adult nervous system.** *Neuron* 2000, **28**:681–96.
258. Tanaka T, Serneo FF, Higgins C, Gambello MJ, Wynshaw-Boris A, Gleeson JG: **Lis1 and doublecortin function with dynein to mediate coupling of the nucleus to the centrosome in neuronal migration.** *The Journal of cell biology* 2004, **165**:709–21.
259. Hirotsune S, Fleck MW, Gambello MJ, Bix GJ, Chen a, Clark GD, Ledbetter DH, McBain CJ, Wynshaw-Boris a: **Graded reduction of Pafah1b1 (Lis1)**

activity results in neuronal migration defects and early embryonic lethality. *Nature genetics* 1998, **19**:333–9.

260. Yang H, Xie X, Deng M, Chen X, Gan L: **Generation and characterization of Atoh1-Cre knock-in mouse line.** *Genesis (New York, N.Y. : 2000)* 2010, **48**:407–13.

261. Dillman JF, Pfister KK, Biology C, Health V: **Differential phosphorylation in vivo of cytoplasmic dynein associated with anterogradely moving organelles.** *The Journal of cell biology* 1994, **127**:1671–81.

262. Gambello MJ, Darling DL, Yingling J, Tanaka T, Gleeson JG, Wynshaw-Boris A: **Multiple dose-dependent effects of Lis1 on cerebral cortical development.** *The Journal of neuroscience : the official journal of the Society for Neuroscience* 2003, **23**:1719–29.

263. Kubo A, Sasaki H, Yuba-Kubo A, Tsukita S, Shiina N: **Centriolar satellites: molecular characterization, ATP-dependent movement toward centrioles and possible involvement in ciliogenesis.** *The Journal of cell biology* 1999, **147**:969–80.

264. Zimmerman W, Doxsey SJ: **Construction of Centrosomes and Spindle Poles by Molecular Motor-Driven Assembly of Protein Particles.** *Traffic* 2000, **1**:927–934.

265. Guo J, Yang Z, Song W, Chen Q, Wang F, Zhang Q, Zhu X: **Nudel contributes to microtubule anchoring at the mother centriole and is involved in both dynein-dependent and -independent centrosomal protein assembly.** *Molecular biology of the cell* 2006, **17**:680–9.

266. Balczon R, Bao L, Zimmer WE: **PCM-1, A 228-kD centrosome autoantigen with a distinct cell cycle distribution.** *The Journal of cell biology* 1994, **124**:783–93.

267. Dammermann A, Merdes A: **Assembly of centrosomal proteins and microtubule organization depends on PCM-1.** *The Journal of cell biology* 2002, **159**:255–66.

268. Quintyne NJ, Gill SR, Eckley DM, Crego CL, Compton D a, Schroer T a: **Dynactin is required for microtubule anchoring at centrosomes.** *The Journal of cell biology* 1999, **147**:321–34.

269. Smith DS, Niethammer M, Ayala R, Zhou Y, Gambello MJ, Wynshaw-Boris a, Tsai LH: **Regulation of cytoplasmic dynein behaviour and microtubule organization by mammalian Lis1.** *Nature cell biology* 2000, **2**:767–75.

270. Harada a, Takei Y, Kanai Y, Tanaka Y, Nonaka S, Hirokawa N: **Golgi vesiculation and lysosome dispersion in cells lacking cytoplasmic dynein.** *The Journal of cell biology* 1998, **141**:51–9.
271. Lam C, Vergnolle M a S, Thorpe L, Woodman PG, Allan VJ: **Functional interplay between LIS1, NDE1 and NDEL1 in dynein-dependent organelle positioning.** *Journal of cell science* 2010, **123**:202–12.
272. Oyadomari S, Mori M: **Roles of CHOP/GADD153 in endoplasmic reticulum stress.** *Cell death and differentiation* 2004, **11**:381–9.
273. Haynes CM, Ron D: **The mitochondrial UPR - protecting organelle protein homeostasis.** *Journal of cell science* 2010, **123**:3849–55.
274. Srinivasan L, Sasaki Y, Calado DP, Zhang B, Paik JH, DePinho R a, Kutok JL, Kearney JF, Otipoby KL, Rajewsky K: **PI3 kinase signals BCR-dependent mature B cell survival.** *Cell* 2009, **139**:573–86.
275. Terawaki S, Kitano K, Mori T, Zhai Y, Higuchi Y, Itoh N, Watanabe T, Kaibuchi K, Hakoshima T: **The PHCCEX domain of Tiam1/2 is a novel protein- and membrane-binding module.** *The EMBO journal* 2010, **29**:236–50.
276. Shepherd TR, Hard RL, Murray AM, Pei D, Fuentes EJ: **Distinct ligand specificity of the Tiam1 and Tiam2 PDZ domains.** *Biochemistry* 2011, **50**:1296–308.
277. Muzumdar MD, Tasic B, Miyamichi K, Li L, Luo L: **A global double-fluorescent Cre reporter mouse.** *Genesis (New York, N.Y. : 2000)* 2007, **45**:593–605.
278. Michiels F, Stam JC, Hordijk PL, Van der Kammen R a, Ruuls-Van Stalle L, Feltkamp C a, Collard JG: **Regulated membrane localization of Tiam1, mediated by the NH2-terminal pleckstrin homology domain, is required for Rac-dependent membrane ruffling and C-Jun NH2-terminal kinase activation.** *The Journal of cell biology* 1997, **137**:387–98.
279. Tsai J-W, Chen Y, Kriegstein AR, Vallee RB: **LIS1 RNA interference blocks neural stem cell division, morphogenesis, and motility at multiple stages.** *The Journal of cell biology* 2005, **170**:935–45.
280. Yamada M, Toba S, Yoshida Y, Haratani K, Mori D, Yano Y, Mimori-Kiyosue Y, Nakamura T, Itoh K, Fushiki S, Setou M, Wynshaw-Boris A, Torisawa T, Toyoshima YY, Hirotsune S: **LIS1 and NDEL1 coordinate the plus-end-directed transport of cytoplasmic dynein.** *The EMBO journal* 2008, **27**:2471–83.

281. Markus SM, Punch JJ, Lee W-L: **Motor- and Tail-Dependent Targeting of Dynein to Microtubule Plus Ends and the Cell Cortex.** *Current Biology* 2009, **19**:196–205.
282. Laan L, Pavin N, Husson J, Romet-Lemonne G, Van Duijn M, López MP, Vale RD, Jülicher F, Reck-Peterson SL, Dogterom M: **Cortical Dynein Controls Microtubule Dynamics to Generate Pulling Forces that Position Microtubule Asters.** *Cell* 2012, **148**:502–14.
283. Tahirovic S, Bradke F: **Neuronal polarity.** *Cold Spring Harbor perspectives in biology* 2009, **1**:a001644.
284. Slaughter BD, Smith SE, Li R: **Symmetry breaking in the life cycle of the budding yeast.** *Cold Spring Harbor perspectives in biology* 2009, **1**:a003384.
285. Chang F, Martin SG: **Shaping fission yeast with microtubules.** *Cold Spring Harbor perspectives in biology* 2009, **1**:a001347.
286. Ségalen M, Johnston C a, Martin C a, Dumortier JG, Prehoda KE, David NB, Doe CQ, Bellaïche Y: **The Fz-Dsh planar cell polarity pathway induces oriented cell division via Mud/NuMA in Drosophila and zebrafish.** *Developmental cell* 2010, **19**:740–52.
287. Johnston C a, Hirono K, Prehoda KE, Doe CQ: **Identification of an Aurora-A/PinsLINKER/Dlg spindle orientation pathway using induced cell polarity in S2 cells.** *Cell* 2009, **138**:1150–63.
288. Walsh T, Shahin H, Elkan-Miller T, Lee MK, Thornton AM, Roeb W, Abu Rayyan A, Loulus S, Avraham KB, King M-C, Kanaan M: **Whole exome sequencing and homozygosity mapping identify mutation in the cell polarity protein GPSM2 as the cause of nonsyndromic hearing loss DFNB82.** *American journal of human genetics* 2010, **87**:90–4.
289. Yariz KO, Walsh T, Akay H, Duman D, Akkaynak a C, King M-C, Tekin M: **A truncating mutation in GPSM2 is associated with recessive non-syndromic hearing loss.** *Clinical genetics* 2012, **81**:289–93.
290. Gundersen GG, Bulinski JC: **Selective stabilization of microtubules oriented toward the direction of cell migration.** *Proceedings of the National Academy of Sciences of the United States of America* 1988, **85**:5946–50.
291. Etienne-Manneville S, Hall a: **Integrin-mediated activation of Cdc42 controls cell polarity in migrating astrocytes through PKCzeta.** *Cell* 2001, **106**:489–98.

292. Palazzo a F, Joseph HL, Chen YJ, Dujardin DL, Alberts a S, Pfister KK, Vallee RB, Gundersen GG: **Cdc42, dynein, and dynactin regulate MTOC reorientation independent of Rho-regulated microtubule stabilization.** *Current biology : CB* 2001, **11**:1536–41.
293. Vallee RB, Stehman S a: **How dynein helps the cell find its center: a servomechanical model.** *Trends in cell biology* 2005, **15**:288–94.
294. DeRosier DJ, Tilney LG: **The structure of the cuticular plate, an in vivo actin gel.** *The Journal of cell biology* 1989, **109**:2853–67.
295. Kitajiri S, Sakamoto T, Belyantseva I a, Goodyear RJ, Stepanyan R, Fujiwara I, Bird JE, Riazuddin S, Riazuddin S, Ahmed ZM, Hinshaw JE, Sellers J, Bartles JR, Hammer J a, Richardson GP, Griffith AJ, Frolenkov GI, Friedman TB: **Actin-bundling protein TRIOBP forms resilient rootlets of hair cell stereocilia essential for hearing.** *Cell* 2010, **141**:786–98.
296. Johnson GL: **NIH Public Access.** 2007, **1773**:1341–1348.
297. Gupta S, Barrett T, Whitmarsh a J, Cavanagh J, Sluss HK, Dérijard B, Davis RJ: **Selective interaction of JNK protein kinase isoforms with transcription factors.** *The EMBO journal* 1996, **15**:2760–70.
298. Koushika SP: **“JIP”ing along the axon: the complex roles of JIPs in axonal transport.** *BioEssays : news and reviews in molecular, cellular and developmental biology* 2008, **30**:10–4.
299. Xia Y, Karin M: **The control of cell motility and epithelial morphogenesis by Jun kinases.** *Trends in cell biology* 2004, **14**:94–101.
300. Kaltschmidt J a, Lawrence N, Morel V, Balayo T, Fernández BG, Pelissier A, Jacinto A, Martinez Arias A: **Planar polarity and actin dynamics in the epidermis of Drosophila.** *Nature cell biology* 2002, **4**:937–44.
301. Sabapathy K, Jochum W, Hochedlinger K, Chang L, Karin M, Wagner EF: **Defective neural tube morphogenesis and altered apoptosis in the absence of both JNK1 and JNK2.** *Mechanisms of development* 1999, **89**:115–24.
302. Weston CR, Wong A, Hall JP, Goad MEP, Flavell R a, Davis RJ: **JNK initiates a cytokine cascade that causes Pax2 expression and closure of the optic fissure.** *Genes & development* 2003, **17**:1271–80.
303. Chang L, Jones Y, Ellisman MH, Goldstein LSB, Karin M: **JNK1 is required for maintenance of neuronal microtubules and controls phosphorylation of microtubule-associated proteins.** *Developmental cell* 2003, **4**:521–33.

304. Kawauchi T, Chihama K, Nabeshima Y, Hoshino M: **The in vivo roles of STEF/Tiam1, Rac1 and JNK in cortical neuronal migration.** *The EMBO journal* 2003, **22**:4190–201.
305. Huang C, Jacobson K, Schaller MD: **MAP kinases and cell migration.** *Journal of cell science* 2004, **117**:4619–28.
306. Muñoz-Descalzo S, Gómez-Cabrero A, Mlodzik M, Paricio N: **Analysis of the role of the Rac/Cdc42 GTPases during planar cell polarity generation in Drosophila.** *The International journal of developmental biology* 2007, **51**:379–87.
307. Boutros M, Paricio N, Strutt DJ, Mlodzik M: **Dishevelled activates JNK and discriminates between JNK pathways in planar polarity and wingless signaling.** *Cell* 1998, **94**:109–18.
308. Wang W, Shi L, Xie Y, Ma C, Li W, Su X, Huang S, Chen R, Zhu Z, Mao Z, Han Y, Li M: **SP600125, a new JNK inhibitor, protects dopaminergic neurons in the MPTP model of Parkinson's disease.** *Neuroscience research* 2004, **48**:195–202.
309. Wang J, Van De Water TR, Bonny C, De Ribaupierre F, Puel JL, Zine a: **A peptide inhibitor of c-Jun N-terminal kinase protects against both aminoglycoside and acoustic trauma-induced auditory hair cell death and hearing loss.** *The Journal of neuroscience : the official journal of the Society for Neuroscience* 2003, **23**:8596–607.
310. Pirvola U, Xing-Qun L, Virkkala J, Saarma M, Murakata C, Camoratto a M, Walton KM, Ylikoski J: **Rescue of hearing, auditory hair cells, and neurons by CEP-1347/KT7515, an inhibitor of c-Jun N-terminal kinase activation.** *The Journal of neuroscience : the official journal of the Society for Neuroscience* 2000, **20**:43–50.
311. Warchol ME, Montcouquiol M: **Maintained expression of the planar cell polarity molecule Vangl2 and reformation of hair cell orientation in the regenerating inner ear.** *Journal of the Association for Research in Otolaryngology : JARO* 2010, **11**:395–406.
312. Kaltenbach J a, Falzarano PR: **Postnatal development of the hamster cochlea. I. Growth of hair cells and the organ of Corti.** *The Journal of comparative neurology* 1994, **340**:87–97.
313. Shin J-B, Streijger F, Beynon A, Peters T, Gadzala L, McMillen D, Bystrom C, Van der Zee CEEM, Wallimann T, Gillespie PG: **Hair bundles are specialized for ATP delivery via creatine kinase.** *Neuron* 2007, **53**:371–86.

314. Drummond MC, Belyantseva I a, Friderici KH, Friedman TB: **Actin in hair cells and hearing loss.** *Hearing research* 2012, **288**:89–99.
315. Ríos-Barrera LD, Riesgo-Escovar JR: **Regulating cell morphogenesis: The drosophila jun n-terminal kinase pathway.** *Genesis (New York, N.Y. : 2000)* 2012, **16**:1–16.
316. Ori-McKenney KM, Vallee RB: **Neuronal migration defects in the Loa dynein mutant mouse.** *Neural development* 2011, **6**:26.
317. Hafezparast M, Klocke R, Ruhrberg C, Marquardt A, Ahmad-Annuar A, Bowen S, Lalli G, Witherden AS, Hummerich H, Nicholson S, Morgan PJ, Oozageer R, Priestley J V, Averill S, King VR, Ball S, Peters J, Toda T, Yamamoto A, Hiraoka Y, Augustin M, Korthaus D, Wattler S, Wabnitz P, Dickneite C, Lampel S, Boehme F, Peraus G, Popp A, Rudelius M, Schlegel J, Fuchs H, Hrabe de Angelis M, Schiavo G, Shima DT, Russ AP, Stumm G, Martin JE, Fisher EMC: **Mutations in dynein link motor neuron degeneration to defects in retrograde transport.** *Science (New York, N.Y.)* 2003, **300**:808–12.
318. Firestone AJ, Weinger JS, Maldonado M, Barlan K, Langston LD, O'Donnell M, Gelfand VI, Kapoor TM, Chen JK: **Small-molecule inhibitors of the AAA+ ATPase motor cytoplasmic dynein.** *Nature* 2012, **484**:125–9.
319. Söderberg O, Leuchowius K-J, Gullberg M, Jarvius M, Weibrecht I, Larsson L-G, Landegren U: **Characterizing proteins and their interactions in cells and tissues using the in situ proximity ligation assay.** *Methods (San Diego, Calif.)* 2008, **45**:227–32.
320. Suzuki A, Ohno S: **The PAR-aPKC system: lessons in polarity.** *Journal of cell science* 2006, **119**:979–87.
321. Zhang H, Macara IG: **The polarity protein PAR-3 and TIAM1 cooperate in dendritic spine morphogenesis.** *Nature cell biology* 2006, **8**:227–37.
322. Chen X, Macara IG: **Par-3 controls tight junction assembly through the Rac exchange factor Tiam1.** *Nature cell biology* 2005, **7**:262–9.
323. Peyre E, Morin X: **An oblique view on the role of spindle orientation in vertebrate neurogenesis.** *Development, growth & differentiation* 2012, **54**:287–305.
324. Siller KH, Doe CQ: **Lis1/dynactin regulates metaphase spindle orientation in Drosophila neuroblasts.** *Developmental biology* 2008, **319**:1–9.

325. Wittmann T, Bokoch GM, Waterman-Storer CM: **Regulation of leading edge microtubule and actin dynamics downstream of Rac1.** *The Journal of cell biology* 2003, **161**:845–51.
326. Wittmann T, Bokoch GM, Waterman-Storer CM: **Regulation of microtubule destabilizing activity of Op18/stathmin downstream of Rac1.** *The Journal of biological chemistry* 2004, **279**:6196–203.
327. Sells MA, Knaus UG, Bagrodia S, Ambrose DM, Bokoch GM, Chernoff J: **Human p21-activated kinase (Pak1) regulates actin organization in mammalian cells.** *Current Biology* 1997, **7**:202–210.
328. Grohmanova K, Schlaepfer D, Hess D, Gutierrez P, Beck M, Kroschewski R: **Phosphorylation of IQGAP1 modulates its binding to Cdc42, revealing a new type of rho-GTPase regulator.** *The Journal of biological chemistry* 2004, **279**:48495–504.
329. Young A, Dictenberg JB, Purohit A, Tuft R, Doxsey SJ: **Cytoplasmic Dynein-mediated Assembly of Pericentrin and gamma Tubulin onto Centrosomes.** *Mol. Biol. Cell* 2000, **11**:2047–2056.
330. Burakov A, Kovalenko O, Semenova I, Zhapparova O, Nadezhdina E, Rodionov V: **Cytoplasmic dynein is involved in the retention of microtubules at the centrosome in interphase cells.** *Traffic (Copenhagen, Denmark)* 2008, **9**:472–80.
331. Quintyne NJ, Schroer T a: **Distinct cell cycle-dependent roles for dynactin and dynein at centrosomes.** *The Journal of cell biology* 2002, **159**:245–54.
332. Hannak E, Kirkham M, Hyman a a, Oegema K: **Aurora-A kinase is required for centrosome maturation in Caenorhabditis elegans.** *The Journal of cell biology* 2001, **155**:1109–16.
333. Lüders J, Patel UK, Stearns T: **GCP-WD is a gamma-tubulin targeting factor required for centrosomal and chromatin-mediated microtubule nucleation.** *Nature cell biology* 2006, **8**:137–47.
334. Dhanasekaran DN, Reddy EP: **JNK signaling in apoptosis.** *Oncogene* 2008, **27**:6245–51.
335. Ylikoski J, Xing-Qun L, Virkkala J, Pirvola U: **Blockade of c-Jun N-terminal kinase pathway attenuates gentamicin-induced cochlear and vestibular hair cell death.** *Hearing research* 2002, **166**:33–43.

336. Morrison DK, Davis RJ: **Regulation of MAP kinase signaling modules by scaffold proteins in mammals.** *Annual review of cell and developmental biology* 2003, **19**:91–118.